ON HEPATIC STEM CELLS AND THEIR ROLE IN CHRONIC LIVER DISEASE AND CARCINOGENESIS

by

LAURENCE JOSEPH HOPKINS

A Thesis submitted to
The University of Birmingham
for the degree of
DOCTOR OF PHILOSOPHY

Centre for Liver Research
School of Immunity and Infection
College of Medical Sciences
The University of Birmingham
February, 2014

ABSTRACT

Hepatic stem cells are found in the liver at all stages of development, including adult, and have the potential to give rise to daughter cells of biliary, hepatocytic and pancreatic lineages. Hepatic stem cells contribute significantly to liver regeneration, but may be associated with development of primary liver cancer, and are being investigated as a cellular therapy for liver failure.

This thesis describes the development of methods for the immunohistochemical quantification of hepatic stem cell activation, allowing assessment of the association between hepatic stem cell activation in needle biopsy tissue and subsequent development of HCC in a retrospectively identified cohort of cirrhotic patients. A murine dietary model of NASH and HCC was developed and characterised in detail demonstrating progressive hepatic stem cell activation with increasing injury severity. We then went on to describe and prospectively isolate a resident population of stromal stem/progenitor cells in adult, uninjured mouse liver with the potential to give rise to both myofibroblasts, and under selective conditions, epithelial stem/progenitor cells. Finally, we demonstrated the isolation of hepatic stem cells from explanted cirrhotic liver and normal common bile duct and assessed their utility as a source of hepatic stem cells for cellular or regenerative therapy.

PUBLICATIONS

Correspondence:

1. Houlihan DD, **Hopkins LJ**, Suresh SX, Armstrong MJ, Newsome PN. Autologous bone marrow mesenchymal stem cell transplantation in liver failure patients caused by hepatitis B: short-term and long-term outcomes. Hepatology. 2011 Nov;54(5):1891-2
2. **Hopkins LJ**, Rowe IA, Houlihan DD. Oncofetal gene SALL4 in aggressive hepatocellular carcinoma. N Engl J Med. 2013 Sep 19;369(12):1170

Original Articles:

3. Dowman JK, **Hopkins LJ**, Reynolds GM, Armstrong MJ, Nasiri M, Nikolaou N, van Houten EL, Visser JA, Morgan SA, Lavery GG, Oprescu A, Hübscher SG, Newsome PN, Tomlinson JW. Loss of 5α-reductase type 1 accelerates the development of hepatic steatosis but protects against hepatocellular carcinoma in male mice. Endocrinology. 2013 Dec; 154(12):4536-47
4. **Hopkins LJ**, Dowman JK, Reynolds GM, Nikolaou N, Armstrong MJ, SHaw JC, Houlihan DD, Lalor PF, Hübscher SG, Tomlinson JW, Newsome PN. Hepatic stem cell activation and hepatocellular carcinoma in a mouse model of non-alcoholic steatohepatitis. Am. J. Path. 2014 May (in press)

5. Musso G, Gambino R, Tabibian JH, Ekstedt M, Kechagias S, Hamaguchi M, Hultcrantz R, Hagström H, Yoon SK, Charatcharoenwitthaya P, George J, Barrera F, Hafliðadóttir S, Björnsson ES, Armstrong MJ, **Hopkins LJ**, Gao X, Francque S, Verrijken A, Yilmaz Y, Lindor KD, Charlton M, Haring R, Lerch MM, Rettig R, Völzke H, Ryu S, Li G, Wong LL, Machado M, Cortez-Pinto H, Yasui K, Cassader M. Is non-alcoholic fatty liver disease associated with chronic kidney disease? A systematic review and meta-analysis. PLOS Medicine

To be published:

6. Hopkins LJ, Suresh S, Mabuchi Y, Wilhelm A, King A, Hübscher SG, Houlihan DD, Matsuzaki Y, Newsome PN. Prospective isolation of a novel population of mesenchymal stem/progenitor cells from adult murine liver

7. Hopkins LJ, Than S, Reynolds GM, Armstrong MA, Houlihan DD, Rowe IA, Lalor PF, Hübscher SG, Newsome PN. Quantification of liver stem/progenitor cell activation in cirrhotic biopsies and subsequent risk of HCC

PRESENTATIONS AND PUBLIC APPEARANCES

Published abstracts:

1. Dowman JK, **Hopkins LJ**, Armstrong MJ, Gathercole L, Shaw J, Hübscher SG, Tomlinson JW, Newsome PN. P86 5α-reductase-1 knockout promotes steatosis but protects against hepatocarcinogenesis in a murine model of NAFLD. Gut 60 (Suppl 2), A39-A40

2. Dowman JK, **Hopkins LJ**, Armstrong MJ, Gathercole LL, Lalor PF, Hübscher SG, Tomlinson JW, Newsome PN. 1233 5-alpha-reductase-1 knockout protects against hepatocarcinogenesis in a murine model of NASH. Journal of Hepatology 56, S488-S489

Poster Presentations:

3. Origins of Tissue Stem Cells (Abcam Stem Cells Conference), Edinburgh, June 2012. "Hepatic Stem Cell Activation and Hepatocellular Carcinoma in a Murine Model of Non-Alcoholic Steatohepatitis"

Oral presentations:

4. 20th United European Gastroenterology Week, Amsterdam, October 2012. OP100 "Chronic metabolic-induced liver injury, hepatic stem cell activation and hepatocellular carcinoma in a murine obesity model". *Oral free-paper prize winner*

DEDICATION

This thesis is dedicated to my parents Terry and Jackie who gave me the confidence to dream, the courage to believe, the determination to do and to my siblings Faye and Timothy who share this gift with me

“Imagination is more important than knowledge” - Albert Einstein

ACKNOWLEDGEMENTS

I have been extremely fortunate to have met so many generous and inspirational people through scientific research. I am grateful to Prof. Philip Newsome, Prof. Stefan Hübscher and Dr. Patricia Lalor for affording me the opportunity to undertake this project and their support and guidance whilst allowing me the freedom to explore and make my own mistakes. I am indebted to Dr. Diarmaid Houlihan, Dr. Matthew Armstrong and Shankar Suresh for their constant support, encouragement and mentorship. I will always be thankful to Prof. Warren Strittmatter for introducing me to the challenging and rewarding world of clinical research and instilling me with self-belief, Dr. Jim Morgan for the hard lessons and excellent advice, and Prof. Lola Reid for her incredible generosity and tutorship. Science is by its nature a collaborative effort and I thank all members of the Centre for Liver Research for their guidance and assistance during my studies there.

TABLE OF CONTENTS

LIST OF FIGURES

LIST OF TABLES

LIST OF ABBREVIATIONS

2-DG, 2-deoxy-D-glucose;

AFP, alpha-foetoprotein;

ALIOS, American Lifestyle Induced Obesity Syndrome;

ANOVA, analysis of variance;

APC, allophycocyanin;

AUC, area under the curve;

αSMA, alpha-smooth muscle actin;

BEC, biliary epithelial cells;

BSA, bovine serum albumin;

CCC, cholangiocarcinoma;

cDNA, complimentary deoxyribonucleic acid;

CD, cluster of differentiation;

CFU, colony formation unit;

CK, cytokeratin;

CLR, Centre for Liver Research;

ColI, Collagen type 1;

DAB, 3,3'- Diaminobenzidine;

DAPI, 4',6-diamidino-2-phenylindole;

ddH_2O, double-distilled water;

DMEM, Dulbecco's modified eagle medium;

EDTA, ethylenediaminetetraacetic acid;

EGF, epidermal growth factor;

EMT, epithelial-mesenchymal transition;

EpCAM, epithelial cell adhesion molecule;

FACS, fluorescent-activated cell sorting;

FAH, fumarylacetoacetate hydrolase;

FCS, foetal calf serum;

FFA, free fatty acids;

FFPE, formalin-fixed paraffin-embedded;

FGF, fibroblast growth factor;

FITC, fluorescein isothiocyanate;

FRG, $FAH^{-/-}/RAG2^{-/-}/IL2RG^{-/-}$;

FS, forward scatter;

gDNA, genomic deoxyribonucleic acid;

GPS, glutamine-penicillin-streptomycin;

GS, glutamine synthetase;

GTT, glucose tolerance test;

H&E, haematoxylin and eosin;

HBSS, Hank’s balanced salt solution;

HCC, hepatocellular carcinoma

HEPES, 4-(2-hydroxyethyl)-1-piperazineethanesulfonic acid;

HGF, hepatocyte growth factor;

hHpSC, human hepatic stem cell;

HFD, high-fat diet;

HSC, haematopoietic stem cell;

i.v., intra-venous;

IHC, intermediate hepatobiliary cells;

IL2RG, interleukin-2 receptor, gamma;

IMS, industrial methylated spirit;

ITS, insulin-transferrin, sodium selenite;

LWBR, liver-body weight ratio;

MCD diet; methionine, choline deficient diet;

MEM, minimal essential medium;

MET, mesenchymal-epithelial transition;

mHpSC, murine hepatic stem cell;

MKM, modified Kubota's medium;

MKM-C, modified Kubota's medium, cholangiocyte differentiation;

MKM-H, modified Kubota's medium, hepatocyte differentiation;

mrEGF, murine recombinant epidermal growth factor;

mrFGF-4, murine recombinant fibroblast growth factor-4;

mrHGF, murine recombinant hepatocyte growth factor;

mrOSM, murine recombinant oncostatin-M;

mrTNFα, murine recombinant tumour necrosis factor-alpha;

MSC, mesenchymal stem cell;

NAFLD, non-alcoholic fatty liver disease;

NaOH, sodium hydroxide;

NAS, non-alcoholic fatty liver disease activity score;

NASH, non-alcoholic steatohepatitis

NC, normal chow;

NCAM, neural cell adhesion molecule;

NTBC, 2-[2-nitro-4-(trifluoromethyl)benzoyl]cyclohexane-1,3-dione;

ORO, oil red O;

OSM, oncostatin-M;

PαS, haematopoietic-lineage ($CD45^{-}Ter119^{-}$), $PDGFR\alpha^{+}Sca1^{+}$ cells

PBS, phosphate-buffered saline;

panCK, pan-cytokeratin;

PBG, peri-biliary gland;

PBMC, peripheral blood mononuclear cell;

PCR, polymerase chain reaction;

PDGFRα, platelet-derived growth factor-alpha;

PE, R-phycoerythrin;

PI, propidium iodide;

QEHB, Queen Elizabeth Hospital Birmingham;

qPCR, quantitative polymerase chain reaction;

RAG-2, recombination activating gene-2;

RNA, ribonucleic acid;

ROCK, rho-associated protein kinase;

rpm, revolutions per minute;

RPMI, Roswell Park Memorial Institute;

Sca1, stem cell antigen-1;

SEM, standard error of the means;

SS, side scatter;

TBS, Tris-buffered saline;

TNFα, tumour necrosis factor-alpha;

TFA, trans-fatty acid;

VG, Van Gieson;

VSC, vascular stem cell;

w/v, weight per volume (expressed as a percentage ie. 1% w/v = 10g/L)

CHAPTER 1

GENERAL INTRODUCTION

1.1 OVERVIEW

Liver disease prevalence and death rates are rising with the unmet clinical need for improved prevention, detection and treatment. The prevalence of liver disease is increasing, driven by the concomitant increase in the prevalence of chronic metabolic disease, predominantly alcoholic liver disease (ALD) and non-alcoholic fatty liver disease, and infectious disease, predominantly hepatitis C virus (HCV) and hepatic B virus (HBV). Other causes of liver disease, including biliary, autoimmune, and genetic disorders, have largely constant, but considerable, incidence rates. Clinical management of liver disease largely focusses on removing the cause of liver injury and preventing liver scarring and progression to end stage liver disease. The liver has considerable regenerative capacity and functional reserve and may withstand ongoing injury for years. Chronic liver diseases are progressive and, if untreated, ultimately lead to impairment of liver function below physiological demand resulting in liver failure. Currently there are no artificial devices that can be used to augment or replace lost liver function analogous to approaches used in kidney (dialysis), heart or lung failure. Consequently the only treatment for end stage liver disease is orthotopic liver transplantation involving high risk and relying on organ donation. Thus there is a great unmet need for clinical therapies with utility in slowing or preventing disease progression, avoiding liver transplantation and reducing deaths as a result of liver disease.

Hepatic stem cells are present in adult liver, are activated in all liver diseases and contribute to liver regeneration. The recent definitive identification of adult hepatic stem cells, and development of techniques for their isolation, culture and differentiation into mature, functional cells of the liver, has altered our understanding of liver tissue homeostasis,

disease and regeneration. The isolation of human hepatic stem cells from foetal and adult liver without significant disease has been well demonstrated[1] and has allowed detailed characterisation of the proliferative capacity and differential potential of hepatic stem cells[2, 3]. Human hepatic stem cells can be maintained in culture for weeks and retain the potential to differentiate into mature hepatic parenchymal populations, hepatocytes and cholangiocytes with function comparable to cells derived from induced pluripotent[4], or embryonic[5, 6], stem cells. Consequently, there is considerable interest in the use of *in vitro* cultured human hepatic stem cells a cellular therapy for chronic liver disease or in devices providing short-term liver function, or a bridge to transplantation, in cases of acute liver failure.

Research using *in vitro* cultured human hepatic stem cells has greatly increased our understanding of the maturation lineage of hepatic stem cells allowing the expression and morphological profiles of cell types at each stage of differentiation to be defined[3]. This has allowed more accurate assessment of hepatic stem cell activation in clinical disease and experimental animal models. These studies have demonstrated the proliferation and differentiation of hepatic stem cells towards mature, functional cell types occurs in response to all causes of liver injury and disease[7-9]. The liver has substantial regenerative capacity in non-pathological settings, with much of the regenerative capacity thought to be contributed by the ability of mature hepatocytes to proliferate and restore lost tissue and function. However, hepatic stem cells provide a second regenerative mechanism allowing complete regeneration of the liver even in cases where the proliferative capacity of mature hepatocytes is completely lost due to chronic disease or experimentally in animal models. Ongoing work is defining the relative contribution, and clinical significance, of hepatic stem cell-mediated regeneration.

1.2. LIVER ANATOMY

1.2.1. General anatomy of the liver and hepatic plate. The liver is the largest glandular organ in the human body and has functions in: glucose and lipid metabolism; immunity; protein production; the filtering of waste products and toxins; the storage of nutrients; and the production of bile. The liver is supplied with blood from both the hepatic artery and the hepatic portal vein, which drains directly from the gut, and drained by the central veins and ultimately the inferior vena cava. Hepatocytes produce bile which is collected and transported through the hepatic plate by the biliary canaliculi (**Fig 1.1A**). Hepatic arteries, portal veins and bile ducts are found in close proximity throughout the liver in portal tracts and are commonly referred to as the portal triad (**Fig 1.1B**). The regions of the parenchyma between portal tracts and central veins are exposed to a gradient of gradually decreasing supply of oxygen and nutrients highest in portal regions and lowest at central veins. By convention, the regions of the lobule are termed peri-portal, mid-zonal, and centri-lobular to reflect their location in relation to the the portal tract and central veins (**Fig 1.1B, annotated in italics**). Bile ducts are observed as lumen, generally smaller than adjacent hepatic arteries (**Fig 1.1B, arrowheads**) and portal veins, and are constituted by columnar epithelial cells termed biliary epithelial cells (BEC) or cholangiocytes (**Fig 1.1B, arrows**). The parenchyma predominantly comprises hepatocytes, the cells responsible for the majority of functions performed by the liver. Stromal and mononuclear cells are also found throughout the hepatic lobule with greater numbers observed in disease states.

1.2.2. Micro-anatomy of the biliary tree. The most proximal branches of the biliary tree, termed the Canals of Hering[10], are lined by both cholangiocytes and hepatocytes and connect directly to the hepatocyte cannicular system that extends throughout the lobule and collects bile produced and secreted by hepatocytes. Bile is principally composed of water, bile salts, mucus, pigments and lipids but also contains many fragments of molecules released by hepatocytes during their normal function or during cellular injury and death in response to liver insult or disease. Bile flows through the hepatic plate into the Canals of Hering in peri-portal regions before entering into increasing large branches of the biliary tree. The Canals of Hering drain into the hepatic ductules, channels formed entirely by cholangiocytes. 'Intralobular ductules' are often observed as isolated strings of cholangiocytes in liver sections and are contiguous with the 'intraportal ductules' within the portal tract which flow into the terminal ductules adjoining the bile ducts of the portal triad. These continue into the progressively larger and more distal structures of the biliary tree: the interlobular bile ducts, septal ducts, segmental ducts, right or left bile ducts and ultimately the common hepatic bile duct. Larger branches of the biliary are lined by peri-biliary glands that function in secreting mucus facilitating the transport of bile. Peri-biliary glands have recently been shown to harbour high proportions of epithelial stem cells with the potential to differentiate into functional hepatocytes, cholangiocytes and pancreatic beta cells *in vitro*[11-13]. Thus, the entire biliary epithelium, from the Canals of Hering through to the common bile duct, contains potent biliary tree/hepatic stem cells. The function and contribution of these cells, particular the newly identified cells of the peri-biliary glands, to tissue homeostasis and regeneration has yet to be fully elucidated.

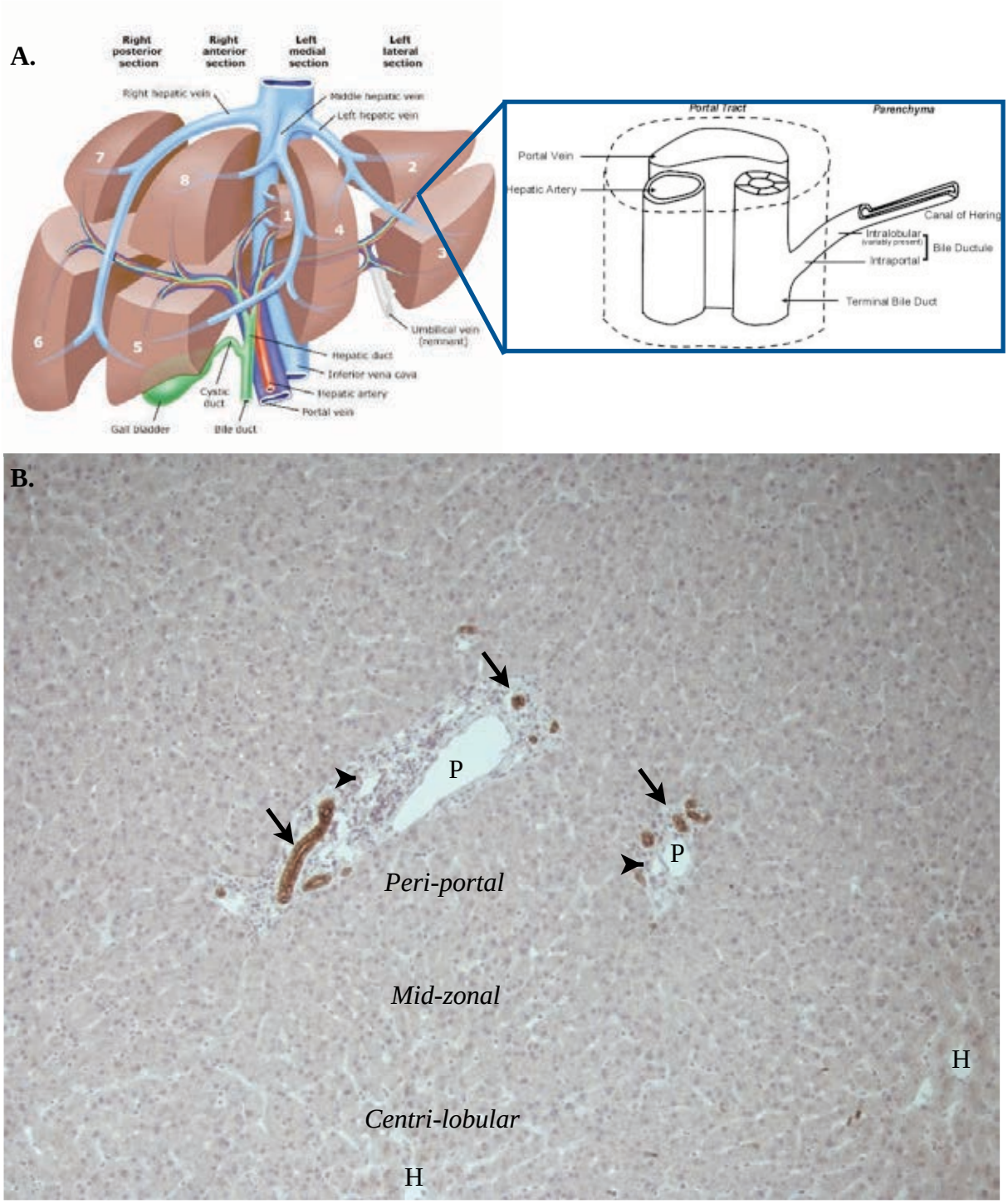

Figure 1.1. Anatomy of the adult liver. A, Gross anatomy of the adult liver including hepatic veins (blue), hepatic portal veins (purple), hepatic arteries (red) and bile ducts and gallbladder (green). Enlarged image shows finer branches of the biliary tree including the intra-portal, intra-lobular ducts and Canals of Hering. Panel A from review[10]. **B,** Representative image (100x magnification) of cytokeratin 19 immunohistochemistry of normal adult liver demonstrating cytoplasmic staining of biliary epithelium (arrows). Hepatic arteries (arrowheads), portal veins (P) and hepatic veins (H) are also annotated along with peri-portal, mid-zonal and centri-lobular regions of the liver parenchyma (italics)

1.2.3. Cell types present in adult liver.

Hepatocytes

Hepatocytes are the main functional epithelial cell type of the liver and function in protein production, breakdown or toxins and waste products and are key mediators of lipid and carbohydrate metabolism. Hepatocytes are the predominant cellular component of the liver parenchyma and have considerable proliferative capacity, able to maintain tissue homeostasis independently of hepatic stem cells and undergo compensatory growth to restore liver mass when up to 75% is lost through trauma[14]. There is evidence for a hepatocyte maturational lineage and functional spectrum spanning the hepatic plate[15], where 'small' hepatocytes originate from peri-portal regions and migrate and mature into larger, often polyploid cells in centri-lobular and peri-venular locations[3].

Biliary epithelial cells (BEC)

Biliary epithelial cells form the lumen of the entire biliary tree and function in the transport of bile and production of mucus and factors maintaining bile consistency. It is increasingly recognised that functional and phenotypic heterogeneity exists amongst biliary epithelial cells[16]. The larger, proximal branches of the biliary tree contain peri-biliary glands that produce mucus and facilitate mucus transport. A high proportion of cells within peri-biliary glands have been shown to express primitive endodermal stem cells markers and have be shown to have hepatocytic, biliary and pancreatic beta cell differentiation potential *in vitro*[11-13]. As hepatic stem cells have also been identified in the most distal portion of the biliary tree, the Canals of Hering[10], it is possible that all cells of the biliary tree have a degree

of stem/progenitor potential and plasticity but to date this has proved difficult to definitively assess.

Liver sinusoidal endothelial cells (LSEC)

Liver sinusoidal endothelial cells LSEC form the liver sinusoids, the not-continuous fenestrated endothelium of the hepatic lobule. LSEC are key mediators of lympocyte recruitment in liver injury and inflammation and secrete factors controlling hepatocyte function and influencing patterning and differentiation of activated hepatic stem cells[3, 17].

Fibroblasts

Fibroblasts are the main structural cell type of liver and are mainly found in peri-portal regions, associated with large vessels and biliary epithelium. Portal fibroblasts contribute to fibrosis and may have particularly prominent role in biliary fibrosis and cirrhosis[18], contributing to the ‘cocooning’ phenomenon commonly observed in chronic biliary disease where bile ducts become enveloping by thick layers of fibrosis[19]. Portal fibroblasts appear to be important for the maintenance of patterning of BEC, in a similar manner to that of LSEC and hepatocytes[3, 17].

Stellate cells

Hepatic stellate cells (HSCs) are peri-sinusoidal mesenchymal cells located within the Space of Disse of adult liver. The origin of stellate cells is yet to be definitively elucidated but embryological fate tracing experiments suggest a mesodermal origin; deriving from the primitive mesothelium of the developing septum transversum and later integrating with

invading epithelial cells of the hepatic bud to form the foetal liver[20, 21]. In normal liver HSCs are quiescent lipid storing cells with characteristic cytoplasmic protrusions that interact closely with surrounding endothelium and epithelium. In response to injury HSCs rapidly transdifferentiate into myofibroblasts playing key roles in scar formation, inflammation and regeneration via the secretion of extra-cellular matrix proteins, cytokines and growth factors[22]. Stellate cells are also thought to be the key mediators of injury resolution[23].

Kupffer cells and infiltrating mononuclear cells

The liver is an important immunological organ as it directly receives blood from small intestine via hepatic portal vein, including all nutrients and consumed pathogens. Liver immunity is usually conferred by specialised, resident macrophages termed Kupffer cells[24]. In injury and liver inflammation, monocytes are recruited by LSEC and differentiate into macrophages and have important roles in the regulation of fibrogenesis, injury resolution and activation/patterning of hepatic stem cells[25-27].

1.3. LIVER EMBRYOLOGY

Liver ontogenesis begins with specification of primitive endoderm by *Nodal* signaling from the surrounding mesenchyme of the septum transversum, shown to be necessary for correct specification and alignment of mesendoderm. A strong graded patterning signal is established across the primitive endoderm where high concentrations of WNT and FGF4 in the most dorsal regions specify gastrointestinal fate and low concentration in ventral regions results in the ventral foregut endoderm escaping restriction to GI fate to subsequently form the pancreas, liver, lung and thymus.

Liver ontogeny and maturation is a continuous process involving a number of cell types and complex regulatory mechanisms. Our increased understanding of these interactions has greatly enhanced our knowledge of hepatic stem cell maturation and improved our ability to culture, maintain and differentiation hepatic stem cell *in vitro*[6, 28]. The first stage of liver ontogeny involves the formation of the 'hepatic bud', derived from the primitive endoderm of the ventral foregut At this point the epithelial layer begins to change from a columnar pattern to pseudostratified through thickening and. A layer of endothelial precursors lie between the hepatic diverticulum and cells of the septum transversum. Signals from the developing heart (mainly FGF1/2) and from the septum transversum (BMPs), assist in the patterning of the hepatic bud and development of hepatic competence[20]. Hepatic competence is achieved early in development, demonstrated be experiments showing only a small proportion of the primitive endoderm ie. the foregut, is capable of developing into liver by engraftment and *in vitro* studies. At this point the key transcription factor HHEX becomes enriched in the cells of the hepatic diverticulum. HHEX is thought to be responsible for activating key early hepatic

genes ie. albumin, AFP, HNF4. Gata4 and Gata6 also play important roles at this point[29]. The hepatic diverticulum delaminates, with the loss of laminin and other associated matrix proteins. The endothelial progenitors ($Flk1^+$ *as per* adult angioblasts[30]) are absolutely required for delamination indicating their key role in patterning the endodermal cells. The cells of the hepatic diverticulum and associated endeothelial precursors then invade the septum transversum and mix with the mesenchymal cells that will go on to form the fibroblast and stellate cell populations of the liver. This interaction is then maintained throughout hepatic development and signalling between cell types is key to the patterning of the adult lobules[20, 31, 32]. At this early point the mix of cells is supplied by 2 pairs of symmetrical vitellin and umbilical veins. From here, the newly formed hepatic bud grows disproportionately, vascularises and is invaded by primitive HSCs becoming the first, and at this stage only, source of haemopoeitic cells in the foetus. Growth continues and the vascular structures of the liver become assymetrical and begin to form shunts that will eventually form the adult vessels. Sinusoidal cells begin to aggregate and form the earliest hepatic plates. At first the parenchyma is populated be a homogeneous population of bipotential hepatoblasts that restrict to cholangiocytes in periportal regions and hepatocytes in centrilobular regions. This process is largely mediated by signals from the endothelial cells and mesenchyme of the portal regions. The formation of the biliary tree involves a number of complex remodeling steps of the primitive ductal plates. At embryological day 12 (e12) the liver parenchyma is comprised entirely of hepatoblasts (**Fig 1.2AB**). By embryological day 14 (e14), hepatoblasts adjacent to portal vein have specified into biliary epithelium and at embryological day 18 remaining hepatoblasts commit to the hepatocytic lineage forming immature hepatocytes. Shortly before birth, biliary epithelial cells surrounding the portal vein condense into the

structures of the biliary tree and immature hepatocytes undergo terminal differentiation into mature, functional hepatocytes.

In the fully developed adult liver, mature cellular population are derived from:

1. Endodermal cells of the hepatic diverticulum; giving rise to hepatocytes and biliary cells
2. Mesenchymal cells of the septum transversum; giving rise to haematopoietic cells, stellate cells, kupffer cells, hepatic arteries and connective tissue
3. Endothelial precursors found between the hepatic diverticulum, and septum transversum before delamination; forming the hepatic arteries
4. Endothelial cells of the vitelline and umbilical veins; forming the hepatic veins and sinusoids and endothelial cells

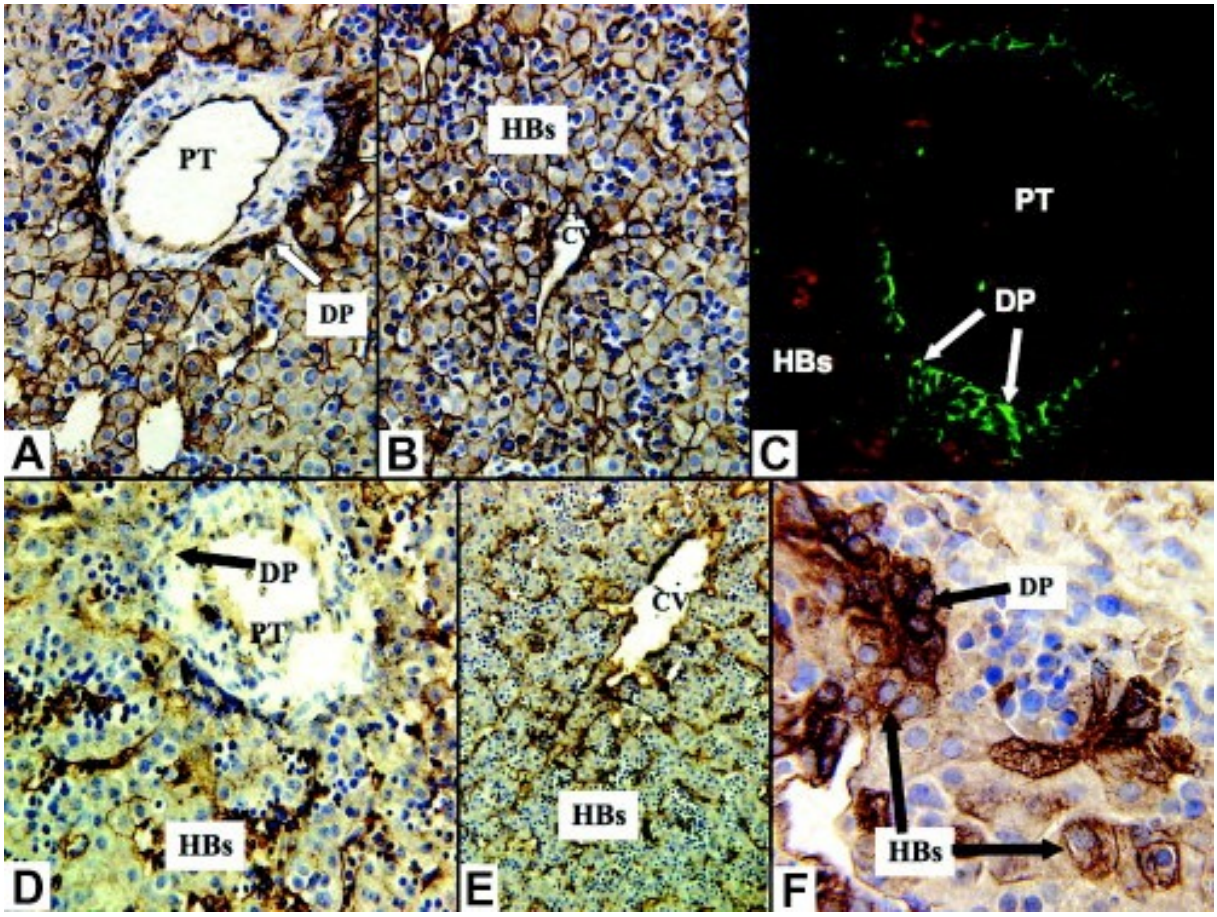

Figure 1.2. Human hepatic stem cells and hepatoblasts in foetal liver. A, EpCAM expression in ductal plate cells and **AB,** parenchymal cells throughout the developing hepatic lobule (nuclear counterstaining with hematoxylin; 10x magnification). **C,** AFP expression (red) found in the hHBs but not in the ductal plates, whereas both stain for EpCAM (green; membranous staining). **D,** ICAM1 expression is not found on the ductal plate nor in bile duct cells but rather is largely in **E,** cells lining the sinusoids within the parenchyma, although hHBs can show a membranous pattern (nuclear counterstaining with hematoxylin). **F**,The ductal plate (DP) cells stain intensely for CK19, whereas CK19 in hHBs is fainter and in a particulate staining pattern (nuclear counterstaining with hematoxylin; 40x original magnification). Figure replicated, and legend adapted, from review[33]

1.4. LIVER DISEASE AETIOLOGIES

1.4.1. Primary biliary cirrhosis. Primary biliary cirrhosis (PBC) is a progressive, chronic disease affecting the intra-hepatic bile ducts with unclear pathogenesis. The disease is characterised by inflammation and destruction of intra-lobular and septal (<100μm) bile ducts leading to a progressive fibrogenic response that initially 'cocoons' florid granulomatous peri-portal infiltrates that may progress to bridging fibrosis and ultimately cirrhosis. In response to inflammation of the biliary epithelium hepatic stem cells proliferate in response to signals predominately produced by adjacent, activated stellate cells and fibroblasts with notch signaling thought to play a particularly prominent role[26]. These signals restrict hepatic stem cells to the biliary lineage ensuring regeneration of the bile ducts without inappropriate production of cells of the hepatocyte lineage.

1.4.2. Hepatitis C virus cirrhosis. Chronic hepatitis C virus (HCV) infection causes hepatocellular injury leading to reduced liver function and progressive fibrosis resulting in cirrhosis. Incidence rates of HCC in patients with HCV-cirrhosis are estimated between 3 and 5% per year, with HCC representing a leading cause of death in patients chronically infected with HCV in the Western world[34].

1.4.3. Definition and prevalence of non-alcoholic liver disease. Non-alcoholic fatty liver disease (NAFLD) encompasses a spectrum of liver pathologies ranging from simple steatosis at its mildest form to non-alcoholic steatohepatitis (NASH) and progression to cirrhosis at its most severe[35]. NAFLD is now recognised as a growing epidemic in western populations[36], correlating with increasing obesity, with prevalence estimates ranging from 20% to 30% in

the general population[37, 38] and up to 90% in obese cohorts[39]. A diagnosis of NAFLD requires the exclusion of alcohol or drug-induced liver disease, cholestatic disease, autoimmune and viral hepatitis and other metabolic or genetic liver disorders[40]. Liver biopsy is currently the only definitive method of diagnosing NASH; the more severe manifestation of NAFLD. Over the past decade significant effort has been directed at developing a non-invasive method of diagnosis including; improved liver functions tests (LFTs)[41] which include biomarkers e.g. CK18[42], a marker of hepatocyte apoptosis; non-invasive imaging techniques such as magnetic resonance spectroscopy and elastography (Fibroscan)[43]; and scoring systems designed to identify afflicted patients[44]. However many of these non-invasive methods for diagnosis of NASH remain crude or have yet to be validated in practice and consequently liver biopsy remains the only truly reliable means of confirming a NASH diagnosis[45]. NASH patients are also at increased risk of HCC[46]. Although much of this risk may be conferred by other characteristics in NASH patients, most notably the metabolic syndrome[47], the presence of NASH may independently increase risk of HCC development even in the absence of cirrhosis[48].

1.4.4. Pathogenesis of non-alcoholic liver disease. NAFLD is closely associated with the metabolic syndrome, and is often described as the 'hepatic manifestation' of the multiplex of metabolic risk factors that define the metabolic syndrome: atherogenic dyslipidaemia; raised blood pressure; abdominal obesity; insulin resistance ± glucose intolerance; proinflammatory state and prothrombotic state[49]. Insulin resistance is recognised as the underlying cause of the metabolic syndrome and the link with NAFLD[50, 51], although whether hepatic insulin resistance is the precipitating factor or develops later as a consequence of peripheral insulin

resistance is still unclear. Worryingly, NAFLD is being increasingly reported in children and is, as in adults, tightly associated with the metabolic syndrome[52, 53] highlighting the growing health problem posed by rising obesity levels not just regarding cardiovascular diseases and diabetes but also chronic liver disease[54]. Our understanding of the progression of NAFLD from simple steatosis to cirrhosis and liver failure is incomplete and consequently our ability to predict which patients with benign steatosis will progress to more serious liver dysfunction is significantly impaired. It is recognised that simple steatosis alone is relatively benign[55], although long-term follow up reveals that a small yet significant proportion of these patients do progress to much more serious disease and ultimately liver failure[56, 57]. The first hypothesis providing a cohesive explanation of the mechanisms underlying the progression of steatosis to the inflammation and fibrosis observed in NASH and cirrhosis was postulated by James and Day with the popular 'two hit hypothesis'[58]. This model proposed that the progression to steatohepatitis firstly requires the accumulation of fat within the hepatocytes of the liver – steatosis, followed by a second hit for which they suggest oxidative stress to be the most likely candidate. More recently it has been accepted that, while the original hypothesis is still valuable with many of its propositions likely to be found correct, this model is unable to completely explain the fundamental mechanisms underlying the original cause of steatosis and subsequent sequelae of NASH and cirrhosis. Although steatosis is undoubtedly associated with NASH, current opinion suggests that the observation of steatosis may be an effect of other initial causal factors established earlier in the pathogenesis of NAFLD and that hepatic steatosis may even be a protective phenomenon. This phenomenon was demonstrated in mice over-expressing diacylglycerol acyltranferase (DGAT), the enzyme responsible for the final step in the synthesis of triglycerides. Over-expression of DGAT resulted in severe steatosis

and lipid accumulation in the livers of these mice, however these mice were found to have normal glucose metabolism, blood glucose levels and did not develop insulin resistance indicating steatosis may not be responsible for the development of insulin resistance in humans and may even be a protective mechanism[59]. Current challenges to our complete understanding of the pathogenesis of NAFLD include: delineating the relationship between insulin resistance and changes in liver metabolism, specifically lipid and glucose homeostasis; understanding the contribution of adiposity, particularly visceral, in light of the strong association with NAFLD and progression to NASH[60-63]; deciphering the mechanisms through which genetic risk factors confer increased susceptibility to NAFLD; and increasing our knowledge of the complex relationship between liver metabolism, inflammation and injury and how these processes are resolved or progress.

1.5. LIVER DISEASE HISTOLOGY

1.5.1. Liver fibrosis. In chronic liver disease, excess accumulation of extracellular matrix molecules, most notably collagen type I, occurs in the liver ultimately leading to cirrhosis and liver failure. A number of cell types are thought to contribute to collagen and matrix deposition including portal fibroblasts, activated stellate cells and their myofibroblastic progeny. Hepatic stellate cells are considered the most important mediators of fibrogenesis and injury resolution. When activated, hepatic stellate cells secrete a number of pro-inflammatory cytokines and transdifferentiate in myofibroblasts, secreting substantial amounts of matrix components and collagen[18]. Fibrosis is progressive and is usually first observed in peri-portal regions[64]. In biliary diseases, fibrosis is usually more prominent

around biliary epithelium, the site of injury, and is generally observed as thick layers of collagen enveloping bile ductules. Fibrosis may also be observed within the liver parenchyma to the extent where wide fibrotic septa are observed bridging portal tracts, characteristic of liver fibrosis[26]. In hepatocytic liver injury, liver fibrosis is predominantly observed in the hepatic lobule, first around portal triads and central veins, and then progressing to bridging and cirrhosis. Hepatic stem/progenitor cells are often observed in close association with fibrotic septa and may represent a common physiological process leading to the migration of hepatic stem cells from the biliary epithelium in portal tracts into the surrounding liver parenchyma before differentiating into mature hepatocytes. Stellate cells have been shown *in vitro* to augment the activation and differentiation of hepatic stem cells and release factors that pattern hepatic stem cells towards the hepatocyte lineage[17].

1.5.2. Ductular reaction. In many disease states cholangiocytes can be observed proliferating in inappropriately large numbers in patterns that do not result in the formation of normal bile ducts. This phenomenon is referred to as "ductular reaction"[10, 65] and is generally acknowledged to have two major types; typical and atypical. Typical ductular reaction is often precipitated by occlusion of bile ducts e.g. gall stones and tumours and results in proliferation of existing ductules forming extra lumen but which do not fully function by carrying bile. This is the type of reaction observed in bile duct ligation experiments conducted in rodent models[66]. Atypical ductular reaction is usually associated with regeneration of the liver after insult, vanishing bile duct diseases and proliferation of liver progenitor cells. This form of ductular reaction does not form discernible lumen and is characterised by the observation of strands of cells extending into the parenchyma in a highly irregular fashion[66-68].

It is now recognised that in many scenarios of chronic liver disease the ductular reaction is, at least in part, mediated by the activation of liver stem cells. Ductular cells within the ductular reaction can express a wide heterogeneous array of markers covering both biliary and hepatocytic lineages including CK19, CK7, EpCAM, HepPar1 and NCAM[10, 69-71]. The field has progressed sufficiently in the last couple of years such that subpopulations of ductular reactive cells can be identified by their expression of specific markers. NCAM is currently regarded as the most important marker in identifying bipotential stem/progenitor cells in ductular reactive processes[72] however recent evidence suggests $NCAM^{+}$ cells are more likely to be in senescence that other ductular reactive cells in chronic disease which may indicate exhaustion of these cells or that a different subpopulation are responsible for much of the proliferation and reconstitution of mature liver populations[73]. Expression of CK19 indicates a more differentiated progenitor cell phenotype primed towards the biliary lineage, whilst progenitor cells primed towards the hepatocytic lose expression of both CK19 and NCAM but may retain EpCAM[74]. Subsequent work in murine models has supported this early hypothesis describing liver stem and progenitor cell phenotypes and have again emphasised the importance of sox9 as a marker of more primitive liver stem cells[75, 76].

One of the most commonly misinterpreted observations in two-dimensional liver sections, specifically when using markers of liver progenitor cells, is the presence of “isolated cholangiocytes” or liver progenitor cells in peri-portal regions. Often the identification of liver progenitor cells in this scenario is erroneous and more likely cross-sections of the Canals of Hering resulting in the observation of single, or small strands, of positively stained cells[10]. Distinguishing between cholangiocytes and liver progenitor cells in this scenario is extremely

challenging using single markers by immunohistochemistry due to shared morphology[77], expression of markers[78], and the demonstration that ductules can extend through the lobule[79, 80].

1.5.3. Histological phenomena related to activation of the hepatic stem cell niche. **A**ctivation of the hepatic stem cell niche is observed in all chronic liver diseases[7, 81]. Histologically, activation is characterised by remodeling of peri-portal regions, in tight association with fibrogenesis, and the proliferation, differentiation and migration of hepatic stem cells into adjacent intra-lobular parenchyma[7, 27].

Intermediate hepatobiliary cells

Intermediate hepatobiliary cells (IHCs) are defined as cells with hepatocytic morphology, located in intra-lobular regions and expressing characteristically biliary markers, most notably CK7 and, to a lesser extent, CK19[82]. The origin of these cells remains controversial. IHCs may represent a population of hepatoblasts; cells that are derived from hepatic stem cells but have not fully differentiated into mature hepatocytes and retain expression of biliary and/or hepatic stem cell markers[72]. However, as these cells are often observed some distance from periportal regions, the accepted location of the hepatic stem cell niche, how these cells migrate from periportal regions to intralobular regions without obvious adjacent parental/ ancestral cells remains to be elucidated. It is possible that these cells represent mature hepatocytes that have re-expressed biliary markers in response to injury-mediated signals[10].

Hepatocytes newly derived from hepatic stem/progenitor cells

One of the most important markers of human hepatic stem cells in both the adult and foetal liver is epithelial cell adhesion molecule (EpCAM), with the use of EpCAM antibodies and immunoselection techniques forming the basis of the most commonly used current techniques for the isolation of hepatic stem cells. EpCAM is a homophilic type I transmembrane glycoprotein[83] reported to be normally expressed in; almost all epithelial tissues[84]; the mammalian germ line[85]; normal adult stem and progenitor cells[86], including liver stem cells[2] and progenitor cells[87]; and cancer-initiating cells[88]. This has led to great interest in EpCAM as a marker of cancer-initiating cells and as a prognostic tool since EpCAM-positive tumours have been shown to be more aggressive and tumourigenic *in vitro*[88, 89]. EpCAM is exclusively expressed by cells of the biliary epithelium in normal liver. However, EpCAM has recently been described as marking hepatocytes that have newly been derived from proliferating hepatic stem cells[74]. $EpCAM^+$ hepatocytes are found in peri-portal and peri-septal regions of diseased liver and display a distinctive membranous pattern of EpCAM expression in contrast with the cytoplasmic distribution observed within biliary cells.

1.5.4. Histological techniques for the identification of hepatic stem cells. Sox9 has been shown to mark somatic stem cell populations in organs derived from the primitive endoderm of the foregut, namely the intestine, pancreas, biliary tree and liver[90]. Cell fate tracing experiments have elegantly shown that, over time, the progeny of $Sox9^+$ cells reconstitute the entire epithelial lining of the intestine, biliary tree and parenchymal cells of the liver indicating the presence of adult stem cells within the $Sox9^+$ population in these organs. In

liver, injury stimulates increased proliferation and accumulation of progeny of $Sox9^+$ cells that include mature hepatocytes and biliary epithelial cells[9].

The objective quantification of immunohistochemical (IHC) staining of liver specimens is an ongoing challenge in pathology. Many liver-related histological phenomena, including fibrosis, steatosis and inflammation[44], are currently quantified using semi-quantitative scoring systems which rely upon the expertise of experienced pathologists. Scoring systems for the quantification of NAFLD were originally designed to allow the standardisation of histological endpoints in clinical trials but are now frequently used in basic research, including assessment of animal models, despite being prone to large inter-rater variability and low reducibility[91]. As such, the development of an objective, computer-assisted method to quantify and analyse immunohistochemical staining would remove user bias and issues associated with inter-rater variability improving on currently used scoring systems. Many reports have demonstrated the use of image analysis in quantifying hepatic fibrosis by calculating collagen percentage area (CPA)[92] and steatosis by quantification of oil red O staining[93]. However, standardised techniques for the quantification of histological phenomena and cell populations involved in hepatic stem cell mediated liver regeneration remain lacking. Previous studies have defined criteria for the presence or absence of $CK19^+$ or $CK7^+$ intermediate hepatobiliary cells[94], total quantification of hepatic progenitor cell numbers per portal tract[95] and quantification of total area covered by biliary and ductular epithelium by CK7 immunohistochemistry[96].

Although each of the markers described above identify hepatic stem/progenitor cells, none of them do so specifically. CK19, CK7 and EpCAM are observed on all cells of the biliary

epithelium. There are conflicting reports of the proportion of biliary cells that express Sox9 under normal conditions, ranging from a small proportion to all cells. In injured liver, Sox9 is also upregulated by activated stellate cells undergoing transdifferentiation to myofibroblasts. Currently no markers have been described that exclusively mark adult hepatic stem cells, although markers that define an increasingly restricted population continue to be regularly reported, the most recent including Foxl1[76, 97], CD133[98], Lgr5 and CD24[99]. As such, the use of a combination of different markers is required to identify hepatic stem cells. Further, as these cells give rise to multiple lineages in response to injury, whose antigenic profiles vary during the process of proliferation, lineage restriction and differentiation, assessing and quantifying hepatic stem cells in during liver injury and regeneration remains challenging.

1.5.5. Hepatic stem cell activation in chronic liver disease. The activation and differentiation of hepatic stem cells is observed in a wide range of acute and chronic liver disease aetiologies[100, 101]. The presence of ductular reactive cells, or cells with intermediate or combined phenotypes, is observed in all common chronic aetiologies, including viral, biliary, alcohol-induced, autoimmune and fatty liver diseases. In biliary disease, hepatic stem cells are restricted to a biliary fate and contribute to regeneration of the biliary epithelium with few, if any, hepatocytes thought to be derived from activated hepatic stem cells. Ductular reactions are often prominent in primary biliary diseases, with increasing evidence suggesting these structures are at least partly derived from hepatic stem/progenitor cells. Consequently, in these diseases the proportion of cells with a predominantly biliary phenotype, ie. Sox9, CK19, CK7, is greatly increased in peri-portal areas with hepatic stem/progenitor cells contributing to the expansion of biliary and ductular structures[9].

In chronic metabolic, or hepatocytic, liver disease hepatic stem cells can be seen proliferating from biliary epithelium and peri-portal regions into adjacent parenchymal areas and contribute to regeneration of lost hepatocyte numbers and function. Ductular reactive structures with predominantly biliary (also stromal[78] but rarely hepatocytic) phenotypes are also commonly seen in these aetiologies, potentially representing intermediate, or transitional, cells, or cells that are proliferating and/or differentiating in an abnormal manner in response to inappropriate patterning. Hepatic stem cells differentiating towards mature hepatocytes progress through a maturational lineage, commonly described as hepatic stem/progenitor cell, hepatoblast, immature/small hepatocyte and functional mature hepatocytes[2]. Whether 'intermediate hepatobiliary cells'[94] belong within this lineage remains controversial but would most likely constitute immature/small hepatocytes.

1.6. HEPATIC STEM CELLS

1.6.1. Historical overview of the identification and characterisation of hepatic stem cells.

The liver has long been known to possess substantial regenerative capacity. In 1902, McCallum was first to provide a clinical description of the regenerative process in a John Hopkins Hospital Report where "regenerative changes are represented by an ingrowth of sprout from the interlobular bile ducts toward the central veins" resulting from acute yellow atrophy[102]. Higgins and Andersen reported the first experimental model of liver regeneration in 1932 using partial hepatectomy (PHx) in rats[103]. During the same year azo dyes were shown to reliably induce hepatocellular tumour formation in rats[104] leading to the liver being adopted as the model organ for the study of the effects of carcinogens[105-108]. Among the

myriad of changes observed in response to these toxic agents, there is invariably an increased proliferation of biliary ductules with an accompanying accumulation of cells in periportal regions with distinctive oval-shaped nuclei that commonly abut biliary ductules. In early reports these cells were commonly referred to as ‘oval’ cells and were distinguished by their distinctive histological characteristics; small (relative to mature hepatocytes); high nuclear to cytoplasmic ratio; basophilic; oval-shaped nuclei; peri-portal location[109]. At this time there was much controversy regarding the fate of ‘oval’ cells. One hypothesis stated oval cells could be transformed into hepatocytes whilst the counter argument suggested oval cells underwent cell death upon removal of the precipitating insult. Most studies into the 1970’s reported similar findings, ie. circumstantial evidence for oval cells being derived from proliferating ductules and potentially giving rise to hepatocytes and/or hepatomas[110, 111].

Alpha-foetoprotein (AFP) is largely absent in adult liver, but is ubiquitous in the foetal liver and highly over-expressed in the majority of HCC lesions, allowing its use clinically as a serum biomarker for HCC. However, AFP levels in adult liver are significantly elevated from negligible levels in response to partial hepatectomy[112]. In response to this observation, the source of AFP production in this scenario was widely debated, with hypotheses including; retro/dedifferentiating hepatocytes to allow proliferation; transformed hepatocytes, or a separate cell type, ie oval cells. Ultimately it was conclusively demonstrated that oval cells were the sole source of AFP in regenerating adult liver; a critical step in the definition of oval cells as a distinct cellular entity in adult liver.

The first crucial demonstration of a distinct stem or progenitor cell within the liver was the pharmacological blockade of hepatocyte proliferation (usually with retrorsine or 2-AAF) in

rodent models. Under these conditions, liver regeneration occurs but is mediated by the rapid proliferation of a distinct population of cells located within the Canals of Hering[10], then termed ‘oval cells’ due to their distinct morphology, capable of differentiating into mature hepatocytes[113]. Oval cells were characterised as being smaller than the surrounding mature cholangiocytes and hepatocytes, have a high nucleus/cytoplasm ratio, distinctive ovoid nucleus. Oval cells proliferate rapidly in response to liver injury with or without inhibition of hepatocyte proliferation, although their proliferation is more muted when hepatocytes retain some proliferative and functional capacity. It is currently unclear to what extent the activation and proliferation of hepatic stem cells contributes to the restoration of lost mature cell types in chronic liver disease, although it is entirely feasible that liver stem cells convey the liver with its ability to remain in a ‘compensated’ state of cirrhosis for years despite severe ongoing injury.

1.6.2. Currently unresolved aspects of hepatic stem cell biology and function. The study of hepatic stem cells, from the first description over 100 years ago to the present day, has been controversial due to a number of apparent contradictions in reported observations and/or hypotheses. Our understanding of hepatic stem cells remains incomplete and many contentious issues remain.

Firstly, the question of whether adult hepatic stem cells fully meet the criteria for true somatic stem cells remains inconclusively addressed. The liver has an extraordinary capacity for regeneration in response to injury and yet the contribution of hepatic stem cells to this process is largely unknown and perhaps negligible in many scenarios where damage is limited or transient due to the significant regenerative capacity of mature hepatocytes. In many tissues

where cell turnover is high (ie. skin, gut) all epithelial cells are apparently derived from somatic stem cells, however it is unclear whether this is the case for liver. Our current benightedness permits the potential role of hepatic stem cells to range from a self-contained reservoir, necessary only in cases of severe injury, through to the source of all mature hepatic parenchymal cell types.

Further, the location and source of hepatic stem cells are in the process of being redefined whilst the mechanisms underlying the maintenance and activation of the hepatic stem cell niche are are in the early stages of being fully elucidated. Early work described a small distinct niche for hepatic stem cells within the most proximal branches of the biliary tree; the Canals of Hering. However recent studies have contributed compelling evidence for the presence of multipotent stem cells throughout the entire biliary tree, perhaps in all biliary epithelia. Whilst chemokines and mitogens known to activate hepatic stem cells have been identified along with many of the major signaling cascades, the precise mechanisms and complex interactions between hepatic stem cells and their environment, including other closely associated cells types, are poorly described. Specifically, how appropriate; patterning to biliary or hepatocytic fate; maintenance in quiescent or activated states; and niche remodeling and recovery after injury, are mediated remains to be elucidated.

The clinical implications of hepatic stem cell activation potentially represents a double edged sword. Greatly increased numbers of hepatic stem cells are seen to accumulate in all chronic liver disease aetiologies and presumably contribute positively to regeneration. Yet, hepatic stem cells are closely associated with the ductular reaction and fibrogenesis, processes considered to adversely effect outcomes and increased numbers of hepatic stem cells and the duration of their activation may be associated with an increased risk of hepatocellular and

cholangiocarcinoma. Thus, the consequences of increasing hepatic stem cell numbers, either through stimulating increased proliferation of the native stem cell niche or by the administration of non-autologous hepatic stem cells, are as yet unknown. Further, there is growing evidence suggestive of a direct link between hepatic stem cells numbers and risk of primary liver carcinogenesis and in some cases hepatic stem cells may be the cell of origin.

Hepatic stem cells also hold great promise as a cellular therapy for liver disease yet many technological hurdles and unknowns regarding the true potential of adult hepatic stem cells remain. Studies of freshly isolated cells *in vitro* have demonstrated extensive long-term undifferentiated proliferation yet the differentiation of cultured hepatic stem cells to fully functional daughter cells, particularly hepatocytes, has yet to be demonstrated to an extent comparable to mature cells *in vivo*.

However, despite recent advances in the prospective isolation and fate-tracking of hepatic stem cells, our understanding of the contribution of hepatic stem cells to the development and progression of disease remains limited whilst many technical challenges remain in the development of hepatic stem cell-based cellular therapies.

1.6.3. Evidence for hepatic stem cells as true somatic stem cells. The two defining characteristics of a stem cell are *potency*; the capacity to give rise to multiple different mature cell types, and *continuous self-renewal*; the ability to generate daughter cells without loss of potency or proliferation potential[114].

Thus the term ‘adult hepatic stem cell’ should specifically refer to a cell that is:

1. found in adult
2. located in the liver
3. multipotent, able to give rise to all hepatic cell types of at least one lineage, through tissue homeostasis or regeneration in response to injury, ie. hepatocytes and cholangiocytes for epithelial cells, stellate and endothelial cells for mesodermal cells types or all parenchymal types for a multipotent stem cell (for liver this would require hepatocyte and cholangiocyte differentiation for an endodermal cell type)
4. self-renewing with considerable proliferative capacity. Experimentally, the ability to repopulate numerous livers by serial transplantation using a suitable recipient model, ie. FRG mice

Studies that have provided evidence contributing to the confirmation of adult hepatic stem cells are summarised below (**Table 1**).

Table 1.1. Studies contributing to the evidence required for the definition of an adult hepatic stem cell.

Requirement	Demonstration	Reference
Location; adult, liver	Canals of Hering	1, 9, 10, 79, 115
	Biliary tree	9, 12
Self-renewal	Serial transplantation	196, 197
Proliferative capacity	Long-term undifferentiated *in vitro* growth	11, 12, 75, 76
	Fate tracing	9, 97, 115
Multipotency	Hepatocyte and cholangiocyte differentiation	1, 13, 75, 115

To fully define hepatic stem cells by these criteria involves the use of several complimentary approaches. Firstly, the antigenic profile of a candidate cell must be fully defined to allow robust identification of a homogeneous population. A major limitation of the hepatic stem cell field has been the lack of a single, specific marker of hepatic stem cells which has subsequently precluded the use of cre-lox lineage tracing models to definitively trace the progeny of hepatic stem cells. However, the use of inducible cre-lox models has furthered our understanding of the location, expansion and contribution of hepatic stem cells to the generation of other cell types. Currently Sox9[9, 75], Foxl1[76] and Lgr5[115] mark the most restricted population of cells encompassing hepatic stem cells, but each also captures a more differentiated population of biliary epithelial cells (**Table 1.2**).

Interestingly, none of the 3 inducible models detect tracing events in the developing liver other than Sox9 at E16.5. In adult liver, Sox9 marks all cells of the biliary epithelium and tracing labels all hepatocytes over a period of 12 months suggesting continuous supply of mature hepatocytes from $Sox9^{+}$ cells even in the absence of hepatic injury. A smaller proportion of biliary epithelial cells are marked by Foxl1 but there is no evidence of tracing events in hepatocytes. No tracing events are observed using Lgr5 in adult liver. These studies in uninjured adult liver demonstrate the variability of results produced by models targeting hepatic stem cells, most likely as a result of marking cells at different stages of the maturational lineage with Lgr5 presumably marking the most primitive cells, followed by Foxl1 and Sox9 the most mature populations that possibly include cells restricted to a biliary fate.

A multitude of injury models can be utilised to stimulate proliferation of hepatic stem cells. Hepatic stem cells are activated in commonly used models of hepatocellular injury (DDC, APAP, MCD - with further stimulation possible with the inclusion of ethionine; MCDE), biliary injury (BDL), fibrosis (CCl_4) and liver regeneration (PHx, the use of retrosine, an inhibitor of hepatocytes proliferation, results in entirely stem-cell mediated regeneration).

The results of hepatic stem cell fate tracing experiments in liver injury models are varied between strains (summarised in **Table 1.2**). Whilst Lgr5, Sox9 and Foxl1 marked cells generate mature hepatocytes and biliary epithelial cells in response to injury, the results from specific injury models can vary considerably between strains. Using MCDE, the most commonly used model for the generation of a robust hepatic stem cell response, $Lgr5^+$ cells generate small clusters of mature hepatocytes, $Sox9^+$ cells generate substantial numbers of peri-portal hepatocytes, whilst no mature hepatocytes appear to be derived for $Foxl1^+$ cells. Taken together, the results from these studies conclusively demonstrate the generation of mature hepatocytes and biliary epithelial cells from rare populations of peri-portal cells with expression of stem cell related markers, yet each marker, Lgr5, Sox9, and Fox1, appears to label populations that yield differing progeny in response to injury.

Table 1.2. Summary of observations from lineage tracing experiments designed to target hepatic stem cells

Condition	Strain		
	Lgr5	***Sox9***	***Foxl1-cre***
Foetal	No studies	Extra-hepatic bile ducts but not liver at E13.5. Observed in intrahepatic bile ducts at E16.5	Not observed in hepatic bud at E12.5.
Adult	Virtually undetectable. No tracing events	99.4% of traced cells found in biliary epithelium after 1 day. Numbers of labelled hepatocytes increased over time. All of parenchyma labelled 12 months after induction	0.1% of total cells, 10% of CK19
DDC	Small clusters of hepatocytes and a small proportion of biliary epithelial cells 9 days after induction	Biliary epithelium with minimal contribution to hepatocytes 21 days after induction	Up to 1% of total cells, >30% of CK19 predominantly hepatocytes 21 days after induction
MCDE	Small clusters of hepatocytes and a small proportion of biliary epithelial cells observed 9 days after induction	Biliary epithelium with substantial numbers of peri-portal hepatocytes labelled 3 weeks after induction. Not all AFP^+ cells	Subpopulation of CK19 biliary epithelial cells. No traced hepatocytes observed 35 days after induction
CCl	Observation of small proliferative cells 2 days after induction that evolved into fully mature hepatocytes from 2 days onwards	Biliary epithelium with substantial numbers of peri-portal hepatocytes labelled 4 days after induction	No studies
BDL	No studies	Biliary epithelium with substantial numbers of peri-portal hepatocytes labelled 10 days after induction	Up to 0.3% of total cells, >30% of CK19 predominantly biliary up to day 7, then hepatocytes by day 14
APAP	No studies	Biliary epithelium with minimal contribution to hepatocytes 21 days after induction	No studies
PHx	?No studies	Biliary epithelium with minimal contribution to hepatocytes 21 days after induction	?No studies

DDC, 3,5-diethoxycarbonyl-1,4-dihydrocollidine; MCDE, methionine choline deficient diet supplemented with ethionine; BDL, bile duct ligation; APAP, acetaminophen; PHx, 70% partial hepatectomy; CK19, cytokeratin 19; AFP, alpha-foetoprotein

1.6.4. The maturational lineages of hepatic stem cells. Foetal and adult hepatic stem cells have now been extensively described both in vitro and in vivo[1, 2, 69]. In foetal liver hepatic stem cells derive from the primitive endoderm and go on to form functional cholangiocytes and hepatocytes as the liver develops. In adult liver the presence of adult hepatic stem cells in small numbers at the finer branches of the biliary tree, the Canals of Hering, in peri-portal regions of the hepatic lobule has been well described for many years. More recent work has described the presence of multipotent biliary tree/hepatic stem cells throughout the biliary tree from the sphincter of Oddi, at the most proximal point, through all regions of the biliary tree through to the Canals of Hering[12]. However it has not been conclusively shown that these cells represent a single, connected population where cells migrate through the biliary tree toward the liver undergoing progressive maturation and patterning. It is possible that at different points of the biliary tree, multipotent stem cells observed that are distinct populations with roles specific to their location, whereby hepatic stem cells of the Canals of Hering are solely responsible for stem-cell mediated liver regeneration in response to chronic hepatocytic liver disease. As such the contribution of biliary tree stem cells to liver regeneration, and specifically reconstitution of hepatocytes, is currently unknown and so were not studied.

In adult liver the intra-lobular hepatic stem cells are located within the Canals of Hering, the most proximal branches of the biliary tree found in portal regions abutting the hepatic plate[10]. There is increasing evidence for the presence of small proportions of hepatic stem cells in all

biliary epithelia but most studies focussed on hepatic injury and stem-cell mediated regeneration have focussed on cells of the Canals of Hering[71, 79, 116]. The location of these cells, between mature cholangiocytes and mature hepatocytes, suggests that these may be the only hepatic/biliary stem cells that contribute to hepatocytic regeneration.

The peribiliary glands of the extrahepatic bile duct are thought to harbour potent tri-potential (hepatocyte, cholangiocyte, pancreatic beta cell) stem cells. Detailed anatomical studies have demonstrated cells expressing the most primitive markers[11] are located in the crypts of the peribiliary glands with more distal cells expressing proportionately less. Further studies have demonstrated the growth and differentiation potential of these cells both *in vitro* and *in vivo*[11-13] posing the hypothesis that potent stem/progenitor cells may be found throughout the intra and extrahepatic biliary tree.

1.6.5. Techniques for the isolation of hepatic stem cells. The robust isolation of a pure, well-defined, homogeneous population of adult hepatic stem cells is an ongoing challenge. Varying methods have been utilised to isolate, maintain in long-term culture and fully differentiate hepatic stem cells, particularly in attempts to address the technological hurdle of producing functional hepatocytes. The isolation of hepatic stem cells is now routine from foetal and adult liver of human and mouse (**Table 1.3**) using FACS or immunoselection. Challenges still remain in defining conditions allowing the long-term undifferentiated culture, expansion and directed terminal differentiation of pure populations. To date, the demonstration of terminally differentiated functional hepatocytes and cholangiocytes from hepatic stem cells with comparable function to mature cells has not been demonstrated.

Where with production of proteins associated with mature hepatocyte function levels and function are often orders of magnitude less than mature hepatocytes.

Prospective isolation by FACS is currently the gold standard for defining and selecting populations based on antigenic profile. However, the isolation of homogeneous populations of hepatic stem/progenitor cells is currently hampered by the lack of single, or combinations of, markers specific for cells early in the maturational lineage. Further, it is possible that cell-cell interaction, either between hepatic stem cells or with companion cells, are necessary for the growth and maintenance of phenotype that is necessarily lost in producing single cell suspensions. Many approaches for the isolation of epithelial stem cells take the approach of isolating the entire niche rather than single cell types[115]. Many commonly used surface markers are also expressed by mature biliary epithelial cells, whilst more specific markers (Sox9, Lgr5) are not expressed on the cell surface precluding their use for prospective isolation of live populations by FACS. Consequently alternative methods that isolate less pure populations have been used in combination with hormonally defined media and growth conditions that specifically select for immature hepatic stem cell/progenitor populations.

Table 1.3. Summary of methods for isolating hepatic stem cells from adult human and mouse liver.

	Isolation Method		
	Magnetic immunoselection	***Fluorescence activated cell sorting (FACS) by antigen***	***FACS by enzymatic activity***
Group	Reid, LM	Grompe, M	van Grunsven, LA
Species	Human	Mouse	Human and Mouse
Antigen	Epithelial cell adhesion molecule (EpCAM)	Lgr5, Sox9	Aldehyde dehydrogenase
Marker expression	CK7, CK19,	Sox9, Cd44, Prom1, CK7, CK19	EpCAM, CK7, CK19, Sox9
Growth conditions	Adherent; plastic; Modified Kubota's medium	Matrigel embedded; AdDMEM/F12, B27, N2, NAC, gastrin, EGF, Rspo1, Fgf10, nicotinamide; noggin and Wnt3a for first 4 days.	Adherent; Collagen type I; DMEM+10% FCS
Growth duration	Long	>8 months (P30)	Short (not passaged, 23 days)
Proliferation	Rapid	Rapid (estimated doubling time = 3 days)	Rapid (estimated doubling time = 2 days)
Hepatocyte differentiation	Y	Matrigel embedded; AdDMEM/F12, B27, N2, NAC, gastrin, Fgf10, EGF, A8301, DAPT.	For mouse: DMEM/F12, ITS, HGF, EGF for 6 days; William's E, HGF, OSM, dex for 6 days.
Cholangiocyte differentiation	Y	N, but undifferentiated cultures have biliary phenotype	N
In vivo engraftment	Y	Y; increased survival in FAH mice; 500-800k cells, intra-splenic injection	N

1.6.6. The hepatic stem cell niche and factors necessary for the long-term culture and maintenance of undifferentiated hepatic stem cells. Maintaining phenotype and differentiation potential is critical for the study or therapeutic use of hepatic stem cells cultured long-term. Culture conditions must provide appropriate signals that both maintain the undifferentiated growth and prevent inappropriate differentiation/restriction of hepatic stem cells that also allow for controlled experimentation or expansion. More recent techniques, that include embedding in gels/matrices, organoid culture and organ specific stroma/feeder layers, have improved on conventional 2D approaches on plastic or collagen by more accurately recreating the conditions of the quiescent hepatic stem cell niche.

The local extracellular matrix is known to play critical roles in patterning the proliferation and restriction of hepatic stem cells. Laminin has been shown to be specifically expressed in regions adjacent hepatic stem cells and is required for appropriate expansion and differentiation of stem cells in response to injury. Much work has been conducting in elucidating the presence and role of several types of collagen in the hepatic stem cell niche. Culture on collagen type I, predominantly found in scar tissue, has been shown to increase the proliferation of hepatic stem cells and induce rapid differentiation to hepatoblasts. Culture on collagen III and IV, more commonly located in peri-portal regions, appear to maintain the phenotype of hepatic stem cells and slow proliferation. Co-culture with hepatic stromal populations has demonstrated the ability of stromal layers to maintain undifferentiated hepatic

stem cells long-term, whilst culture on activated myofibroblasts/ stellate cells results in rapid proliferation and differentiation similar to that seen with culture on collagen type I. Many studies have repeatedly demonstrated the close spatial association between hepatic stem cells and stromal populations, particularly during niche remodeling in response to injury, indicating important functions of stroma in regulating and patterning the growth and expansion of hepatic stem cells. Stroma are also thought to play key roles in ECM remodeling and chemokine/cytokine production thereby altering the niche and allowing expansion of hepatic stem cell populations towards parenchyma and ensuring appropriate differentiation to hepatocyte or cholangiocyte lineages dependent on type of injury.

Harry Kubota conducted many detailed experiments defining the most minimal media components necessary for the survival and growth of hepatic stem cells. These experiments demonstrated the selection and growth of hepatic stem cells in serum-free media containing essential ions/minerals and only insulin and hydrocortisone as growth factors[1]. Usefully, this media precludes the survival of mature epithelial cells and slows, or even prevents, proliferation of stromal cells except when in close association with hepatic stem cell colonies. The nature of the selection method used, immunoselection without the need for strict single cell suspensions, may allow for the isolation of clumps of cells that are presumably mixed with respect to maturation status and potentially including associated stromal/companion cells that may contribute to the survival and patterning of hepatic stem cell colonies cultured in this method. Indeed cells with distinct stromal morphology and antigenic profiles are commonly observed at the peripheries (also infiltrating bands in the case of larger colonies) of hepatic stem cell colonies. There is growing literature not only describing detailed cross talk between

epithelial and mesenchymal populations within stem cell niches but also of the supportive role stroma plays in providing nutrients and factors required for the quiescent maintenance and rapid expansion of stem cell niches. In particular to liver, it is thought that during liver regeneration adjacent stromal cells[17] access energy (lipid) stores to produce and secrete lactate then utilised by rapidly proliferating hepatic stem cells essentially fuelling the rapid hepatic stem cell-mediated regeneration of the liver observed in response to acute injury[117]. This process may be occurring in cultured hepatic stem cell colonised isolated in this manner, with stromal cells allowing the survival of hepatic stem/progenitor populations in such minimal media by maintaining their undifferentiated state through secretion of patterning factors whilst also producing nutritional molecules hepatic stem cells, with limited metabolic machinery, are unable to produce.

Our understanding of the milieu soluble and bound factors in normal and injured liver is far from complete. Many of the soluble factors increased in response to acute and chronic liver injury that stimulate activation of the hepatic stem cell niche have been described (TNFa, IL6, TWEAK etc.) and the producing cell type, mechanism of action and functional effects are also well characterised in many cases[19, 26]. Yet, factors critical for hepatic stem cell function continue to be identified and our understanding of the complex interaction between each of these signals remain limited. In addition, there is an increasing appreciation of the importance of conformational state and availability of growth factors on signaling outcomes, further complicated by the discovery that growth factors can convey differing, and even opposing, signals when bound to ECM molecules or in free solution[29, 118]. This is particularly pertinent in the case of liver regeneration where substantial ECM remodeling occurs in peri-portal

regions surrounding the hepatic stem cell niche, potentially leading to the release of growth factors or modulation of signaling outcomes as a result of altered ECM conformation or composition.

Gradients of signaling molecules are commonly observed in development and allow information regarding relative spatial positioning to be received by a substantial numbers of cells over considerable distances[119]. Similar mechanisms are thought to contribute to patterning of hepatic stem cell identity and maturation in both developing and adult liver, with particular functional importance in regeneration and hepatic stem cell activation. Firstly, oxygen concentrations decrease from their highest levels in peri-portal regions, where hepatic stem cells reside, as oxygenated blood enters the hepatic plates, perfuses the hepatic lobules and drains into the hepatic vein where oxygen concentrations are lowest. Consequently a gradient of oxygen concentration exists across the liver lobule from the portal triad to the central vein. This is the same axis through which hepatic stem cells migrate and differentiate into mature hepatocytes. More work is required in assessing the importance of this signaling gradient in the patterning hepatic stem cells, but is of note that the hepatic stem cells is highly vascularised and oxygenated, in contrast to many other stem cell niches. This may be a necessity due to the need for rapid increases in metabolic output of hepatic stem cells and progeny during differentiation in mature hepatocytes.

1.6.7. Hepatic stem cell niche remodeling and fibrogenesis. The extra-cellular matrix of the hepatic stem cell niche is closely associated with the basement membrane, principally composed of fibronectin, laminin[7, 19], collagen type III[27], hyaluronan[120], chondroitin sulphates[121] and minimally sulphated proteoglycans[122, 123]. The remodeling and expansion of

laminin has been shown to be particularly important for the activation of hepatic stem cells. Laminin is exclusively expressed in the hepatic stem cell niche in normal liver. In response to injury, hepatic stem cells contribute to increased laminin secretion during activation and laminin is observed in peri-portal parenchyma areas in close association with ductular reactive cells and proliferating stem/progenitor cells. Studies have shown the remodeling and secretion of laminin is required for effective activation and maturation of hepatic stem cells[19, 124]. Other structural proteins, particularly collagens and proteoglycans, have been shown to play important roles in the regulation and patterning of hepatic stem cells and are thought to convey lineage specific cues through compositional differences between ductal and hepatic plates. Appropriate remodeling of ECM is thought to be critical for the effective expansion and differentiation of hepatic stem cells in response to injury[118]. Histologically, ECM remodeling can be observed as increased deposition of ECM components, increased numbers of fibroblasts and hepatic stem/progenitors and architectural changes in peri-portal regions (**Fig 1.3**.[125]). In chronic injury, these processes are tightly associated with fibrogenesis, with scarred regions composed of myofibroblasts, hepatic progenitors, inflammatory and endothelial cells, observed forming bridges between peri-portal regions and eventually encapsulating regenerative nodules.

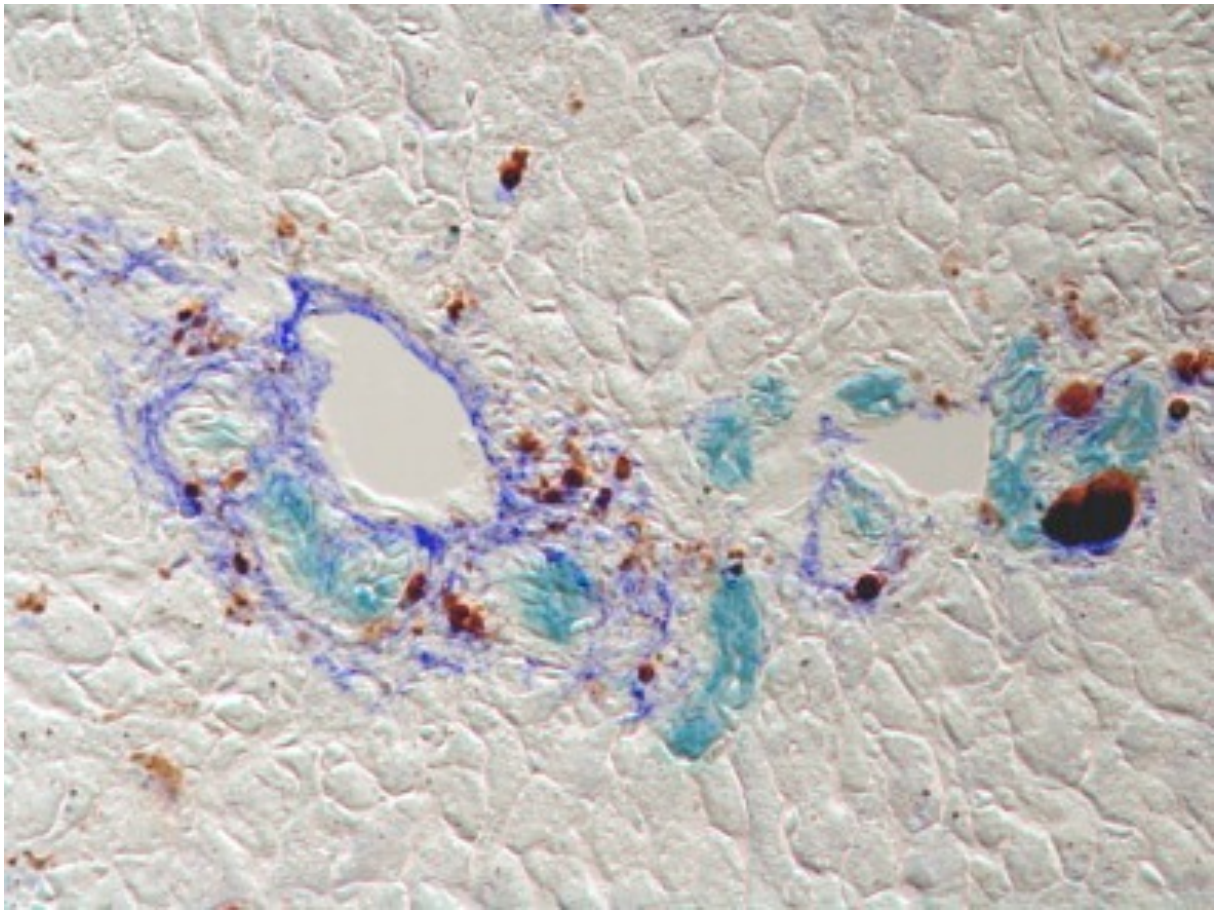

Figure 1.3. Hepatic stem cell niche remodeling in response to chronic liver disease. Lineage traced Foxl1^{+} hepatic progenitors (aqua blue) encapsulated by elastin^{+} portal fibroblasts (dark blue) are seen expanding from peri-portal regions into the surrounding parenchyma in response to DDC-induced liver injury. Brown precipitates are breakdown products of DDC. Image replicated from review[125]

1.7. LIVER REGENERATION

The suggestion of the liver's extraordinary ability to regenerate at least dates back to the ancient Greek myth of Prometheus, whilst it was Higgins and Anderson who were the first to scientifically demonstrate this phenomenon using partial hepatectomy in rats[103]. Their study involved the surgical removal of a significant proportion of the rat's liver and observation of its regeneration. Higgins and Anderson noted that after removal of as much as two-thirds of the liver the entire mass could be reconstituted in as little as a week, a remarkable regenerative capability not observed in other viscera. It is now understood that this regeneration is mediated entirely by the mature cell types of the adult liver, namely hepatocytes and cholangiocytes[14]. This is notable as other constantly regenerating organs such as the skin and gut[126, 127] are replaced by the proliferation and differentiation of stem cell populations. Upon two-thirds partial hepatectomy, an estimated minimum of 95% of mature hepatocytes rapidly enter mitosis followed by a smaller proportion of hepatocytes undergoing a second round of division to fully reconstitute original liver mass and function. This process was first demonstrated using continual administration of tritiated thymidine (a means of labelling cells that have undergone DNA replication and thus proliferation) after PHx. This resulted in the labelling of 99% of hepatocytes, significantly more than the 2/3 that would be expected if the hepatocytes of the remnant liver had not proliferated, as would be the case if liver regeneration was performed but an alternate, distinct population of stem cells[128]. A subsequent study by the same lab highlighted the enormous regenerative capacity of mature hepatocytes by demonstrating complete regeneration of the liver after up to 12 sequential hepatectomies in the same animal[129]. Further work has shown that hepatocytes transplanted into models of liver failure can rescue liver failure and repopulate the liver completely[130] and

serial transplantation, isolation and re-transplantation of labelled of hepatocytes can fully regenerate consecutive livers up to 10 times[131]. How the proliferation of hepatocytes is controlled in such a way that the original liver mass is restored almost exactly to its original size is unknown, but clearly feedback mechanisms are present ensuring sufficient regeneration whilst preventing excessive or uncontrolled growth.

1.8. LIVER CANCER

The majority of tumours found in the liver are metastases from distant sites, however primary liver cancers are increasingly prevalent with a poor prognoses. Hepatocellular carcinoma (HCC) is the most common primary adult liver cancer and is characterised by tumours with predominantly hepatocellular features[46, 132]. The major risk factors for HCC are chronic liver injury, viral infection or alcoholism, and cirrhosis, all increasing in Western populations. HCC surveillance is recommended for all patients with cirrhosis, usually involving bi-annual ultrasound screening and measurement of circulating α-fetoprotein (AFP) levels. As early diagnosis of HCC significantly improves outcome, identifying patients with end-stage liver disease at particularly high risk of developing HCC could allow the use of more frequent, targeted and accurate surveillance methods, notably MRI. however current strategies are problematic with not all patients being screened routinely and modest decreases in mortality observed in those that are[133]. Consequently, there is a need for more accurate tests for the prediction of risk of liver cancer development with preliminary studies indicting potential utility of biopsy material through assessment of hepatic stem cell activation.

Cholangiocarcinoma (CCC), the second most common primary adult liver cancer, is characterised by tumour cells with biliary characteristics as opposed to the hepatocellular features seen for HCC. However, it is increasingly recognised that a spectrum exists between HCC and CCC, and combined HCC-CCC (mixed carcinoma) has been well described. With increasing understanding of the characteristics of hepatic stem cells and their activation in chronic liver diseases and cirrhosis, it has been hypothesised that mixed carcinomas may be derived from primitive, bi-potential hepatic stem/progenitor cells. Further, there is substantial experimental evidence of a direct causal contribution of hepatic stem cells to the development of both HCC and CCC, although this association has proved difficult to test clinically[88, 89, 94, 134].

CHAPTER 2

MATERIALS AND METHODS

2.1. HUMAN TISSUE SAMPLES

2.1.1. Formalin-fixed paraffin-embedded (FFPE) explanted tissue and liver biopsies

FFPE explanted tissue blocks were obtained from the Centre for Liver Research (CLR) tissue collection. FFPE blocks were obtained from the archives of the Department of Pathology (Queen Elizabeth Hospital, Birmingham, UK).

2.1.2. Fresh explanted liver tissue

Human liver explants were obtained from consenting patients undergoing liver transplantation or resection at the Queen Elizabeth Hospital, Birmingham. Livers were evaluated and prepared by Dr. Gary Reynolds. For hepatic stem cell isolation a slice of tissue was cut and placed in cold Dulbecco's Modified Eagle Medium (DMEM) prior to use.

2.1.3. Fresh common bile duct tissue from Whipple's procedures

Common bile duct was obtained from consenting patients undergoing Whipple's procedures at the Queen Elizabeth Hospital, Birmingham. Fresh tissue was placed in cold Dulbecco's Modified Eagle Medium (DMEM) prior to use and stored at 4°C until processed.

2.1.4. Whole peripheral blood from healthy volunteers

Whole blood was obtained from with research ethics approval from consenting volunteers at the Queen Elizabeth Hospital, Birmingham.

2.2. IMMUNOHISTOCHEMISTRY

2.2.1. Sectioning and fixation of formalin-fixed paraffin-embedded (FFPE) tissue

FFPE sections were cut at 4µm and fixed to microscope slides (X-tra Adhesive, Leica, Wetzlar, Germany).

2.2.2. De-waxing and rehydration of FFPE tissue sections

All FFPE sections were de-waxed and rehydrated before tinctorial or histochemical staining. Sections were passed sequentially through Clearene solvent (Leica, Wetzlar, Germany) three times, industrial methylated spirit (IMS) twice, and water for 2 minutes each.

2.2.3. Haematoxylin and Eosin (H&E) staining

Previously de-waxed and rehydrated sections were sequentially moved through the following reagents: Harris Haematoxylin (Leica, Wetzlar, Germany) for 4 minutes; water for 2 minutes; Acid Alcohol (Leica, Wetzlar, Germany) for 30 seconds; water for 2 minutes; Scott's Tap Water Substitute (Leica, Wetzlar, Germany) for 30 seconds; Eosin (aqueous) (Leica, Wetzlar, Germany) for 1 minute; and water twice for 2 minutes each before dehydration and mounting.

2.2.4. Van Gieson staining

Previously de-waxed and rehydrated sections were sequentially moved through the following reagents: Celestine Blue (Leica, Wetzlar, Germany) for 5 minutes; water twice for 2 minutes each; Harris Haematoxylin for 4 minutes; water for 2 minutes; Acid Alcohol (Leica, Wetzlar, Germany) for 30 seconds; water for 2 minutes; Scott's Tap Water Substitute (Leica, Wetzlar,

Germany) for 30 seconds; and water for 2 minutes; Van Gieson's solution for 3 minutes; and rinsed with industrial methylated spirit (IMS) before dehydration and mounting.

2.2.5. Chromogenic immunohistochemistry

Sections previously de-waxed and rehydrated underwent antigen retrieval using Dako Target Retrieval Solution (Dako UK Ltd. Ely, UK). Buffer was microwaved for 5 minutes at full power then sections added and heated for a further 10 minutes before being left to stand for 10 minutes. Sections were then cooled by the slow addition of cold tap water to the hot buffer. Sections were removed, dried and then circled with a wax pen to allow damming of subsequent buffers. Subsequent steps were conducted at room temperature with slow rocking. Sections were blocked in 0.3% MeOH in H_2O_2 for 20 minutes to block endogenous hydrogen peroxidase activity and casein buffer (Vector Laboratories Ltd., Peterborough, UK) for 1 hour to block non-specific antibody binding. Primary antibodies were diluted in Tris-buffered saline (TBS) (pH 7.4) and sections were incubated in primary antibody for 1 hour directly after blocking steps. Sections were washed with three, five minute washes in TBS plus 0.1% Tween20 (Sigma-Aldrich Chemie Gmbh, Munich, Germany). Sections were then incubated with appropriate immPRESS (peroxidase) Polymer Detection Kits (Vector Laboratories Ltd., Peterborough, UK). Sections were again washed as before in TBS plus 0.1% Tween20 then incubated in fresh 3,3'-Diaminobenzidine (DAB) reagent (AbD Serotec, Kidlington, UK) with agitation until brown staining was clearly visible on liver tissue. Excess substrate was then washed off using tap water and sections were counterstained in Mayer's Haematoxylin (Leica, Wetzlar, Germany) for 30 seconds before bluing by incubation in tap water. All experiments included a negative control section (no primary antibody) and a section treated with an

isotype control matched to the primary antibody. This allowed detection of nonspecific binding of the primary or secondary antibodies to the liver sections resulting in false positive results.

2.2.6. Dehydration and mounting and stained sections

Sections were passed sequentially through industrial methylated spirit (IMS) twice, and Clearene solvent (Leica, Wetzlar, Germany) three times before mounting glass coverslips with DPX mountant (Sigma-Aldrich Chemie Gmbh, Munich, Germany).

2.2.7. Fixation of cultured cells for immunohistochemistry

Cells were washed twice in phosphate-buffered saline (PBS) and then incubated in 100% methanol at -20°C for 10 minutes. Fixed cells were then washed three times in PBS to remove methanol and stored in PBS at 4°C until further use.

Table 2.1. Anti-human antibodies used

Antigen	Host	Clone	Supplier	Concentration Used (µg/ml)
Albumin	Rabbit	F0117	**Dako**, Glostrup, Denmark	1
CK7	Mouse	OV-TL 12/30	**Dako**, Glostrup, Denmark	2
CK18	Mouse	CD10	**Dako**, Glostrup, Denmark	2
CK19	Mouse	RCK108	**Dako**, Glostrup, Denmark	2
EpCAM	Mouse	MOC-31	**Dako**, Glostrup, Denmark	5
NCAM	Mouse	0567	**Ebiosciences,** Hatfield, UK	2
panCK	Rabbit	Z0622	**Dako**, Glostrup, Denmark	2
Sox9	Rabbit	ab5535	**Millipore**, Billerica, MA, USA	1

Table 2.2. Anti-mouse antibodies used

Antigen	Host	Clone	Supplier	Concentration Used (µg/ml)
AFP	Rabbit	A0008	**Dako**, Glostrup, Denmark	13
αSMA	Rabbit	E184	**Abcam**, Cambridge, MA, USA	1:1000 dilution*
β-catenin	Goat	SC-1496	**Santa Cruz Biotech.**, Santa Cruz, CA, USA	1
CAM 5.2	Mouse	CAM 5.2	**BD biosciences,** San Jose, CA, USA	5
CD45-PE	Rat	30-F11	**BD biosciences,** San Jose, CA, USA	0.2
CK18	Mouse	ab668	**Abcam**, Cambridge, MA, USA	40
Desmin	Rabbit	ab8592	**Abcam**, Cambridge, MA, USA	2
Glutamine Synthetase	Mouse	MAB302	**Millipore**, Billerica, MA, USA	5
Ki67	Rabbit	ab9260	**Millipore**, Billerica, MA, USA	0.4
Pan-CK	Rabbit	Z0622	**Dako**, Glostrup, Denmark	2
PDGFRα	Rat	APA5	**Ebiosciences,** Hatfield, UK	2
PDGFRα	Goat	AF1062	**R&D systems**, Minneapolis, MN	2
PDGFRα-APC	Rat	APA5	**BD biosciences,** San Jose, CA, USA	0.2
Sca1	Rat	E13 161-7	**Abcam**, Cambridge, MA, USA	1
Sca1-FITC	Rat	E13 161-7	**BD biosciences,** San Jose, CA, USA	0.2
Ter119-PE	Rat	TER119	**BD biosciences,** San Jose, CA, USA	0.2
Ubiquitin	Rabbit	Z0458	**Dako**, Glostrup, Denmark	1:1000 dilution*
Ubiquitin	Rabbit	ab19247	**Abcam**, Cambridge, MA, USA	5
Vimentin	Rabbit	SP20	**Abcam**, Cambridge, MA, USA	2

*Antibody concentration not supplied with this product.

2.2.8. Fluorescent immunohistochemistry

Either sections or cells fixed *in situ* were blocked for one hour in casein buffer (Vector Laboratories Ltd., Peterborough, UK), incubated with primary antibody diluted in TBS for 2 hours, washed three times for 5 minutes in TBS plus 0.1% Tween20 and incubated in appropriate secondary antibodies for 2 hours. Further steps were conducted with cells or sections protected from light using aluminium foil. Cells or sections then underwent three, five minute washes in TBS plus 0.1% Tween20 before incubation in 4',6-diamidino-2-phenylindole (DAPI) solution (0.5µg/ml in water, Sigma-Aldrich Chemie Gmbh, Munich, Germany) for 2 minutes. Cells or sections were then washed with PBS three times to remove excess DAPI. All steps were conducted at room temperature with rocking. Fixed cells were left under PBS. Coverslips were mounted using VECTASHIELD mounting medium with DAPI (Vector labs, Peterborough, UK).

2.2.9. Oil Red O staining

Cells were stained in 96-well plates. Cells were incubated in 60% isopropanol (diluted in DI water) for 5 minutes, Oil Red O working solution for 60 minutes and 60% isopropanol again for 5 minutes. Cells were then wasted twice in water and counterstained with Mayer's haematoxylin for 1 minute. Haematoxylin was rinsed with tap water and cells were left under PBS before imaging.

2.3. IMAGE CREATION AND ANALYSIS

2.3.1. Imaging

Images of chromogenic immunohistochemistry were taken with a conventional light microscope (Carl Zeiss AG, Oberkochen, Germany). Images of fluorescent staining of fixed cells were taken with an inverted microscope (Carl Zeiss AG, Oberkochen, Germany). Images of fluorescent staining of sections were taken with a confocal microscope (Carl Zeiss AG, Oberkochen, Germany).

2.3.2. ImageJ

ImageJ was used for quantitative analysis of chromogenic and tinctorial staining. Total area of biopsies was calculated by manually drawing around tissue fragments and using the ‘measure’ function within ImageJ. DAB and Van Gieson staining was quantified using the ‘Color Threshold’ function of ImageJ. The ‘Color Threshold’ function of ImageJ produces histograms quantifying the hue, saturation and brightness of the overall image and allows pixels within user defined ranges for each parameter to be excluded.

2.3.3. NAFLD activity and fibrosis scoring

The NAFLD activity score (NAS) was assigned to each section through blinded assessment by an experienced liver pathologist (Prof. Stefan Hübscher) according to the Kleiner scoring system[44]. The Kleiner system generates a composite score (out of a total of 8) based on the degree of steatosis (0-3), lobular inflammation (0-3), and hepatocyte ballooning (0-2), with a

separate score for fibrosis (0-4). Steatosis scores are assigned according to the extent of steatosis as: 0 for <5%; 1 for 5-33%; 2 for 33-66%; and 3 for >66%. Lobular inflammation scores are assigned according to the number of inflammatory foci as: 0 for no foci; 1 for <2 foci per 200x field; 2 for 2-4 foci per 200x field; and 3 for >4 foci per 200x field. Hepatocyte ballooning scores are assigned according the number and prominence of ballooned hepatocytes as: 0 for none; 1 for few, or borderline, cases of ballooning; and 2 for many cases of ballooned hepatocytes that typically contain Mallory's hyaline. Fibrosis is assessed separately for the NAS composite and scores are assigned based on the degree and location of fibrosis as: 0 for none; 1 for peri-sinusoidal or peri-portal; 2 for peri-sinusoidal and peri-portal; 3 for bridging; and 4 for cirrhosis. A score of 1 is often subdivided into: 1a, mild, or delicate, peri-sinusoidal; 1b, moderate, or dense, peri-sinusoidal; and 1c, portal or peri-portal fibrosis without the presence of peri-cellular or peri-sinusoidal fibrosis.

2.4. ISOLATION OF PRIMARY HUMAN CELLS

2.4.1. Immunoselection of biliary epithelial cells (BEC)

Slices of approximately 100g of explanted, resected or donor liver were stored at 4°C in DMEM for up to 2 days (liver progenitor cells may be viable in cadaveric liver for up to 6 days). Slices were removed from DMEM and diced finely with scalpels before digestion with 0.2% collagenase Type 1A (Sigma-Aldrich, UK) in PBS for between 20 and 45 minutes at 37°C depending on the condition of liver tissue. After digestion the liver suspension was passed through a fine mesh with moderate pressure and washed with PBS until 200ml of cell suspension was obtained. The suspension was transferred to eight 25ml universal tubes and spun at 2000rpm for 5 mins. Supernatant was discarded and pellets were combined and

resuspended in 25ml PBS in four 25ml universal tubes. Pellets were combined 2:1 resuspended and spun as above until a single pellet was obtained. Eight tubes for density centrifugation gradients were set up each containing 3ml of 77% Percoll (GE Healthcare Life Sciences, Little Chalfont, UK) in PBS layered under 3ml of 33% Percoll in PBS. The pellet was resuspended in 25ml of PBS and 3ml layered over each of the Percoll gradients. Percoll gradients were then spun at 2000rpm for 20 mins with no brake. Bands formed at the second interphase were removed and combined 2:1 in four 25ml universal tubes, resuspended in PBS and spun at 2000rpm for 5 mins with brake. All pellets obtained were transferred into a single universal, resuspended and spun again at 2000rpm for 5 mins. The final pellet was resuspended in 500µl PBS and EpCAM primary antibody. Cells were incubated in primary antibody for 30 mins at 37C with periodic shaking. Cells were then washed in PBS and spun at 2000rpm for 5 mins with the pellet resuspended in 500µl ice-cold PBS with anti-mouse IgG dynal beads. Cells were incubated on ice with shaking for 30 minutes then made up to a final volume of 5ml in further ice-cold PBS. Cell suspensions were then placed on magnet for 5 mins and all PBS removed. Remaining cells represent all $EpCAM^+$ parenchymal cells present in the liver and consist largely of mature biliary epithelial cells (BEC). These cells can be plated on type I collagen coated plates or flasks in media containing insulin, IT3, EGF, HGF and cholera toxin, cultured to confluence and subsequently passaged using trypsin.

2.4.2. Selection of hepatic stem cells from $EpCAM^+$ cells from explanted liver tissue

Immunoselected $EpCAM^+$ cells from explanted liver were plated onto culture plastic in modified Kubota's medium resulting in the selection and growth of hepatic stem cells only. Media was changed weekly.

2.4.3. Isolation of biliary tree stem cells from explanted common bile duct

Common bile duct was removed from DMEM and diced finely with scalpels before digestion with 0.2% collagenase Type 1A (Sigma-Aldrich, UK) in PBS for 20 minutes at 37°C. After digestion tissue was passed through a fine mesh and washed in 5mM EDTA in PBS for 30 minutes at 37°C to dissociate peri-biliary glands. The resulting suspension was passed through fine mesh, spun at 2000rpm for 5 mins and seeded in collagen-coated plates in modified Kubota's medium for 1 hour. Non-adherent cells/glands were then transferred to fresh collagen-coated plates and incubated in modified Kubota's medium.

2.4.4. Isolation of $CD14^{+}CD16^{+}$ monocytes from peripheral blood

Monocyte subsets from peripheral blood were isolated using the CD16 nonocyte isolation kit and CD14 Microbeads (Miltenyi Biotec, Bisley, Surrey, UK) according to manufacturer's instructions.

2.5. ANIMAL HUSBANDRY

2.5.1. Housing

All mice were housed in accordance with the animal care protocols at the University of Birmingham, UK. Mice were maintained on a 12:12 hour light-dark schedule at 22°C, with up to 4 mice per cage.

2.5.2. Genotyping

Tissue for genotyping was obtained from ear clippings used to number and identify animals. Genomic DNA (gDNA) was isolated by digesting tissue in 100µl of sodium hydroxide

(NaOH) for 40 minutes at 95°C with occasional agitation. The resulting solution was neutralised with 8µl of Tris-HCl (pH 8.0). All genotyping PCR reactions were performed using the following mixture: 12.5µl 2x BioMix Red (Bioline, London, UK); 0.3µl of each primer; 2.9µl water; and 4µl of isolated gDNA solution (total 25µl). FAH primers were designed to yield a product of 250bp. Cycling conditions for FAH were as follows: 94°C for 3 mins; 35 cycles of (94°C for 30 seconds, 60°C for 30 seconds and 72°C for 60 seconds); and finally 72°C for 7 minutes. RAG-2 primers were designed to yield a product of 200bp. Cycling conditions for RAG-2 were as follows: 94°C for 5 mins; 35 cycles of (94°C for 45 seconds, 58°C for 45 seconds and 72°C for 60 seconds); and finally 72°C for 5 minutes. IL2RG primers were designed to yield a product of 250bp. Cycling conditions for IL2RG were as follows: 94°C for 3 mins; 35 cycles of (94°C for 30 seconds, 60°C for 30 seconds and 72°C for 60 seconds); and finally 72°C for 7 minutes. Products were run on a 2% agarose gel for 40 minutes at 124V. Band size was determined using Hyperladder IV (Bio-rad, Hemel Hempstead, UK).

2.5.3. American Lifestyle-Induced Obesity Syndrome (ALIOS) diet

ALIOS mice were fed a trans-fat custom diet (TD.06303 Harlan Teklad, Madison, WI, USA) containing 45% kcal from fat (30% of the fat was from hydrogenated vegetable oil, which contains 30% trans-fat), 37% from carbohydrate and 18% from protein. Drinking water was replaced by a HFCS equivalent, prepared by adding 42ml/litre of a 55% fructose and 45% glucose solution. Control mice were fed a standard chow diet with normal drinking water. Food and drink was provided *ad libitum* to all animals.

2.5.4. Preparation of Nitisinone stock and drinking water

NTBC drinking water was prepared as a 2mg/ml stock solution by firstly dissolving 3g of sodium bicarbonate (Sigma-Aldrich Chemie Gmbh, Munich, Germany) in 30ml of sterilised water at 42ºC for 2 hours with agitation. A further 220ml of sterilised water was then added to make a total of 250ml before dissolving 500mg of NTBC (Nitinisone, Swedish Orphan Biovitrum, Stockholm, Sweden) by heating at 50ºC for 3 hours with stirring. The resulting solution was then sterilised by filtering in a laminar flow hood. Stock solution was protected from light and stored at 4ºC for up to 3 months. Drinking water was autoclaved with the addition of food colouring to distinguish from normal drinking water. NTBC stock was then added to the cooled, coloured water under sterile conditions at 8ml/L to a final NTBC concentration of 16mg/L. The amount of NTBC stock added was adjusted accordingly to prepare 25% (4mg/L), 12.5% (2mg/L) and 6.25% (1mg/L) NTBC drinking water for cycling. NTBC was administered to mice *in lieu* of normal drinking water.

2.5.5. Adoptive transfer via intra-venous (i.v.) tail vein infusion

Freshly isolated cells were resuspended in a total volume of 230µl of PBS and kept on ice before infusion into the tail vein. Mice were observed for 5 minutes then returned to normal conditions.

2.5.6. Tissue preservation and preparation for histological assessment

Mice were killed by cervical dislocation under terminal general anaesthesia using isoflurane. Livers were excised and tissue placed in formalin for paraffin embedding or snap frozen in liquid nitrogen. For formalin-fixed paraffin embedded (FFPE) samples, tissue was left to fix

in formalin overnight, then paraffin wax embedded. Sections were cut at 3.5µm and and fixed to microscope slides (X-tra Adhesive, Leica, Wetzlar, Germany). Frozen tissue was used for RNA isolation.

2.6. ISOLATION OF PRIMARY MURINE CELLS

2.6.1. Isolation of non-parenchymal cells from murine liver

Mice were killed by cervical dislocation and whole livers dissected and transferred to a sterile petri dish 56.5cm^2 petri dish (Fisher Scientific, Hampton, NH, USA). Livers were mechanically dissociated by fine chopping with two scalpels until a homogenous paste was formed. Tissue was then placed in a first digestion buffer (2mg/ml collagenase in DMEM) and incubated at 37°C for 10 minutes with robust agitation (200rpm). Digested tissue was placed over coarse mesh (pore size 0.45µm, Millipore, Billerica, MA, USA) and debris was washed through with PBS and discarded. Remaining tissue was transferred to a second digestion buffer (1mg/ml collagenase in DMEM) and re-digested at 37°C for 40 minutes with robust agitation. The resulting suspension was placed over fine mesh (pore size 0.45µm, Millipore, Billerica, MA, USA) and washed through with HBSS wash buffer with firm pressure applied to dissociate and force through any remaining tissue fragments. The resulting suspension was made up to 200ml with HBSS, split into four 50ml conical tubes and spun at 2000rpm for 5 minutes to remove debris. Pellets were resuspended in 100ml HBSS, split into two conical tubes and spun again at 2000rpm for 5 minutes. Pellets were resuspended in 100ml of HBSS and spun at 50g for 10 minutes to remove mature hepatocytes. Supernatant was collected and spun again at 50g for 10 minutes. Supernatant was collected and spun at 2000rpm for 5 minutes to collect remaining cells. Pellets were resuspended and pooled in

10ml of Red Cell Lysing Buffer (Sigma-Aldrich Chemie Gmbh, Munich, Germany) and incubated at room temperature for 5 minutes with agitation. The suspension was made up to 50ml with HBSS and spun at 2000rpm for 5 minutes to collect cells. Cells were resuspended in 120ml 30% Percoll (GE Lifesciences, Pittsburgh, PA, USA) in PBS and split into four 50ml conical tubes. Percoll suspensions were spun at 2000rpm for 20 minutes with no brake applied. Supernatants were removed and pellets resuspended and pooled in HBSS and spun at 2000rpm for 5 minutes to collect viable non-parenchymal cells.

2.6.2. Fluorescence activated cell sorting of hepatic stem cell populations

Isolated murine hepatic non-parenchymal cells were resuspended in 1ml HBSS and incubated with CD45 (PE; 1µl/liver), Ter-119 (PE; 1µl/liver), Sca-1 (FITC; 1µl/liver) and PDGFRα (APC; 2µl/liver) (all antibodies from eBiosciences, Hatfield, UK) on ice for 30 minutes protected from light. The suspension was made up to 15ml with HBSS and spun at 2000rpm for 5 minutes to wash out conjugated antibodies. Cells were then resuspended in 1ml HBSS with 2µg/ml propidium idodide (PI) (Sigma-Aldrich Chemie Gmbh, Munich, Germany) and incubated on ice for 15 minutes protected from light. Cells were strained through a 50µm filter and placed on ice protected from light until sorting.

2.7. FLUORESCENCE ACTIVATED CELL SORTING (FACS)

2.7.1. Equipment setup

Cells were sorted using the MoFlo XDP high-speed cell sorter (Beckman Coulter, Brea, CA, USA). Both the blue (488nm) and red (640nm) lasers were used. The blue laser was used for

forward scatter (FS) and side scatter (SS) detection. The following channels were used for detection of fluorescence: FL1 (FITC), FL2 (PE), FL3 (PI), FL9 (APC).

The cell sorter was initialised and optimised before each sort. Briefly, this consisted of a crude and fine stream alignment, drop delay using Flowcheck beads (Beckman Coulter, Brea, CA, USA), and compensation of fluorescent bleeding between channels using small samples of cells stained for each individual antibody.

2.7.2. Sorting strategy

Cells were stained with: PI, CD45-PE, Ter119-PE, Sca1-FITC and PDGFRα-APC and identified through the combination of the following plots: PI (X axis)/FSC-height (Y axis) (**Fig 2.1A**), PE/FITC (**Fig 2.1B**), PE/FSC-Height (**Fig 2.1C**) and FITC/APC (**Fig 2.1D**). PI was used to positively identify and exclude dead cells (R1; PI^+,) from further analysis. Haematopoietic lineage cells ($CD45^+$, $Ter119^+$) were positively identified and excluded on PE/FSC-Height plots (R3) (**Fig 2.1A**) from further analysis. The presence and intensity of PDGFRα and Sca1 staining was visualised on a FITC/APC plot (**Fig 2.1D**) after exclusion of dead and lineage positive cells allowing identification of populations of interest.

2.7.3. Prospective isolation of cells from adult murine liver

Gates were drawn around viable (R3; PI^-,) and haematopoietic lineage negative (R4) cells and distinct populations of Lin^-Sca1^+ cells (R6) and PαS cells (R5) observed on the FITC/APC plot. Lin^-Sca1^+ cells were sorted from all cells found inside gates R3, R4 and R6 and outside gates R1, R2, and R5. PαS cells were sorted from all cells found inside gates R3, R4 and R5 and outside gates R1, R2 and R6.

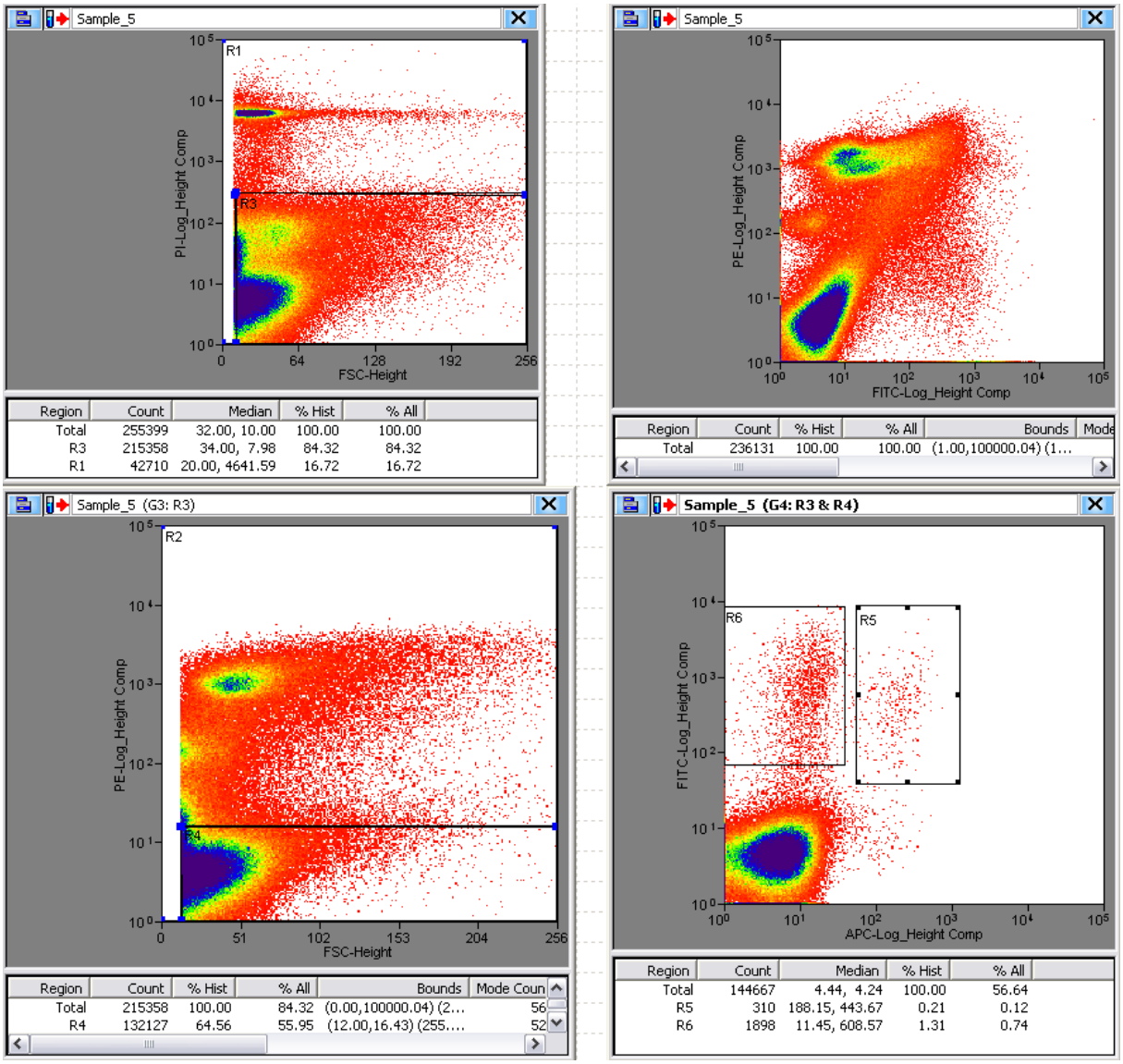

Figure 2.1. Gating strategy for the prospective isolation of stem/progenitor cell populations from adult murine liver. A, live/dead cells identified with PI/FSC-Height, **B**, visualisation of PE/FITC compensation, **C**, haematopoietic lineage cells identified with a combination of CD45 and Ter119 (PE) against FSC-Height, **D**, Two distinct, non-haematopoietic, resident hepatic cell populations with Sca1 (FITC) and PDGFRα (APC) antigenicity.

2.8. *IN VITRO* CELL CULTURE

2.8.1. Cell culture conditions

All cells were maintained in two-dimensional culture conditions at 37°C in 5% CO_2 in Corning plastic cell culture flasks or wells (Sigma-Aldrich Chemie Gmbh, Munich, Germany).

2.8.2. Preparation of coated culture flasks and plates

Collagen solution type I from rat tail (Sigma-Aldrich Chemie Gmbh, Munich, Germany) was diluted to a final dilution of 0.01% (w/v) in sterile water. The diluted preparation was added to plates or flasks at 10µg/cm^2 and left for 4 hours at room temperature. Diluted collagen was stored at 4°C for up to 2 weeks. Coated plates were washed once with PBS and cells plated directly.

2.8.3. Preparation of collagen gels

Collagen gels were prepared using the 3D Collagen Cell Culture System (Millipore, Billerica, MA, USA) according to manufacturer's instructions. Collagen gel solutions were made and kept on ice before cells were added a density of 100,000/ml and allowed to set at 37°C.

2.8.4. Preparation of stock solutions

100µM Dexamethasone stock solution. 100mg of dexamethasone powder (Sigma-Aldrich Chemie Gmbh, Munich, Germany) was added to 250ml of ddH_2O resulting in a 1mM stock solution. Dexamethasone stock was stored at 4°C until further use.

200µg ml^{-1} EGF stock solution. 500µg of lyophilised recombinatn murine epidermal growth factor (EGF) (Peprotech, Rocky Hill, NJ, USA) was added to 2.5ml ddH_2O resulting in a 200µg ml^{-1} stock solution. Stocks were aliquoted and stored at -20°C until further use.

40µg ml^{-1} HGF stock solution. 20µg of lyophilised hepatocyte growth factor (HGF) (Peprotech, Rocky Hill, NJ, USA) was added to 0.5ml of ddH_2O resulting in a 40µg ml^{-1} (? molarity) stock solution. Stocks were aliquoted and stored at -20°C until further use.

100x Insulin-transferrin-sodium selenite (ITS) stock solution. 50ml of ddH_2O was added to 1 vial (≈40mg) of insulin-transferrin-sodium selenite (ITS) media supplement (Sigma-Aldrich Chemie Gmbh, Munich, Germany) to form a 100x stock. Stocks were aliquoted and stored at -20°C until further use.

20mM Y-27632 stock solution. Y-27632, a molecular inhibitor of rho-associated protein kinase (ROCK) was prepared as a 20mM stock solution from 1mg of Y-27632 dihydrochloride (Sigma-Aldrich Chemie Gmbh, Munich, Germany) by diluting in 200µl of ddH_2O. Stocks were aliquoted and stored at -20°C and used at a working concentration of 20µM.

40µg ml^{-1} mrOSM stock solution. 25µg of lyophilised murine recombinant oncostatin-M (Peprotech, Rocky Hill, NJ, USA) was reconstituted in 625µl of ddH_2O resulting in a 40µg ml^{-1} stock solution. Stocks were aliquoted and stored at -20°C until further use.

10µg ml^{-1} mrFGF4 stock solution. 25µg of lyophilised murine recombinant fibroblast growth factor-4 (FGF-4) (Peprotech, Rocky Hill, NJ, USA), was reconstituted in 2.5ml of ddH_2O resulting in a 10µg ml^{-1} stock solution. Stocks were aliquoted and stored at -20°C until further use.

1.25M 2-DG stock solution. 1g of lyophilised 2-deoxy-D-glucose (2-DG,(Sigma-Aldrich Chemie Gmbh, Munich, Germany) was reconstituted in 4.8ml of ddH_2O to a final concentration of 1.25M solution. Stocks were aliquoted and stored at -20°C until further use. 2-DG was used at a final concentration of 1.25mM.

50µg ml^{-1} mrTNFα stock solution. 5µg of murine tumour necrosis factor-alpha (TNFα) recombinant protein (eBiosciences, San Diego, CA, USA) was reconstituted in 100µl of ddH_2O to a concentration of 50µg ml^{-1}. Stocks were aliquoted and stored at -20°C until further use.

2.8.5. Preparation of culture media

Stromal expansion media. 10% foetal calf serum (FCS) and glutamine-penicillin-streptomycin (GPS) antibiotic media supplement (Life Technologies Ltd., Paisley, UK) were added to alpha-minimal essential media (αMEM) (Life Technologies Ltd., Paisley, UK).

Hank's Balanced Salt Solution (HBSS) wash buffer. 5ml of glutamine-penicillin-streptomycin (GPS) antibiotic media supplement, 5ml of foetal calf serum (FCS) and 1M 4-(2-hydroxyethyl)-1-piperazineethanesulfonic acid (HEPES, Sigma-Aldrich Chemie Gmbh, Munich, Germany) were added to 500ml of hank's balanced salt solution (HBSS) (Life Technologies Ltd., Paisley, UK).

OC^- medium. To make up 100ml of OC^- medium, 45ml of DMEM and 45ml Ham's F12 were mixed then the following supplements were added; 10ml FCS; 250µl 1M HEPES; 1ml 100x ITS stock;10µl EGF stock; 100µl HGF stock; and 1ml dexamethasone stock. Media was stored at 4°C until further use.

OC complete (OC^+) medium. Before use, 100ml of OC^- medium was completed with the addition of 12.2mg nicotinamide and 10µl Y-227632 stock.

Murine hepatocyte differentiation medium (MKM-H). For 10ml of hepatocyte differentiation medium, 4.5ml of DMEM (Life Technologies Ltd., Paisley, UK) and 4.5ml Ham's F12 (Life Technologies Ltd., Paisley, UK) were mixed then the following supplements were added; 1ml FCS; 25µl 1M HEPES; 100ul 100x ITS stock; 5ul HGF stock, 10ul FGF-4 stock, 10ul OSM stock, 10ul dexamethasone stock and 20% Matrigel.

Murine cholangiocyte differentiation medium (MKM-C). For 10 mL of cholangiocyte differentiation medium, 4.5ml of DMEM and 4.5ml Ham's F12 were mixed then the following supplements were added; 1ml FCS; 100ul 100x ITS stock; 5ul HGF stock; and TNFα (50ng/ml).

Modified Kubota's Medium (MKM). Modified Kubota's Medium contains albumin 0.3mM calcium (Sigma-Aldrich Chemie Gmbh, Munich, Germany), 4.5mM Nicotinamide (Sigma-Aldrich Chemie Gmbh, Munich, Germany), 0.1nM Zinc Sulfate heptahydrate (Sigma-Aldrich Chemie Gmbh, Munich, Germany), 10nM hydrocortisone (Sigma-Aldrich Chemie Gmbh, Munich, Germany), 1x Insulin-Transferrin-Selenium (Life Technologies Ltd., Paisley, UK) and a mixture of free fatty acids (FFA supplement, Sigma-Aldrich Chemie Gmbh, Munich, Germany) bound to 0.1% bovine serum albumin (BSA) (Sigma-Aldrich Chemie Gmbh, Munich, Germany) in RPMI 1640 medium (Life Technologies Ltd., Paisley, UK).

2.8.6. Preparation of miscellaneous solutions

Preparation of digestion solutions (collagenase). Digestion solutions were prepared at 0.2% w/v and 0.1% w/v collagenase by adding 40mg and 20mg of collagenase (WAKO, Odawara, Japan) respectively to 20ml of dulbecco's modified eagle medium (DMEM) .

Propidium iodide (PI) stock solution. - SXS

0.4% w/v Trypan Blue solution. Trypan blue powder (Sigma-Aldrich Chemie Gmbh, Munich, Germany) was dissolved in PBS to a 0.5% w/v solution and boiled briefly before cooling to room temperature. The solution was further diluted to 0.4% w/v with PBS and stored at room temperature until further use.

14.3mM (5mg/ml) 4′,6-diamidino-2-phenylindole (DAPI), dihydrochloride solution.

DAPI (4',6-Diamidino-2-Phenylindole, Dihydrochloride, Life Technologies Ltd., Paisley, UK) was prepared as a 5 mg/ml (14.3mM) stock solution by dissolving 10mg of DAPI in 2ml of ddH_2O. DAPI stock solution was stored at 4°C and protected from light until further use.

1mg/ml propidium iodide (PI) stock. Propidium iodide (Sigma-Aldrich Chemie Gmbh, Munich, Germany) was dissolved in ddH_2O to a concentration of 1mg/ml and stored at 4°C until further use.

Preparation of Oil Red O stock and working solutions. Oil red O stock solution was made up by adding 300mg of Oil Red O powder (Sigma-Aldrich Chemie Gmbh, Munich, Germany) to 100 ml 99% isopropanol (Sigma-Aldrich Chemie Gmbh, Munich, Germany). Stock solution was stored at room temperature. Oil red O working solution was made by adding 2 part ddH_2O to 3 parts oil red O stock. Working solution was left at room temperature for 10 minutes before filtering with filter paper and funnel. Working solution of oil red O was used immediately.

2.8.7. Cell passage

Spent media was removed and cells were washed twice in PBS. Pre-warmed (37°C) TrypLE Express (Life Technologies Ltd., Paisley, UK) was added to cells at 100µl/cm2 and incubated at 37°C for 5 minutes or until cells were fully detached. TrypLE was quenched in DMEM +10% FCS and pipetted over the flask or plate several times to ensure all cells were collected. Cells were transferred to conical tubes and pelleted by spinning at 2000rpm for 5 minutes. Cells were then resuspended and plated in appropriate media.

2.8.8. In situ fixation of cultured cells

Media was removed and cells were washed twice in PBS. Cells were then covered with ice-cold 100% methanol (Sigma-Aldrich Chemie Gmbh, Munich, Germany) and incubated at -20°C for 20 minutes. Methanol was removed and cells were washed twice with PBS to remove excess methanol before storage at 4°C under PBS until further use.

2.8.9. Preparation of cell lyses for RNA isolation

Media was removed and cells were washed twice in PBS. Cells were then either trypsinised, pelleted and frozen at -20°C or RLT buffer was added directly to cells after PBS wash and cells were scraped, collected and stored at -20°C.

2.9. *IN VITRO* FUNCTIONAL ANALYSES

2.9.1. Hepatocyte differentiation of murine hepatic stem cells

For hepatocyte differentiation of murine hepatic stem cells, 0.5 x 10^{-6} cells were plated onto 6-well collagen-coated plates and placed in hepatocyte differentiation media for 2 weeks with

media changed weekly. Cells were then fixed with 100% methanol and stored at 4°C until further use.

2.9.2. Cholangiocyte differentiation of murine hepatic stem cells

For cholangiocyte differentiation of murine hepatic stem cells, cell were suspended in collagen gels at a density of 100,000 cells per ml. Cholangiocyte differentiation media was then added on top of the set gels and cells were incubated for 7 days. Cells were then fixed with 100% methanol and stored at 4°C until further use.

2.9.3. Fibroblast differentiation of murine hepatic stem cells

For fibroblast differentiation differentiation of murine hepatic stem cells, 0.5×10^{-6} cells were plated onto 6-well culture plastic plates and placed in αMEM for 2 weeks with media changed weekly. Cells were then fixed with 100% methanol and stored at 4°C until further use.

2.10. GENERIC LAB TECHNIQUES

2.10.1. RNA isolation

Total ribonucleic acid (RNA) was isolated using RNeasy Minikits (Qiagen, Gaithersburg, MD, USA) according to manufacturer's instructions. Whole tissue, either snap frozen or stored in RNA later (Life Technologies, Paisley, UK) was added to appropriate amounts of RLT buffer and homogenised with a hand-held homogeniser. Cells were either scraped in RLT buffer or pelleted and resuspended in RLT buffer before homogenisation using QIAshredder kits (Qiagen, Gaithersburg, MD, USA). Isolated RNA was eluted in ddH_2O for all

downstream applications. RNA concentration and quality was determined using Nanodrop spectrophotometers (Nanodrop, Wilmington, DE, USA).

2.10.2. Quantitative polymerase chain reaction (qPCR)

Taqman 20x gene expression singleplex quantitative real-time polymerase chain reaction (qPCR) assays (Applied Biosystems, Carslbad, CA, USA) were used to measure mRNA expression. Reactions were performed in singleplex and levels were normalised to the 18S housekeeping gene. For the gene of interest in a single 10µl reaction the following components were added: 5µl of 2x MasterMix (Applied Biosystems, Carlsbad, CA, USA), 0.5µl of 20x expression assay or 18S primers and probes, 1µl cDNA, and nuclease-free H_2O up to a final volume of 10µl. Samples were run on the 7500 real-time PCR system (Applied Biosystems, Carlsbad, CA, USA). Data were expressed as Ct values, (Ct = cycle number at which logarithmic PCR plots cross a calculated threshold line), and used to determine ΔCt values (ΔCt = Ct of the target gene – Ct of the housekeeping gene). Fold changes were calculated using transformation [fold increase = 2^- difference in ΔCt].

2.11. STATISTICS

Statistical analyses were performed using GraphPad Prism software All data were tested for normal distribution. Comparison of grouped data was performed using student's t-test or Welch's t-test where variances were significantly different. Statistical analysis of qPCR data was performed using ΔCt values. Glucose tolerance was analysed by 1-way ANOVA and

student’s t-test comparison of the mean (± standard error of the mean (SEM)) area under the curve (AUC) of the different groups. A value of $p \leq 0.05$ was considered statistically significant. Significance was represented as: *≤0.05; **≤0.01; ***≤0.001; ****≤0.0001.

CHAPTER 3

HEPATIC STEM CELL ACTIVATION AND HEPATOCELLULAR CARCINOMA IN A MOUSE MODEL OF NON-ALCOHOLIC STEATOHEPATITIS

(Modified from May 2014 publication in the American Journal of Pathology)

I am grateful to Dr. Joanna Dowman, a previous PhD student, for setting up the mouse model and collecting the data contributing to Figure 3.1A-G

3.1. RATIONALE FOR STUDY

Non-Alcoholic Fatty Liver Disease (NAFLD) is an increasingly common disease with severe complications. Non-alcoholic fatty liver disease (NAFLD) represents one of the most common causes of liver disease in the western world[135], ranging in severity from steatosis to non-alcoholic steatohepatitis (NASH) and cirrhosis[40]. Although simple steatosis alone is relatively benign, the presence of steatohepatitis greatly increases the risk of progression to cirrhosis, with its concomitant risk of developing hepatocellular carcinoma (HCC)[46] and death[136]. Currently, our knowledge of the pathogenesis of NAFLD is incomplete and there are no pharmacological therapies for the specific treatment of NAFLD. As such further research, and the continued development of appropriate models, is critically needed.

Hepatic stem cells are activated in clinical NAFLD yet their contribution to repair or progression remains unclear. Chronic liver diseases (including NAFLD) lead to the activation of a secondary proliferative pathway of human hepatic stem cells (hHpSC). hHpSC constitute 1-2% of the cells of the adult biliary tree and are slow-cycling under normal conditions[11]. Whilst hHpSC have been implicated in the reconstitution of parenchymal cell populations in situations where the proliferative capacity of mature parenchymal cells is impaired[74, 79, 137], they have also been linked to the promotion of a peri-portal ductular reaction, which in turn may provoke progressive peri-portal fibrogenesis[138]. Moreover, hHpSC proliferation has been associated with increased risk of HCC[94], although a direct link has not been proven in murine or human settings. Thus, the overall impact of hHpSC in chronic liver damage remains uncertain. In murine models of liver injury where endogenous

hepatocyte proliferation is inhibited[139], or where injury is extensive[140], proliferation of murine hepatic stem cells (mHpSC) contributes to tissue repair. However, our understanding of the initiating mechanisms, and subsequent consequences, of mHpSC activation during fatty liver injury remains limited due to a lack of suitably representative murine models.

There is a need for more pathophysiologically relevant *in vivo* models of NAFLD. Current rodent models of fatty liver disease rely upon strains carrying spontaneous mutations (ob/ob[141], db/d[142]), genetic manipulations[143], or formulated diets (MCD[144], HFD[145]), yet none of these models accurately reproduce the broad range of factors that contribute to the histological spectrum of human NAFLD and its sequelae. More recently, combinatorial use of diets with high proportions of fat, trans-fatty acids, oxidised lipoproteins[146] or high fructose drinking water[147] have resulted in patterns of liver injury closer to that observed in NASH, although aspects such as significant fibrogenesis and carcinogenesis are still lacking. Tetri *et al.* added a sedentary lifestyle to a diet rich in trans-fatty acids (TFA), and high-fructose corn syrup (HFCS) for a 16-week period, and demonstrated that mice developed glucose intolerance and hepatic steatosis and inflammation[148]. However, the activation of human HpSC in this, or much more extended versions (12 months) of the 'American Lifestyle-Induced Obesity Syndrome' (ALIOS) model had not previously been studied.

3.2. RESULTS

3.2.1. American lifestyle induced obesity syndrome (ALIOS) mice develop metabolic changes and liver injury characteristic of NAFLD. Weight gain was greater in ALIOS mice than NC mice after 6 months, although their weights converged by 12 months (**Fig 3.1A**). Glucose tolerance was reduced in ALIOS mice compared with NC mice at 6 months, but this difference was not maintained at 12 months, by which time NC mice were similar (**Fig 3.1B**). Liver to body weight ratios (LWBR) were higher in ALIOS mice compared to chow-fed mice at both 6 and 12 months (**Fig 3.1C**) with greater levels of hepatic triglycerides measured in livers of ALIOS mice compared to NC mice (**Fig 3.1D**). ALIOS mice had elevated levels of serum alanine aminotransferase (ALT) (**Fig 3.1E**) and aspartate aminotransferase (AST) (**Fig 3.1F**) at 12 months compared to NC mice. Expression of *TNFA* and *COL1A1* was increased in the ALIOS cohort at 6 and 12 months compared with chow-fed mice at the same time points in keeping with induction of inflammatory and fibrogenic processes in response to ALIOS diet (**Fig 3.1G**). Mature hepatocytes are known to proliferate in response to hepatic injury. To assess the proliferation of hepatocytes in response to the ALIOS diet, sections were stained with Ki67, a protein closely associated with cell proliferation and specifically found in the nucleus of proliferating cells. Proliferation index, quantified by nuclear Ki67 staining, was significantly higher in mice fed ALIOS for 12 months than those fed normal chow for 12 months or baseline animals (**Fig 3.1H**). Activated stellate cells demonstrated by alpha-smooth muscle actin (αSMA) immunohistochemistry were clearly increased in number in the ALIOS cohort at 12 months but were infrequent or absent at 6 months and in the other cohorts (**Fig 3.2**).

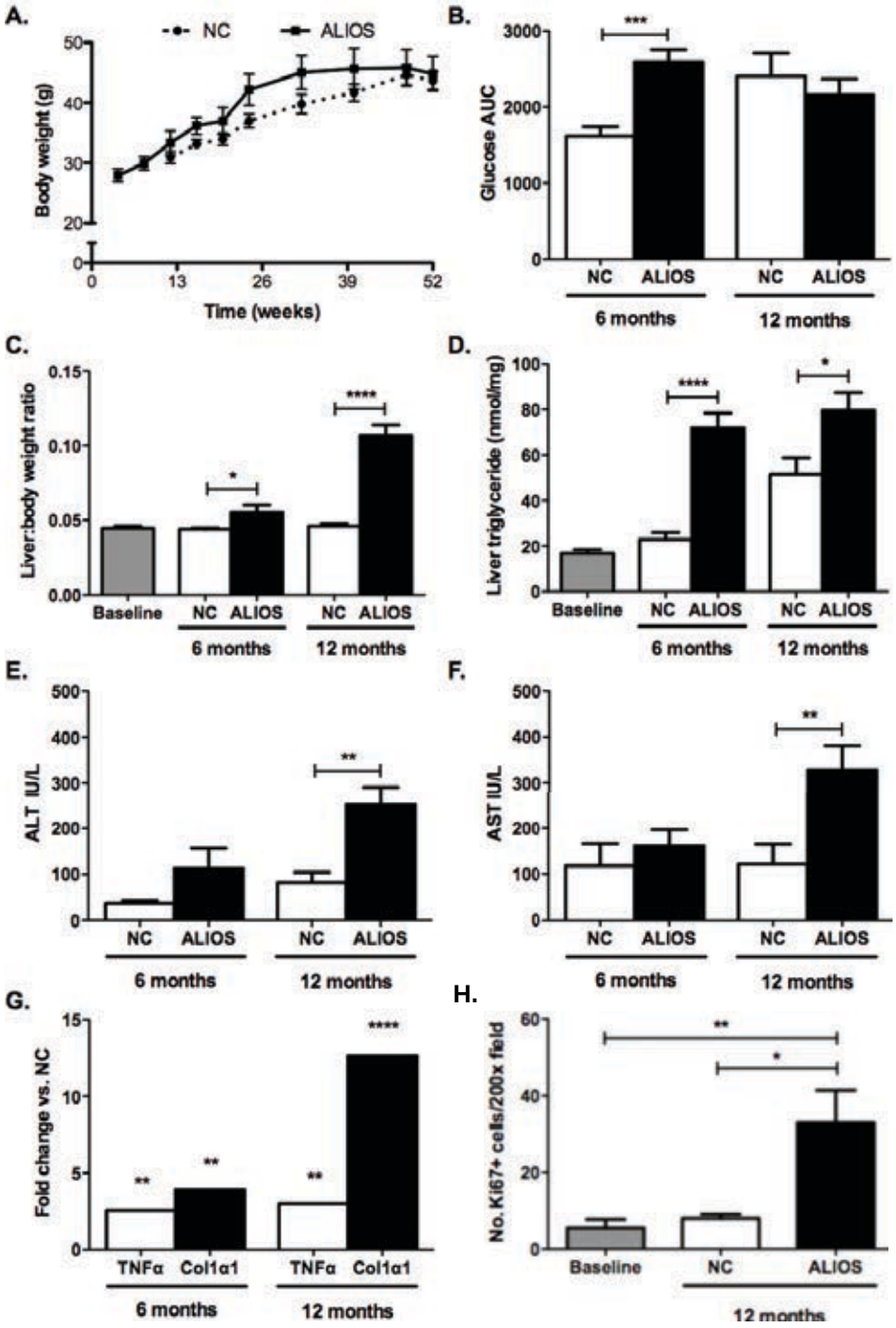

Figure 3.1. ALIOS mice develop metabolic changes and liver injury characteristic of NAFLD. A, Combined body weight curves for co-housed NC mice (blue) or ALIOS diet (red) for 6 months and 12 months. **B,** Area under the curve (AUC) of intra-peritoneal (i.p.) glucose tolerance tests (GTT). **C,** Liver to body weight ratios. **D,** Liver triglyceride content. **E,** Circulating concentrations of alanine aminotransferase and **F,** aspartate aminotransferase. **G,** Fold change in expression levels of *TNFA* and *COL1A1* in ALIOS mice at 6 and 12 months over NC mice. **H,** Proliferation index calculated from Ki67 immunohistochemistry. Error bars represent SEM *p ≤ 0.05; **p ≤ 0.01; ***p ≤ 0.001; ****p ≤ 0.0001 (student's t-test)

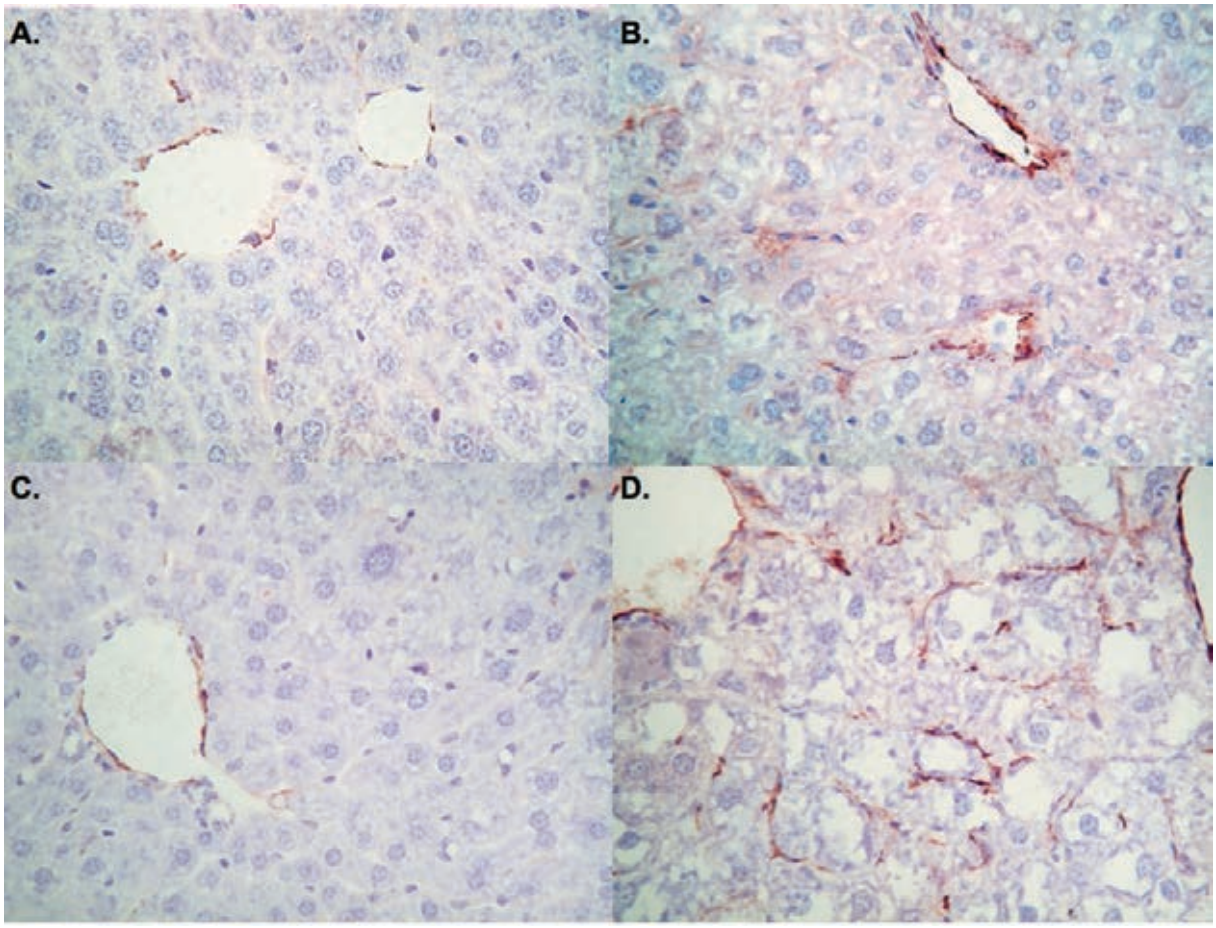

Figure 3.2. Alpha smooth muscle actin (αSMA) immunohistochemistry demonstrates hepatic stellate cell activation in ALIOS mice. Representative examples of livers from mice fed: **A**, normal chow for 6 months; **B**, ALIOS for 6 months; **C**, normal chow for 12 months; and **D**, ALIOS for 12 months. Numerous αSMA-positive perisinusoidal cells, in keeping with activated stellate cells, are present in mice fed ALIOS for 12 months (D). In the other groups, αSMA staining is largely confined to blood vessels

3.2.2. Increased expression of lipid metabolism and insulin signalling genes in ALIOS mice. Expression of *ACACA* (acetyl-CoA carboxylase 1) and *FASN* (fatty acid synthase), genes coding for key regulators of lipogenesis, were increased in ALIOS mice at 6 months and decreased at 12 months compared to NC mice (**Fig 3.3A,B**). Expression of *CPT1A* (carnitine palmitoyltransferase 1), a rate-limiting enzyme necessary for beta-oxidation of long chain fatty acids, was increased in ALIOS mice at 6 months compared to NC mice (**Fig 3.3C**). Although the activity of these gene products is mainly regulated at the post-transcriptional levels, these data represent increased lipid turnover (increased lipogenesis and beta-oxidation) in livers of ALIOS mice. Expression of *INSR* (insulin receptor), *IRS1* (insulin receptor substrate 1) and *IRS2* (insulin receptor substrate 2) were increased in ALIOS mice at 6 months compared to NC mice but not at 12 months (**Fig 3.3D,E,F**). Up-regulation of these genes at 6 months that is lost by 12 months may demonstrate a failure to compensate for dietary stresses in ALIOS mice by 12 months.

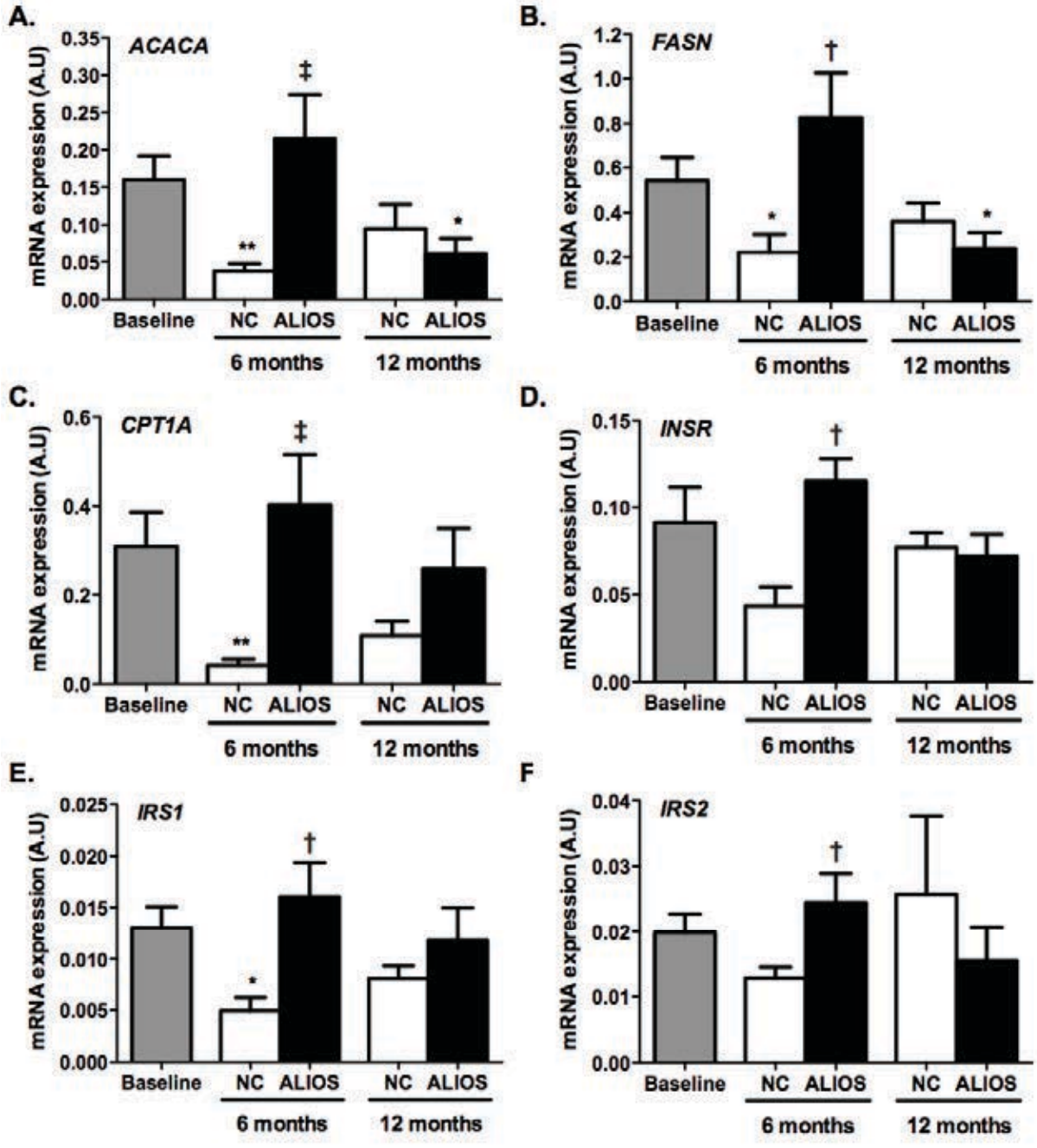

Figure 3.3. Increased lipid turnover in ALIOS mice at 6 months. Hepatic mRNA expression of: **A,** acetyl CoA carboxylase; **B,** fatty acid synthase; **C,** carnitine palmitoyltransferase; **D,** insulin receptor; **E,** insulin receptor substrate 1; and **F,** insulin receptor substrate 2 measured by real-time PCR in mice fed normal chow (black bars) or ALIOS diet (grey bars) for either 6 or 12 months. Additional comparisons are made against baseline liver samples (white bars) (* $p<0.05$, **$p<0.01$ vs. baseline, † $p<0.05$, ‡ $p<0.01$ vs. normal chow). Data are expressed as arbitrary units (A.U.) with data from 8-10 animals in each group

3.2.3. ALIOS mice develop histological features of NASH. Baseline (8-week old) mice displayed no evidence of liver injury or steatosis (**Fig 3.4A**), whereas NC mice developed mild steatosis with mixed droplet size which had a predominantly peri-venular distribution at 12 months (**Fig 3.4B**). In mice on ALIOS steatosis was more severe and diffuse, and progressed with time. Moderate steatosis was observed in NC mice by 12 months.

Moderate macro-vesicular steatosis with a predominantly peri-portal distribution was typically seen at 6 months (**Fig 3.4C**). This pattern of steatosis persisted for ALIOS mice at 12 months by which time there was also prominent micro-vesicular steatosis in peri-venular regions (**Fig 3.4D)**. Steatosis was mild or moderate after 6 months of ALIOS diet (**Fig 3.4C**) and severe in 9/10 mice at 12 months (**Fig 3.4D**). The presence of ballooned hepatocytes and Mallory-Denk bodies are characteristic features of NASH[149].

Distinction of ballooned hepatocytes from the frequently extensive micro-vesicular steatosis made assessment of this histological feature difficult. Although occasional cells with a ballooned appearance were initially thought to be present in H&E stained sections from ALIOS mice at 6 and 12 months (**Fig 3.6A**), no definite Mallory-Denk bodies were identified by immunostaining for ubiquitin or K18 (**Fig 3.5**).

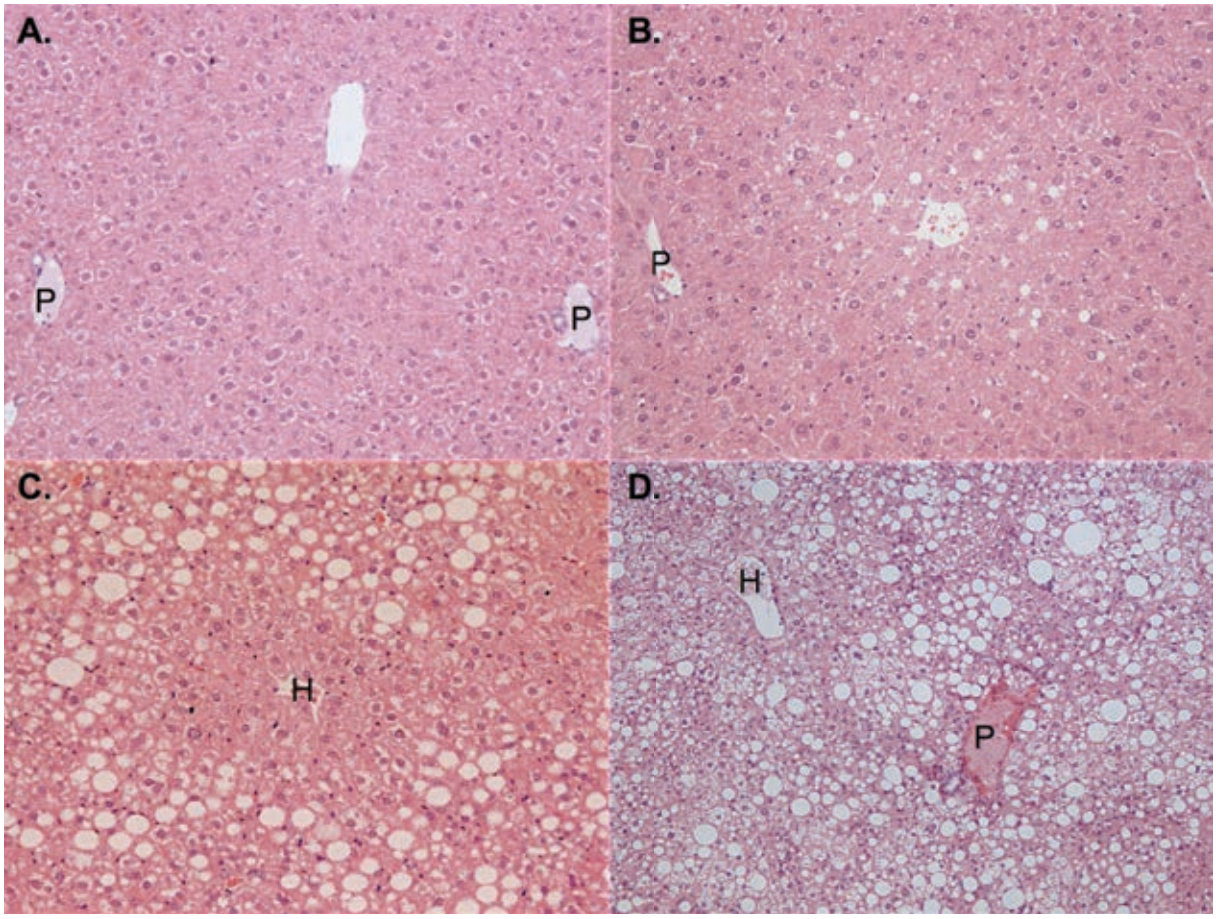

Figure 3.4. ALIOS mice develop moderate steatosis at 6 months becoming severe at 12 months. All sections stained with haematoxylin and eosin. **A,** Baseline mouse (8 weeks old) shows no evidence of steatosis. **B,** Normal chow mouse at 12 months shows very mild peri-venular steatosis. **C,** Moderate macro-vesicular steatosis with a predominantly peri-portal distribution in an ALIOS mouse at 6 months. **D,** Severe pan-lobular steatosis in an ALIOS mouse at 12 months. Macro-vesicular steatosis still has a mainly peri-portal distribution. Micro-vesicular steatosis is more prominent in peri-venular regions. H = hepatic vein, P = portal tract

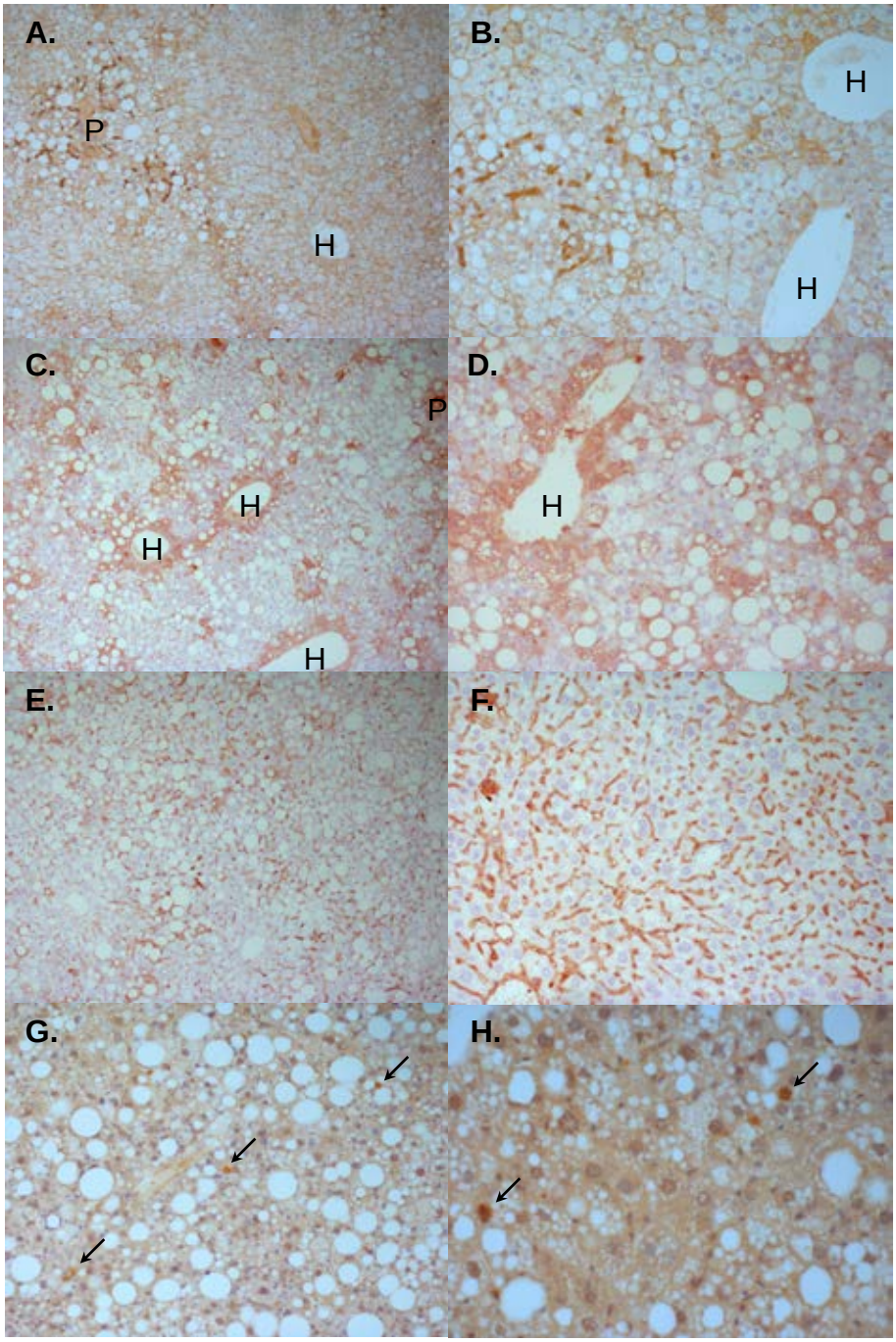

Figure 3.5. CK18 and ubiquitin immunohistochemistry fail to detect evidence of hepatocyte ballooning in response to ALIOS. A, 100x image and **B,** 200x image of CK18 immunohistochemistry of 12 month ALIOS liver showing prominent staining of ductular reactive cells and less intense membranous staining of hepatocytes. **C-F,** CAM5.2 immunohistochemistry of 12 month ALIOS liver showing both patchy, predominantly peri-venular cytoplasmic staining of hepatocytes (**C**, 100x, **D**, 200x) and diffuse sinusoidal staining (**E**, 100x, **F**, 200x) in different regions of the same section. **G**, 200x image and **H,** 400x image of ubiquitin immunohistochemistry of 12 month ALIOS liver demonstrating presence of highly stained aggregates in hepatocytes (arrows). H = hepatic vein, P = portal tract

For all animals the ballooning component of the NAS was thus scored as 0. ALIOS induced lobular inflammation in 7/10 ALIOS-fed at 6 months that was not observed in any NC mice at this time point. At 12 months lobular inflammation was present in 9/10 of the ALIOS cohort and 2/9 chow-fed mice. Lobular inflammatory cells comprised a mixed population of lymphocytes and neutrophils (**Fig 3.6B**), with peri-portal inflammatory infiltrates observed in 4/10 ALIOS mice at 12 months (**Fig 3.6C**). Fibrosis was observed histologically in 8/10 ALIOS and 1/9 chow-fed mice at 12 months. In all cases, fibrosis had a peri-sinusoidal pattern similar to that observed in human NASH. Amongst ALIOS mice at 12 months, fibrosis severity ranged from mild peri-portal through to bridging fibrosis. The latter was characterised by the presence of diffuse dissection of the parenchyma by delicate strands of peri-sinusoidal collagen without the development of broader fibrous septa (**Fig 3.6D)**. The single NC mouse with fibrosis at 12 months only had mild peri-portal fibrosis. Cirrhosis was not observed in any mice.

The use of the Kleiner histological system (NAS) demonstrated significantly increased severity of steatosis grade (**Fig 3.7A,** $p=0.003$), lobular inflammation (**Fig 3.7B,** $p<0.0001$) and fibrosis stage (**Fig 3.7C,** $p=0.001$**)** in ALIOS mice compared to NC mice at 12 months. At 6 months, 0/10 NC mice scored for any components of NAS, whilst ALIOS fed mice had a mean NAS of 2.4 (SEM 0.6). By 12 months, NC mice had a mean NAS of 1.3 (SEM 0.4) and ALIOS-fed mice a mean NAS of 5.0 (SEM 0.6) (**Fig 3.7D,** $p<0.001$).

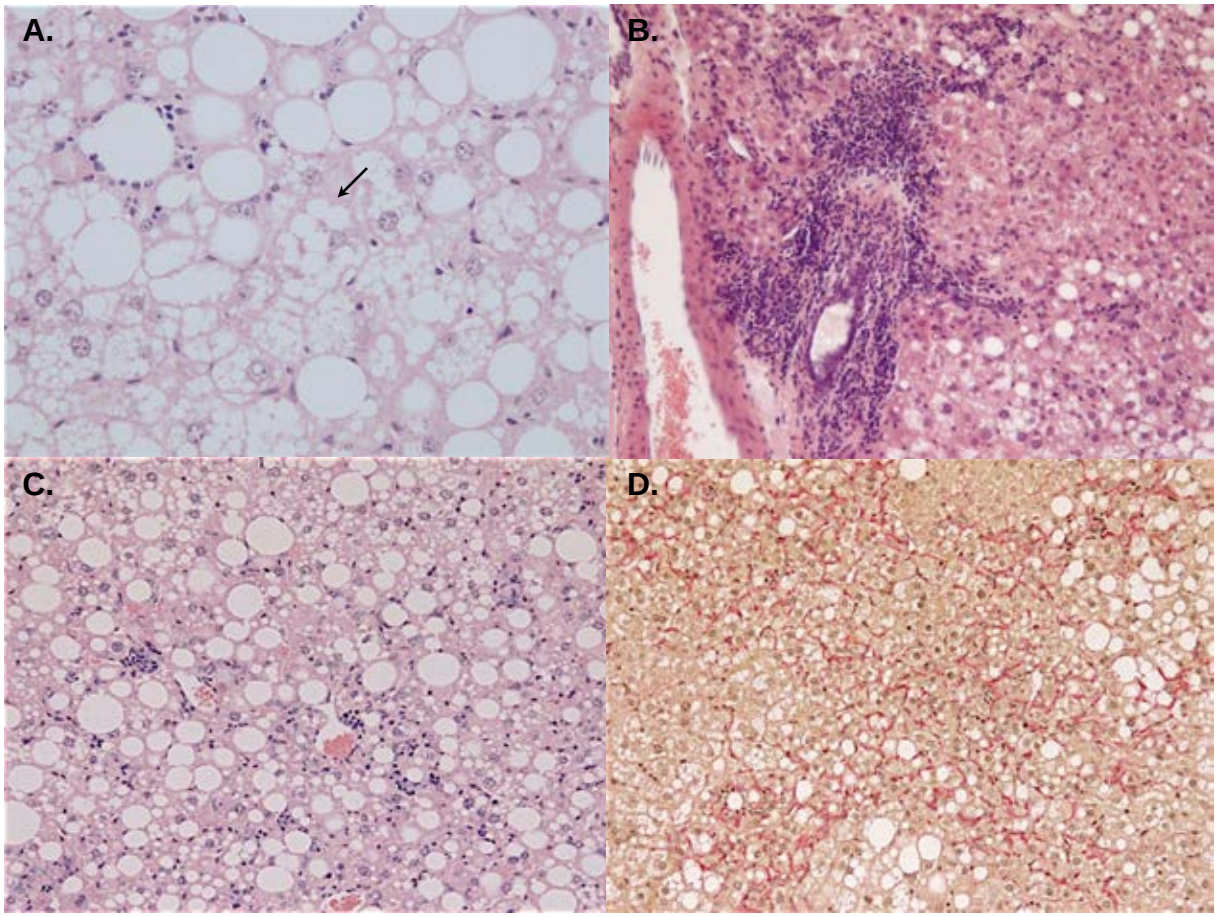

Figure 3.6. ALIOS mice develop histological features of NASH. A, Mixed large and small droplet fatty change in an ALIOS mouse at 12 months. The arrow indicates a cell thought to have possible ballooning. However, no definite Mallory-Denk bodies were demonstrated by immunostaining for ubiquitin and K18 (data not shown). **B,** Portal inflammation and **C,** lobular inflammation in an ALIOS mouse at 12 months. **D,** Peri-cellular and bridging fibrosis in an ALIOS mouse at 12 months. **Figs A-C** - Haematoxylin and Eosin, **Fig D** - Van Gieson

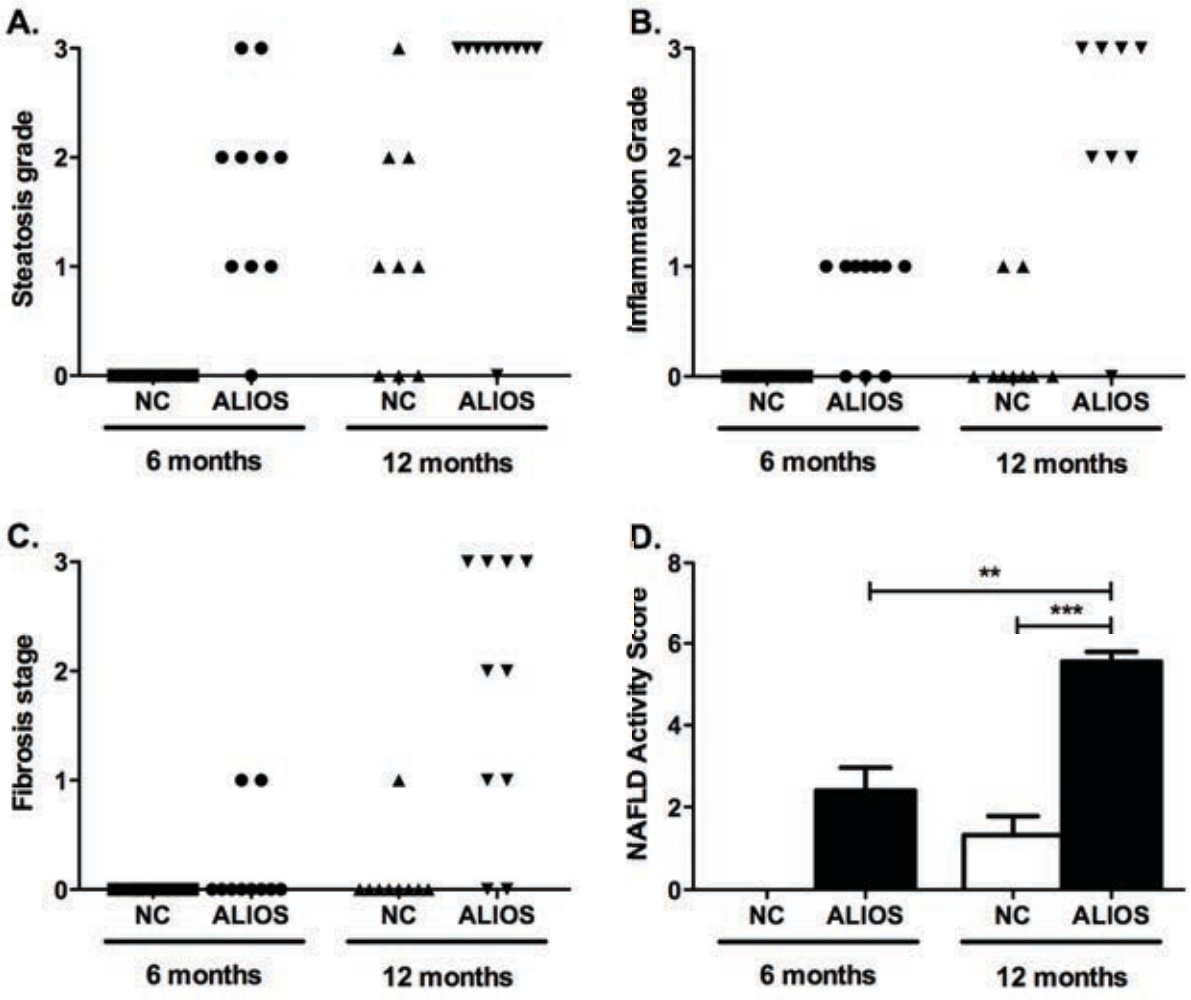

Figure 3.7. Histological scoring of non-alcoholic liver disease severity in ALIOS mice. A, Steatosis grade scores, **B,** lobular inflammation scores, **C,** fibrosis stage scores and **D,** total NAFLD activity scores (NAS) according to the Kleiner histological scoring system. Error bars represent SEM *$p \leq 0.05$; ***$p \leq 0.001$; (student's t-test).

3.2.4. Hepatic stem cell activation in ALIOS mice correlates with histological features of NASH. Pan-CK immunohistochemistry has been previously used to identify hepatic progenitor (oval cells) and ductular reactive cells in rodents[150]. More recently Sox9, a nuclear transcription factor, has been reported as a marker of hepatic progenitor cells[75], allowing a more specific population of stem/progenitor cells to be identified by immunohistochemistry than with pan-CK. Pan-CK and Sox9 expression in livers of baseline mice had a similar pattern to those of NC mice at 12 months. Pan-CK expression was largely restricted to the biliary epithelium (**Fig 3.8A**), and Sox9 immunostaining was likewise positive within the biliary epithelium (**Fig 3.8B**). In contrast, by 12 months ALIOS mice had greatly increased numbers of pan-CK^+ and $Sox9^+$ cells observed throughout the parenchyma in addition to cells located within the biliary epithelium seen in chow-fed animals (**Fig 3.8C,D**). This observation was confirmed by quantification of the percentage area covered by pan-CK^+ cells and the number of observed $Sox9^+$ cells per area (**Fig 3.8E,F**). Increased accumulation of pan-CK^+ and $Sox9^+$ cells was seen with severe steatosis (score = 3), lobular inflammation (score $\geq$ 2) and fibrosis severity (**Fig 3.8G,H**).

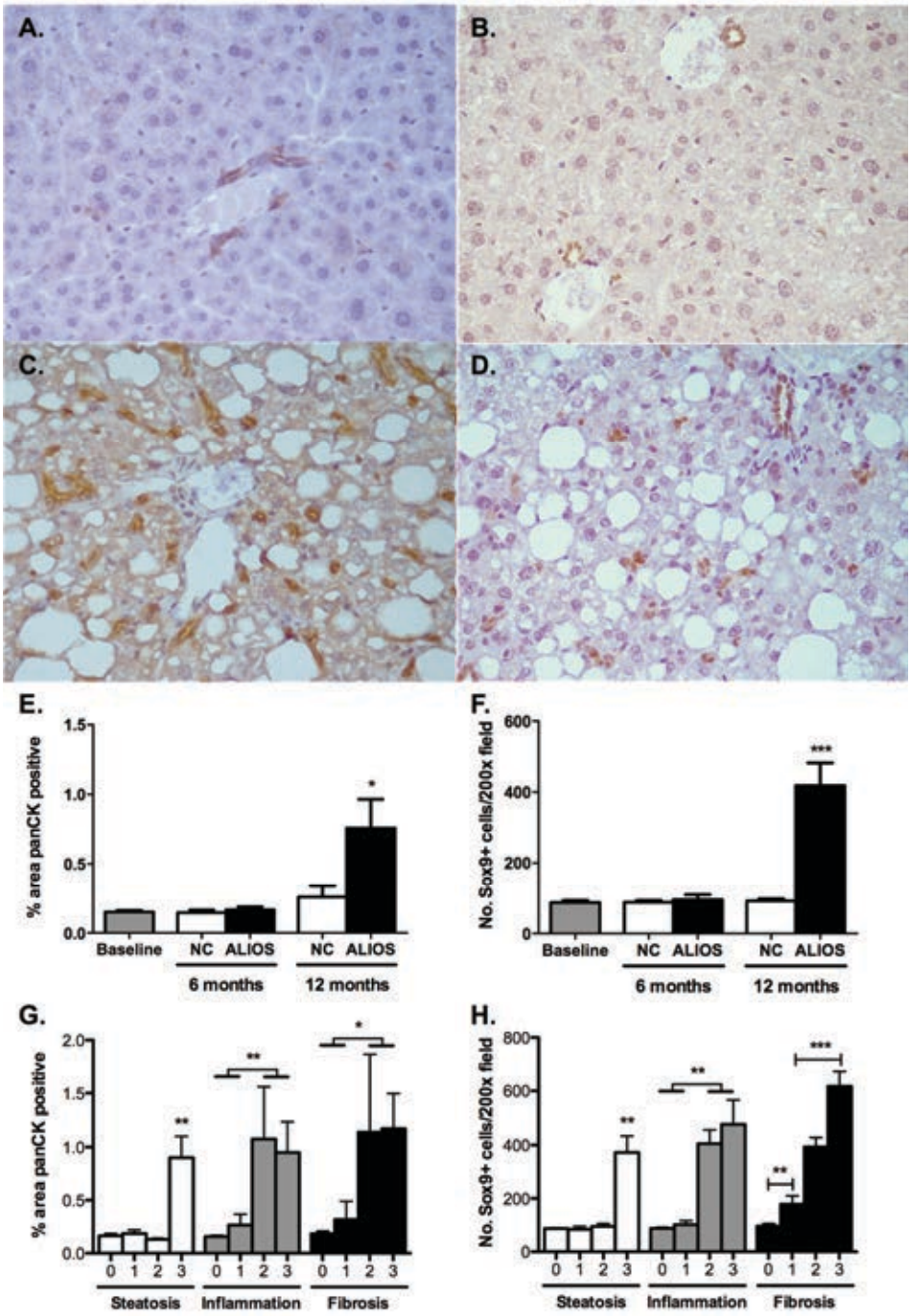

Figure 3.8. Hepatic stem cell activation in ALIOS mice correlates with histological features of NASH. Representative examples of **A,** pan-CK and **B,** Sox9 immunohistochemistry of livers from NC mice at 12 months. Representative examples of **C,** pan-CK and **D,** Sox9 immunohistochemistry of livers from ALIOS mice at 12 months. **E,** Mean percentage area covered by pan-CK$^+$ cells and **F,** average number of Sox9$^+$ per 200x field, in liver sections from baseline, NC and ALIOS mice. Correlation between histological scores and **G,** mean percentage covered by pan-CK$^+$ cells and **H,** average number for Sox9$^+$ cells per 200x field. Error bars represent SEM *$p \leq 0.05$; **$p \leq 0.01$; ***$p \leq 0.001$ (ANOVA with Bonferroni's correction)

3.2.5. ALIOS mice develop hepatocellular neoplasms containing perivascular Sox9^{+} tumour cells. At 12 months mice were killed and organs were harvested for analysis and storage. At this time point some livers excised from ALIOS mice had macroscopically visible growths. As tumours had not previously been reported in murine dietary models of steatosis or liver disease we undertook a detailed histological examination of all livers from both ALIOS and NC mice at 12 months.

A total of 9 lesions (5 macroscopic and 4 microscopic) were observed in 6/10 (60%) ALIOS mice (**Table 3.1**). Macroscopically visible nodules (diameter >3mm) developed in 4/10 (40%) of ALIOS mice at 12 months (**Fig 3.9A**), of which two were found in one mouse. No macroscopic nodules or microscopic foci of atypical hepatocytes were seen in any NC mice.

All of the lesions identified macroscopically and microscopically were well–circumscribed and well-differentiated. Macroscopic lesions (**Fig 3.9A)** were associated with compression of adjacent non-lesional tissue, but no invasion of blood vessels, portal tract stroma or surrounding liver tissue was seen. Histological examination showed lesions composed of hepatocytes with low-grade cytological atypia in the form of mild nuclear pleomorphism, a slightly increased nuclear/cytoplasmic ratio and occasional mitoses. Microscopic foci (< 1mm diameter) composed of atypical hepatocytes with a similar appearance were present in a further two ALIOS-fed mice (**Fig 3.9B**). In the absence of evidence of invasion to confirm a definite diagnosis of malignancy lesions were further characterised using additional markers (**Table 3.1**) that have been shown to be altered in previous studies of rodent models[151, 152], and/or human HCC[153, 154].

Table 3.1. Characteristics of hepatic lesions in mice fed ALIOS diet for 12 months

Lesion Number	Animal Number	Lesion Description	Size	Reticulin Fibre Depletion	Glutamine Synthetase	β-cat	Sox9	AFP	PI-FC
1	2	Microscopic	<1mm	+	2	-	-	-	1.61
2	2	Microscopic	<1mm	+	N/A	-	+	-	2.05
3	3	Macroscopic	3mm	+	3	-	+	-	2.82
4	3	Macroscopic	3mm	+	2	+	-	-	17.58
5	3	Microscopic	<1mm	+	2	+	-	-	14.17
6	4	Microscopic	<1mm	-	2	+	-	-	7.89
7	4	Macroscopic	6mm	+	2	-	+	+	3.42
8	5	Macroscopic	5mm	+	1	-	+	+	6.8
9	6	Macroscopic	10mm	+	3	-	+	+	6.96

Glutamine synthetase, 1-normal perivenular pattern, 2-diffuse upregulation, 3-absence; **β-cat**, presence of nuclear accumulation of β-catenin; **AFP,** presence of alpha-foetoprotein; **PI-FC**, Proliferation index (% $Ki67^{+}$) fold change in tumour vs. background liver

Alpha-foetoprotein (AFP) is expressed by hepatoblasts during liver development but is absent in rodent and adult liver[2]. AFP has been shown to be re-expressed by a subset of HCC associated with increased aggression and worse prognosis with features characteristic of hepatic stem/progenitor cells. Detection of circulating AFP is routinely utilised clinically in the screening and early detection of HCC in high-risk patients[133]. A small proportion of AFP^+ tumour cells in 3/5 macroscopic lesions were observed in ALIOS mice (**Fig 3.9C**) but absent in microscopic lesions and background liver of all mice. Loss of the normal reticulin fibre pattern is a characteristic feature of human HCC, although reticulin fibres are sometimes retained in well-differentiated neoplasms. Reticulin staining was difficult to assess as it was somewhat patchy in non-lesional liver tissue. However, a clear reduction in the number of reticulin fibres present could be observed in all (5/5) macroscopically visible nodules from ALIOS-fed mice **(Fig 3.9D)**. Reticulin fibres also appeared to be reduced, to a lesser extent, in 3/4 microscopic foci. Up-regulation of glutamine synthetase (GS) expression is a feature that has been used to distinguish well-differentiated HCC from pre-malignant lesions in the human liver[155]. In non-lesional liver, a peri-venular distribution of GS was observed, similar to the pattern of expression seen in normal human liver (**Fig 3.10A**). Diffuse staining for GS was present in 3/4 of the atypical microscopic foci seen in ALIOS-fed mice, similar to the pattern that has been described in human HCC (**Fig 3.10B**). Interestingly, 3/5 macroscopic nodules appeared to have a reduced expression of GS, with loss of the normal peri-venular pattern of staining (**Fig 3.10A,B**). Aberrant nuclear accumulation of β-catenin is indicative of tumourigenesis and associated with increased tumour progression and a worse prognosis[156]. A small proportion (<5%) of tumour cells in three lesions (one macroscopic and two microscopic) displayed nuclear accumulation of β-catenin (**Fig 3.10C**).

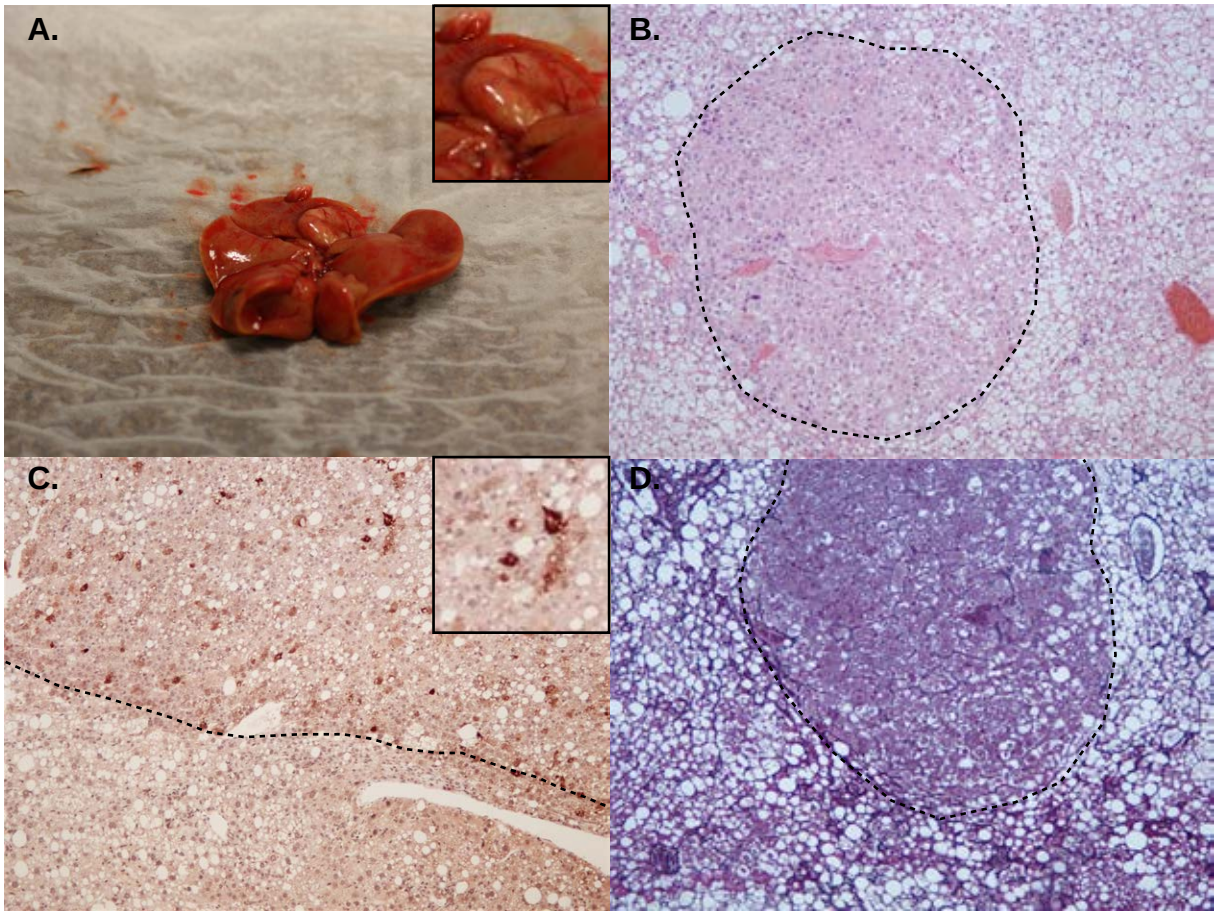

Figure 3.9. ALIOS mice develop hepatocellular carcinoma after 12 months duration. **A,** Representative example of macroscopic hepatocellular lesion from ALIOS mouse at 12 months. **B,** Representative example of microscopic hepatocellular lesion from NC mouse at 12 months by H&E staining. **C,** AFP immunohistochemistry of macroscopic hepatocellular lesion demonstrating presence of AFP^{+} tumour cells. **D,** Representative example of absent reticulin staining in a macroscopic hepatocellular lesion from ALIOS mouse at 12 months. There is compression of the normal reticulin framework in surrounding non-lesional tissue

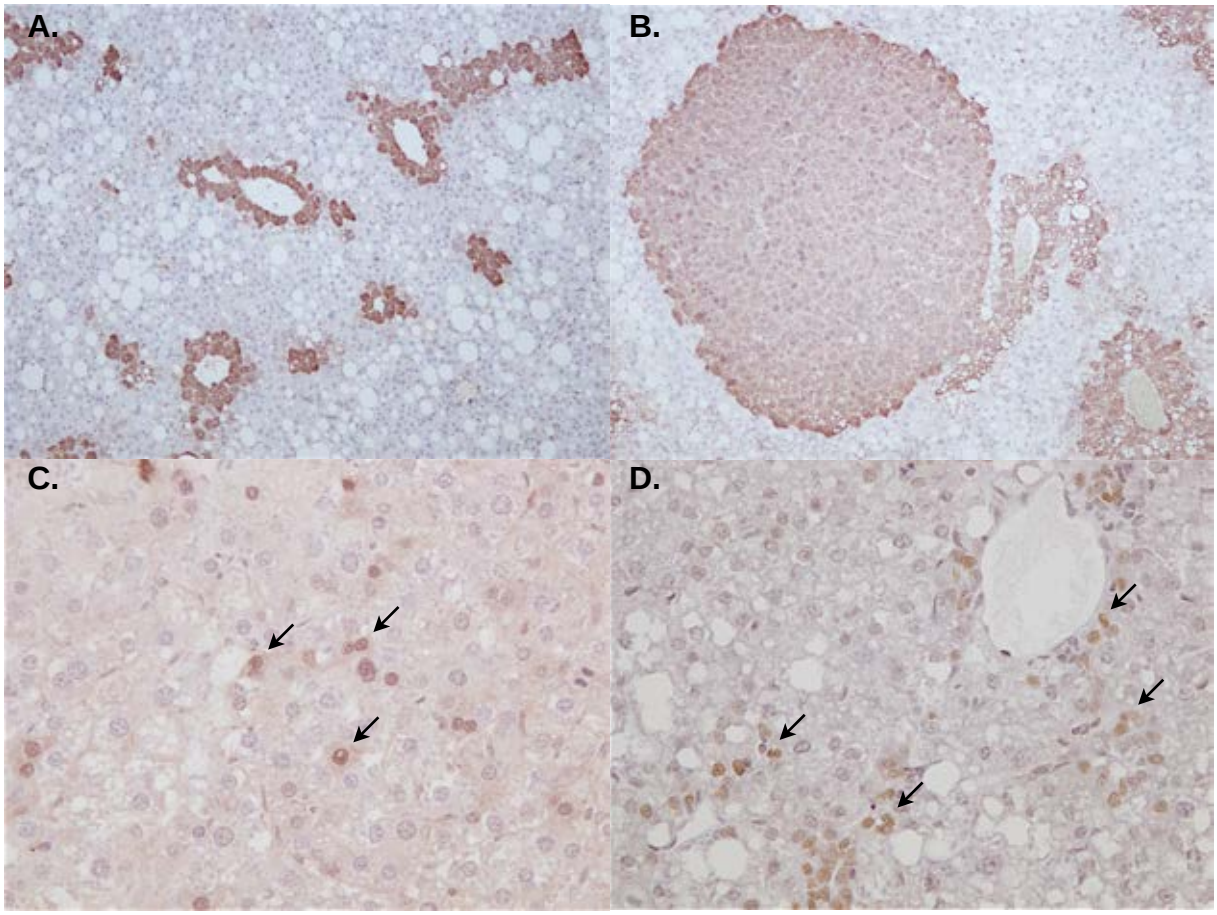

Figure 3.10. Hepatocellular lesions from ALIOS mice have aberrant glutamine synthetase expression and contain Sox9^{+} tumours cells. Examples of glutamine synthetase immunohistochemistry of **A,** liver from baseline mice and **B,** microscopic lesion from ALIOS mouse at 12 months. **C,** Example of nuclear accumulation of β-catenin (arrows) in cells of hepatocellular lesion from ALIOS mouse at 12 months. **D,** Example of perivascular Sox9^{+} tumour cells (arrows) of hepatocellular lesion from ALIOS mouse at 12 months

Sox9, a marker of mHpSC and primitive stem cells of the biliary and intestinal epithelium[9], was observed in the nuclei of neoplastic hepatocytes in five nodules (four macroscopic and one microscopic). These appeared to be preferentially located in a perivascular distribution, but otherwise had a similar morphology to surrounding tumour cells, without obvious evidence of biliary differentiation (**Fig 3.10D**).

Using Ki67 immunohistochemistry (**Table 3.1**), increased proportions of proliferating hepatocytic tumour cells were observed when compared with the proportion of proliferating hepatocytes in background liver (16.0±7.3% vs. 3.0±1.6%, p=0.001). Moreover, turnover was higher in nodules containing tumour cells with nuclear accumulation of β-catenin; fold change in proliferation index over background (13.2±4.9 vs. 3.9±2.4, p=0.005).

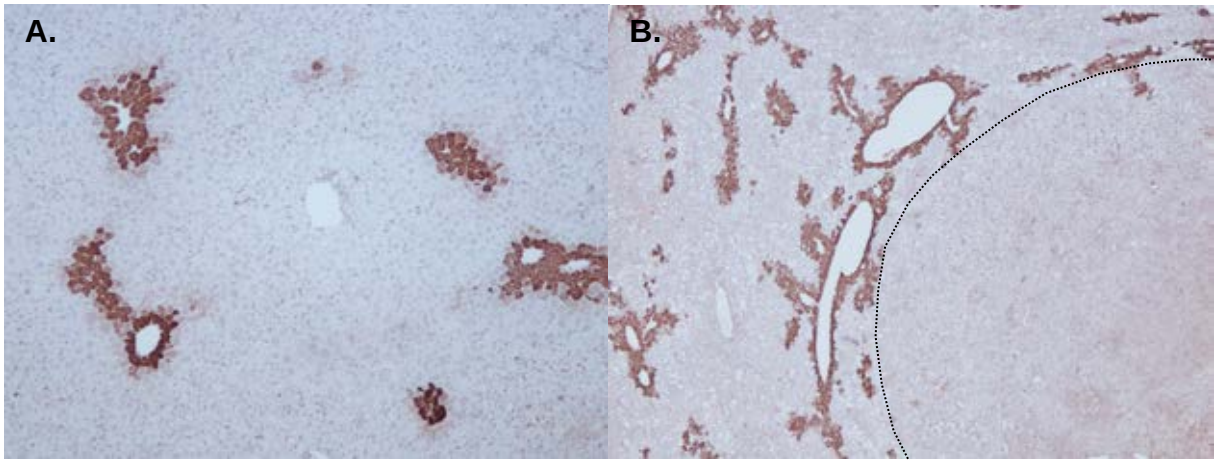

Figure 3.11. Glutamine synthetase immunohistochemistry of baseline liver and a representative hepatic neoplasm from ALIOS mouse at 12 months. A, Glutamine synthetase immunohistochemistry in liver of baseline mouse demonstrating perivenular pattern of expression. **B,** Glutamine synthetase immunohistochemistry in liver of ALIOS mouse demonstrating perivenular pattern of expression in background liver and absence in hepatic neoplasm (dashed line)

3.3. DISCUSSION

Mice exposed to the ALIOS lifestyle for an extended period of 12 months develop a broad spectrum of NAFLD-related histological changes including severe steatosis, lobular inflammation, fibrosis and hepatocellular neoplasia. This study demonstrates for the first time in a clinically relevant model of NASH, a marked expansion of mouse HpSC, and their close association with neoplastic foci in response to high fat diet alone.

NAFLD is an increasingly prevalent cause of liver disease, but no satisfactory murine model of NAFLD has been developed restricting our ability to dissect disease processes and the development of new treatments. Combination of TFA and HFCS, two common dietary components implicated in NAFLD pathogenesis, with restricted access to exercise was reported to induce features of NASH after 16 weeks by Tetri *et al.*, although histological fibrosis was not seen[148]. In this study, extending the ALIOS diet in mice for up to 12 months recapitulated the full spectrum of disease with inflammation (NASH), advanced fibrosis and the development of hepatocellular neoplasia.

The distribution of steatosis observed in ALIOS mice was of an initial predominantly macro-vesicular peri-portal steatosis with relative sparing of acinar zones 2 and 3. With time and disease progression, increasing micro-vesicular steatosis extending into the centri-lobular region was observed. A similar zonal variation in the distribution of micro and macro-vesicular steatosis in ALIOS mice was also observed in the study by Tetri *et al.*[148]. The mechanisms accounting for these differences in fat distribution remain to be elucidated, however possible explanations include differences in lipid and/or glucose metabolism, or a differential responsiveness of hepatocytes to insulin signalling in different acinar zones. Of

note, the extensive microvesicular steatosis observed with the ALIOS diet may also reflect more progressive disease, as a recent large study demonstrated that this feature correlated with more severe histological changes in human NAFLD liver biopsies[157]. Quantification of liver triglyceride confirmed these histological findings, with significantly greater triglyceride in the ALIOS livers compared with controls at 6 months, although by 12 months this difference was reduced by a significant increase in the control group. This observation is again consistent with the predisposition of ageing mice to the development of a metabolic phenotype[158].

Although developed for assessing the severity of NAFLD in human liver tissue, the NAS has also been used in other murine studies. In the current study NAS was significantly higher in the ALIOS cohort at both 6- and 12-months. By 12 months, although several of the control mice had developed some features of NAFLD (i.e. mainly steatosis), NAS scores in the ALIOS group were significantly higher. The assessment of hepatocyte ballooning in humans is used diagnostically, yet our understanding of the causative contribution of hepatocyte ballooning in the pathogenesis of NASH remains unclear. Despite applying three staining techniques routinely used for the assessment of ballooning (H&E, Ubiquitin, and K18) the presence of hepatocyte ballooning was not observed in response to ALIOS**.** The use of haematoxylin and eosin staining revealed occasional cells that had changes potentially suggestive of ballooning that was difficult to fully discern from the presence of micro-vesicular steatosis. Ubiquitin and CK18 immunohistochemistry allow for more specific identification of ballooned hepatocytes through the detection of ubiquitinylated cytokeratin aggregates (Mallory-Denk bodies) that are characteristic of ballooning resulting from

NASH[149]. The use of a CK18 primary antibody (Dako) routinely used in the Histology Department at the QEHB and predicted to cross-react with mouse yielded a pattern of expression in mouse that significantly differed to that seen in humans. CK18 immunohistochemistry of clinical liver specimens demonstrates prominent membranous staining of hepatocytes, the condensation and aggregation of which into Mallory-Denk bodies signifies hepatocyte ballooning. However in murine sections from ALIOS mice, CK18 immunohistochemistry predominantly stained ductules and ductular reactive cells with weak, patchy staining of hepatocytes that was variably cytoplasmic and membranous making assessment of hepatocyte ballooning difficult. The use of a second antibody utilised clinically (CAM5.2, Dako) again yielded different expression patterns in mouse versus human samples. CAM5.2 immunohistochemistry demonstrated areas of both hepatocytic and sinusoidal staining within the same section suggesting non-specific staining possibly due to variation in fixation levels. CAM5.2 staining of hepatocytes was largely cytoplasmic with no obvious examples of hepatocyte ballooning observed. Ubiquitin immunohistochemistry revealed infrequent staining of apparent protein aggregates in parenchymal cells that possibly represent Mallory-Denk bodies. These observations appear to be similar to those of Tetri *et al.* who observed in their 16-week model of ALIOS that “some cytoplasm alterations and clumping suggestive of “ballooning” and possible Mallory hyaline were noted in zone 3”[148]. However, only H&E staining was reported in this study and additional immunohistochemistry was not used to confirm the presence of Mallory-Denk bodies. It was not possible to discern whether the lack of ballooning in this study was due to intrinsic variation between rodent and human liver injury, or the extended duration of the ALIOS diet to 6 and 12 months. Severe steatosis, bridging fibrosis and hepatic stem cell activation was observed in the ALIOS model at 12

months. However, differences between murine and human histopathology was observed in the pattern and distribution of steatosis, fibrosis and stem cell proliferation (**Table 3.2**).

Histological fibrosis was observed in only two of the ALIOS mice and no control animals at 6 months, and in both cases was in a peri-portal (stage 1c) distribution. However *COL1A1* mRNA expression was 4.2-fold higher in the ALIOS mice at this time point, providing additional evidence of an early fibrotic response. By 12 months, fibrosis was observed in only one (10%) of the controls but in eight (80%) of the ALIOS mice, four of which demonstrated bridging fibrosis. The >10-fold increase in Col1α1 expression in the ALIOS cohort at this time point was consistent with these findings.

The presence of hHpSC was originally suggested by immunohistochemical studies that placed the intra-hepatic stem cell niche within the canals of Hering[79]. Isolation of adult human hepatic and biliary stem cells has since demonstrated substantial expansion potential *in vitro* with differentiation to both biliary and hepatocyte lineages, prompting interest in hepatic stem cells as a potentially viable therapeutic option for liver disease. Complementary studies utilising transgenic mice have identified and characterised bipotential mHpSCs that readily proliferate and differentiate to cholangiocytes and hepatocytes in culture[75]. However, murine models of liver injury that faithfully replicate the complex pathogenesis of human liver disease are currently lacking and as such the role of hepatic stem cells, and the mechanisms of their activation, in these settings remains poorly understood.

Table 3.2. Comparison of human NASH and the murine ALIOS model

	Human NASH	Murine ALIOS
Clinical features		
Cause	Multifactorial (Diet/environment/ genetics)	Diet alone
Body weight	Significant association with obesity and central adiposity	Weight gain (then subsequent loss with severe disease burden)
Hepatomegaly	Clinical sign (not present in all cases)	Increased liver to body weight ratios at 6 and 12 months
Glucose intolerance (diabetes)	Significant association with insulin resistance and type 2 diabetes. Reciprocal risk factors	Glucose intolerance observed at 6 months
Blood markers	Elevated ALT and AST, but can have significant disease with normal LFTs	Elevated ALT and AST at 12 months
Hepatic Tumourigenesis	Significant risk of HCC development in NASH cirrhosis (vs. normal population)	Hepatocellular lesions observed in 50% of animals at 12 months
Histopathology		
Steatosis distribution and pattern	Early stages = perivenular macrovesicular Later stages = panacinar with mixture of macro- and microvesicular steatosis	6-months = Periportal macrovesicular steatosis 12-months = Periportal macrovesicular and perivenular microvesicular steatosis
Steatosis severity	Variable. In end-stage cirrhosis steatosis may be absent	6-months = Moderate 12-months = Severe
Inflammation	Portal and lobular inflammation	Portal and lobular inflammation
Hepatocyte ballooning	Diagnostic of ‘definite’ NASH (AGA guidelines 2012)	Not identified
Fibrosis	Perisinusoidal +/- periportal progressing to bridging fibrosis. Broad septa and nodules (cirrhosis) in late stage disease	Perisinusoidal +/- periportal progressing to bridging pericellular fibrosis at 12 months. No broad septa or cirrhosis at 12 months
Hepatic stem/progenitor cells	Activation of hepatic progenitor cells commonly seen in periportal and periseptal ductular reactions	Periportal expansion of hepatic progenitors into surrounding parenchyma observed as single cells and ductules

Currently used rodent models of chronic hepatic injury, HpSC activation and hepatocarcinogenesis rely upon the use of toxic agents[159] or genetic manipulations[160] that fail to replicate the complex pathogenesis of NAFLD. This study provides the first detailed characterisation of a clinically relevant murine model of metabolic liver injury and provides new data on the spatio-temporal association between NAFLD, mHpSC activation and the development of hepatic dysplasia/cancer. In human disease, loss of mature biliary epithelial cells and hepatocytes, as occurs in chronic biliary diseases and metabolic liver disease respectively, results in a marked accumulation of hHpSC[10, 100, 138]. Activation of the mHpSC niche has been extensively studied in a range of murine liver injury models, including genetic[140], diet[116], bile duct ligation[97] and alcohol[161], but activation in non-toxic diet models using wild-type mice has previously not been reported. This study demonstrates activation of the mHpSC niche in response to the ALIOS model of chronic metabolic liver injury using pan-CK and Sox9 immunohistochemistry. The number of mHpSC observed increased with duration, and severity of liver injury, but were largely absent from NC mice. These findings support the observation of a close association between hHpSC activation and histological features of chronic liver injury in humans[69].

The novel finding of hepatocellular neoplasms in 6/10 ALIOS mice has not been previously reported, and is of significant concern given the high population consumption of both HFCS and TFA. HCC is a well-recognised complication of advanced NASH in humans, and is also increasingly recognised to occur in non-cirrhotic NASH[162]. Most cases of HCC in this study developed on a background of significant fibrosis, however one occurred in the absence of any detectable fibrosis in the surrounding liver. Potential carcinogenic mediators associated

with both the metabolic syndrome and NASH include hyperinsulinaemia, lipid peroxidation and oxidative stress, which may promote cellular proliferation or epigenetic aberrations.

Previous rodent models of HCC have described the development of a spectrum of similar focal hepatocellular lesions[151, 152], which have been variously classified as "pre-neoplastic foci", "dysplastic foci" "adenoma" and "benign hepatoma" as well as hepatocellular carcinoma. Similar problems have been encountered with the classification of precursor lesions and early HCC in human livers[153, 154].

The extent to which the murine lesions are comparable to hepatocellular neoplasms in human liver has not been fully established. In an attempt to address this problem, detailed characterisation was carried out, using many of the markers used to diagnose early HCC in human livers. This revealed many features consistent with that of early human HCC including the loss of biliary structures, disruption or loss of reticulin fibres, aberrant expression of glutamine synthetase and AFP and nuclear accumulation of β-catenin. These changes were accompanied by varying degrees of cytological atypia that are also recognised as a feature of human HCC, establishing this as a novel model for the study of HCC development on the background of NASH.

Sox9 is a marker of endodermal stem cells in liver, pancreas, biliary tree, and intestine[9] and its expression is associated with progression of a number of tumours[163-165]. Whilst studies have suggested a causal link between hHpSC and HCC development[140], a direct link between $Sox9^+$ hHpSC and HCC development and progression has yet to be described. In this study we report for the first time the presence of small foci of perivascular $Sox9^+$ tumour cells in murine HCC, which also notably express higher levels of Ki67 indicative of higher

proliferative rates. Increasing evidence suggests small populations of tumour cells possess significantly greater abilities for self-renewal and tumour initiation than other cells of the tumour bulk[166]. These cells also frequently express stem cell-related markers and are found in peri-vascular locations[167] suggesting the presence of peri-vascular $Sox9^+$ tumour cells may represent a cancer stem cell niche within HCC tumours of ALIOS mice. It is possible that these $Sox9^+$ cells represent a form of transitional cell between a stem cell and a neoplastic hepatocyte. We are unable to determine the cell of origin for the tumours observed in ALIOS mice or assess the contribution of $Sox9^+$ tumour cells to the development and progression of HCC, although their close spatial association requires further research. Further work utilising cell fate tracking experiments specifically labelling mHpSC in a relevant injury model will aid in determining the origin of $Sox9^+$ HCC tumour cells but was not possible in this study.

This clinically relevant murine model of NASH replicates many of the features seen in human disease as well as demonstrating activation of the hepatic stem cell niche. This study increases our limited understanding of stem cell mediated-regeneration and hepatocarcinogenesis in response to chronic metabolic liver injury and validates ALIOS as an appropriate model for further studies of NAFLD and HCC.

CHAPTER 4

PROSPECTIVE ISOLATION OF STEM/PROGENITOR CELLS FROM ADULT MURINE LIVER

4.1. RATIONALE FOR STUDY

Tissue-resident adult mesenchymal stem/progenitor cells have been described in the bone marrow, heart, lung and kidney. The presence of mesenchymal stem cells (MSCs) in adult bone marrow with the ability to form fat, bone, and cartilage is well accepted[168-170]. The selective isolation of multipotent mesenchymal stem cells from adult murine bone marrow using PDGFRα and Sca-1 was originally reported by Matsuzaki *et al.*[168, 171]. Tissue resident stromal stem/progenitor cell populations enriched for these antigens have subsequently been described in the heart[172-174], lung[175], kidney[176], and synovium[177]. Isolation of Sca-1^{+} cells from murine adult[178] and foetal/neonatal liver[31] has previously been described, where isolated cells display a predominantly stromal morphology with the appearance of small proportions of hepatocytic, ductal and endothelial cells observed after long-term *in vitro* culture. Although these studies have been unable to conclusively exclude the possibility that these cultures contained mixed populations of mature resident liver cells, they do provide evidence suggesting the presence of a rare, homogeneous population of somatic stem cells with liver-specific multipotency, including hepatocytic, biliary and stromal potential.

The presence of adult mesenchymal stem/progenitor cells in the liver is currently controversial. The presence of tissue specific somatic mesenchymal progenitors cells is increasingly accepted. In visceral organs, similar cells have been described and are variously termed angioblasts, vascular wall stem/progenitor cells or endothelial progenitor cells[30, 179]. These terms are likely to refer to similar, overlapping populations of cells found in, or directly

adjacent to, adult vasculature with the ability to differentiate into mesodermal lineages, notably endothelium and smooth muscle.

Prospective isolation of stromal populations from wild-type mouse liver has not been previously demonstrated. The prospective isolation of both murine hepatic stem cells (mHpSCs) and hepatic stellate cells from adult mouse liver remains challenging due to the lack of specific markers and culture conditions allowing long-term undifferentiated growth. Recent methods for the isolation of mHpSCs have relied upon the use of liver injury in transgenic mice to induce, and/or increase the number of, mHpSCs labelled by specific cre-lox recombination in $Lgr5^{+}$[115],$Sox9^{+}$[75] or $Foxl1^{+}$[76] cells. Hepatic stellate cells are most commonly isolated through density centrifugation by virtue of their lower density due to high lipid content[180]. The prospective isolation of HSCs, either by immuno-selection or cell sorting, has not been previously reported.

Stellate cells, or their precursors, may give rise to epithelial populations during regeneration. Recent studies have reported expression of markers of mature hepatocytes and cholangiocytes on freshly isolated stellate cells with lineage tracing experiments utilising markers specific to stellate cell markers in liver demonstrating the presence of mature hepatocytes and cholangiocytes derived from stellate cells in response to liver injury[18, 181].

PDGFRα has previously been reported as having a role in liver development and regeneration[182], Sca1 has been described as a marker of hepatic stem cells[178] and the combination of these antigens has been shown to identify potent mesenchymal stem/ progenitor cells in many visceral organs. Therefore, PDGFRα^{+}, Sca-1^{+} cells from adult, wild-type, uninjured mouse liver were isolated and their fibrogenic potential and capacity to give rise to epithelial stem/progenitor cells was assessed.

4.2. RESULTS

4.2.1. Presence of cells with characteristic mesenchymal stem cell expression profile in adult (6-8 week old) murine liver. Platelet derived growth factor-alpha (PDGFRα) immunohistochemistry on normal liver demonstrated the presence of PDGFRα$^+$ cells in predominantly peri-vascular locations with small numbers of positive cells observed in parenchymal regions. Immunohistochemistry with two PGFRα antibody clones stained the walls of all major vessels including the hepatic artery, portal and central veins. No obvious staining was observed in biliary epithelium or on mature hepatocytes. Parenchymal staining appears to mark cells with elongated, spindle-like morphology characteristic of stromal cells, although it was not possible to distinguish between fibroblasts and hepatic stellate cells by morphology alone. Positive cells were commonly observed in clusters forming strands in a pattern typical of peri-sinusoidal fibrosis despite the absence of injury **(Fig 4.1A-D).**

Stem cell antigen-1 (Sca1) immunohistochemistry on normal liver demonstrated the presence of Sca1$^+$ cells in predominantly peri-vascular locations, and possibly adjacent to biliary epithelium, with fewer numbers of positive cells observed than with PDGFRα immunohistochemistry. The majority of staining was restricted to vascular walls with staining more intense in the walls of hepatic arteries and portal veins than central veins. Sca1$^+$ cells are present in parenchymal locations commonly adjacent to vasculature. It was not possible to definitely determine the parenchymal cell type expressing Sca1 due to more diffuse and less intense staining on parenchymal cells (**Fig 4.1E,F**).

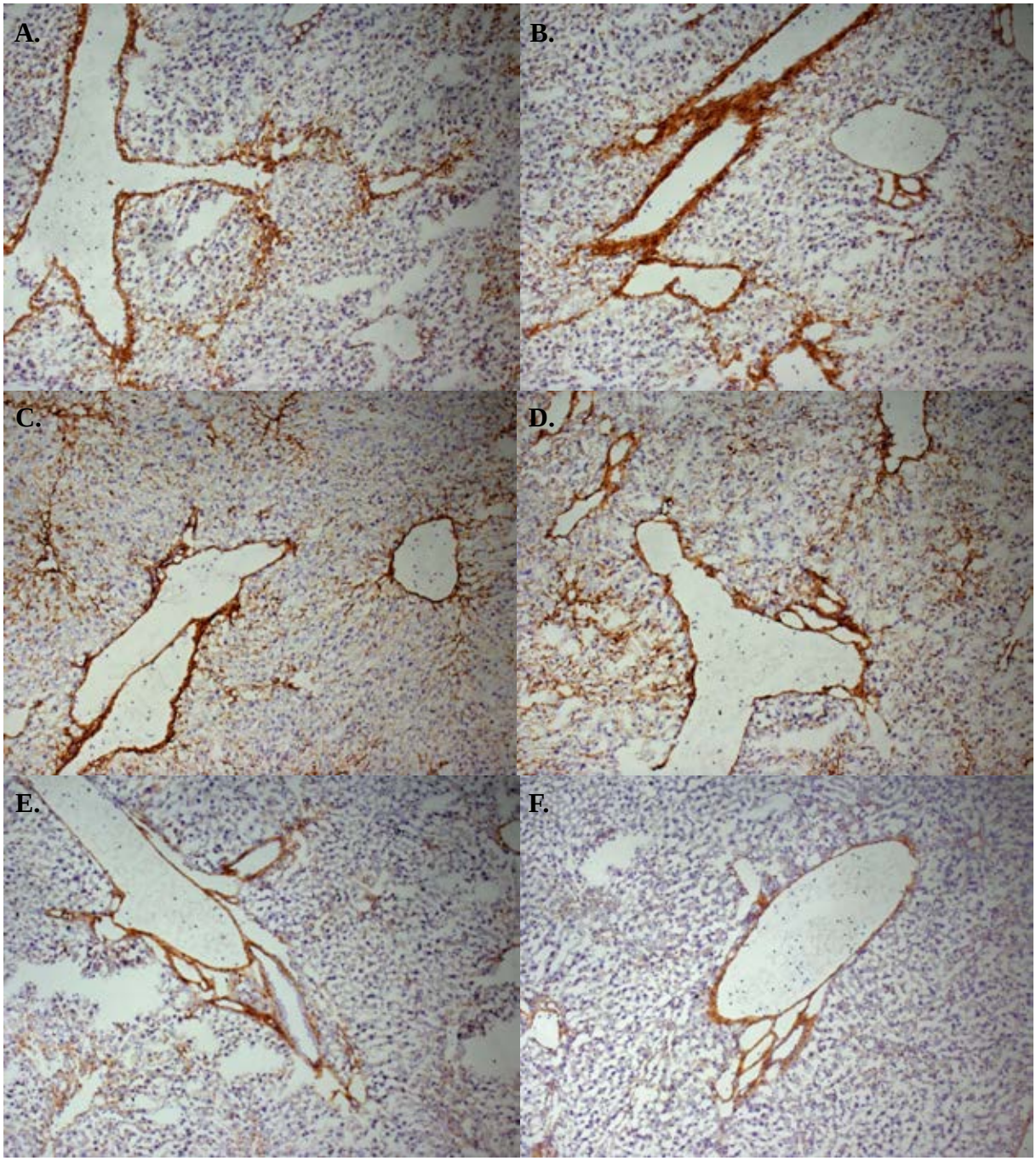

Figure 4.1. PDGFRα and Sca1 immunohistochemical staining localises to peri-vascular regions in uninjured adult murine liver. Representative examples of immunohistochemical staining of adult mouse liver sections using **AB,** PDGFRα (ebiosciences), **CD**, PDGFRα (R&D Systems), and **EF**, Sca1 antibodies

4.2.2. Prospective isolation of PαS and Sca1$^+$ cells from adult normal uninjured liver. Non-parenchymal cells were isolated by fluorescence-activated cell sorting (FACS) from excised adult, wild-type, uninjured liver by mechanical dissociation, collagenase digestion, red cell lysis and density centrifugation (detailed in methods chapter). Viability was consistently >80% as determined by propidium iodide (PI) staining (**Fig 4.2A**). CD45$^+$/ Ter119$^+$ haematopoietic lineage-positive (PE$^+$) cells constituted roughly a third of all viable cells and were excluded (**Fig 4.2B**). PDGFRα$^+$ Sca1$^+$ (PαS) cells constituted 0.2% of the viable, lineage-negative fraction yielding roughly 2,000 cells per digested liver. PDGFRα$^-$ Sca1$^+$ (Sca1) cells constituted roughly 1% of all viable, lineage-negative cells with an approximate yield of 10,000 cells per digested liver (**Fig 4.2C**).

To optimise the isolation of single cell preparations from digested adult murine liver density centrifugation was used to select conditions to improve overall yield and purity of isolated PαS cells. A 1.033g/ml solution (33% Percoll in phosphate buffered saline) was selected based on previous reports of methods for the isolation of hepatic stem cells from adult rodent[75]. The use of gradient centrifugation allowed the segregation of cellular populations based on density into those denser (pellet, **Fig. 4.3A**) and lighter (supernatant, **Fig. 4.3B**) than the solution used. Cells in the supernatant (<1.033g/ml) were less viable than those in the pellet (>1.033g/ml) (14.2% vs 51.2%). Of the viable cells, similar proportions of lineage negative (CD45$^-$ Ter119$^-$) cells were found in both populations. Higher yields of PαS and Sca1$^+$ cells were detected in the pellet faction than the supernatant fraction (0.20% and 0.46% vs. <0.01% and 0.02% of total sorted cells respectively).

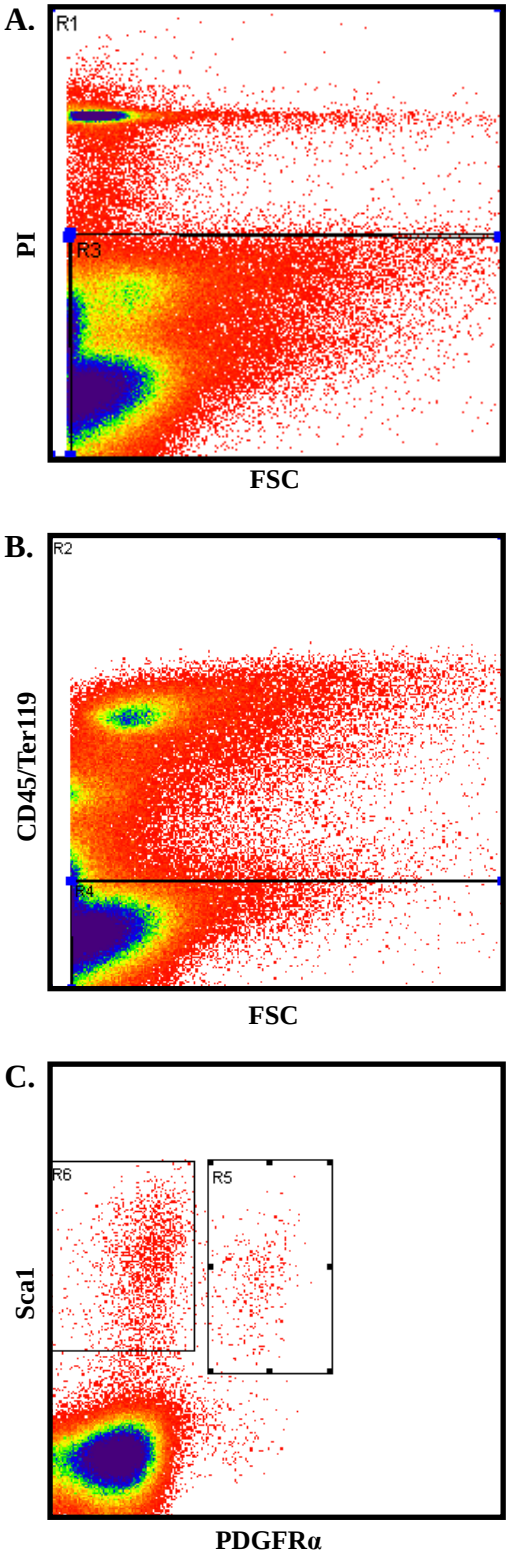

Figure 4.2. Gating strategy for isolation of PDGFRα$^+$ Sca1$^+$ cells from adult murine liver. Fluoresnce-activated cell sorting of viable CD45$^-$ Ter119$^-$ Sca1$^+$ PDGFRα$^+$ (PαS) cells by sequential excluding gates: **A,** Forward side scatter vs. propidium iodide allowing exclusion of dead cells. **B,** Forward side scatter vs. CD45/Ter119 allowing exclusion of haematopoietic lineage populations. **C,** Sca1 Vs. PDGFRα allowing selection of PαS and Sca1$^+$ populations

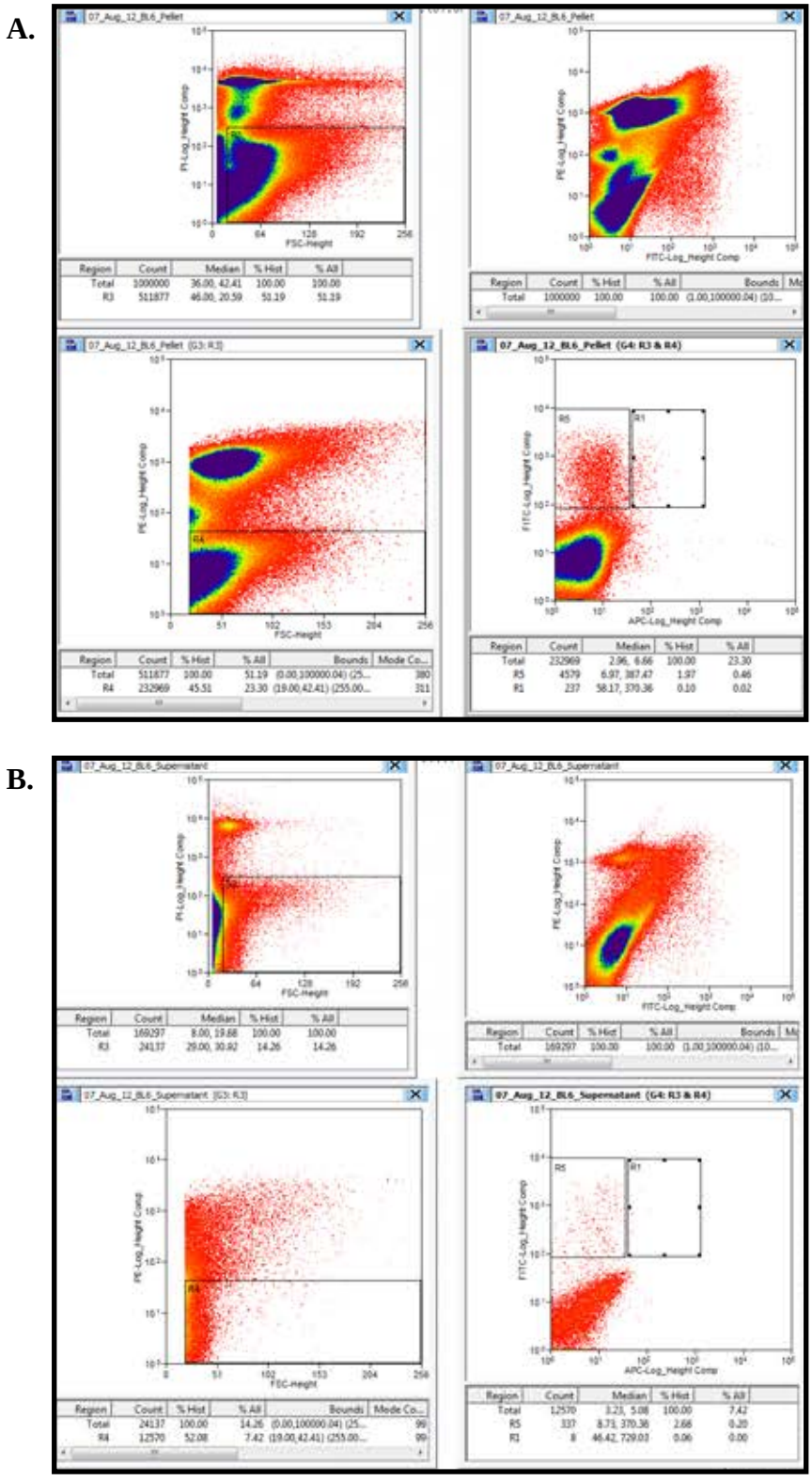

Figure 4.3. Density centrifugation improves viability and yield of PDGFRα⁺ Sca1⁺ cells. FACS plots from prospective isolation of PαS and Sca1⁺ cells from **A,** pellet fraction (density >1.033g/ml) and **B,** supernatant fraction (density <1.033g/ml) after density centrifugation

Three selection protocols were selected with varying length of collagen digestion (30 minutes vs 60 minutes) and the use of density centrifugation to assess the effect on viability and yield of isolated cells. Due to the cost of the experiment this optimisation experiment was only run once. The total viability of sorted cells was found to increase across the groups, with 30 minutes digestion with no Percoll (30 min -) having the lowest viability followed by 30 minutes with Percoll (30 min +) and 60 minutes digestion with Percoll (60 min +) having the highest viability (43.7% vs. 47.9% vs. 65.8%, **Fig 4.4A**). The total proportion of viable lineage negative ($CD45^-Ter119^-$) cells was decreased when a Percoll gradient density centrifugation step was utilised (42.8% and 42.1% vs. 79.0%, **Fig 4.4B**). The total proportion of viable lineage negative cells with PαS and Sca1 expression was highest with 60 minutes digestion with a Percoll gradient step (0.30% PαS and 2.26% $Sca1^+$), and less in the other conditions, 30 minutes digestion with a Percoll gradient step (0.07% PαS and 0.44% $Sca1^+$) and 30 minutes digestion without a Percoll gradient step (<0.01% PαS and 0.05% $Sca1^+$) (**Fig 4.4C**). As a result, 60 minutes collagenase digestion with a Percoll gradient centrifugation step was used for all subsequent isolations.

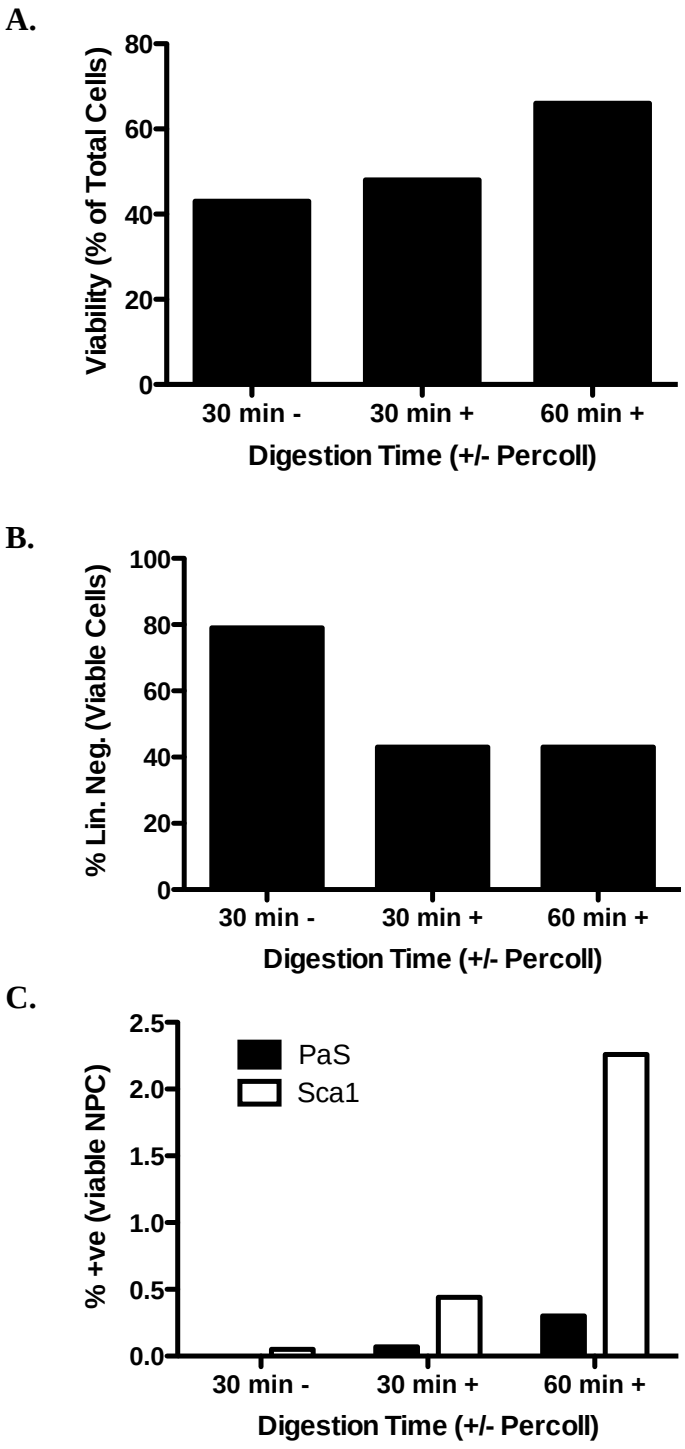

Figure 4.4. Increased digestion time further improves viability and yield of PDGFRα^+ Sca1$^+$ cells. Bar charts showing **A,** viability; **B,** proportion of haematopoietic lineage (CD34/ Ter119) negative cells; and **C,** proportions of PαS and Sca1$^+$ cells after 30 minutes collagenase digestion without density centrifugation (30 min -), 30 minutes collagenase digestion with density centrifugation (30 min +) and 60 minutes collagenase digestion with density centrifugation (60 min +)

4.2.3. Prospectively isolated hepatic PαS and Sca1$^+$ cells can be cultured *in vitro.* Freshly isolated PαS and Sca1$^+$ cells can be cultured on plastic in αMEM + 10% foetal calf serum (FCS), conditions designed for the expansion and maintenance of mesenchymal stem cells. Under these conditions PαS and Sca1$^+$ cells adhered, proliferated readily to confluence and could be passaged. PαS cells were small and spindle-shaped in the first few days post-isolation and grew as individual cells suggesting contact inhibition between adjacent cells, morphology characteristic of stromal cells (**Fig 4.5B**). After 7 days culture on plastic PαS had characteristic myofibroblast morphology and strongly expressed alpha smooth muscle actin (**Fig 4.5A**). Sca1 cells were not viable on plastic in αMEM + 10% foetal calf serum (FCS) but were viable on type I collagen if plated at much higher densities than PαS cells. Viable Sca1 cells take longer to emerge than PαS cells, are commonly observed in small clusters and are larger with more substantial cytoplasm than PαS cells (**Fig 4.5C**). Oil red O staining failed to demonstrate presence substantial amount of intracellular lipid in PαS cells after 3 days (**Fig 4.5D**) or 7 days (**Fig 4.5E**) culture on plastic in αMEM + 10FCS.

Colony forming unit assays were utilised to quantify colony forming potential of PαS cells and Sca1$^+$ cells. Cells were plated at very low density (40 cells/cm^2). Cultured in αMEM on plastic, 2.7% of freshly isolated PαS cells and 0.10% of Sca1$^+$ cells formed colonies. In OC+ media on collagen type I, 0.61% of PαS and 0.07% of Sca1$^+$ cells formed colonies (**Fig 4.6A**). PαS colonies were larger with greater numbers of cells than those formed by Sca1 cells. PαS colonies were comprised of cells with a more stromal morphology and were generally more homogeneous (**Fig 4.6B**). Sca1$^+$ colonies typically comprised large, occasionally binucleate cells, with adjacent smaller spindle-shaped cells (**Fig 4.6C**).

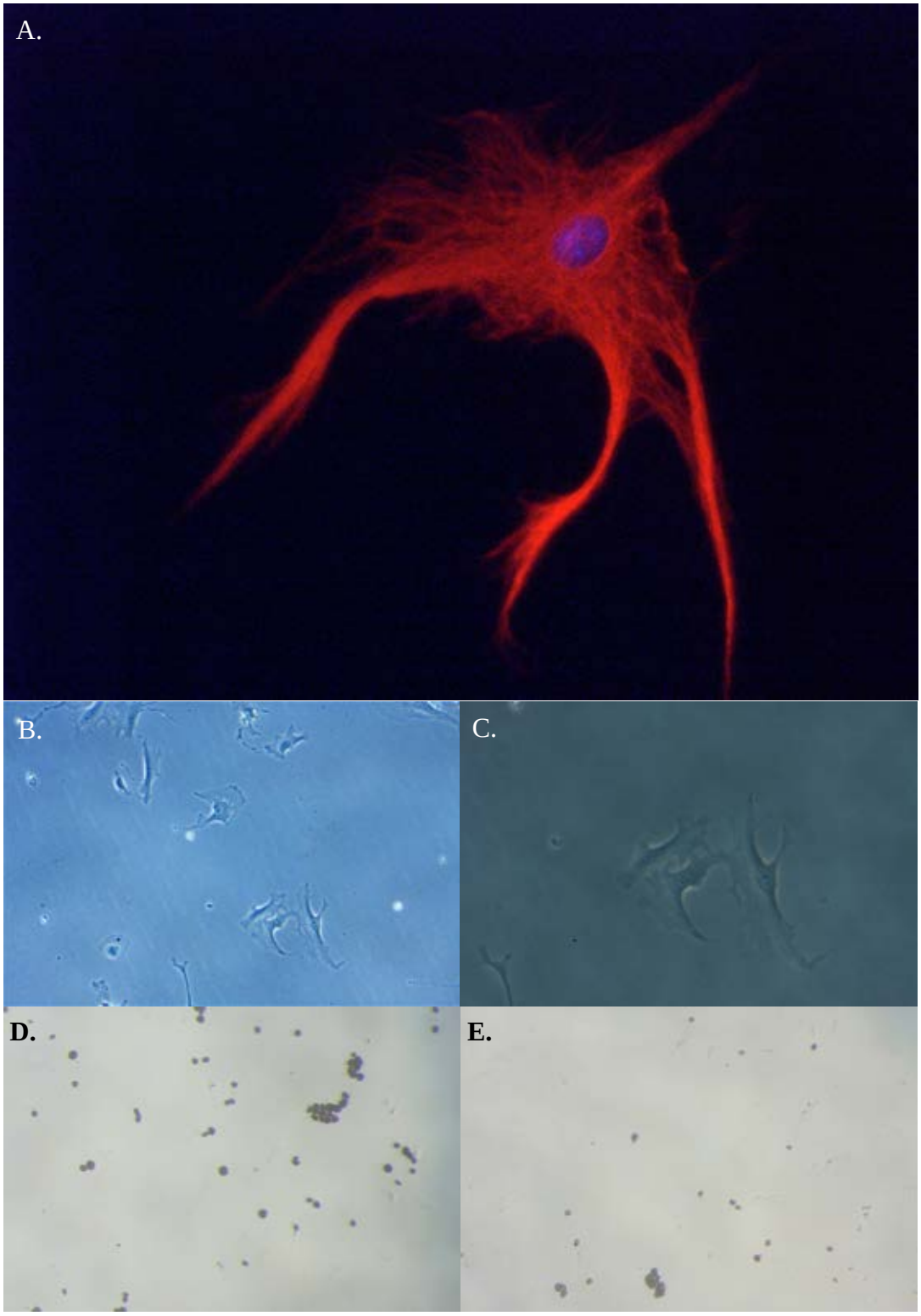

Figure 4.5. ***In vitro*** **culture of freshly isolated cells from adult murine liver. A,** Vimentin immunohistochemistry with DAPI nuclear counterstain of a single representative PαS cell cultured for 7 days on plastic in αMEM +10% FCS. Light microscopy of **B,** PαS cells after 3 days culture on plastic in αMEM +10% FCS and **C,** $Sca1^{+}$ cells after 3 days culture on collagen in OC. Oil red O staining fails to detect intracellular lipid (stained red) in freshly isolated PαS cells after **D,** 3 days and **E,** 7 days culture on plastic in αMEM +10% FCS

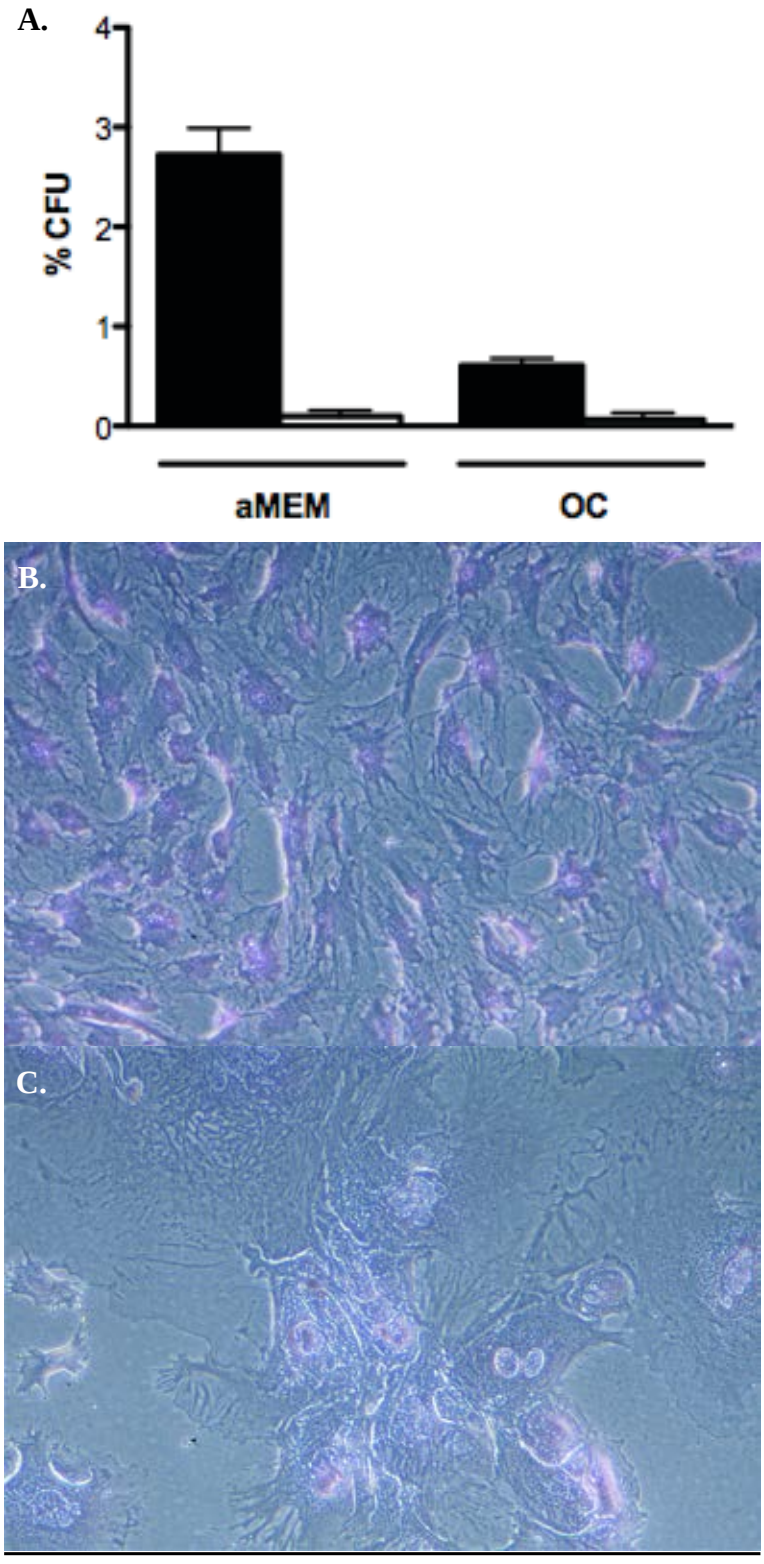

Figure 4.6. Colony formation assays of PαS and Sca1^{+} cells. A, Proportion of freshly isolated PαS (black bars) and Sca1+ cells (white bars) forming colonies after 2 weeks culture in αMEM +10% FCS or OC media. Crystal violet staining of colonies formed by **B,** PαS and **C,** Sca1+ cells

4.2.4. Hepatic PαS cells proliferate on plastic and gain expression of myofibroblast markers over time which is further augmented by culture on type I collagen. Freshly isolated PαS cells were plated at a density of 160 cells per mm^2 and cultured in αMEM + 10% foetal calf serum on plastic to assess proliferation. PαS cells rapidly gain expression of markers associated with activated myofibroblasts, including αSMA, and lose expression of PDGFRα. Expression of PDGFRα is only maintained on infrequent clusters of small, rounded cells after 7 days culture that may represent slowly proliferating cells with stem/progenitor characteristics. Culture on type I collagen resulted in almost complete loss of PDGFRα expression after 7 days with only infrequent clusters of small, rounded PDGFRα$^+$ cells observed (**Fig 4.7A**). PαS cells were viable and proliferated readily on plastic (number of cells per field = 13.1 at day 3 vs 23.3 at day 7 , p=0.018, student's t test). PαS cells plated on collagen type I proliferated at a faster rate than on cultured on plastic (number of cells per field at 7 days = 23.3 on plastic vs 52.3 on collagen type I, p=0.005) (**Fig 4.7B**). Staining with markers associated with hepatic fibroblast and stellate lineages allowed assessment of the activation of PαS cells over time on plastic and in response to culture on collagen type I. The proportion of cells expressing alpha small muscle actin (αSMA) was found to increase with time in culture on plastic from around 70% at day 3 to almost 100% at day 7. All cells were αSMA$^+$ after 7 days culture on collagen type I. Around a third of cells were positive for desmin and all cells were positive for vimentin across all 3 conditions utilised. PαS cells were consistently around 20-40% desmin-positive across all conditions.

Vimentin, an intermediate filament protein, was expressed by all PαS cells across all conditions and allowed the morphology and distribution of cells across the 3 conditions to be visualised in greater detail. After 3 days culture on plastic PαS cells were small and spindle shaped with minimal branched cytoplasm and long cellular processes characteristic of fibroblasts or quiescent stellate cells. Cells were distributed throughout the plate and were most often observed as isolated single cells. After 7 days culture on plastic PαS cells were larger than at day 3 with greater cytoplasm and more extensive cellular processes characteristic of myofibroblasts. At day 7 PαS cells were more densely distributed due to increased size and number but do not form obvious cell-cell adhesions or nexi characteristic of epithelial cells. After culture on collagen type I for 7 days PαS cells were confluent due to increased cell number. Cells were slightly smaller than after 7 days on culture on plastic most likely due to spatial restriction. Cells appeared to display appropriate contact inhibition with no evidence of cells growing atop each other instead forming homogenous sheets without characteristic muscle fibre polarity (**Fig 4.7C**).

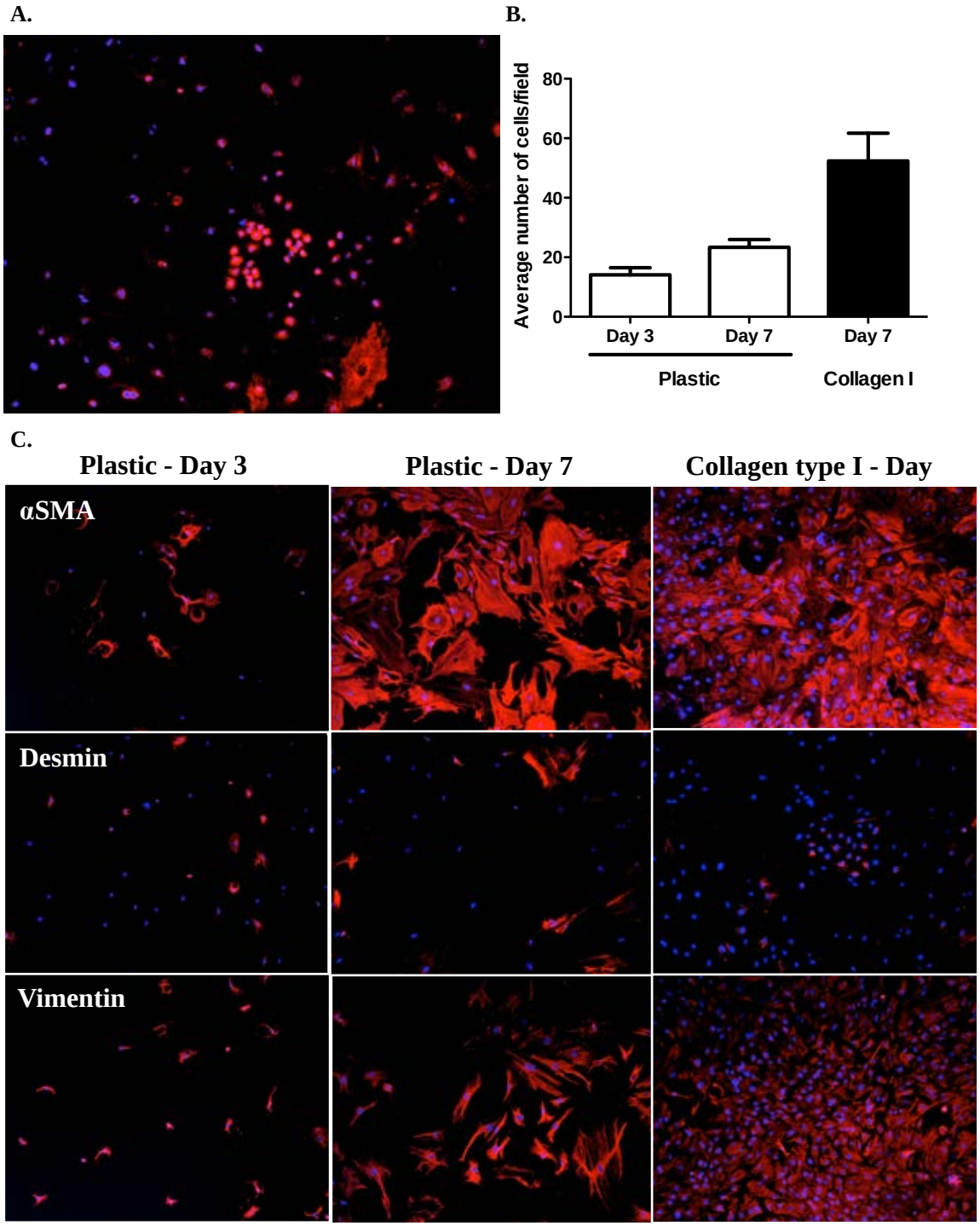

Figure 4.7. Freshly isolated PαS cells lose PDGFRα expression and gain morphology and phenotype characteristic of hepatic stellate cells. A, PDGFRα immunofluorescent staining of PαS cells after 7 days culture on plastic demonstrating a small cluster of cells maintaining PDGFRα expression. **B,** Proliferation of PαS cells after 3 and 7 days culture on plastic and 7 days culture on collagen type I. **C,** Alpha smooth muscle actin, desmin and vimentin immunofluorescent staining of PαS cells after 3 and 7 days culture on plastic and 7 days culture on collagen type I. Counterstained with DAPI (blue) was performed for all immunofluorescent analyses

4.2.5. 2-deoxyglucose inhibits proliferation and activation of PαS cells cultured on plastic and type I collagen. Isolated primary stellate cells activate in response to culture on plastic within the first few days of culture and this process is augmented by culture on type I collagen. 2-deoxyglucose (2-DG) has previously been described as a potent inhibitor of the activation of freshly isolated hepatic stellate cells through the inhibition of glycolysis[183]. 2-DG was added to αMEM media at a concentration of 5mM to assess its effects on PαS cell proliferation and activation on plastic and type I collagen and its potential use in maintaining PαS cells in a quiescent state.

Freshly isolated PαS cells were plated at a density of 160 cells per mm^2 and cultured in αMEM + 10% foetal calf serum on plastic or collagen type I with or without addition of 1.25mM 2-DG. All PαS cells in all conditions were positive for vimentin (**Fig 4.11B**). Vimentin immunohistochemistry demonstrated PαS cells cultured in the presence of 2-DG were small with scanty cytoplasm and maintained spindle-like morphology characteristic of quiescent or freshly isolated stellate cells after 7 days (**Fig 4.8**). PαS cells cultured in the absence of 2-DG took on myofibroblastic morphology described previously (**Fig 4.7**). PαS cells cultured on type I collagen proliferated more rapidly than on plastic with a greater number of cells observed per field at day 7 (52.4 Vs. 26.4, p=0.01). 2-DG inhibited the proliferation of freshly isolated PαS cells and the activating effect of type I collagen with significantly fewer cells observed after 7 days culture with 2-DG on both plastic and collagen type I (plastic, 13.1 vs. 26.4, p<0.001; collagen type I, 12.5 vs. 52.4, p<0.001). There was no difference in the total number of PαS cells observed after 7 days culture with 2-DG between culture on plastic or collagen type I (**Fig 4.11A**).

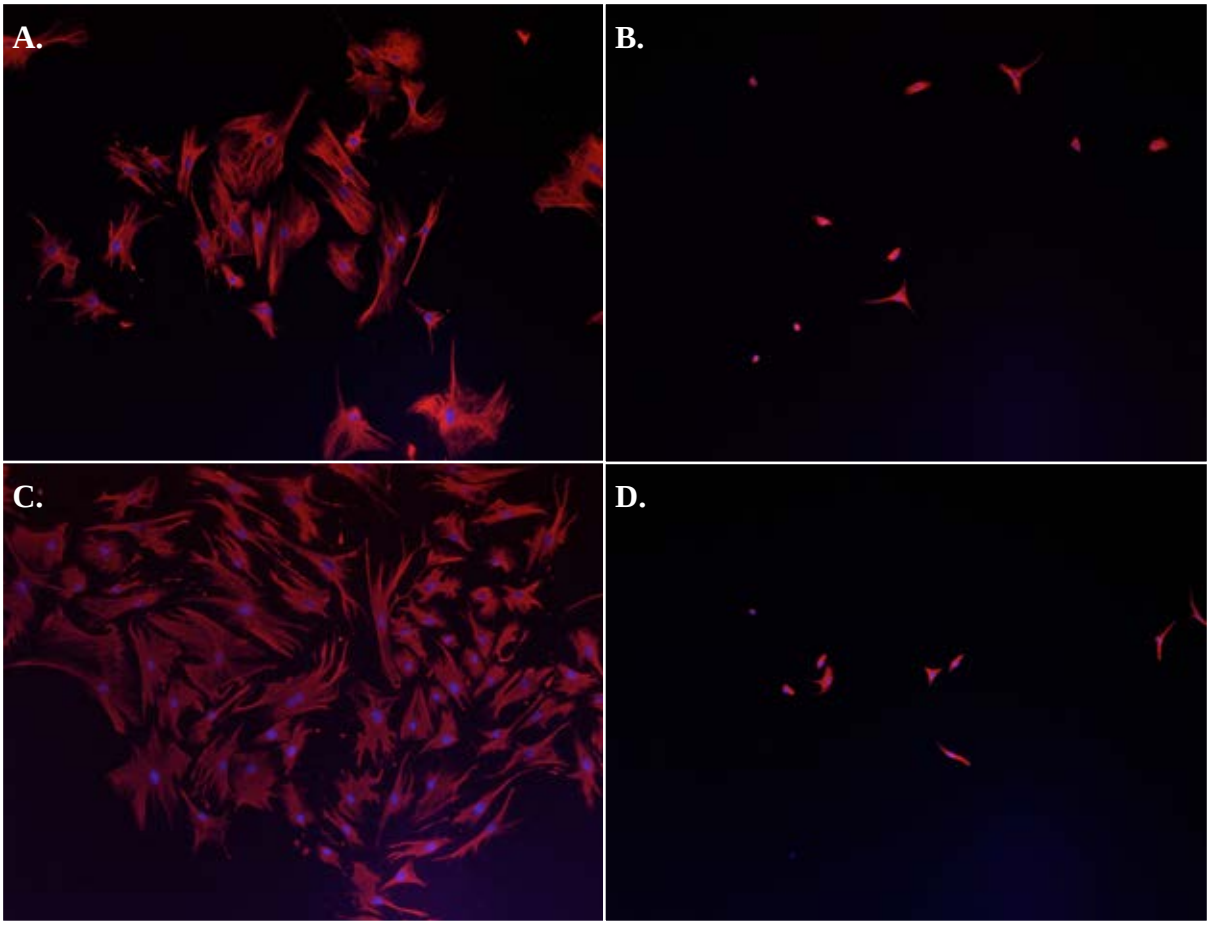

Figure 4.8. Vimentin immunohistochemistry of PαS cultured in the presence of 2-DG. Vimentin staining of PαS cells after 7 days culture on: **A,** plastic without 2-DG; **B,** plastic with 2-DG; **C,** collagen type I without 2-DG; and **D,** collagen type I with 2-DG

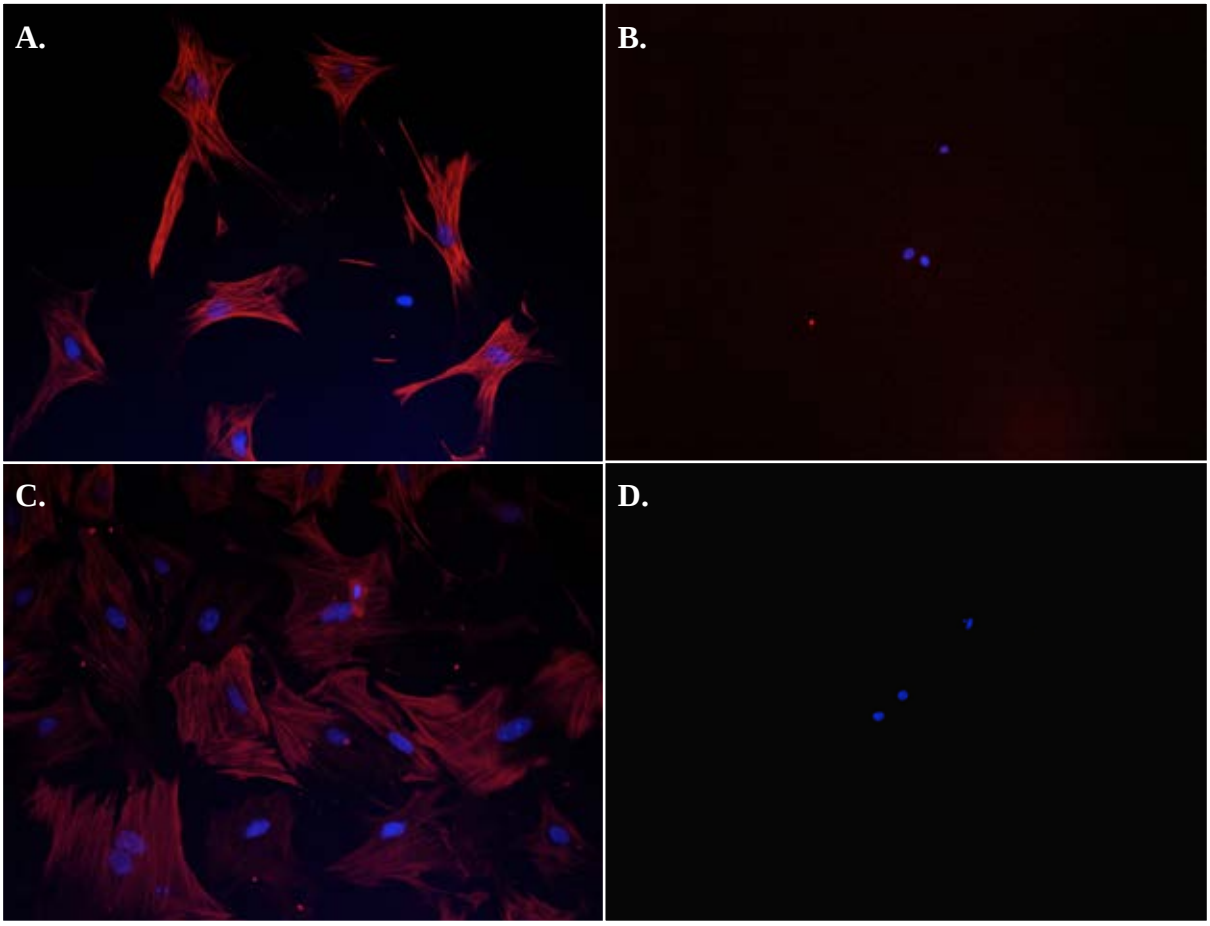

Figure 4.9. Alpha-smooth muscle actin (αSMA) immunohistochemistry of PαS cultured in the presence of 2-DG. αSMA staining of PαS cells after 7 days culture on: **A,** plastic without 2-DG; **B,** plastic with 2-DG; **C,** collagen type I without 2-DG; and **D,** collagen type I with 2-DG

αSMA immunohistochemistry demonstrated a high proportion of PαS cells cultured in the absence of 2-DG expressed αSMA at day 7 after culture on plastic and collagen type I (plastic, 91%; collagen type I 95%). However, a significantly smaller proportion of cells were found to express αSMA after culture with 2-DG on both plastic and collagen (plastic, 26% vs. 91%, $p<0.001$; collagen type I, 19% vs. 95%, $p<0.001$) suggesting failure of PαS to undergo myofibroblastic differentiation and maintenance of a quiescent state. There was no significant difference in the proportion of cells expressing αSMA between culture on plastic of collagen type I with 2-DG. (**Fig 4.9, 4.11B)**.

The proportion of cells expressing desmin was consistently around 30% across culture conditions with no significant difference observed (**Fig 4.10, 4.11D**).

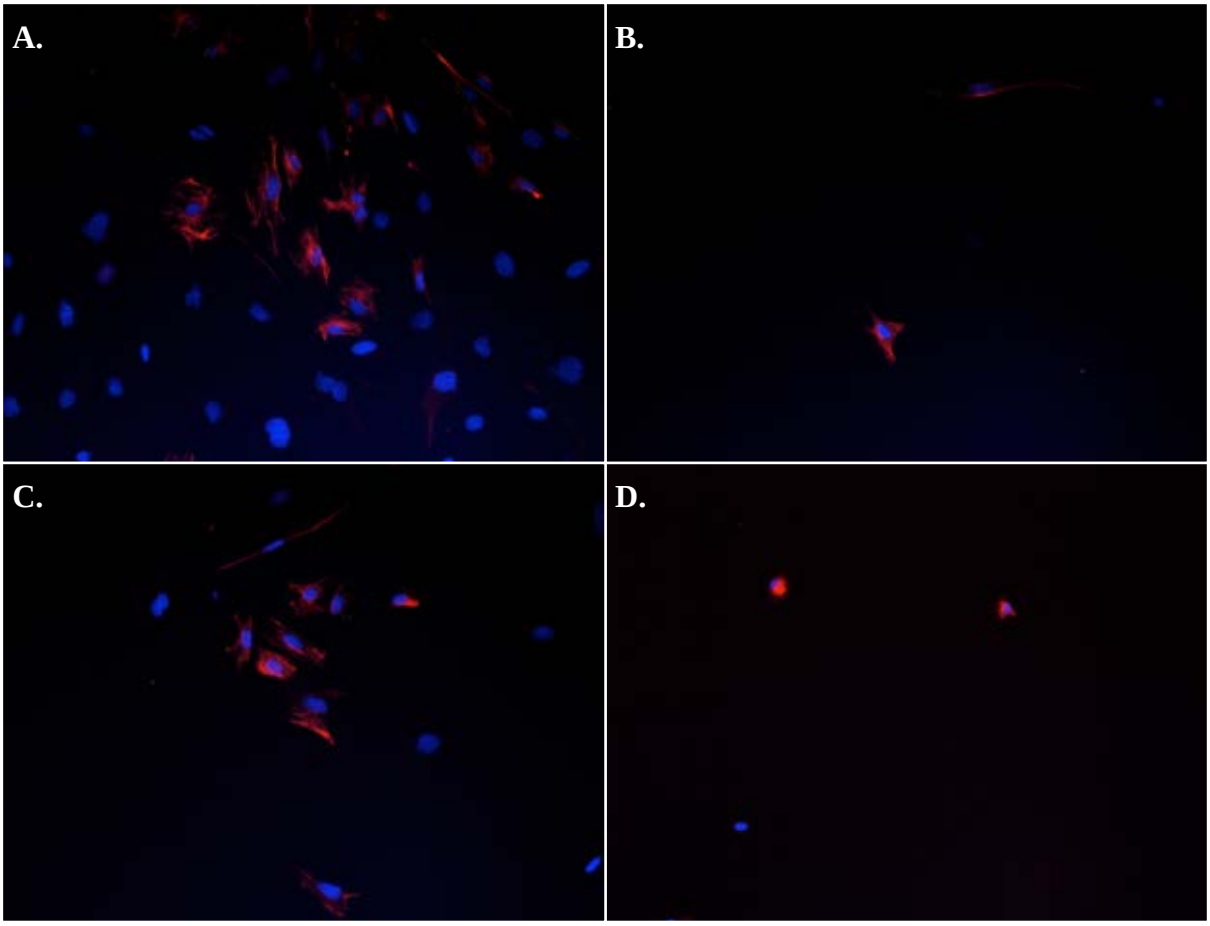

Figure 4.10. Desmin immunohistochemistry of PαS cultured in the presence of 2-DG. Desmin staining of PαS cells after 7 days culture on: **A,** plastic without 2-DG; **B,** plastic with 2-DG; **C,** collagen type I without 2-DG; and **D,** collagen type I with 2-DG

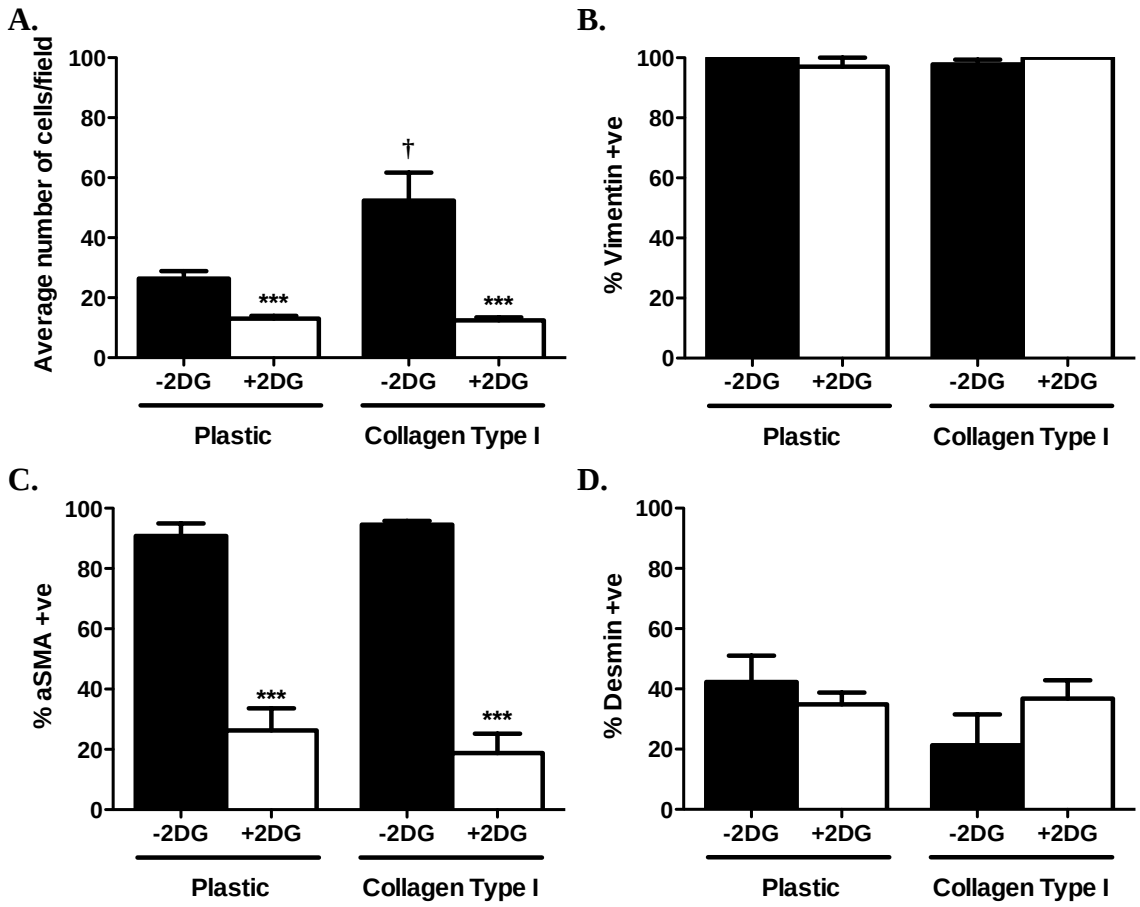

Figure 4.11. 2-DG inhibits proliferation and maintains quiescent phenotype of freshly isolated PαS cells. PαS cells were cultured on plastic or collagen type I in αMEM +10% foetal calf serum with or without 2-DG for 7 days. Mean values from 4 wells for **A,** average numbers of cells per field and proportions of cells expressing **B,** vimentin; **C,** alpha smooth muscle actin; and **D,** desmin. Error bars represent standard error of means. ***$p<0.001$ vs. identical culture conditions without 2-DG, † $p<0.05$ vs. plastic without 2-DG

4.2.6. Selection of rapidly proliferating epithelial colonies by culture in conditions designed for selection and maintenance of hepatic stem/progenitor cells. When cultured in conditions (OC^+) originally designed for the selection of hepatic (epithelial) progenitor cells[76] PαS and $Sca1^+$ cells grew rapidly to confluence and demonstrated morphological heterogeneity. As $Sca1^+$ cells were found to have low colony formation potential (approximately 1 colony per 1000 freshly isolated cells), freshly isolated $Sca1^+$ cells were first plated at very high density in an attempt to increase viability and examine their growth and characteristic after long term *in vitro* culture. $1x10^5$ cells (density approximately $1x10^5$ cells/ cm^2) were plated in single wells of a 48-well plate coated with collagen type 1 in OC+ and left to proliferate to confluence. Immediately after plating all cells had spindle-shaped morphology and proliferated rapidly (estimated doubling time ≈ 2 days). After roughly 7 days small clusters of cells with typical epithelial morphology can be observed. After 14 days these regions occupied a proportionally larger area than fibroblastic cells After 2 weeks culture cells had a large degree of heterogeneity. Areas of cells with characteristic stromal morphology (spindle shaped, contact inhibition) were observed (**Fig 4.12A**) directly abutting cells with epithelial morphology (**Fig 4.12B**). Cells of differing morphology were not observed in mixed populations, instead forming clearly demarcated boundaries (**Fig 4.12B**, dashed line). Epithelial cells were generally smaller than accompanying stromal cells, were ovoid, had a high nuclear-to-cytoplasmic ratio and grew with a high degree of cell-to-cell contact. Interestingly, these cells were frequently observed growing as three dimensional aggregates (**Fig 4.12C,D**). The addition of the ROCK inhibitor Y-27632 to culture media prevented formation of aggregates and maintained all cells as a monolayer and was used in all subsequent cultures using OC+ media to ease passaging and imaging.

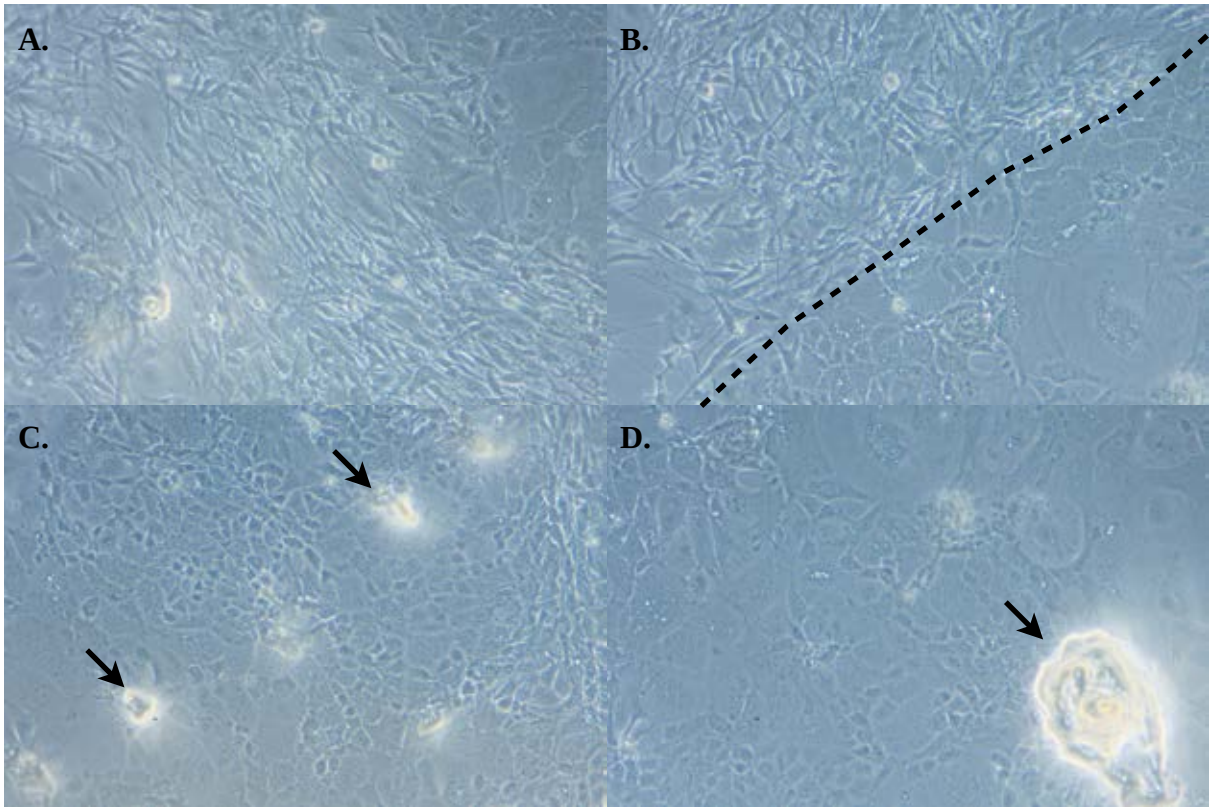

Figure 4.12. Heterogeneous morphology of freshly isolated Sca1$^+$ cells cultured on collagen type I in OC+ media for 2 weeks. Representative images of light microscopy on Sca1$^+$ cells after 14 days culture on collagen type I in OC$^+$ media demonstrating: **A,** cells with predominantly stromal morphology; **B,** distinct boundaries (dashed line) between regions of stromal cells (above) directly abutting cells with epithelial morphology (below); and epithelial cells growing in **C,** monolayers and **D,** three dimensional aggregates (arrows)

Immunohistochemistry with wide spectrum pan-cytokeratin (pan-CK), routinely used as a marker of murine hepatic stem/progenitor cells in liver, specifically stained all cells of the epithelial colonies and was not observed on surrounding stromal cells. PanCK immunohistochemistry demonstrated the rapid growth of the epithelial colonies (**Fig 4.13A**, day 7; **Fig 4.13B**, day 10; **Fig 4.13C**, day 14). All cells were positive for vimentin at day 14 (**Fig 4.13D**). As all cells expressed vimentin this was used to demonstrate the contrasting morphology of the epithelial colonies with surrounding stromal cells. Cells within colonies were smaller, oval shaped, had a greater nucleus to cytoplasmic ratio, and grew in tight aggregates. After long-term culture (**Figure 4.14**) single colonies could reach considerable size and appeared to proliferate into, and displace the surrounding stroma with occasional single, large stromal cells observed within the colony, presumably enveloped. Cells were often smallest at the centre of colonies and demonstrated a ‘swirling’ pattern (**Fig 4.15**) previously reported as characteristic of biliary tree/hepatic stem cell cultures.

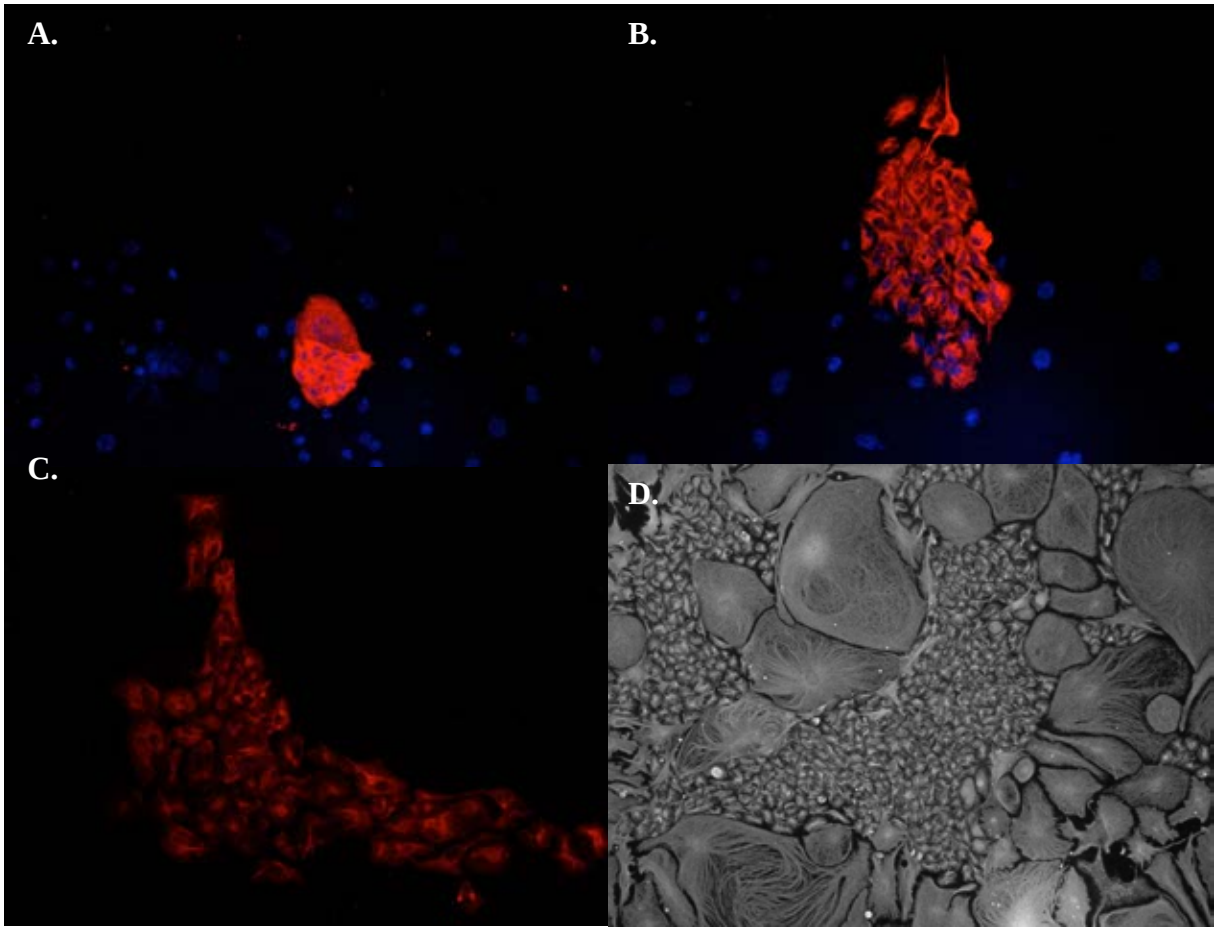

Figure 4.13. Selection of highly proliferative epithelial colonies from Sca1 cultures with hepatic stem cell expression profiles. Representative images (200x magnification) of pan-cytokeratin immunofluorescent staining of Sca1 cells cultured in OC^+ at **A,** day 7, **B,** day 10 and **C,** day 14. **D,** Representative example (100x magnification) of vimentin immunofluorescent staining of Sca1 cells cultured in OC^+ on collagen type I for 14 days

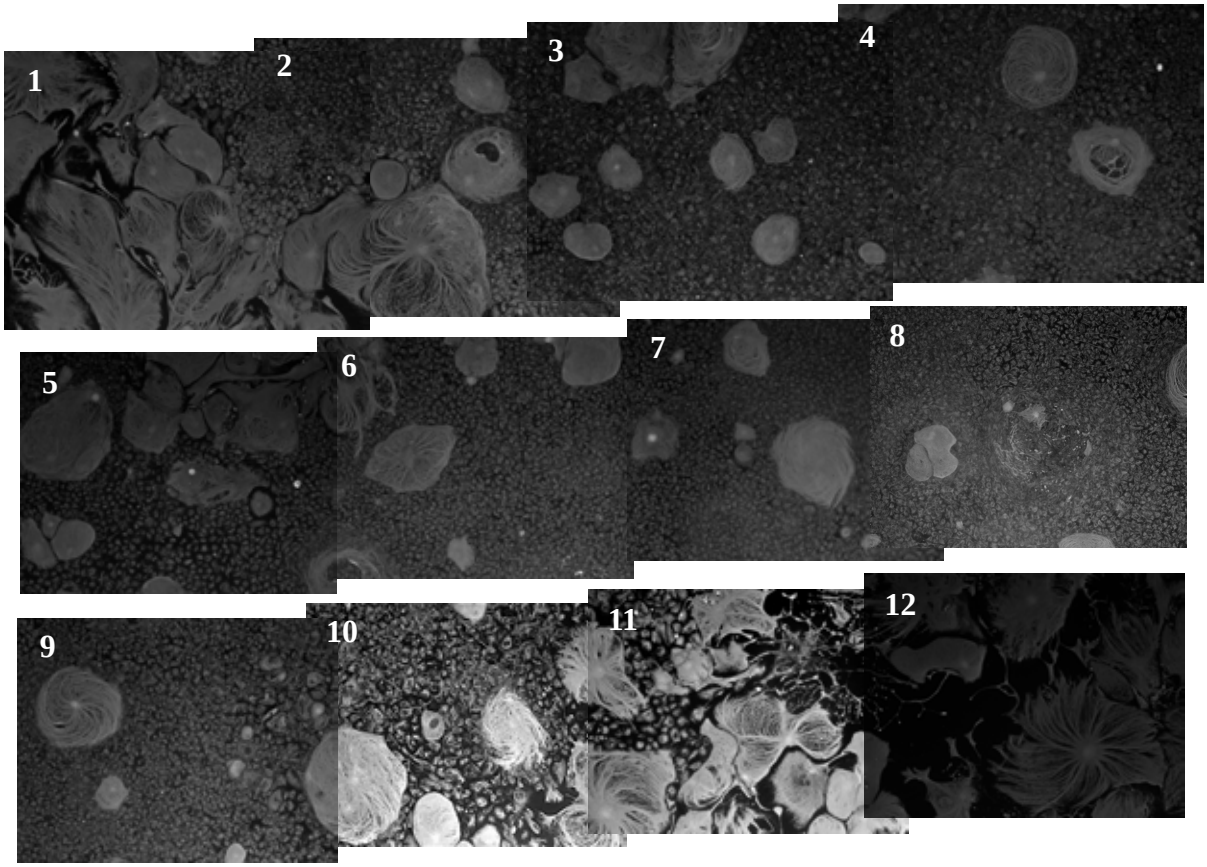

Figure 4.14. Sequential cross-sectional images of a large epithelial stem/progenitor cell colony observed after 8 weeks culture. Vimentin immunofluorescent staining of PαS cells cultured in OC^+ after approximately 8 weeks culture. Panels 1 through 12 are composed of consecutive, overlapping images arranged horizontally across from left to right across the centre of a single epithelial stem/progenitor colony with surrounding and occasional isolated, enveloped stromal cells

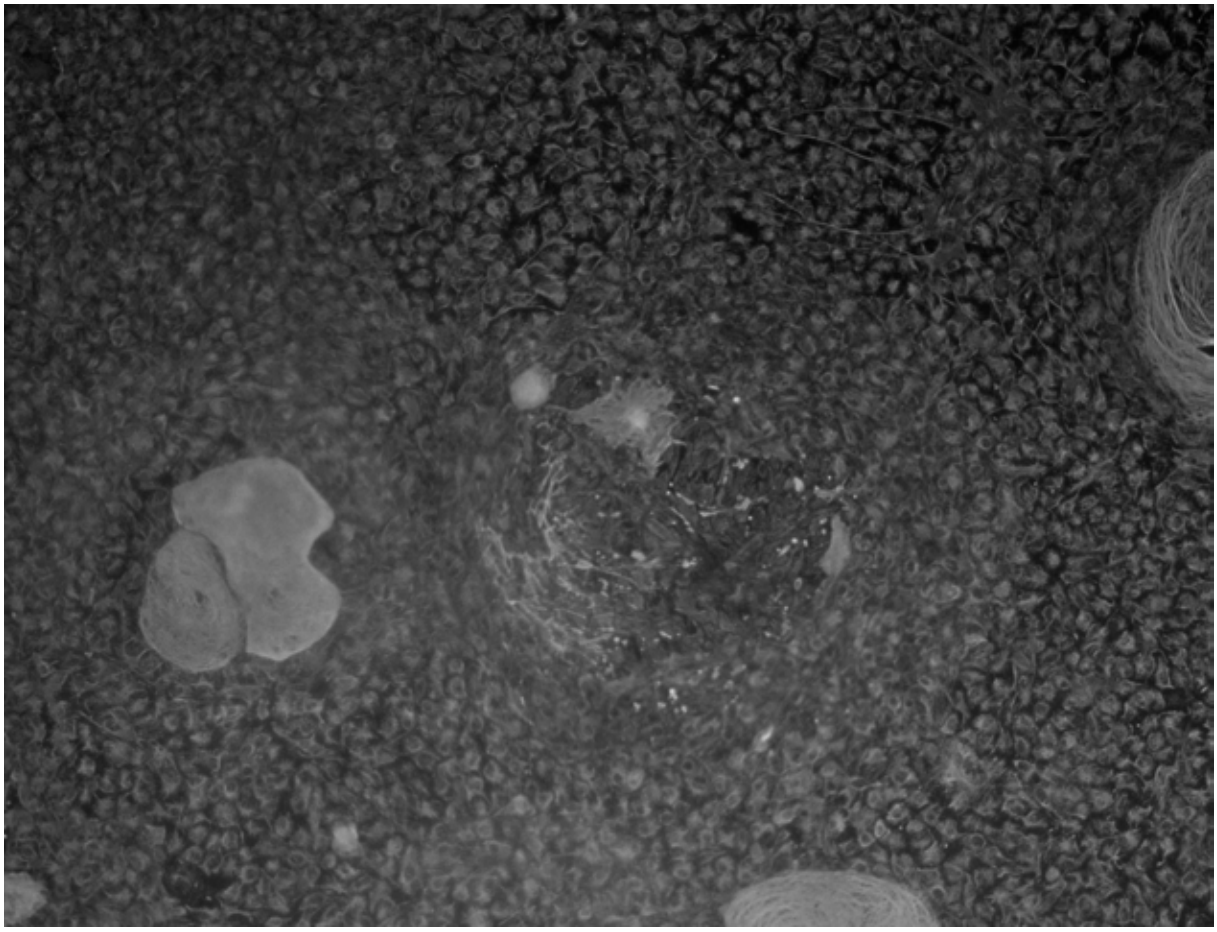

Figure 4.15. Presence of cells with swirling pattern characteristic of biliary tree stem cells at the centre of a large epithelial stem/progenitor cell colony. Vimentin immunofluorescent staining of freshly isolated Sca1 cells cultured in $OC^{+}$for approximately 6 weeks

4.2.7. Characterisation of selected epithelial stem/progenitor cells. Epithelial cells were allowed to outgrow surrounding stroma (around 8 weeks culture) and then selected and passaged as a homogeneous culture. A 2 minute Trypsin digestion step was used to remove remaining stroma whilst sparing epithelial colonies, then a longer Trypsin step was used to passage epithelial cells. Selected epithelial cells grew rapidly as a confluent monolayer **(Fig 4.16A)**. Interestingly, the morphology of cells at the edges of confluent colonies differed from those at the centre. Where cells at the centre of colonies had a typical epithelial stem/ progenitor cell phenotype, namely: small; ovoid; densely packed; and with a high nuclear to cytoplasmic ratio, those at the peripheries were generally larger, had greater cytoplasmic processes and were arranged in a more polygonal pattern, all characteristics of more mature epithelial cells **(Fig 4.16B)**.

Selected epithelial cells proliferated rapidly and were split at a ratio of 1 to 6 twice per week for over 3 months. Fluorescent immunohistochemistry demonstrated selected epithelial stem/ progenitor cells were all positive for vimentin (**Fig 4.16C**) and pan-CK. All selected epithelial stem/progenitor cells were negative for αSMA (**Fig 4.16D**) and desmin (**Fig 4.16E**) and a small proportion displayed patchy alpha-foetoprotein (AFP) staining (**Fig 4.16F**).

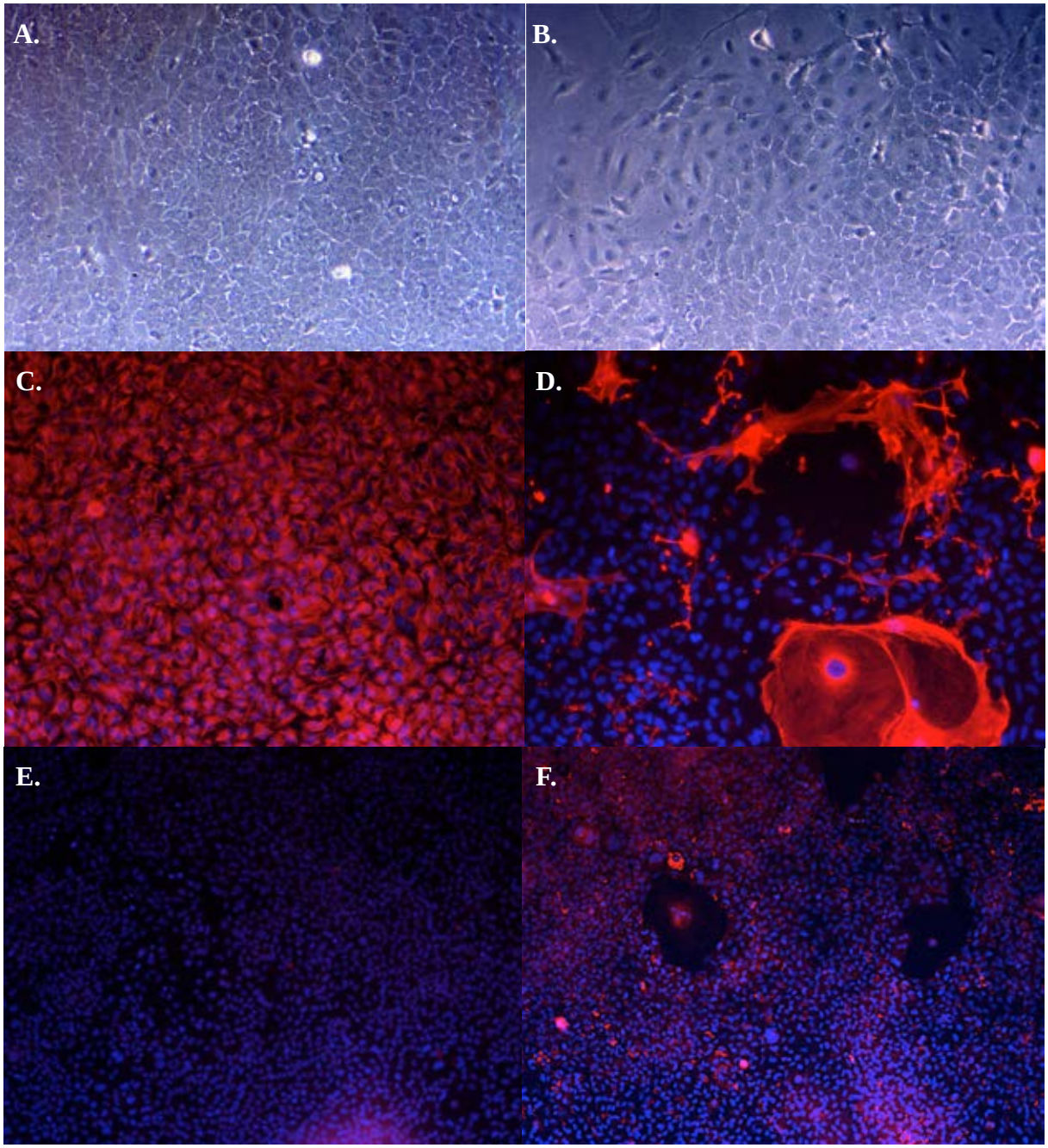

Figure 4.16. Characteristics of long-term cultured epithelial stem/progenitor cells. Representative images (100x magnification) of passage 6 epithelial stem/progenitor cells showing the **A,** centre and **B,** edge of confluent area of growth 2 days after passaging. Examples of fluorescent immunohistochemistry of fixed, confluent passage 6 epithelial stem cells stained for myofibroblastic markers **C,** vimentin (100x magnification); **D,** αSMA (200x magnification); and **E,** desmin 100x magnification). **F,** Representative image (100x magnification) of fluorescent immunohistochemistry on confluent passage 6 epithelial stem cells stained for the hepatoblast marker AFP

4.2.8. Epithelial stem/progenitor cells cultured long-term in selective media show limited hepatocytic differentiation but rapid myofibroblastic differentiation. To assess the plasticity of selected epithelial stem/progenitor cells that had been cultured long term, passage 6 cells were cultured in conditions to assess myofibroblast, hepatocyte and biliary epithelial cell differentiation potential. When cells were cultured in αMEM + 10% foetal calf serum for 7 days they displayed morphology highly similar to that described for freshly isolated PαS cell cultured in the same conditions. Compared to epithelial stem cells cultured in OC+ media for the same duration (**Fig 4.17A)**, cells were significantly fewer in number, most likely due to decreased proliferation, larger with greater, branched cytoplasma and demonstrated contact inhibition (**Fig 4.17B**).

Hepatocyte differentiation assays, utilising media previously reported to induce hepatocytic differentiation of isolated murine hepatic stem/progenitor cells, were conducted in triplicate to assess the potential of selected cells to form functional, mature hepatocytes. Prolonged culture of cells in normal growth conditions resulted in very dense cultures with cell shedding and evidence of cell death observed (**Fig 4.17C**) due to over-confluence. Shedding and cell death was also observed in cells cultured in hepatocyte differentiation media for 14 days, although cells appeared larger (**Fig 4.17D**). Morphological changes other than size were subtle and may be a result of slightly decreased proliferative rate, a known effect of oncostatin-M including in differentiation media used. Immunohistochemical analysis of cells cultured in differentiation media for 14 days revealed patchy AFP expression (**Fig 4.17E**) and absent albumin staining (**Fig 4.17F**) that was not significantly different from previous analysis (**Fig 4.16**) of undifferentiated epithelial stem/progenitor cells derived from $Sca1^{+}$ cells.

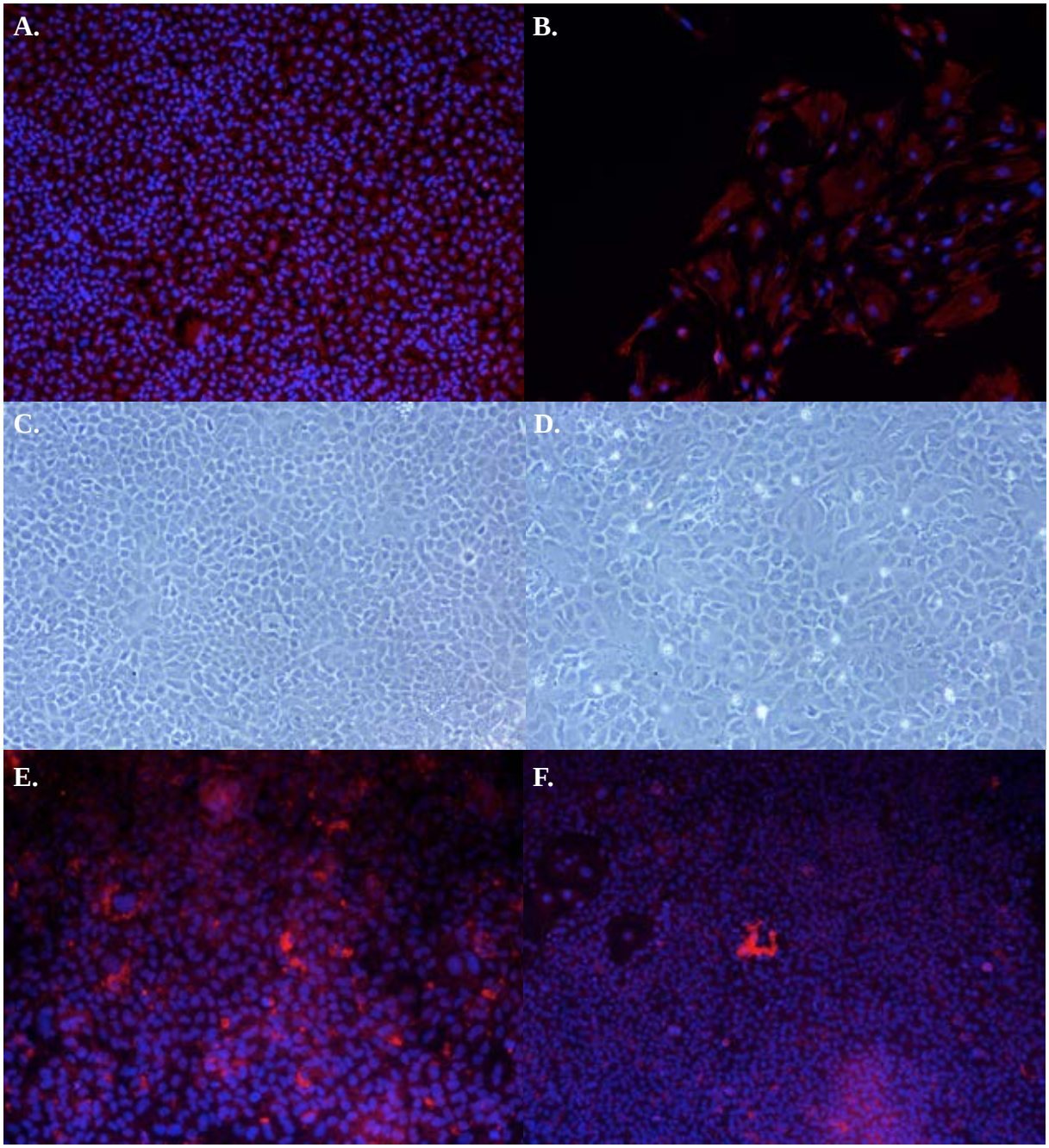

Figure 4.17. Selected epithelial stem/progenitor cells demonstrate rapid differentiation to myofibroblasts and limited differentiation to hepatocytes. Representative examples of vimentin immunohistochemistry of passage 6 epithelial stem/progenitor cells after 7 days culture in: OC+ on collagen type I **A,** with, and **B,** without 2-DG. Light microscopy of passage 6 cells after 7 days culture in **E,** OC^{+} and **F,** hepatocyte differentiation media on collagen type I. Immunohistochemical analysis of cells after 14 days culture in hepatocyte differentiation media showing **E,** patchy AFP expression and **F,** absent albumin expression

Suspension of epithelial stem/progenitor cells in three-dimensional collagen gels for biliary differentiation resulted in non-viable cultures where passaged cells failed to migrate or proliferate, preventing assessment of biliary differentiation potential.

4.2.9. *In vivo* assessment of engraftment and repopulation potential of freshly isolated Sca1^{+} cells. 1x10^{5} freshly isolated Sca1^{+} cells were suspended in saline and injected directly into the tail vein of a single male FAH$^{-/-}$ RAG2$^{-/-}$ IL2RG$^{-/-}$ (FRG) triple knockout transgenic mouse (treated). Normal saline was injected into the tail vein of a single male littermate as a control (untreated). Mice were weighed daily and a weight loss of greater than 10% from initial weight was used as the end-point, where mice would be killed and the experiment ended. NTBC was gradually reduced once immediately after infusion (4mg/L for 2 days, 2mg/L for 2 days and 1mg/L for 2 days). Mice were put back onto 16mg/ml (100%) NTBC at day 18 following rapid weight loss and NTBC was again gradually reduced as per first the protocol at day 21 up to day 27. The untreated mouse was found dead on day 46 and the treated mouse was found dead on day 52, both before weight loss was greater than 10% of initial weight. Recorded weights were similar until around day 40 when weights began to converge with the treated mouse demonstrating slower weight loss than some recovery from day 48 (**Fig 4.18**). No obvious fluid retention or ascites were found *post-mortem* on day 52.

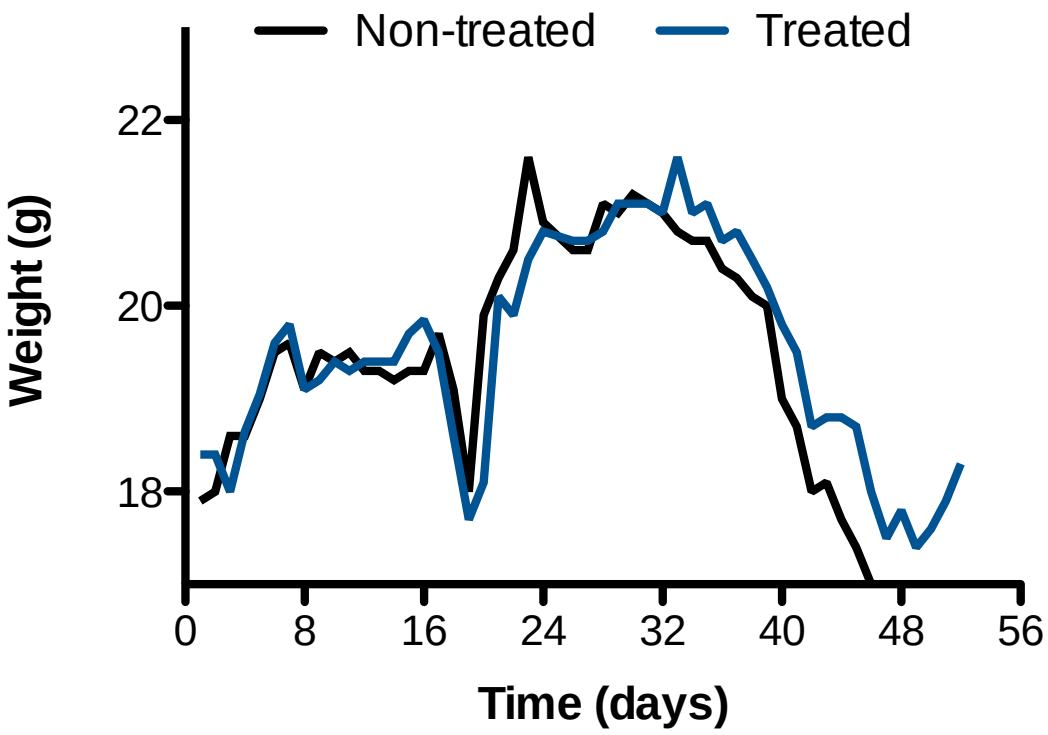

Figure 4.18. Increased survival time in a single FRG mouse infused with freshly isolated Sca1$^+$ cells versus saline only. Daily recorded weights of FRG mice after infusion of 1x10^5 Sca1$^+$ cells suspended in saline (blue line) versus saline only (black line). Drinking water was gradually reduced in two cycles beginning immediately after infusion and on day 21. NTBC levels in drinking water were: 16mg/ml on days 18-21; 4mg/ml on days 1, 2, 22 and 23; 2mg/ml on days 3, 4, 24 and 25; 1mg/ml on days 5, 6, 26 and 27 and absent on all other days.. Survival of treated mouse versus untreated mouse = 46 versus 52 days, n=1 for each treatment

4.3. DISCUSSION

Here, PDGFα^{+} Sca1^{+} (PαS) cells are shown to be present in adult murine liver and their prospective isolation using fluorescence-activated cell sorting (FACS) demonstrated. Detailed characterisation studies indicate PαS cells are a potent source of fibrogenic cells and may have the potential to give rise to epithelial stem/progenitor cells. Preliminary functional studies were conducted, however the contribution of PαS cells to: liver fibrogenesis in chronic disease; regeneration through production of daughter cells capable of differentiation into mature, functional hepatocytes and/or biliary epithelial cells; and injury resolution, where they may have value as a novel target for anti-fibrosis therapy; remains to be demonstrated.

In this study cells expressing both PDGFα and Sca1, an expression profile used to define potent mesenchymal stem cells in previous studies in other organs, were detected by immunohistochemistry and reproducibly isolated by prospective FACS. Freshly isolated PαS cells could be cultured *in vitro* on plastic in alpha-minimal essential media plus 10% foetal calf serum, conditions developed for the culture and long-term maintenance of murine mesenchymal stem cells (MSCs) isolated from bone marrow. In contrast to bone marrow MSCs, which maintain their potency and characteristic stromal cell morphology for long periods (weeks and serial passages), freshly isolated PαS cells rapidly take on myofibroblastic characteristics when cultured in identical conditions with significantly increased initial rates of proliferation, more in-keeping with reports of stellate cells isolated by density centrifugation. Activation and proliferation of freshly isolated PαS cells was increased by culture on type I collagen, known to activate stellate cells, and could be strongly inhibited by

culture with 2-deoxyglucose, a potent inhibitor of glycolysis, previously shown to be required for appropriate activation and transdifferentiation of stellate cells. When cultured in conditions allowing the selection and long-term culture of freshly isolated murine hepatic stem/progenitor cells, both PαS and $Sca1^+$ cells formed heterogenous cultures of both stromal and epithelial cells. In the first few days post-isolation, cells were predominantly stromal, however over time areas comprised of cells with epithelial characteristics appeared as clearly defined colonies of tightly aggregated cells and slowly outgrew surrounding stromal cells. Due to the fewer numbers of isolated PαS cells per liver and their use in experiments characterising their fibrogenic potential, in was not possible to examine the long term growth of PαS cells under these conditions or their potential to differentiate into functional hepatic cell types, hepatocytes and biliary epithelial cells. However, it was possible to select and culture epithelial cells derived from cultures of freshly isolated $Sca1^+$ cells for more than 12 weeks and 10 passages without apparent loss of proliferative capacity of changes in morphology. Selected cells had an antigenic profile highly suggestive of, but not definitively, hepatic stem/progenitor cells. Functional assays demonstrated rapid differentiation, or conversion back, to myofibroblastic cells after culture in MSC conditions. However, in conditions designed for the differentiation of murine hepatic stem/progenitor cells into hepatocytes and biliary epithelial cells, it was not possible to demonstrate the differentiation of these cells into functional mature cell types. A single *in vivo* experiment assessing the potential use of selected epithelial cells as a cellular therapy for liver failure was encouraging but inconclusive. Thus, while much work remains to fully characterise prospectively isolated PαS and $Sca1^+$, these results demonstrate the presence of peri-vascular stromal cells resident in adult murine liver with high colony forming potential, the ability to differentiate into

myofibroblastic cells and form long-term cultures of highly proliferative epithelial cells with stem cell characteristics that, with further study, may be definitively demonstrated as hepatic stem/progenitor cells.

The location of PαS in normal liver is in-keeping with previous studies demonstrating the presence of cells with MSC-like characteristics, currently best termed ‘vascular stem cells (VSC)’, in most, if not all, organs. Early reports often described the location of these cells as ‘perivascular’, however more detailed examination has revealed the vascular wall itself as the VSC niche under normal conditions. Immunohistochemistry performed on sections of normal, uninjured mouse liver demonstrated a similar location for PαS cells within the liver as reported for other organs. Although further immunohistochemical analyses using whole-mount samples of large intra-hepatic arteries would be required to conclusively demonstrate presence of PαS cells within the vascular wall itself, PDGFRα and Sca1 staining was observed in all portal vessels and directly adjacent parenchyma. Interestingly this location is also the site of early fibrogenesis seen in chronic hepatocytic diseases, where fibrosis is first predominantly observed in peri-portal regions, before progressing to ‘bridging’ fibrosis where fibrotic septa span the parenchyma between portal triads. This therefore raises the possibility of PαS cells contributing to fibrosis, either directly through the deposition of collagen and/or indirectly by proliferating and differentiating into fibrogenic myofibroblasts. The relative contribution, if any, of PαS to fibrogenesis has yet to be shown but would be best elucidated through the use of chronic hepatocellular injury in cell fate tracking models, particularly the inducible PDGFRα cre recombinase transgenic mouse, where the presence of myofibroblasts

derived from PDGFRα^{+} cells would demonstrate a role for PαS cells in fibrogenesis.

This study demonstrates the prospective isolation of a homogeneous population of PαS that rapidly take on myofibroblast morphology and alpha-smooth muscle actin expression when cultured on plastic or collagen type I. The use of 2-deoxyglucose, a specific inhibitor of glycolysis, inhibited the proliferation and myofibroblastic differentiation of PαS cells, confirmed by the reduced proportion of cells expression αSMA after 7 days culture in the presence of 2-DG. Despite oil red O staining failing to demonstrate substantial intracellular lipid content in PαS cells, the inhibition of PαS cells by 2-DG is likely to be through a similar mechanism to that reported for freshly isolated hepatic stellate cells[183].

The isolation of PαS cells from liver required significant modification and adaptation from the original protocol for isolation of of PαS cells from bone marrow[168]. Firstly, the digestion method for liver was based upon previous reports of isolation of primary murine liver cells and my experience of isolating hepatic stem cells from explanted liver and extra-hepatic bile duct (chapter 6) whilst attempting to maintain as much similarity with the original bone marrow digestion protocol as possible. The major modifications were thus based upon the mechanical dissociation of liver tissue, use of mesh filters and gradient centrifugation while keeping the collagenase digestion approximately the same. A major issue with liver digestion was debris resulting from rapid death and disintegration of hepatocytes which occurs rapidly upon liver excision and is a well described problem in primary hepatocyte isolation resulting in the need for *in situ* liver digestion. Here it was preferable to remove hepatocytes and associated debris from the isolation as soon as possible to prevent technical problems and

minimise the effect of factors released by dying cells on the cells targeted for isolation. From experience and trial and error, it was found that this was best achieved by fine dissociation with scalpels followed by a rapid digestion step with a high concentration of collagenase under vigorous agitation then removal of debris by filtration through fine mesh and re-digestion of remaining tissue. Whilst this increased the degree of tissue dissociation, it did not appear to reduce the yield of PαS cells, indeed increased digestion time appeared to increase PαS yield and viability whilst it is known to have the opposite effect on hepatocyte isolation. The addition of a gradient centrifugation step, routinely used in protocols for the isolation of epithelial stem/progenitor cells from both rodent and human tissues, allowed selection of a fraction containing the majority of cells of interest whilst excluding large amounts of debris and unwanted cells types in the supernatant. This allowed a further increase in yield of PαS cells and speeded up sorting times, known to be a factor influencing the viability of freshly isolated cells.

The prospective isolation of hepatic stellate cells from adult rodent or human liver tissue has not been previously described. The current gold standard method for the isolation of stellate cells exploits their characteristic high lipid content and consequential low density allowing their selection through density centrifugation alone. This approach yields cultures that contain a significant proportion of contaminating cells, notably macrophages and fibroblasts and commonly used culture conditions (plastic and high serum media) leads to rapid activation and transdifferentiation of stellate cells into myofibroblasts.

This method of prospectively isolating cell based on PDGFα and Sca1 expression may have utility in isolating hepatic epithelial stem/progenitor cell populations. Currently used methods for the isolation of hepatic stem/progenitor cells from murine liver rely on injury to facilitate proliferation of hepatic stem/progenitor populations allowing a significant yield. Further, protocols yielding the purest populations with greatest differentiation potential have relied on intracellular markers, preventing the use of prospective isolation with FACS, instead relying on labelling with inducible transgenic mouse models. Sca1 alone has previously used to prospectively isolate progenitor cells from adult murine liver[178] and was shown to yield highly heterogeneous cultures of cells with stromal, endothelial, hepatocytic and biliary morphology and expression profiles. The use of selective culture conditions was not utilised in the study by Clayton *at el.* and thus at the point of isolation, the Sca1 population reported here may be highly similar with the differences in morphology and growth potential conferred by culture conditions only. However, this study demonstrated significantly higher colony formation of PαS compared to $Sca1^{+}$ cells and that PαS cells were also capable of forming large epithelial colonies when cultured in OC+ conditions, indicating PαS cells likely represent a more enriched population of stem/progenitor cells than Sca1 alone. Further work utilising this isolation method may ultimately demonstrate it as a novel and superior method for the isolation of hepatic stem/progenitor cells without the need for liver injury, which almost certainly alters the phenotype and behaviour of stem/progenitor cells prior to isolation, and transgenic labelling models. However there are many of the challenges encountered in this study and limitations that remain to be resolved.

Firstly, the use of selective media was necessary for long-term growth and passaging of epithelial stem/progenitor cells. This study highlights the rarity of true epithelial stem/ progenitor cells in uninjured adult liver, and heterogeneity and plasticity of resulting *in vitro* cultures. Although the use of selective media is routine in both rodent and human, this approach may cause changes to cultured cells that do not accurately represent what occurs *in vivo* and artificially produce cells with stem/progenitor properties. In conditions designed for culture of MSCs only freshly isolated PαS were found to be viable, where they rapidly formed confluent highly homogeneous cultures of myofibroblastic cells, but $Sca1^{+}$ cells failed to grow in these conditions. Both populations could be cultured in conditions for selection of epithelial stem/progenitor cells but gave rise to both stromal and epithelial cell types during the first few days before outgrowth of epithelial colonies. These results would suggest freshly isolated PαS cells are more potent and have the capacity to give rise to a greater range of cell types. Thus, despite epithelial cultures from PαS cells not being characterised, it would appear PαS cells represent a more primitive cell type than $Sca1^{+}$ within the same lineage. Interestingly, although freshly isolated Sca1 cells fail to form myofibroblastic cells, stromal cells were observed in Sca1 cultures in OC+ and selected epithelial stem/progenitor cells from Sca1 cultures were capable of rapid differentiation into myofibroblasts.

Further work is needed to demonstrate robust differentiation of selected epithelial stem/ progenitor cells into hepatocytes and biliary epithelial cells, the mature cell types of the liver. Although attempted several times, it was not possible to culture these cells in 3D collagen gels, conditions necessary for terminal differentiation of hepatic stem cells into biliary

epithelial cells and thus their capacity to form biliary epithelium could not be assessed. Attempts to demonstrate hepatocytic differentiation were also largely unsuccessful. One of the major technical issues was the continued high rate of proliferation even with addition of oncostatin-M, previously demonstrated to effectively halt proliferation of hepatic stem cells and induce differentiation. Although culture in hepatocyte differentiation media for 7 days did result in slight morphological change (cells appeared larger) this may have been largely due to decreased proliferation rate as there was no change in antigenic profile (negative for albumin, low level, patchy AFP expression). Further optimisation of this protocol may have resulted in more robust differentiation. This work is essential in definitively demonstrating PαS do have the capacity to form hepatic epithelial stem/progenitor cells. If selected epithelial colonies from PαS cells are shown to be unable to differentiate into functional hepatocytes, despite their characteristic morphology and expression of pan-CK and AFP, it is possible these cells represent fibroblastic cells that are closely associated with activated and proliferation hepatic stem/progenitor cells in the ductular reaction and are thought to express pan-CK and vimentin along with other stromal markers such as CD56 (NCAM).

Lastly, the single experiment to assess the ability of selected epithelial stem/progenitor cells to engraft into, and reconstitute, chronically injured liver *in vivo* was inconclusive. Hepatic stem cells isolated based on Lgr5 expression have been shown to have this capacity using the FRG model[115] and this experiment is similarly important to hepatocyte differentiation assays in demonstrating the epithelial colonies observed in PαS cell cultures do represent hepatic stem cell colonies. Further replicates of this experiment are required, along with sectioning of

livers to demonstrate engraftment of infused cells. As hepatocytes of FRG mice are deficient in FAH expression, and isolated cells were from wild type mice, FAH immunohistochemistry can be used to identify transplanted cells and assess the degree of engraftment, proliferation and *in vivo* differentiation.

Other future work on this project will investigate the fibrogenic potential of PαS cells by assessing matrix deposition, specifically collagens, and utilise wound healing (scratch) assays to quantify the speed at which cells can proliferate and resolve injury. A direct comparison between PαS cells and stellate cells isolated by density centrifugation would be particularly useful. Fibrogenic liver injury models, particularly acute and chronic carbon tetrachloride administration, could be used to investigate the contribution of PαS cells to fibrogenesis by immunohistochemical analysis to locate and quantify PαS after injury, and isolation to characterise the effect of injury on PαS cells. Cell fate tracing experiments using PDGFRα or Sca1 labelled mice, particularly in injury models, would further elucidate the role of PαS cells in hepatic fibrogenesis.

CHAPTER 5

ACTIVATION OF HEPATIC STEM CELLS IN CHRONIC LIVER DISEASE AND ASSOCIATION WITH RISK OF HEPATOCELLULAR CARCINOMA

5.1. RATIONALE FOR STUDY

Increased understanding of the maturation lineage and antigenic profiles of hepatic stem cells from *in vitro* studies has not been fully applied to histological studies. Recent studies have demonstrated the isolation and long-term *in vitro* culture of adult hepatic stem cells from both rodent[75, 115] and human[1]. These studies, describing as many as 8 distinct stages of the hepatic stem cell maturational lineage[3], have provided detailed characterisation and expression profiles of cells at each stage of differentiation. The use of markers specifically identifying hepatic stem/progenitor cells has not been reported in histological studies until recently. In mouse, markers that also detect mature biliary epithelium, panCK and EpCAM, were commonly used to assess hepatic stem cell activation. In human studies and clinical practice, CK19 and CK7 are used routinely to assess ductular reaction, the histological phenomena mostly closely associated with hepatic stem cell activation.

There is a need for objective methods to objectively quantify hepatic stem cell activation and associated histological phenomena. The lack of specific markers of hepatic stem cells continues to prevent their direct assessment, and validated objective scoring systems that quantify and give clinical relevance to hepatic stem cell activation are still lacking. Currently used methods for quantifying other histological phenomena in liver disease rely on expert liver histopathologist opinion and semi-quantitative scoring systems[44, 184]. Recently there has been progress in the use of objective, fully quantitative assessment methods, particularly for fibrosis through measurement of collagen percentage area[92]. However this approach has yet to be applied to the measurement of hepatic stem activation.

The contribution of hepatic stem cell activation to homeostasis and carcinogenesis in chronic liver disease is incompletely understood. The activation the hepatic stem cell niche is tightly regulated and normally resolves quickly when the insult to the liver is removed[19, 26, 27]. However, in chronic liver diseases, ie. viral, alcoholic and biliary cirrhosis, activation of the hepatic stem cell niche can be maintained over years in an attempt to maintain normal cell number and function. In this scenario, the consequences of rapid cell turnover and continuous supply from the hepatic stem cell niche, and the proportion of functional parenchymal cells derived from stem cells, are unknown. Further, the risk of primary liver cancer is known to be greatly increased in cirrhosis with experimental studies indicating hepatic stem cells may be involved in carcinogenesis[46, 88, 89, 94]. Any association between activation of the hepatic stem cell niche and risk of primary liver cancer, particularly hepatocellular carcinoma, is currently unknown.

Therefore, immunohistochemical techniques allowing visualisation of histological phenomena related to hepatic stem cell activation (ductular reaction, CK19; intermediate hepatobiliary cells, CK7; hepatocytes newly derived from hepatic stem/progenitor cells, EpCAM; and hepatic stem/progenitor cells, Sox9) were assessed and methods for the objective quantification of each were developed. The association of each of these phenomena with risk of HCC development was assessed in two retrospectively identified cohorts of NASH and HCV cirrhotic patients that had undergone fine-needle liver biopsy and had greater than 3 years follow up at the Queen Elizabeth Hospital Birmingham.

5.2. RESULTS

5.2.1 Objective quantification of ductular reaction using Cytokeratin 19 (CK19) immunohistochemistry. Immunohistochemical staining for CK19 was observed on biliary epithelium (**Fig 5.1. arrowheads**) in normal, uninjured, adult liver with very occasional small, isolated, single cells (**Fig 5.1. arrows**) observed in peri-portal parenchyma. All $CK19^{+}$ cells have characteristic biliary morphology, being largely cuboidal (cells of the larger bile ducts may be columnar), smaller than hepatocytes (approximately 8μm vs 20μm), located within the limiting plate arranged in lumen (**Fig 5.1**).

In chronically diseased liver, CK19 marks biliary epithelium and ductular reactive cells, observed as partially formed lumen or strings of cells infiltrating into peri-portal parenchyma in close proximity to inflammatory infiltrates and fibrous septa. $CK19^{+}$ cells are rarely observed in parenchyma distant from peri-portal or peri-septal regions (**Fig 5.2A**). CK19 immunohistochemistry occasionally detects isolated hepatocytic cells potentially representing intermediate hepatobiliary cells or hepatocytes newly derived from hepatic stem cells. Stromal, immune and endothelial cells are invariably negative for CK19.

High quality chromogenic CK19 staining, with intense staining and low background results in a high contrast image that can be analysed by the ‘Color Threshold’ function of ImageJ(39) The production of a binary image by ImageJ (**Fig 5.2B**) allows the quantification of ‘positive’ pixels and percentage area stained, a value that can be used to closely approximate the degree of ductular reaction.

Figure 5.1. CK19 immunohistochemistry on normal liver specifically marks biliary epithelium. Representative image (100x) of CK19 immunohistochemistry on normal, uninjured, adult liver demonstrating specific staining of biliary epithelium (arrowheads)

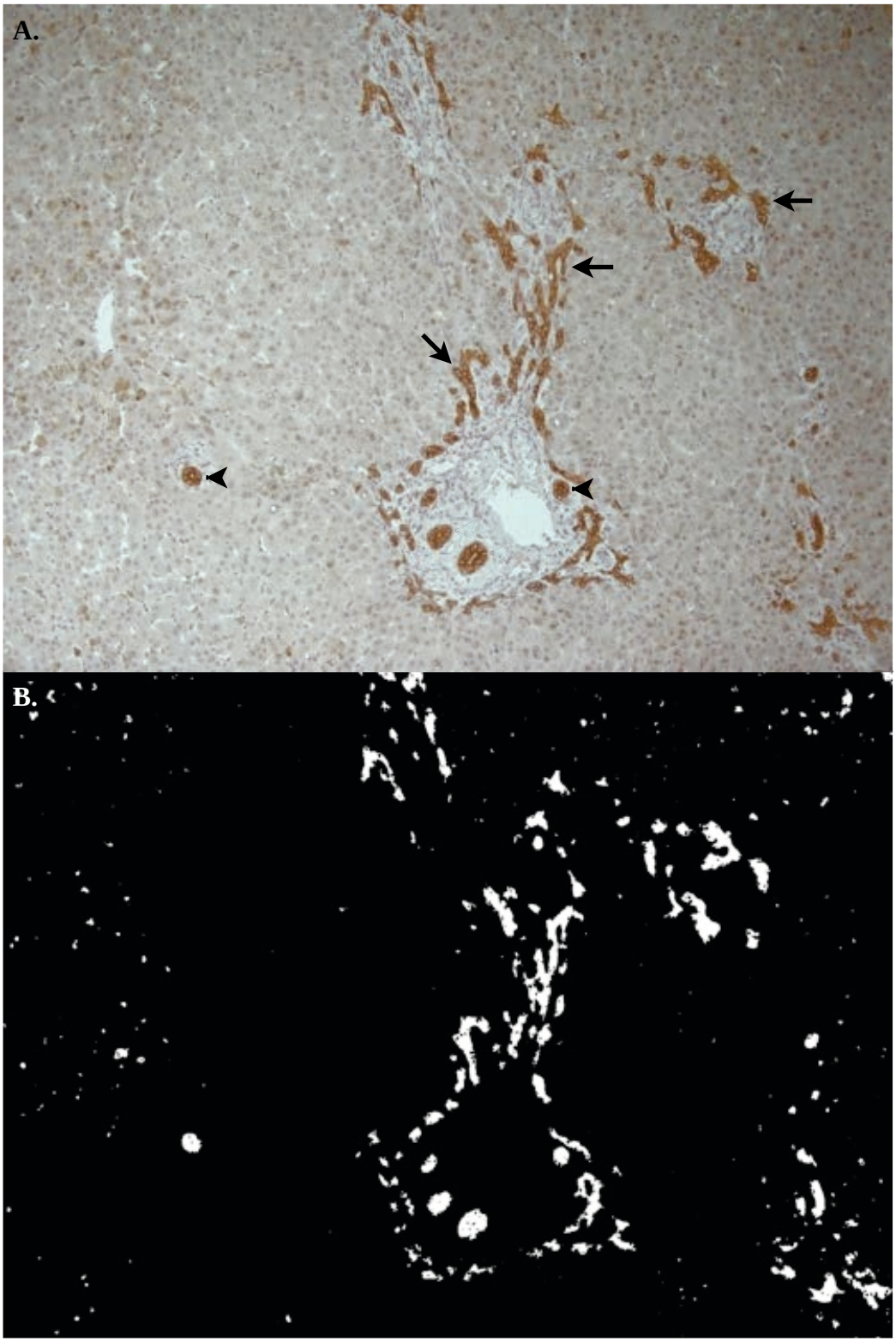

Figure 5.2. CK19 immunohistochemistry can be quantified using ImageJ to measure ductular reaction. A, Representative image of cytokeratin 19 immunohistochemistry on explanted HCV cirrhotic liver (arrowheads, normal epithelium; arrows, ductular reaction; 100x). **B,** Binary image produced from the same image by colour threshold function of ImageJ allowing quantification of CK19 staining and approximation of ductular reaction

5.2.2. Quantification of intermediate hepatobiliary cells using cytokeratin 7 (CK7) immunohistochemistry. Cytokeratin 7 (CK7) immunohistochemistry on normal, uninjured liver sections is similar to that observed for CK19 immunohistochemistry with only the biliary epithelium stained. However, in chronically diseased liver a number of cell types display cytoplasmic CK7 staining. Normal biliary epithelial cells are observed forming distinct lumen with ductular reactive cells seen as strings, or aggregates, of cells that do not form functional lumen. In addition, CK7 marks two other cell types. Occasional cells with distinct biliary morphology and intense cytoplasmic CK7 staining are observed in isolation or small clusters within the liver parenchyma and distant from peri-portal or peri-septal regions (**Fig 5.3. red arrows**). These cells are commonly referred to as isolated cholangiocytes and are considered to be distinct from the ductular reaction with suggestion these cells represent terminal branches of the biliary tree known as the Canals of Hering or possibly hepatic stem/ progenitor cells. If these cells are hepatic stem/progenitor cells distinct from biliary epithelium and ductular reaction, their ancestry, fate and function have yet to be fully elucidated. Larger cells with hepatocytic morphology and less intense cytoplasmic CK7 staining (**Fig 5.3. green arrows**) are also observed throughout the parenchyma, usually as clusters of cells (**Fig 5.3. highlighted in green boxes**), and are commonly referred to as 'intermediate hepatobiliary cells' (IHCs). With high stringency chromogenic CK7 immunohistochemistry, IHCs can be distinguished from biliary epithelium based on size and location, and from isolated cholangiocytes through size, morphology and CK7 staining intensity.

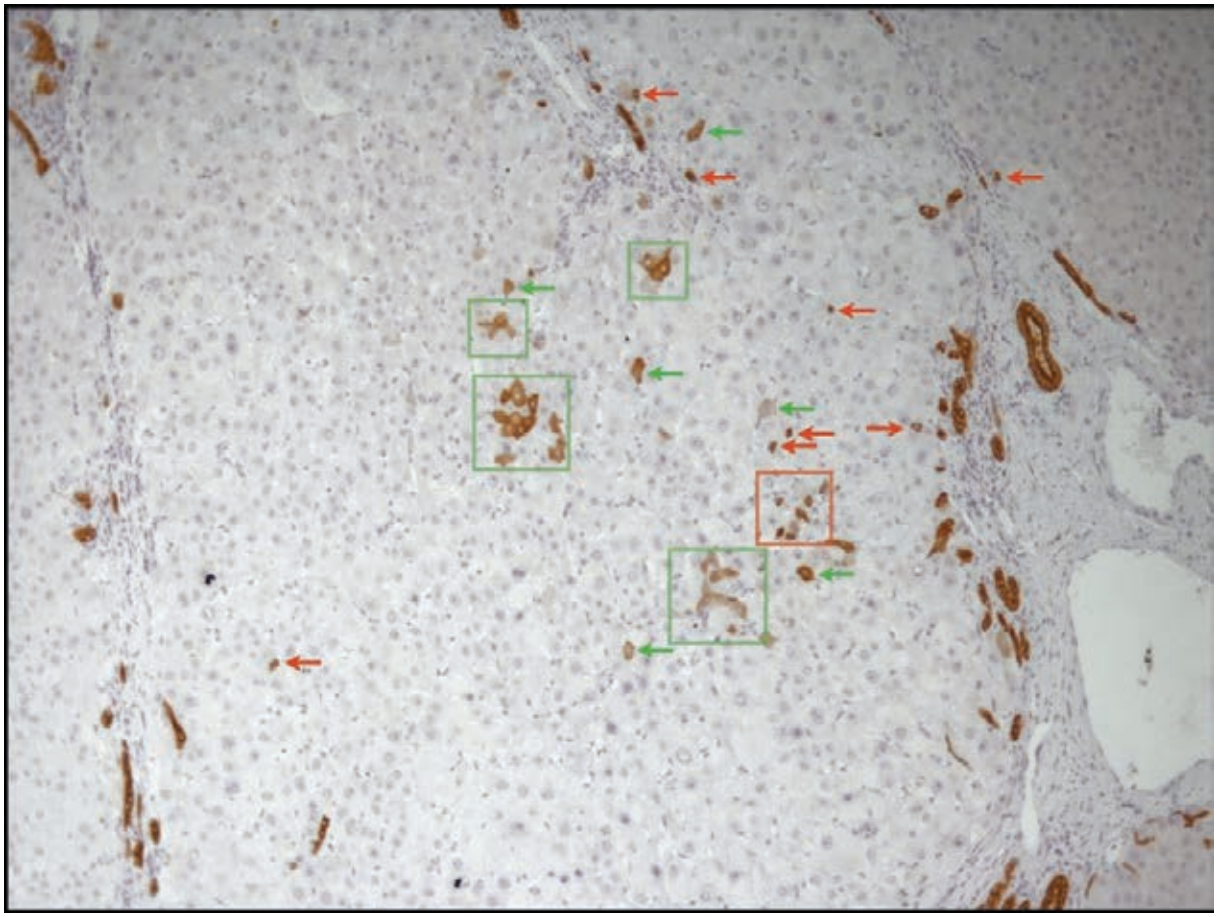

Figure 5.3. CK7 immunohistochemistry detects intermediate hepatobiliary cells in NASH cirrhotic explanted liver. Representative image (100x) of cytokeratin 7 immunohistochemistry of NASH cirrhotic explanted liver. Red arrows highlight isolated mature cholangiocytes (possibly Canals of Hering). Green arrows and boxes highlight intermediate hepatobiliary cells

5.2.3. Quantification of hepatocytes newly derived from hepatic stem cells using epithelial cell adhesion molecule (EpCAM) immunohistochemistry. In normal liver epithelial cell adhesion molecule (EpCAM) is exclusively expressed by mature biliary epithelium, seen as intense cytoplasmic staining (**Fig 5.4A, arrowheads**), and occasional isolated cholangiocytes that are also identified with CK7 and CK19 immunohistochemistry (**Fig 5.4A, arrows**). Polygonal hepatocytic cells invariably have a membranous pattern of EpCAM expression in contrast to cholangiocytes that maintain a cytoplasmic distribution in injured liver. In NASH cirrhosis, EpCAM expression was always membranous and positive hepatocytes were in small foci in peri-portal or peri-septal areas, often in close proximity to ductular reaction (**Fig 5.4B, arrows**).

In cases of HCV cirrhosis large numbers of hepatocytes displaying membranous EpCAM expression are commonly observed, particularly in peri-portal or peri-septal regions (**Fig 5C-F**). Distinct regions of $EpCAM^+$ parenchyma (**Fig 5.4C, arrow**) potentially identify active regeneration from hepatic stem/progenitor cells. Interestingly, $EpCAM^+$ hepatocytes are most commonly observed in regenerating nodules of cirrhotic livers (**Fig 5.4D**), perhaps supporting previous evidence that these nodules are derived from proliferation of adjacent hepatic stem cells[74]. In some cases of HCV cirrhosis almost all hepatocytes were seen to be $EpCAM^+$ (**Fig 5.4E**). Intensity of EpCAM staining appears to decrease gradually from highest in peri-portal and peri-septal areas to weak or no expression on centri-lobular hepatocytes. Smaller cells with more intense membranous expression of EpCAM are observed directly adjacent to fibrotic septa (**Fig5.3F, arrowheads**) with larger, more distal cells seen to have less intense membranous EpCAM expression and were occasionally binucleate (**Fig5.3F, arrows**) characteristic of mature hepatocytes.

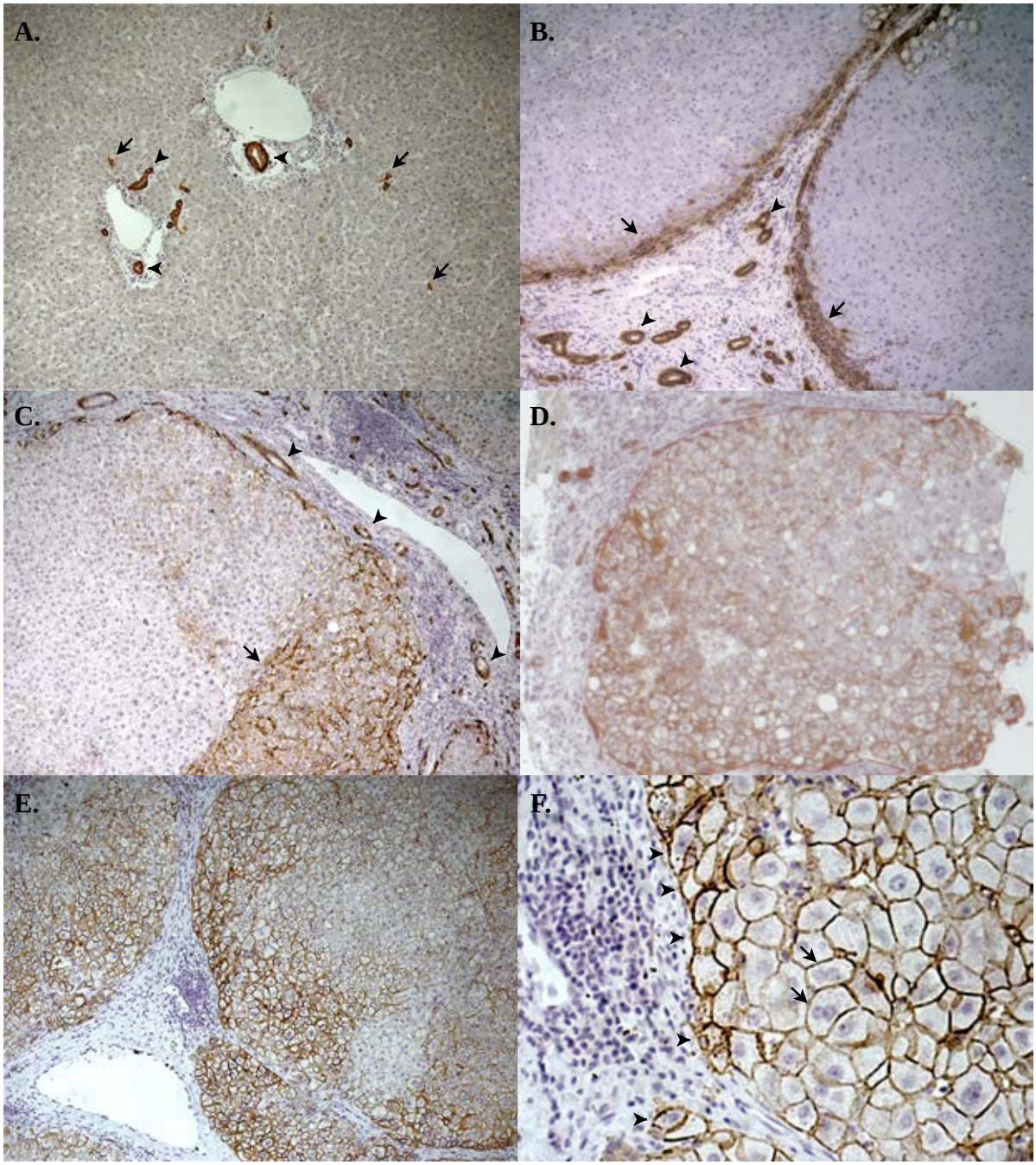

Figure 5.4. EpCAM immunohistochemistry allows identification of hepatocytes newly derived from hepatic stem/progenitor cells. Representative images of EpCAM immunohistochemistry on **A,** normal, uninjured adult liver (arrowheads, normal epithelium; arrows, isolated cholangiocytes; 100x) **B,** NASH cirrhotic explanted liver (arrowheads, normal epithelium; arrows, peri-septal $EpCAM^+$ ductular reaction; 100x), **C,** HCV cirrhotic explanted liver with a distinct region of $EpCAM^+$ parenchyma (arrow) adjacent to an area of $EpCAM^-$ parenchyma (arrowheads, normal epithelium; 100x), **D,** NASH cirrhotic biopsy tissue with $EpCAM^+$ regenerative nodule (demarcated in red, 200x), **E,** HCV cirrhotic liver with a high proportion of $EpCAM^+$ hepatocytes. **F,** high magnification (400x) view demonstrating small hepatocytes (arrowheads) and binuclear hepatocytes (arrowheads) of peri-septal region from panel **E**

As foci of parenchyma expressing EpCAM were reasonably clearly demarcated (**Fig 5.5**), ImageJ can be used to the quantify these areas after delineated by the user and produce a value for the proportion of parenchyma with cytoplasmic EpCAM expression. Thus, by also measuring the total parenchymal area using ImageJ, an approximation of the proportion of $EpCAM^+$ hepatocytes can be calculated (area of $EpCAM^+$ parenchyma divided by total area of parenchyma).

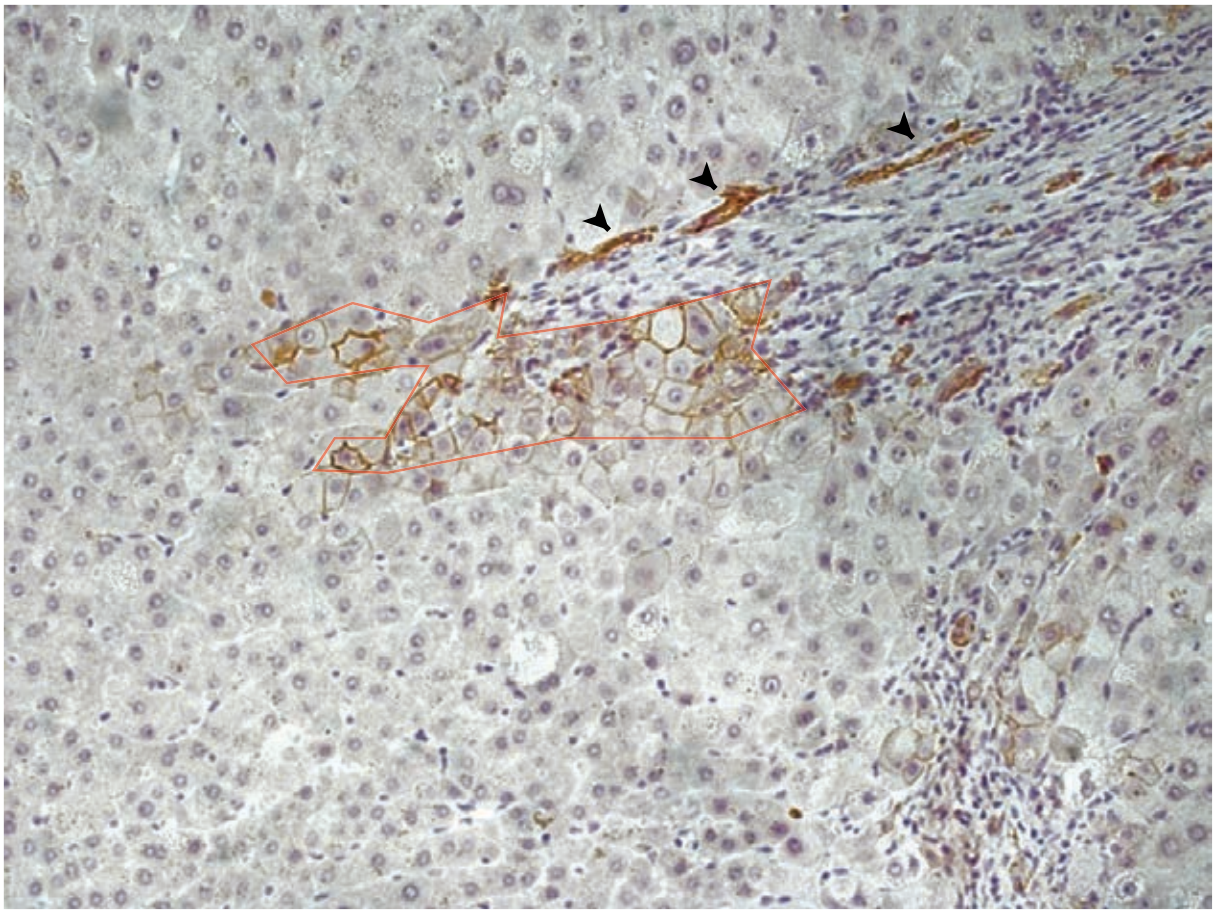

Figure 5.5. Presence of hepatocytes with membranous EpCAM expression in NASH cirrhosis. Representative image (100x) of EpCAM immunohistochemistry demonstrates cytoplasmic EpCAM staining of mature bile ductules (arrowheads) and membranous EpCAM staining of mature hepatocytes (demarcated in red)

5.2.4. Quantification of hepatic stem/progenitor cells using Sox9 immunohistochemistry.

Sox9 has been reported as a specific marker of hepatic stem cells in both rodent and human adult liver. In normal liver, expression of Sox9 is infrequent and restricted to a small proportion of biliary epithelial cells only. In diseased liver, nuclear expression of Sox9 is observed on most biliary epithelial cells of normal lumen (**Fig 5.6, arrowheads**) and ductular reaction. Sox9 expression is predominantly observed in peri-portal regions and with the presence of $Sox9^+$ becoming less frequent in centri-lobular regions. In cases of severe injury, particularly HCV cirrhosis, parenchymal regions are observed where almost all parenchymal cells display nuclear Sox9 expression (**Fig 5.6, arrows**). By morphology alone it is not possible to definitively assess the cell types expressing Sox9 but the close proximity of $Sox9^+$ nuclei suggest Sox9 expressing cells are unlikely to be hepatocytes and most likely hepatic stem/progenitor cells, hepatoblasts or activated stellate cells. Sox9 expression has not been reported for any immune cell types. Although more recent studies have reported Sox9 expression on activated stellate cells, detailed fate tracing studies have demonstrated the utility of Sox9 in identifying hepatic stem cells and failed to demonstrate stromal progeny from $Sox9^+$ cells. Thus, for the purpose of this study the number of $Sox9^+$ nuclei were counted as a measure of the number of hepatic stem cells and degree of hepatic stem activation.

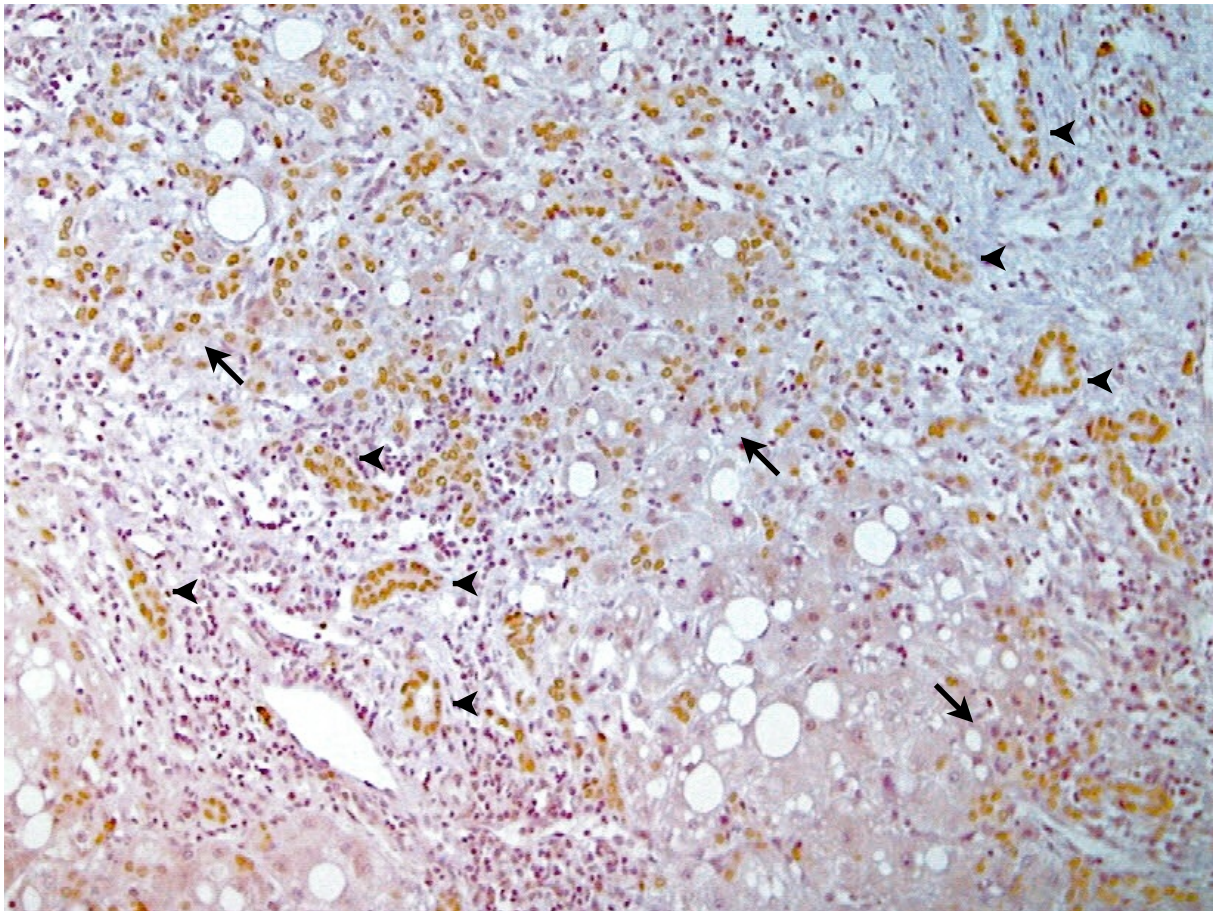

Figure 5.6. Activation of the hepatic stem cell niche in HCV cirrhosis visualised by Sox9 immunohistochemistry. Representative image (200x) of Sox9 immunohistochemistry on HCV cirrhotic explanted liver. Nuclear Sox9 staining is observed on normal biliary epithelium (arrowheads) and on peri-portal parenchymal cells (arrows)

5.2.5. Hepatic stem cell activation occurs in all major aetiologies of chronic liver disease.

To assess hepatic stem cell activation in chronic liver disease, 5 samples of cirrhotic explanted liver tissue for each of the chronic liver diseases PBC, HCV, NASH and ALD were selected from the Centre for Liver Research tissue bank and stained with CK19, CK7, EpCAM and Sox9.

Primary cirrhosis (PBC)

In primary biliary cirrhosis (PBC), cytokeratin 19 (CK19) staining marks large bile ducts, remnant small ducts and peri-septal ductular reactive cells. Cytokeratin 7 (CK7) staining appears to mark the same population of cells as those marked by CK19 along with an expanded population of ductular reactive cells. Foci of $CK7^{+}$ intermediate hepatobiliary cells are occasionally observed in cases of PBC. Through the use of sequential sections, IHCs appear to be negative for CK19, EpCAM and Sox9 and are often observed in centri-lobular locations distinct from ductular reactive cells detected with CK7 or EpCAM. EpCAM and Sox9 immunohistochemistry appears to mark all biliary epithelial and ductular reactive cells. Interestingly, cytoplasmic expression of Sox9 appears to be present in hepatocytic cells directly adjacent to peri-portal fibrotic septa, however EpCAM expression by hepatocytes is not observed in PBC. This observation has not previously been reported in PBC cirrhosis.

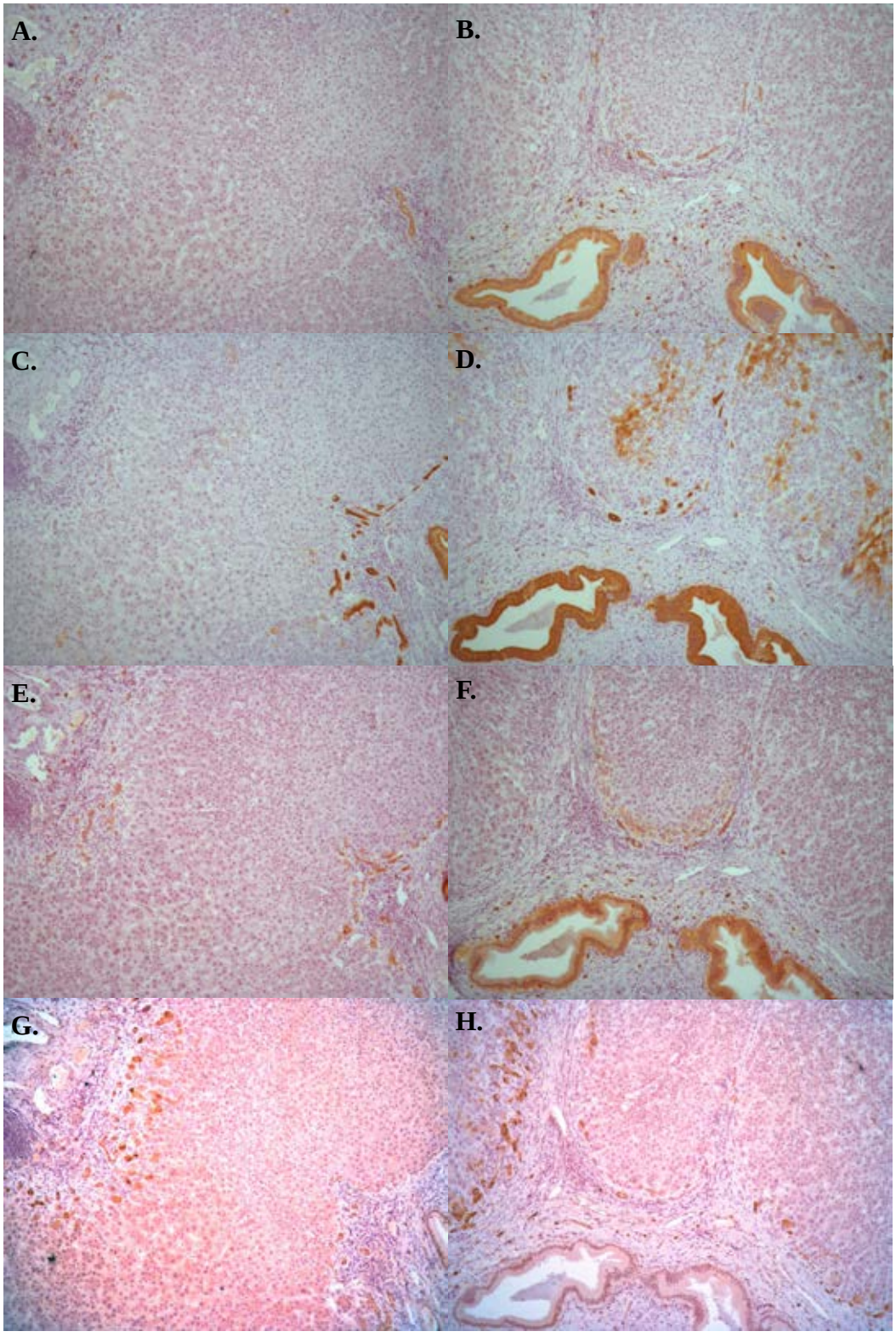

Figure 5.7. Characterisation of hepatic stem cell populations in PBC cirrhosis. Representative images (100x) of immunohistochemical staining for **AB,** CK19; **CD,** CK7; **EF,** EpCAM; and **GH,** Sox9 in serial sections from two cases (**A,C,E,G** and **B,D,F,H**) of PBC cirrhosis

Hepatitis C virus (HCV) cirrhosis

Expression of CK19 in HCV cirrhosis is restricted to the biliary tree and a small proportion of ductular reactive cells. As observed in PBC, CK7 and EpCAM detect all biliary epithelial and ductular reactive cells. Sox9 expression is exclusively observed as nuclear staining of biliary epithelial and ductular reactive cells. The presence of $EpCAM^{+}$ hepatocytes is frequently observed in HCV cirrhosis. EpCAM expression in hepatocytes is typically membranous, in contrast with the cytoplasmic pattern observed in biliary epithelium and ductular reactive cells. $EpCAM^{+}$ cells are most frequently observed in peri-portal and peri-septal regions but may extend to throughout the lobule. Regenerative nodules are commonly entirely composed of $EpCAM^{+}$ hepatocytes that may indicate stem cell mediated regeneration, particularly as previous studies have suggested these nodules may have clonal origins from hepatic stem cells. The proportion of hepatocytes expressing EpCAM is cirrhosis appears to be quite variable, ranging from small numbers of peri-portal hepatocytes to the majority of hepatocytes with membranous EpCAM expression extending throughout the liver parenchyma.

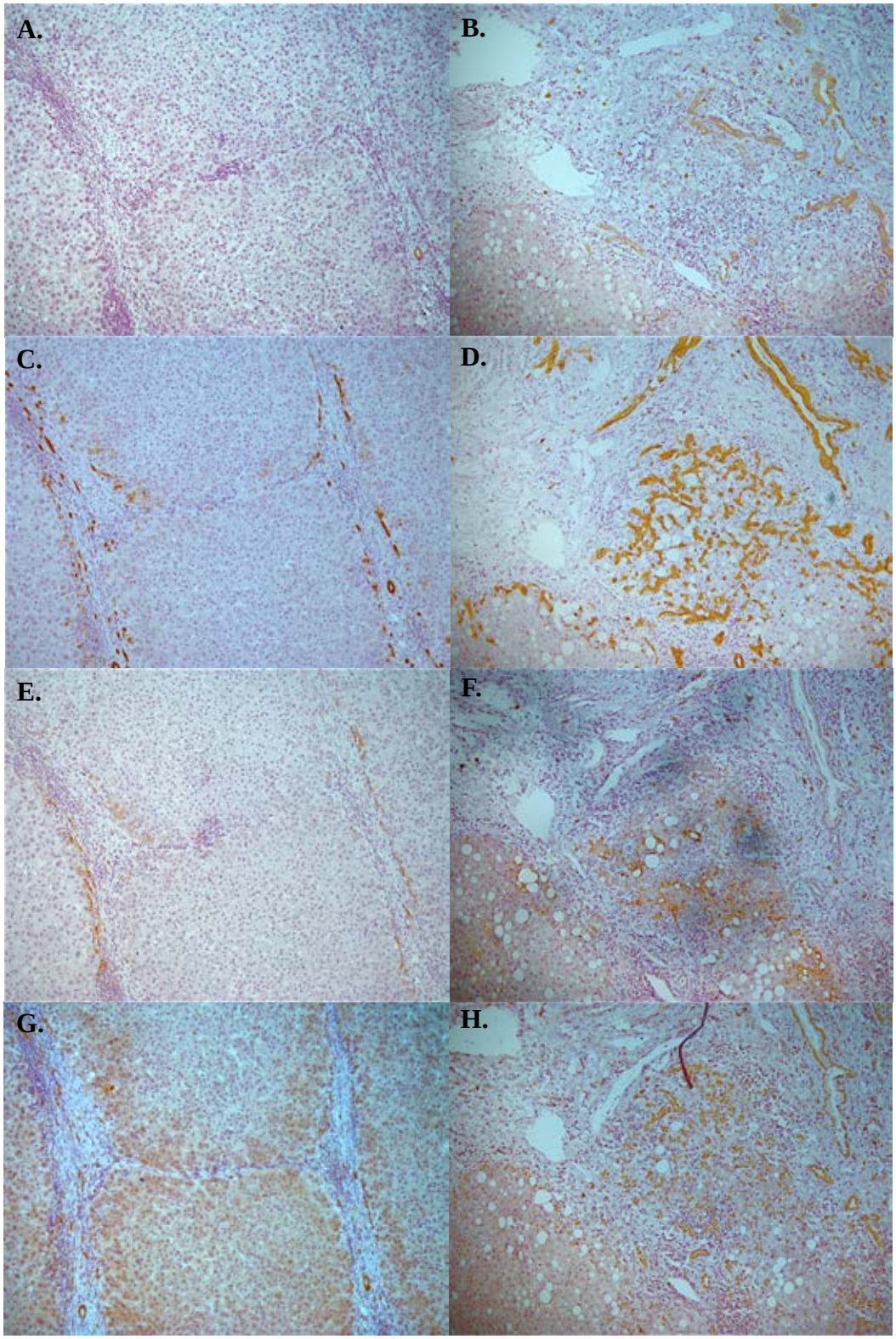

Figure 5.8. Characterisation of hepatic stem cell populations in HCV cirrhosis. Representative images (100x) of immunohistochemical staining for **AB,** CK19; **CD,** CK7; **EF,** EpCAM; and **GH,** Sox9 in serial sections from two cases (**A,C,E,G** and **B,D,F,H**) of HCV cirrhosis

Non-alcoholic steatohepatitis (NASH) cirrhosis

CK7, EpCAM and Sox9 immunohistochemical analysis of NASH cirrhotic sections labelled all biliary epithelial cells and ductular reactive cells, with CK19 expression observed in a small proportion of ductular reactive cells similar to other other chronic diseases described above. Ductular reactive is commonly extensive in NASH cirrhosis and is closely associated spatially with fibrotic septa. The presence of $EpCAM^{+}$ hepatocytes is rarely observed in NASH cirrhosis, being significantly more infrequent than commonly seen in HCV cirrhosis.

Alcoholic liver disease (ALD) cirrhosis

ALD is histologically similar to NASH with concurrent inflammation, fibrosis, ductular reaction and hepatic stem cell activation. Observations with CK19, CK7, EpCAM and Sox9 on ALD cirrhotic samples (not shown) were not substantially different to those observed for NASH.

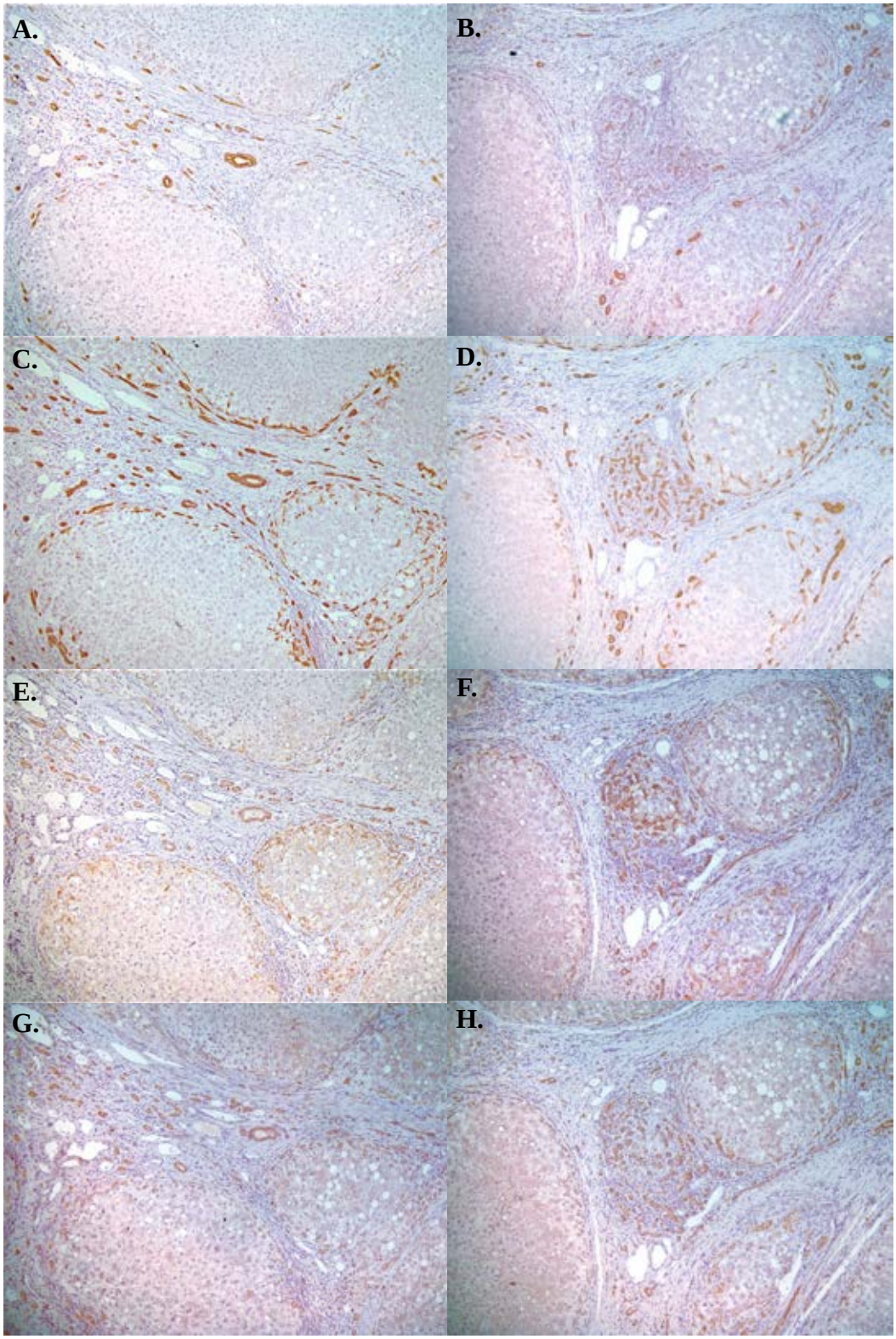

Figure 5.9. Characterisation of hepatic stem cell populations in NASH cirrhosis. Representative images (100x) of immunohistochemical staining for **AB,** CK19; **CD,** CK7; **EF,** EpCAM; and **GH,** Sox9 in serial sections from two cases (**A,C,E,G** and **B,D,F,H**) of NASH cirrhosis

5.2.6. Quantification of histological phenomena and association with subsequent development of HCC in NASH cirrhosis. NASH cirrhotic biopsies were retrospectively identified from patients with greater than 3 years follow up at the Queen Elizabeth Hospital Birmingham allowing any subsequent development of HCC after time of biopsy to be identified. A total of 18 biopsies were identified that had a definitive diagnosis of NASH without overlapping aetiologies or previous history of cancer. Clinical data was retrieved by Dr. Matthew Armstrong for each patient at the time of biopsy used. Not all data for each risk factor were available: gender data were available for all patients; hypertension for 13 of 18; obesity for 8 of 18; hyperlipidaemia for 7 of 18; and diabetes for 14 of 18 (**Fig 5.10A**). No significant differences in the incidence of hypertension, obesity, hyperlipidaemia, or diabetes, risk factors for NASH, were found between patients that did, and patients that did not, subsequently develop HCC (**Fig 5.10B**). Of the 18 patients, 6 were found to have subsequently developed HCC. All patients that developed HCC were male. Of those that did not 6 were male and 4 were female, in-keeping with the previously reported increased risk of HCC in male patients[132].

Ductular reaction was quantified by calculating the percentage area of the entire biopsy covered by CK19 immunohistochemistry. The presence of intermediate hepatobiliary cells using CK7 immunohistochemistry was defined *as per* Ziol *et. al*: “the observation of at least 2 foci of more than 5 polygonal-shaped hepatocytes, measuring from 6 to 40 μm large, with cytoplasmic positivity”[94]. The presence and proportion of $EpCAM^{+}$ hepatocytes was extremely low in this cohort of NASH cirrhotic biopsies and so was not suitable for further assessment. At the time of this analysis Sox9 immunohistochemistry had not been optimised and due to the clinical nature and scarcity of biopsy material, it was felt to be inappropriate to

re-section blocks for the purpose of analysing Sox9 expression for this study alone. Sox9 immunohistochemistry was performed on the HCV cohort identified as a result of this preliminary study in NASH cirrhotics (described in 5.2.7).

Quantification of CK19 immunohistochemistry revealed trend towards greater severity of ductular reaction in biopsies from those patients that subsequently developed HCC (**Fig 5.11A**, p=ns). Due to the lower number of patients included in this study it is possible that this association would reach significance in a larger study with greater statistical power.

Ten biopsies were found to have presence of $CK7^+$ IHCs with IHCs absent in the remaining 8. 4 out of the 10 (40%) biopsies with presence of IHCs and 2 out of the 8 (25%) biopsies with absence of IHCs subsequently developed HCC (**Fig 5.11B**). As some patients had a greater period of follow-up incidence per year was calculated and patients with presence or absence of IHCs on biopsy were compared. Patients with presence of IHCs were found to have an annual incidence of HCC of 7.8% whilst patients with absence of IHCs were found to have an annual incidence of 4.9%. The incidence rates, 8.14% and 3.12% respectively, were similar to those previously reported by Ziol *et. al*[94] (**Table 5.1**) in a cohort of HCV cirrhotic patients, however the difference was non-significant in our cohort possibly due to low numbers of patients included and consequent lack of statistical power. Due to the size of this cohort it was not possible to perform multivariate analysis to determine the contribution of known risk factors for HCC including male gender, age, ethnicity, obesity, and type 2 diabetes. Without this analysis it is not possible to fully assess the association between ductular reaction and presence of $CK7^+$ intermediate hepatobiliary cells and risk of HCC development in this cohort of NASH cirrhotic patients.

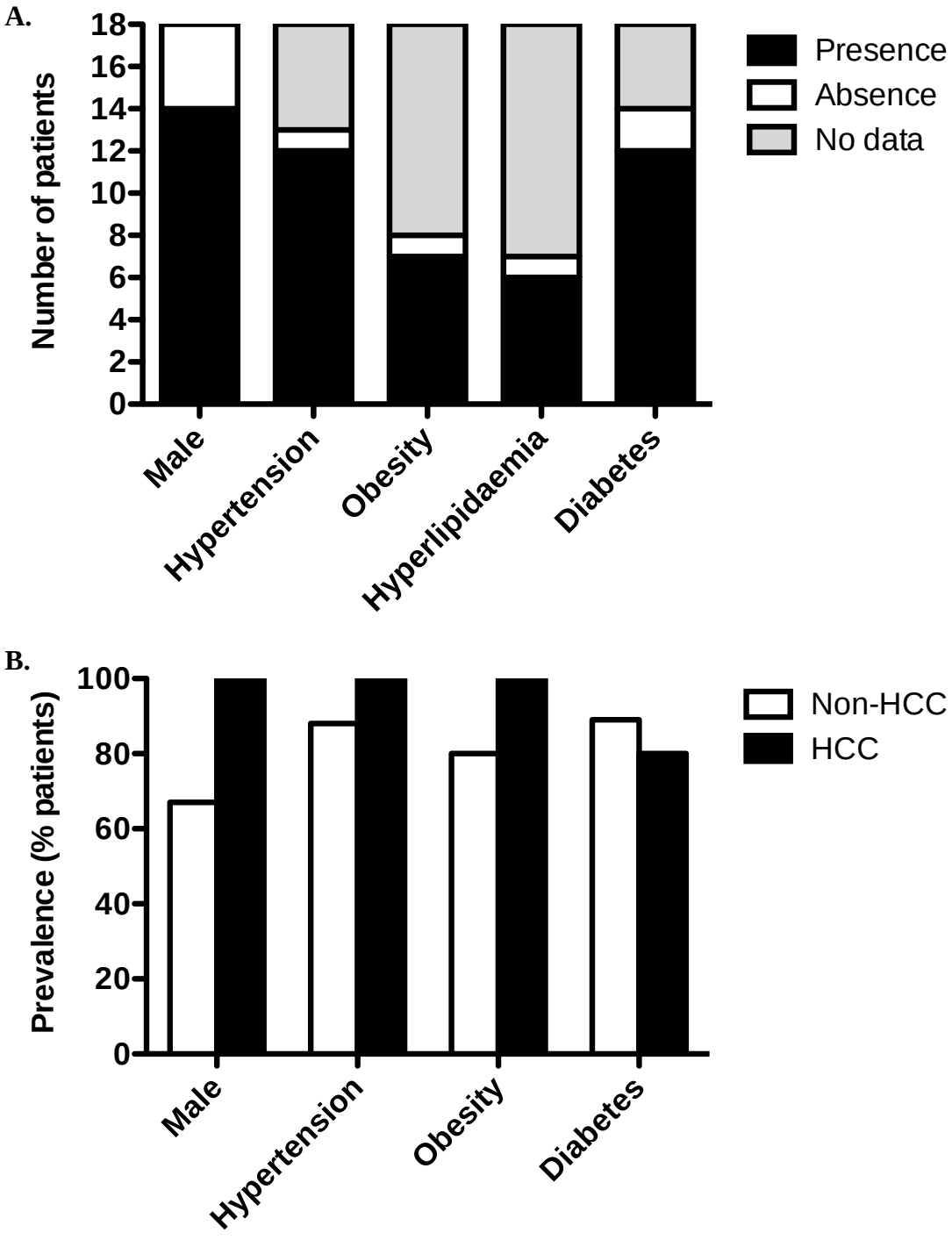

Figure 5.10. Available data on risk factors for NASH reveal no significant associations with development of HCC. Bar charts representing **A,** the total number of patients with presence (black bars) and absence (white bars) and **B,** prevalence of clinical measures: male gender; hypertension; obesity; hyperlipiaemia; and diabetes in the 18 patients used for the NASH cirrhotic biopsy cohort. The number of patients where no data were available for each clinical measure is shown (grey bars)

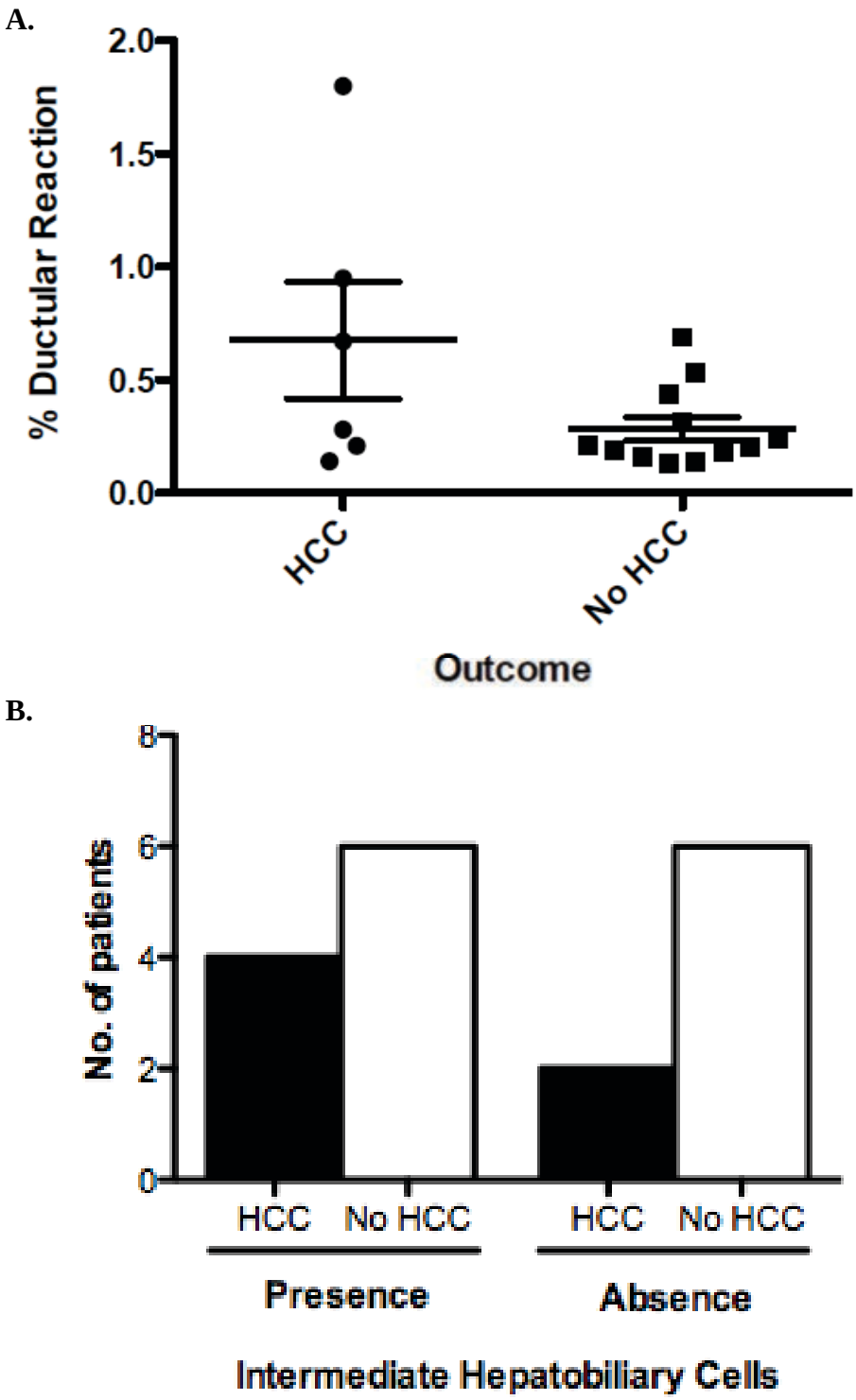

Figure 5.11. Quantification of histological phenomena in NASH cirrhotic biopsies reveals an association with subsequent development of HCC. A, Comparison of percentage area covered by ductular reaction in NASH cirrhotic biopsies in patients that did and did not develop HCC subsequently (p=ns, 0.055, error bars represent S.E.M.). **B,** Number of patients with presence or absence of IHCs that subsequently did or did not develop HCC

Table 5.1. The subsequent incidence of HCC in NASH cirrhotic patients with and without presence of intermediate hepatobiliary cells in liver biopsy.

Intermediate hepatobiliary cells	Present	Absent
Number of biopsies	10	8
Overall incidence of HCC	40%	25%
Average follow-up time (years)	5.1	5.1
Incidence per year	7.8%	4.9%
Incidence per year reported by Ziol *et al.*	8.14%	3.12%

5.2.7. Retrospective identification and characterisation of a large cohort of HCV cirrhotic patients. Due to the low power and inability to detect significant associations using a small number of NASH cirrhotic biopsies, a larger cohort of patients that allowed assessment the association of quantified histological phenomena related to hepatic stem cell activation and risk of HCC development was identified. Liver biopsies from the original diagnosis of HCV cirrhosis were retrospectively identified where patients had at least 3 years follow-up at the Queen Elizabeth Hospital Birmingham allowing subsequent development of HCC to be assessed. All patients with overlapping aetiologies or previous history of cancer were excluded. Unlike with NASH, the diagnosis of HCV is definitive with the most common overlapping aetiologies, co-infection with HIV and/or HBV, being similarly simple to determine. This allowed the identification of a larger cohort of 74 HCV cirrhotic patients, characterised in **Table 5.2**. As with the NASH cohort there was a greater proportion of male patients (54 of 74, 73%). The mean age at biopsy was 51 years. 2 patients were lost to follow-up, of those with data, the mean follow up time was 9 years to February 2014, at which point development of HCC was identified in 16 patients (22%). Ishak scores were recorded from biopsy reports. All biopsies had an Ishak fibrosis score of 5 or 6 out of 6 (cirrhotic) and a median necroinflammation score of 5. Portal inflammation and interface hepatitis were the most reported individual components of the Ishak score (median = 2). All biopsies were stained for CK19, CK7, EpCAM and Sox9. Due to blinding, analysis is ongoing and cannot be completed until all sections have been fully quantified. Final analysis will include correction for all relevant clinical and histological data to assess independent associations between quantified histological phenomena and risk of HCC development.

Table 5.2. Clinical data on retrospectively identified HCV cirrhotic patients.

Number of male patients (%)	54 (73)
Mean age at biopsy in years (standard deviation)	50.7 (8.9)
Median periportal/septal interface hepatitis score (/4)	2
Median confluent necrosis score (/6)	0
Median focal lytic necrosis score (/4)	1
Median portal inflammation score (/4)	2
Median Ishak necroinflammation score (/18)	5
Median Ishak fibrosis score (/6)	6
Mean years of follow up February 2014 (standard deviation)	9.0 (2.0)

5.3. DISCUSSION

Each of the markers used in this study, CK19, CK7, EpCAM and Sox9, identified cells at different stages of the hepatic stem maturational lineage allowing the quantification of ductular reaction, intermediate hepatobiliary cells, hepatocytes newly derived from hepatic stem cells and hepatic stem cells specifically.

Cytokeratin 19 (CK19) is routinely used histologically to specifically stain biliary epithelial cells and has utility in assessing biliary pathologies and characterising tumour phenotype[101]. CK19 was restricted to the biliary epithelium marking only mature biliary epithelial and ductular reactive cells in all aetiologies assessed in this study.

Cytokeratin 7 (CK7) was found to mark the same population of biliary and ductular reactive cells as observed with CK19 immunohistochemistry. CK7 also identifies a population of parenchymal cells that extended throughout the lobule with hepatocytic morphology that have previously been described as ‘intermediate hepatobiliary cells’[94] perhaps representing hepatoblasts. There is currently controversy around the placement of IHCs within the maturational lineage of hepatic stem cells, with the possibility that IHCs are hepatocytes expressing CK7 *de novo* in response to injury. IHCs were found to be particularly common in HCV cirrhosis, were occasionally observed in ALD and NASH cirrhosis and rarely in PBC.

Epithelial cell adhesion molecule (EpCAM) is routinely used to prospectively isolate hepatic stem cells from foetal and normal adult liver through the use of magnetic immunoselection and selective culture conditions[1]. However the cell types expressing EpCAM were only

recently reported in chronic liver injury[74]. These immunohistochemical studies demonstrate EpCAM expression to be restricted to the biliary epithelium in normal adult liver as previously reported[87]. In injured liver EpCAM is found on all cells of the biliary epithelium, ductular reactive cells and hepatocytes. Whilst biliary and ductular cells have a cytoplasmic distribution of EpCAM, in hepatocytes EpCAM expression was invariably restricted to the cell membrane. $EpCAM^+$ hepatocytes are commonly observed adjacent to portal triads and fibrous septa potentially indicating a relationship with the hepatic stem cell niche or ductular reactive cells respectively. Following this study, increased telomere length in $EpCAM^+$ hepatocytes was reported[74] indicating fewer replications and therefore more recent genesis of $EpCAM^+$ hepatocytes supporting the hypothesis that these cells are newly derived from proliferating hepatic stem cells. The large proportion of $EpCAM^+$ hepatocytes possibly indicates rapid proliferation and differentiation of hepatic stem/progenitors contributing to parenchymal regeneration that mature hepatocytes may no longer provide. In these cases regenerative nodules are invariably constituted entirely of $EpCAM^+$ hepatocytes corroborating this hypothesis.

Immunohistochemical studies of Sox9 in chronic liver diseases have not previously been reported. This study demonstrated the presence of $Sox9^+$ cells in explanted diseased adult liver. Sox9 expression was observed on all cells of the biliary epithelium and was frequently observed on parenchymal cells adjacent to fibrotic septa or within regenerating nodules. Sox9 is a nuclear transcription factor and as such is most commonly observed in the nuclei of cells[165]. Interestingly, in PBC livers we observed the presence of hepatocytic cells with cytoplasmic Sox9 expression directly adjacent to fibrous septa. This observation was not seen

in any of the ALD, NASH or HCV livers examined (n=5 for each group) and has not been previously reported. Whether this observation reflects aberrant differentiation of $Sox9^{+}$ (hepatic stem/progenitor) cells in PBC, where presumably these cells should be restricted to the biliary lineage, is unknown. Previous studies have however described the presence of cytoplasmic Sox9 as conferring abrogation of proliferation in breast cancer cell lines[185], increased proliferation of breast cancer cells and poor prognosis[186]. Further study of hepatocytic cells with cytoplasmic expression of Sox9 should determine the clinical relevance and pathophysiological role of these cells.

Once techniques had been optimised for the quantification of histological phenomena using markers associated with hepatic stem/progenitor cells: ductular reaction (CK19), intermediate hepatobiliary cells (CK7); and hepatocytes newly derived from hepatic stem/progenitor cells, a cohort of 19 NASH cirrhotic biopsies were identified. Biopsies were included if they were the first biopsy diagnostic of cirrhosis, from at least 3 years ago and from patients with no previous history of cancer or overlapping liver disease. This allowed the association between the numbers of each cell type and subsequent risk of developing HCC to be assessed.

In this small cohort, no association was detected between the severity of ductular reaction and subsequent risk of developing HCC in NASH cirrhosis. Ductular reaction is currently regarded as the abnormal proliferation of mature cholangiocytes and is seen in almost all aetiologies of chronic liver disease[66, 187]. It is known that activation of the hepatic stem cell niche also occurs in these situations and it is possible that the ductular reaction is driven, at least partly, by the proliferation of hepatic stem cells and their differentiating progeny,

although this hypothesis is currently untested in humans due to the nature of histological sampling. In murine models the ductular reaction is less well described, but the accumulation of hepatic stem cells, has been demonstrated in a number of injury models[69, 161] and fate tracing experiments have shown the accumulation, or increased numbers, of hepatic stem cells based upon marker expression and lineage tracing studies[9, 115]. A larger cohort would have allowed greater statistical power and may have detected a significant association between severity of ductular reaction and risk of HCC. Further, larger cohorts would allow clinical factors influencing severity of ductular reaction to be identified, quantified and adjusted for which would then allow associations between severity of ductular reaction and other quantified populations to be assessed. This provide information on the relationship between ductular reaction and the activation of the hepatic stem cell niche.

The presence of intermediate hepatobiliary cells has recently been reported to be independently associated with increased risk of hepatocellular carcinoma development in a prospectively identified cohort of patients with hepatic C virus cirrhosis[94]. Intermediate hepatobiliary cells were infrequent in NASH cirrhosis biopsies by cytokeratin 7 immunohistochemistry making the quantification of absolute numbers of these cells uninformative. Instead the definition used for assessing the presence or absence of intermediate hepatobiliary cells used in the study by Ziol *et al.* was used. This cohort of 18 NASH cirrhotic patients demonstrated similar incidence of HCC per year for those patients with presence of IHC (7.8% vs. 8.14% per year) and patients with an absence (4.9%. vs. 3.12% per year) in liver biopsies. As with assessing the association between ductular reaction and risk of HCC, a larger cohort of NASH cirrhotic patients is necessary for the potential

association to be fully assessed and a comparison of the association described in HCV cirrhotic patients to be made in patients with NASH cirrhosis.

Although the presence and potential relevance of $EpCAM^+$ hepatocytes could not be assessed in this cohort of biopsies due to the small numbers and scarcity of this cell type in NASH cirrhosis, the use of EpCAM is of great interest in the light of work suggesting these cells are hepatocytes recently derived from liver progenitor cells[74] and the association of EpCAM with a number of cancer related processes and cell types[83, 84, 86, 88, 89].

188

The prevalence of HCC in NASH patients is increasing[46], and not only in those patients with cirrhosis but also in non-cirrhotic patients with other components of the metabolic syndrome[48, 162]. As HCC therapy and survival rates are currently unsatisfactory, largely due to late diagnosis and consequent diminishing of choice and efficacy of treatment options, this approach could assist in identifying patients most at risk, possibly allowing the use of more powerful and effective imaging techniques (CT or MRI vs US) that are currently too expensive for surveillance of all cirrhotic patients. However, it is important that the potential benefits of this approach outweigh the risks associated with liver biopsy[188].

The results obtained from the preliminary work possible with the small cohort of NASH cirrhotic patients identified at the Queen Elizabeth Hospital, Birmingham (QEHB) are encouraging and represent the first work attempting to identify patients that are at increased risk of developing HCC based on the original biopsy from which a diagnosis of NASH

cirrhosis was made following on from demonstration of the utility in HCV cirrhotic biopsies[94]. Obtaining clinically important information about a patients risk of HCC from immunohistochemical analyses, quick and inexpensive technique, using a resource that is already routinely obtained (liver biopsy) has the potential to change the current surveillance and followup strategies employed in this patient cohort.

Due to the limited number of patients with a definitive, non-overlapping diagnosis of NASH, this study was extended through the identification of a larger cohort of patients with hepatitis C virus cirrhosis. HCV was chosen due to the greater number of HCV cirrhotic biopsies available due to the less problematic diagnosis and retrospective identification of HCV cirrhosis. This larger cohort will allow a more powerful analysis of the association between the histological phenomena related to hepatic stem cell activation and subsequent risk of HCC. As IHCs and $EpCAM^{+}$ hepatocytes were also found to be more common in HCV, this cohort will allow the absolute quantification of IHCs rather than a simple score for presence or absence, the proportion of hepatocytes newly derived from the hepatic stem cell niche and the total number of $Sox9^{+}$ hepatic stem cells to be including in the final analysis.

CHAPTER 6

ISOLATION OF HUMAN ADULT BILIARY TREE AND HEPATIC STEM CELLS FROM COMMON BILE DUCT AND EXPLANTED CIRRHOTIC LIVER

6.1. RATIONALE FOR STUDY

The isolation of human hepatic stem cells currently relies on foetal and donor liver tissue. Currently used tissues for the isolation of human hepatic stem cells are foetal cadaveric tissue and livers donated to transplant programs that are unused[1], usually due to long ischaemia times or high fat content. Not only are these tissues scarce, but their use in basic research, and potentially in future clinical trials and therapies, makes them highly controversial. Donor livers deemed unsuitable for transplantation are also unlikely to yield high quality cultures of hepatic stem cells. Consequently methods for the isolation and propagation of human hepatic stem cells from other tissue sources are appealing.

The isolation of adult hepatic stem cells from explanted cirrhotic liver tissue has not previously been demonstrated. The number of liver transplants being performed in the UK and worldwide is increasing. Explanted diseased liver tissue is currently used for research (with patients' consent) or discarded. Robust methods exist for the isolation of hepatic stem cells from foetal and donor liver, currently the main method used to obtain and study hepatic stem cells, however there is a lack of research demonstrating the isolation of significant numbers of potent hepatic stem cells from explanted cirrhotic livers[189]. If the isolation of hepatic stem cells with preserved proliferative and differentiation capacity can be demonstrated, explanted liver tissue could become a major source of hepatic stem cells, potentially negating the need for foetal and donor tissue and increasing the availability of hepatic stem cells for research and therapeutic uses.

Hepatic stem cells isolated from diseased liver are likely to further our understanding of the reciprocal impact of hepatic stem cell niche dysfunction and end stage liver failure. The use of diseased explanted liver also provides a valuable opportunity to study the functions and characteristics of hepatic stem cells that have been exposed to long-term liver injury and regeneration. Currently the relative contribution of the hepatic stem cell niche to long term liver regeneration and tissue homeostasis is unknown, particularly in clinical disease. Furthermore, chronic liver disease may fundamentally alter or damage the hepatic stem cell niche contributing to liver failure or potentiating carcinogenesis. Thus, the development of robust methods for the isolation of hepatic stem cells from explanted liver has the potential to greatly increase our understanding of the impact of chronic disease on the hepatic stem cell niche and how these changes, or defects, in the hepatic stem cell niche worsen or expedite end stage liver disease and liver failure.

6.2. RESULTS

6.2.1. Hepatic stem cells can be isolated from explanted cirrhotic liver can by immuno-selection and selective media conditions. Biliary epithelial cells (BEC) can be routinely isolated from explanted cirrhotic liver tissue through the use of immuno-selection of cells based on expression of EpCAM. Recent work has demonstrated the use of EpCAM immuno-selection for the isolation of hepatic stem cells from foetal and donor liver. This method selects hepatic stem cells through the use of media with very few growth factors (modified Kubota's media (MKM), detailed in methods). The proliferation and morphology of BEC that had previously been passaged three times was assessed when cultured in normal conditions for the culture of BEC or in conditions described for the selection of hepatic stem cells. The number of BEC was found to increase by roughly 200% after 3 days when cultured in BEC media on collagen type I, normal conditions for the culture of BEC. Cell number increased by approximately 500% after 3 days when BEC were plated on low-growth factor Matrigel, matrix designed for the culture of stem cell populations, in BEC media. Cell number decreased by roughly 70% after 3 days when BEC were cultured on Matrigel in MKM (**Fig 6.1A**). BEC cultured under normal conditions retained elongated morphology (**Fig 6.1B**) with similar morphology observed with increased cell density after culture on Matrigel in normal BEC media (**Fig 6.1C**). Fewer cells were observed after culture in MKM on Matrigel for 3 days. Remaining cells were generally more ovoid and smaller than normal BEC cultures, however no obvious hepatic stem cell colonies were observed (**Fig 6.1D**). Direct plating of $EpCAM^{+}$ immunoselected cells from cirrhotic explanted liver in MKM on Matrigel resulted in appearance of small clusters of densely packed ovoid cells with high nuclear to cytoplasmic ratios characteristic of hepatic stem cell colonies (**Fig 6.1E**).

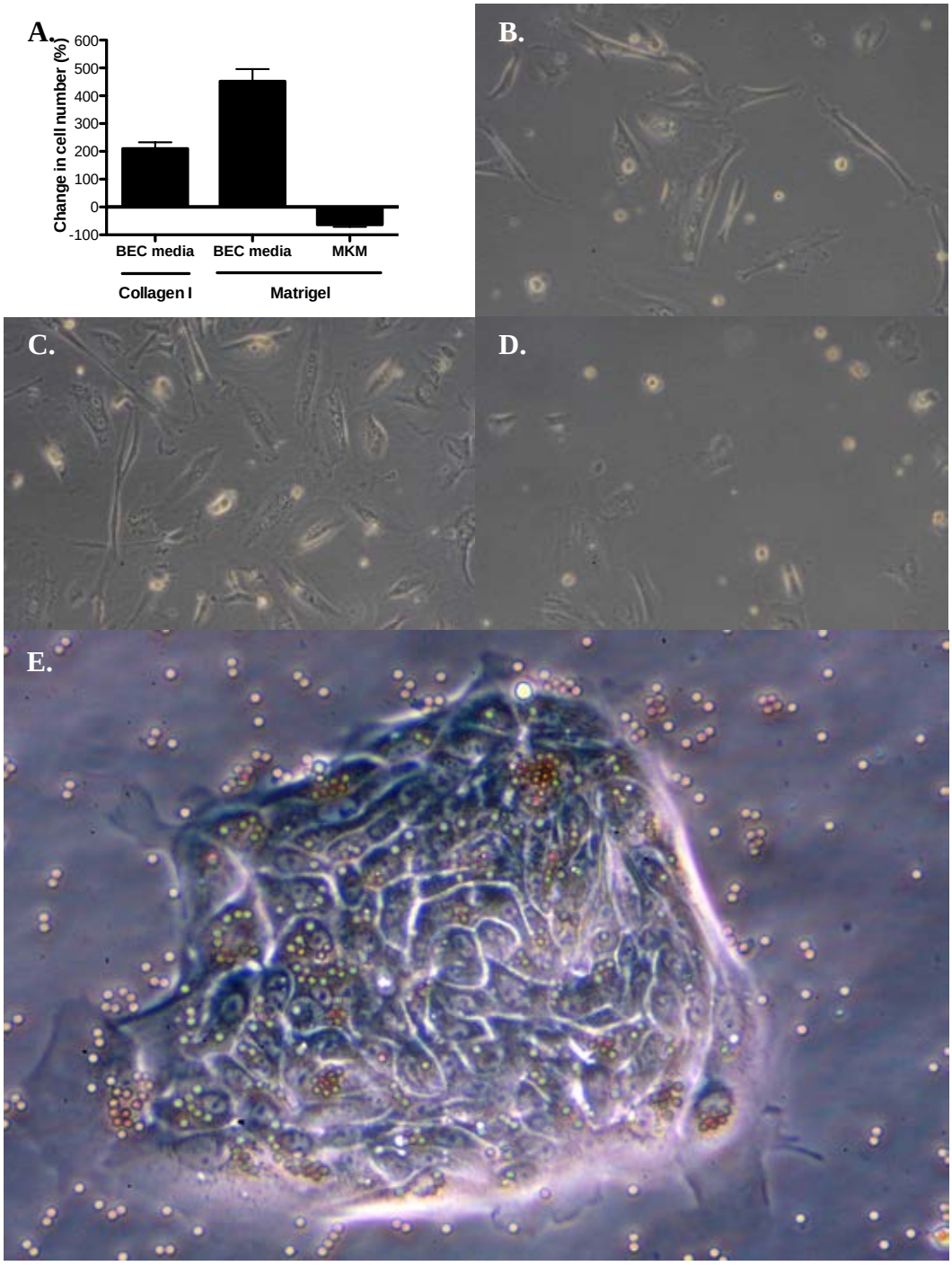

Figure 6.1. Modified Kubota's medium (MKM) allows selection of hepatic stem cells from explanted diseased liver. A, Bar graph representing the change in cell numbers observed in 3 random 200x magnification fields before and after 3 days culture of passage 3 biliary epithelial cells in normal BEC culture conditions, on Matrigel, and in MKM. Representative light microscopy images (200x magnification) of passage 3 biliary epithelial cells from ALD liver after 3 days culture in **B,** BEC media on collagen type I, **C,** BEC media on Matrigel, and **D,** modified Kubota's medium on Matrigel. **E,** Representative light microscopy image of a single hepatic stem cell colony derived from directly plated immuno-selected $EpCAM^+$ cells after culture for one day in modified Kubota's medium on Matrigel

Foetal calf serum (FCS), used in many, including BEC, media, and containing a myriad of growth factors, was found to slow proliferation of hepatic stem colonies and eventually lead to loss of colonies after approximately 3 days culture (**Fig 6.2**). Colonies continue to grow for the first 2 days when cultured in MKM plus 10% FCS then begin to decrease in overall size. The appearance of projections was also noted (**Fig 6.2CD, arrows**). It was difficult to assess whether these processes were the remnants of cells that had died within the colony or represented eruptions of differentiating cells that became unviable in MKM during differentiation towards mature parenchymal cell types. Interestingly, similar observations were occasionally observed spontaneously in cultures of hepatic stem cell colonies in MKM alone after around 4 days culture, particularly in cultures from livers with hepatocytic disease. Decreased growth and eventually loss of all colonies, similar to observations of culture with FCS, occurred in all hepatic stem cell colonies from these livers. It was not possible to ascertain the cause, or underlying processes, responsible for the spontaneous loss of cultured colonies from certain livers.

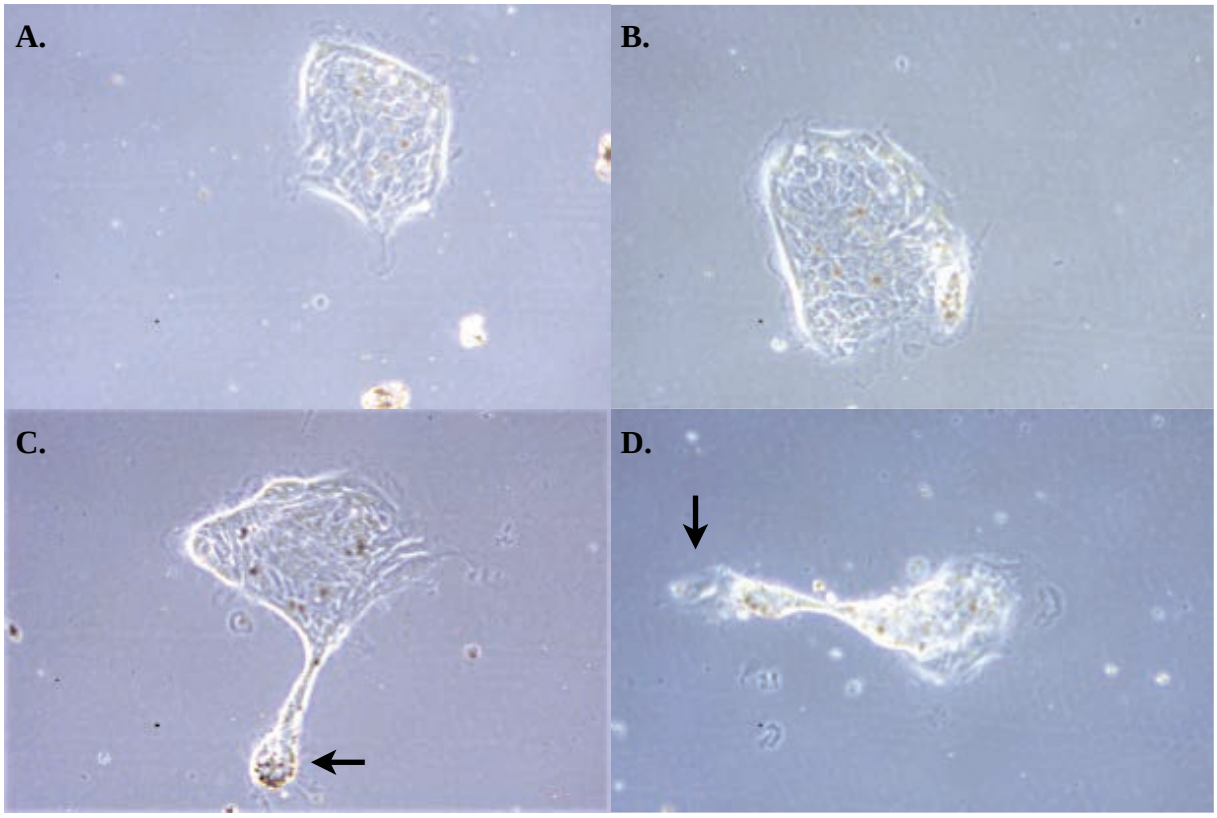

Figure 6.2. Foetal calf serum reduces proliferation and reduces viability of hepatic stem colonies. Light microscopy of a single representative hepatic stem cell colony cultured for 5 days in MKM on Matrigel then in MKM +10% foetal calf serum **A,** immediately after media change and after **B,** 1 day, **C,** 2 days, and **D,** 3 days culture. Arrows highlight projections from dying colonies likely representing remnant dying hepatic stem cells

6.2.2. Hepatic stem cells isolated from explanted cirrhotic liver have similar expression profiles to that reported for hepatic stem cells isolated from foetal and donor liver. Immunofluorescent analysis of hepatic stem cell colonies from ALD cirrhotic explanted liver cultured for 5 days in MKM on Matrigel demonstrated expression of markers previously described for hepatic stem cells isolated from foetal and donor liver tissue. Hepatic stem cell colonies from individual livers were found to have highly homogeneous antigenic profiles. Hepatic stem cells co-expressed NCAM and EpCAM (**Fig 6.3A**), a combination described as specific for hepatic stem cells, with a small proportion of cells at the periphery of colonies expressing NCAM in the absence of EpCAM (stained red). These cells also appeared slightly larger than cells at the centre of colonies and were also slightly more elongated with occasional cytoplasmic processes. Hepatic stem cells were positive for Sox9 (nuclear staining may be obscured by DAPI counterstain), demonstrating nuclear staining and occasional clusters of cells with cytoplasmic staining (**Fig 6.3B**). All hepatic stem cell colonies were found to express cytokeratin 7 (**Fig 6.3C)**, a marker of biliary epithelial cells, and cytokeratin 18 (**Fig 6.3D**), a marker of hepatocytes. Staining of CK7 and CK18 was diffuse and cytoplasmic and observed on all hepatic stem cells.

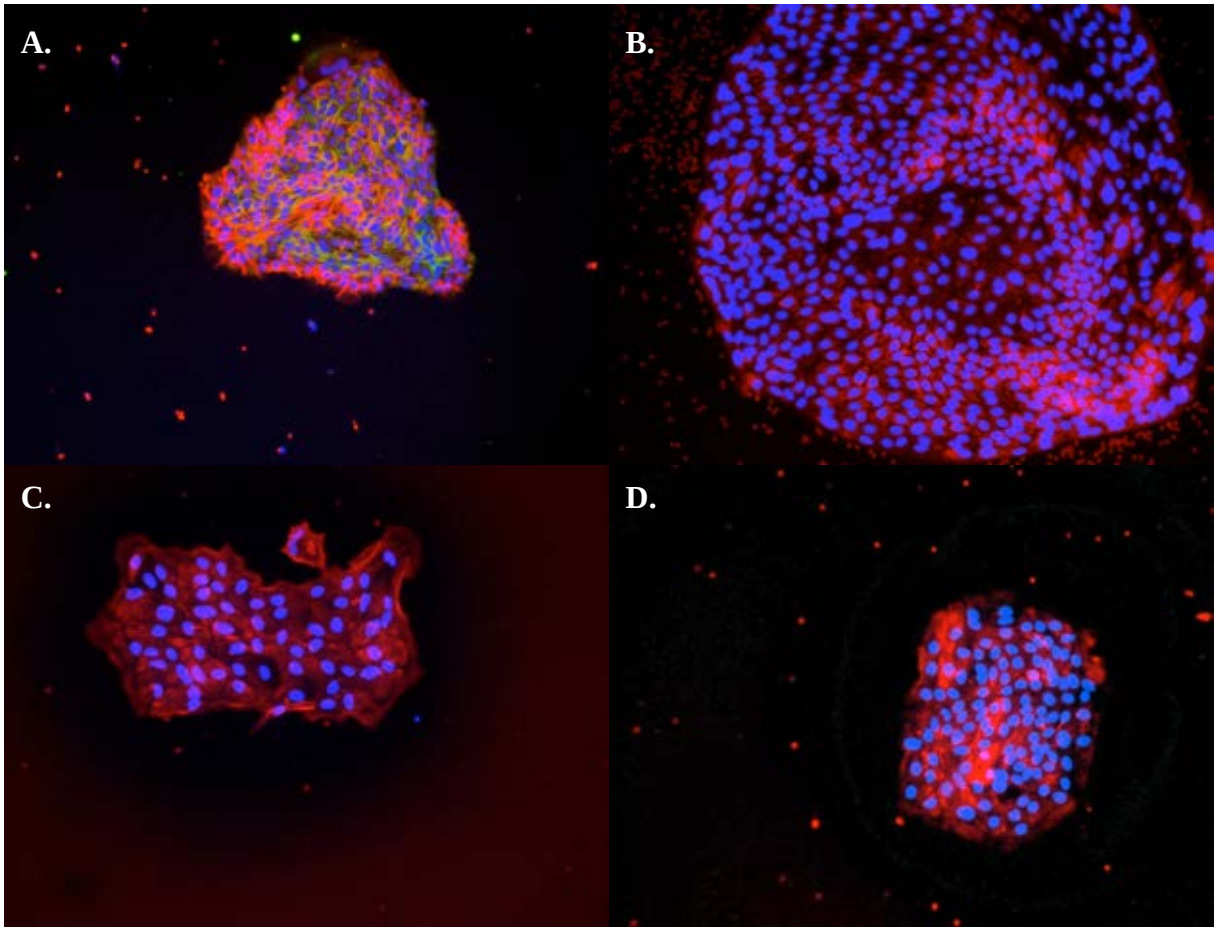

Figure 6.3. Hepatic stem cell colonies from explanted ALD cirrhotic liver express stem cell, biliary and hepatocytic markers. Immunofluorescent staining of representative hepatic stem cell colonies from explanted alcoholic liver disease cirrhotic liver after 5 days culture in modified Kubota's medium on Matrigel type I for **A,** neural cell adhesion molecule (red) and epithelial cell adhesion molecule (green) **B,** Sox9, **C,** cytokeratin 7, and **D,** CK18. All colonies were counterstained with DAPI to visualise cell nuclei (blue)

Hepatic stem cells isolated from explanted primary biliary cirrhosis (PBC) tissue were plated on Matrigel-coated plastic in modified Kubota's medium. Approximately 200 colonies were observed within 24 hours (**Fig 6.4A**) and grew to almost complete confluence within 5 days in single $10cm^2$ well. A conservative estimate of the total number of liver stem/progenitor cells at day 5 would be in excess of 1,000,000 cells with an approximate doubling time of around 12 hours. Hepatic stem cell colonies observed at day 1 generally consisted of uniformly small, densely packed cells. At day 5, regions with typical morphology were still observed (**Fig 6.4B, arrows**) surrounded by larger cells with much more elongated morphology and a much smaller nuclear to cytoplasmic ratio, morphology similar to mature BEC. Throughout the confluent colony, stem cell-like regions and areas of larger, biliary cells were clearly distinct from each other suggesting the sudden increase of larger, apparently more differentiated cells resulted from spontaneous, rapid proliferation and differentiation of hepatic stem cells isolated from this particular explanted PBC liver.

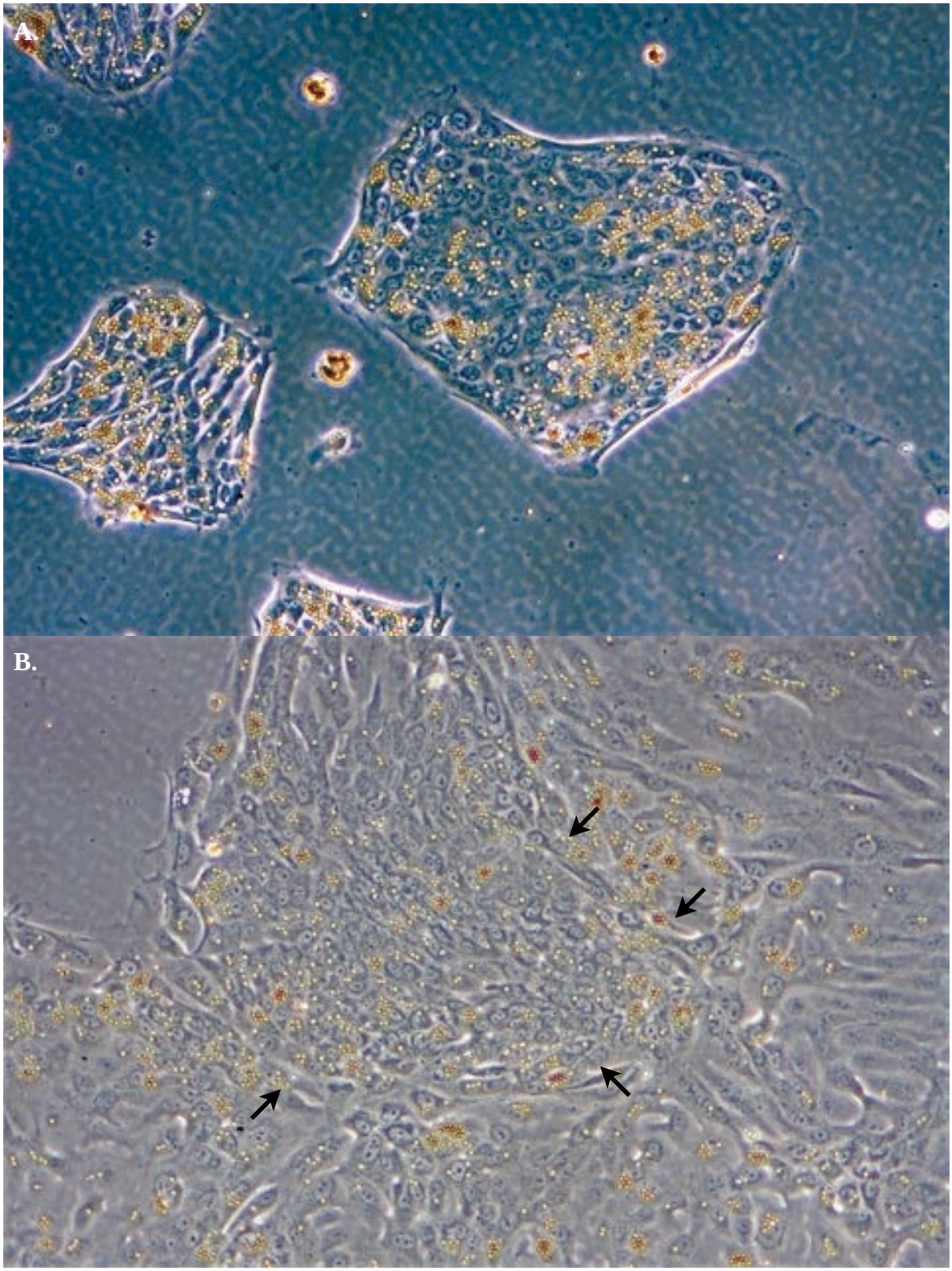

Figure 6.4. Hepatic stem cells isolated from explanted liver with chronic biliary disease form rapidly proliferating heterogeneous cultures. Representative light microscopy images of hepatic stem cells isolated from primary biliary cirrhosis explanted liver after culture in MKM on Matrigel type I for **A,** 1 day and **B,** 5 days. Arrows highlight dense clusters of cells with hepatic stem cell morphology surrounded by larger cells with biliary morphology

6.2.3. Characterisation of the effects of culture conditions on the proliferation and morphology of hepatic stem cells from explanted cirrhotic liver. Hepatic stem cells isolated from an ALD cirrhotic explanted liver were plated on 12 Matrigel-coated wells in MKM for 5 days. Media was changed to give four equal groups of three cultures in: MKM, MKM-C (designed for differentiation to biliary epithelial cells), MKM-H (designed for differentiation to hepatocytes), and MKM co-cultured with $CD14^{+}CD16^{+}$ peripheral blood mononuclear cells for 3 days. Hepatic stem cell colonies cultured in MKM on Matrigel proliferated rapidly with an approximate doubling time of 2 days (**Fig 6.5**). Over time, cells formed a 'swirling' pattern characteristic of biliary tree stem cell cultures previously described by Cardinale *et al.* as "small (7-9um), densely packed, uniform with high nucleus to cytoplasmic ratios" with NCAM and EpCAM duel positivity throughout the colony[11]. Immunofluorescent staining of the colony visualised in **Fig 6.5** demonstrated the presence of a significant proportion of $NCAM^{+}$ $EpCAM^{+}$ dual-positive cells (stained yellow) throughout the colony after 10 days culture. Dual positive cells often constituted the swirling patterns observed towards the centre of colonies (**Fig 6.6, black arrows**). Regions of single positive $EpCAM^{+}$ cells (stained green) with cytoplasmic staining were observed in regions of the colony without the swirling pattern (**Fig 6.6. white arrows**) and may represent cells beginning to differentiate towards a mature biliary phenotype. $NCAM^{+}$ $EpCAM^{-}$ cells (stained red) appeared slightly larger than cells at the centre of colonies with elongated morphology and were most commonly observed at the peripheries (**Fig 6.6, black arrowheads**) potentially representing transitional cells in the maturational lineage of hepatic stem cells[72] or similarity with peri-vascular stromal cells/angioblasts[190] that have previously been reported to have close associations with hepatic stem cells both *in vivo* and *in vitro* culture[17].

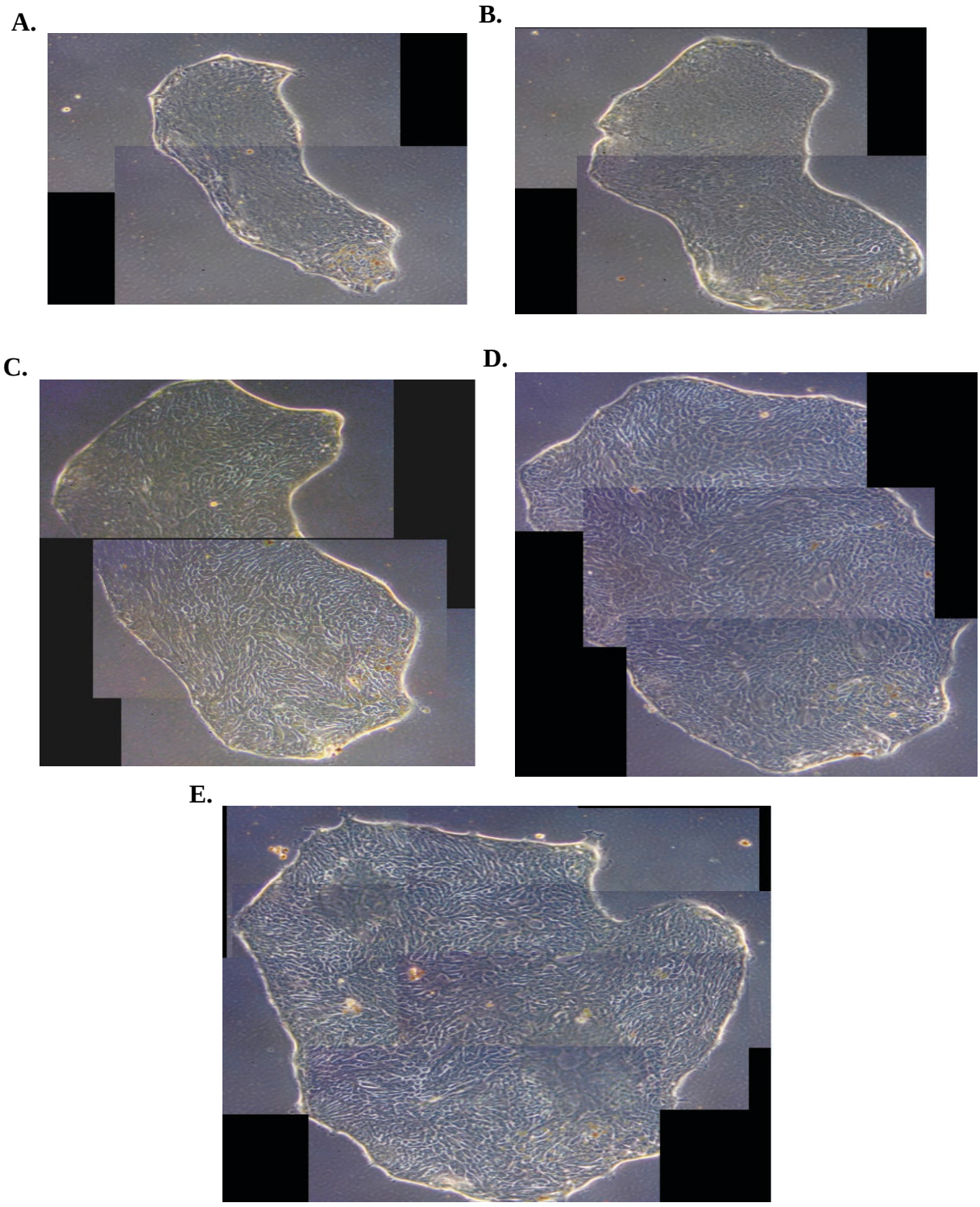

Figure 6.5. Hepatic stem cell colonies proliferate rapidly and maintain morphology in modified Kubota's medium on Matrigel. Light microscopy images (100x magnification) of a single hepatic stem cell colony isolated from explanted ALD cirrhotic liver cultured in modified Kubota's medium on Matrigel after **A,** 6 days, **B,** 7 days, **C,** 8 days, **D,** 9 days, and **E,** 10 days culture

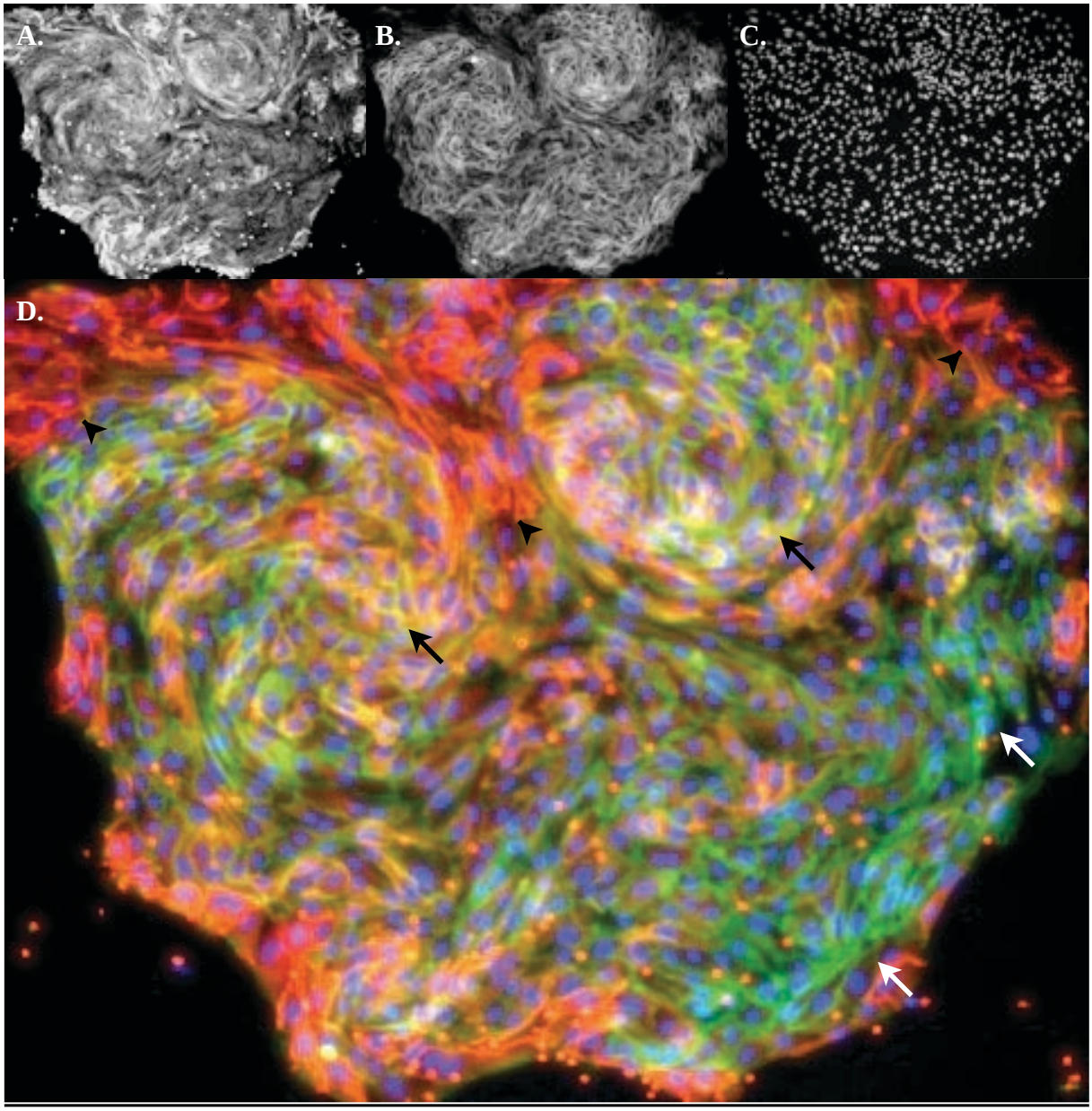

Figure 6.6. NCAM and EpCAM immunofluorescence reveals antigenic heterogeneity within hepatic stem cell colonies. Fluorescent microscopy (100x magnification) for **A,** NCAM **B,** EpCAM **C,** DAPI and **D,** merged image of NCAM (red), EpCAM (green and DAPI (blue) of a large hepatic stem cell colony (imaged in **Fig 6.4.**) from explanted alcoholic liver disease cirrhotic liver after 10 days culture in modified Kubota's medium on Matrigel type I. Dual NCAM and EpCAM staining demonstrates the presence of small, dual positive cells densely arranged in swirling patterns (stained yellow, highlighted by black arrows), larger, elongated cells positive for NCAM only (stained red, highlighted by black arrowheads) and regions of cells positive for EpCAM only (stained green, highlighted by white arrows)

The growth of hepatic stem cell colonies appeared to slow almost immediately after incubation with MKM-C (**Fig 6.7**). After 2 days the borders of hepatic stem cell colonies began to become irregular, with larger more elongated cells observed in the centre of the colony (**Fig 6.7C**). After 5 days culture in MKM-C, the borders of hepatic stem cell colonies appeared highly irregular, with many cells within the colony now displaying more elongated morphology more closely resembling that of primary BEC (**Fig 6.7E**). Growth relative to colonies cultured in MKM was reduced. It was not possible to ascertain whether the reduced growth was due to reduced proliferation of hepatic stem cells in MKM-C, or due to substantial loss of differentiating cells, particularly at the borders of colonies where cells were more irregularly shaped, perhaps undergoing cell death and sloughing.

Hepatic stem cells cultured in MKM-H rapidly stopped proliferating within 24 hours before being lost in a similar manner to that described for hepatic stem cell colonies cultured with foetal calf serum (**Fig 6.2**). Attempts to differentiate hepatic stem cell colonies subsequently isolated from explanted cirrhotic livers resulted in the same outcome.

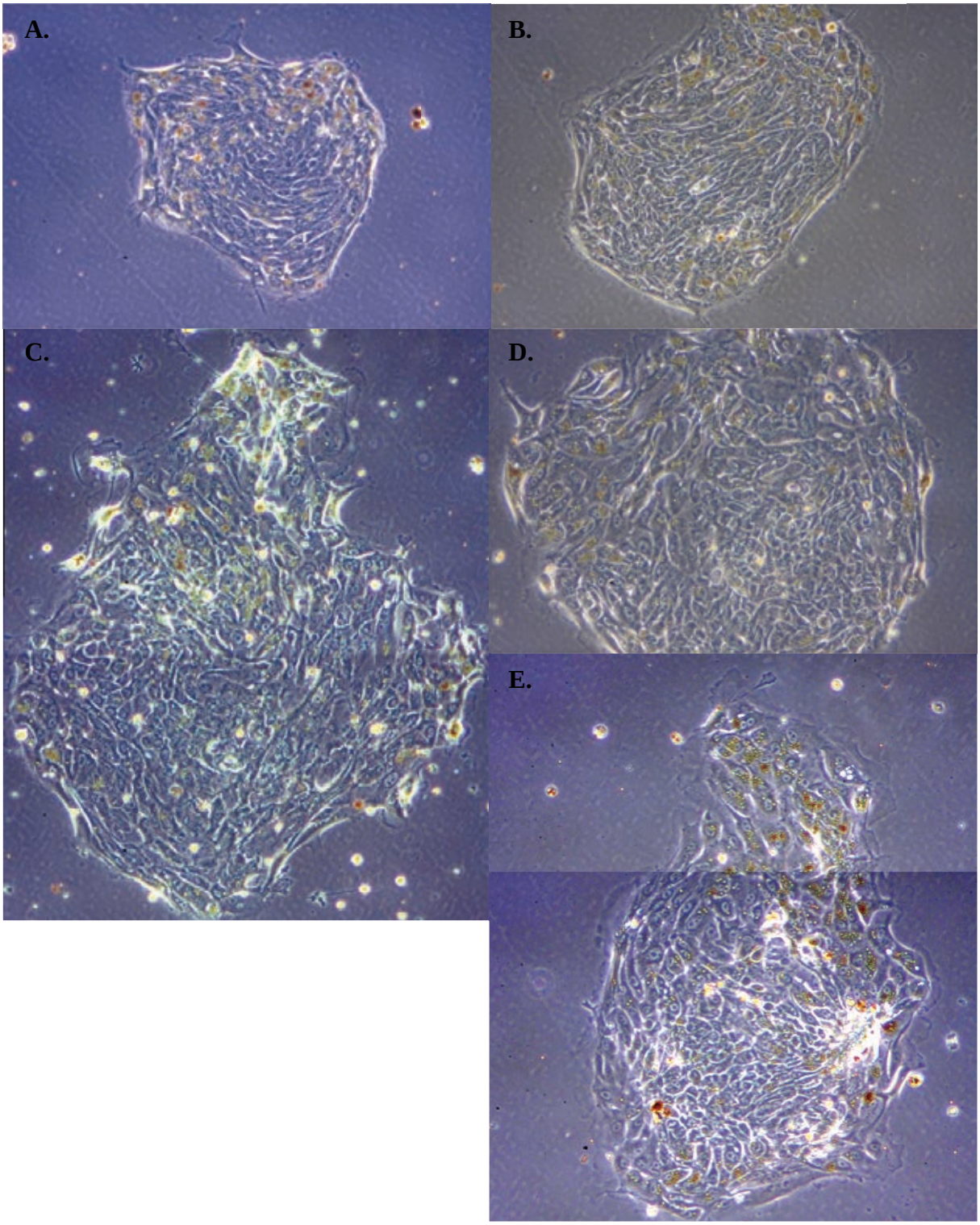

Figure 6.7. Culture of hepatic stem cells in conditions designed for biliary differentiation maintains proliferation and induces limited morphological change. Light microscopy images (100x magnification) of a single representative hepatic stem cell colony cultured for 5 days in MKM on Matrigel type I then in biliary differentiation media (MKM-C) **A,** immediately after media change and after **B,** 1 day, **C,** 2 days, **E,** 3 days, and **E,** 4 days culture

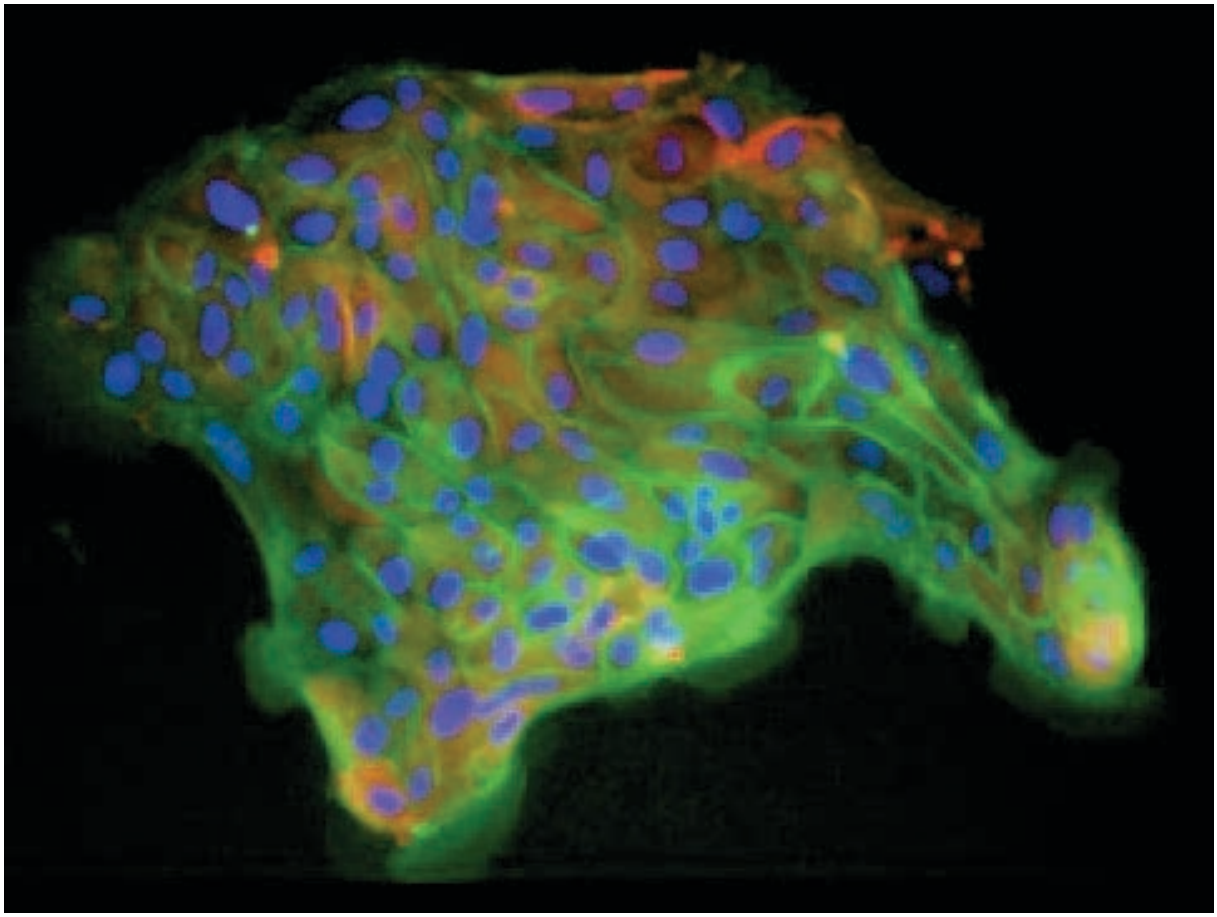

Figure 6.8. Hepatic stem cells cultured in MKM-C for 3 days retain expression of EpCAM and NCAM. Fluorescence immunohistochemistry (400x magnification) for NCAM (red), EpCAM (green) and DAPI (blue) of a single representative hepatic stem cell colony after 3 days culture in MKM-C

$CD14^+CD16^+$ PBMCs are recruited by LSEC into the liver parenchyma during liver inflammation and are the monocyte subset most likely to differentiate into macrophages. Macrophages have been to shown to have potent effects on hepatic stem cell proliferation and have critical function in patterning hepatocytic differentiation[26]. The growth of hepatic stem cell colonies co-cultured with $CD14^+CD16^+$ PBMCs in modified Kubota's medium was immediately inhibited, with no growth observed for the duration of the experiment. Cells retained typical hepatic stem cell morphology, being relatively small, with high cytoplasmic to nuclear ratio, and were observed in a compact, uniform colonies with smooth borders, in contrast to the stem cell colonies cultured in MKM-C (**Fig 6.8**). Immunofluorescent staining with NCAM and EpCAM demonstrated that, although the growth of the liver stem cell colony was strongly inhibited by $CD14^+CD16^+$ PBMCs, hepatic stem cells retained expression of stem cells markers (**Fig 6.9**). EpCAM expression was observed on all hepatic stem cells throughout colonies and around half of hepatic stem cells co-expressed NCAM, results indicating hepatic stem cells were maintained in an undifferentiated state (**Fig 6.10**).

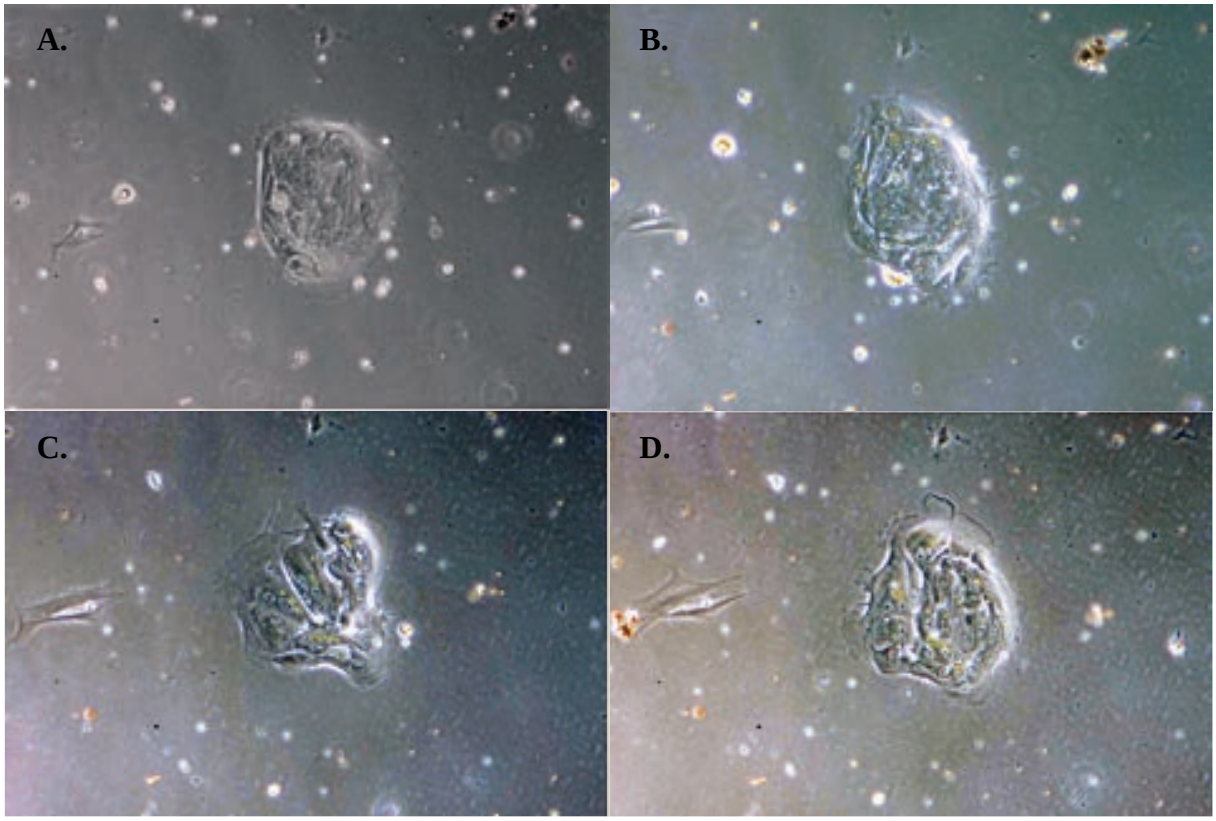

Figure 6.9. Co-culture with $CD14^+CD16^+$ peripheral blood mononuclear cells inhibits proliferation of hepatic stem cells. Light microscopy of a single representative hepatic stem cell colony cultured for 5 days in MKM on Matrigel type I then in the presence of $CD14^+CD16^+$ peripheral blood mononuclear cells **A,** immediately after addition of peripheral blood mononuclear cells and after **B,** 1 day, **C,** 2 days, and **D,** 3 days co-culture

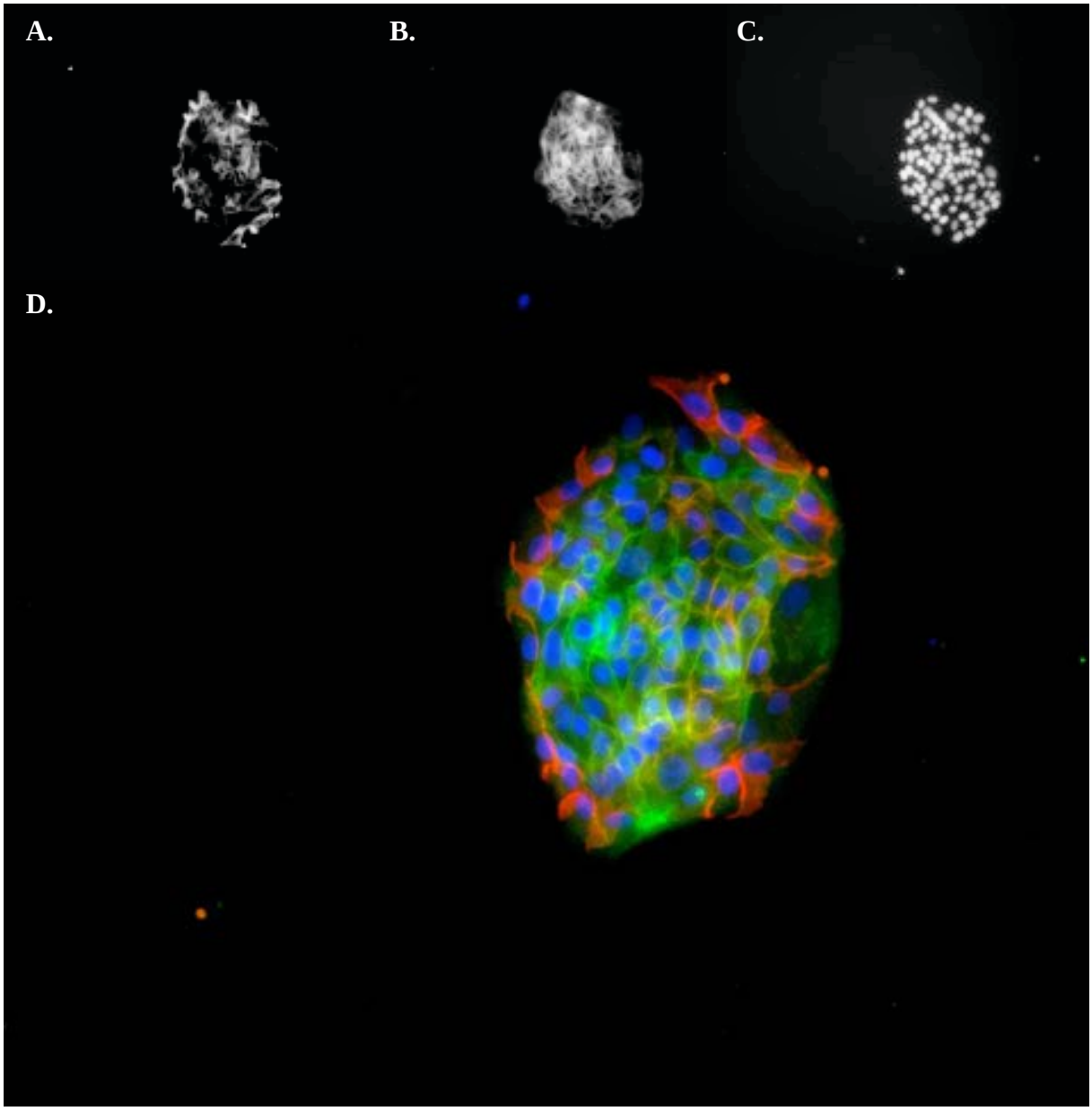

Figure 6.10. Maintenance of EpCAM expression by hepatic stem cells after co-culture with $CD14^+CD16^+$ PBMCs. Fluorescent microscopy (200x magnification) for **A,** NCAM **B,** EpCAM **C,** DAPI and **D,** merged image of NCAM (red), EpCAM (green) and DAPI (blue) of a single hepatic stem cell colony after 3 days co-culture with $CD14^+$ $CD16^+$ peripheral blood mononuclear cells

6.2.4. Biliary tree stem cells can be isolated from common bile duct and have similar characteristics to hepatic stem cells from explanted liver. Peribiliary glands (PBGs) are acinar structures found throughout the biliary tree and are larger and more numerous in proximal regions (**Fig 6.1AB, arrows**). High proportions of epithelial cells of peribiliary glands express stem cell markers and have been hypothesised to be the precursors of all biliary epithelial cells and potentially all epithelial cells of the hepatopancreatic system[11-13]. Successful isolation of intact peribiliary glands from common bile duct samples could be achieved with brief collagenase digestion of bile duct tissue and washes with EDTA resulting in a suspension of intact PBGs (**Fig 6.11CD**). PBGs were cultured on plastic in MKM. In these conditions large numbers (typically over 100) of PBGs adhered to plastic over a few hours and formed colonies of cells with proliferation rates and morphology similar to hepatic stem cells (**Fig 6.12A-D**). PBGs were also found to co-express biliary (CK7, **Fig 6.12E**) and hepatocytic markers (CK18, **Fig 6.12F**).

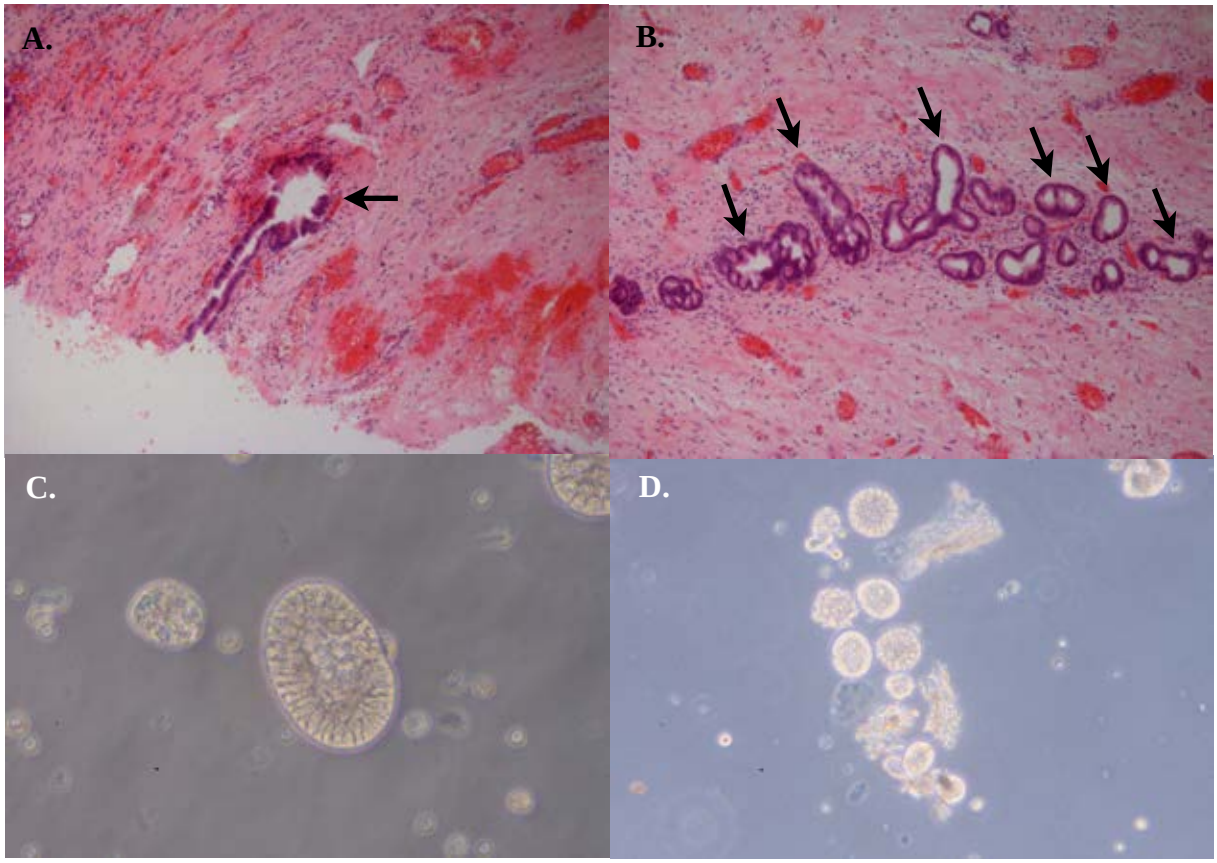

Figure 6.11. Collagenase digestion and EDTA washes of common bile duct tissue allows isolation of intact peri-biliary glands. AB, Representative images (200x magnification) of haematoxylin and eosin staining of common bile duct wall sections demonstrating presence of peri-biliary glands (arrows). **CD,** Light microscopy of freshly isolated intact peri-biliary glands from explanted common bile duct by brief collagenase digestion and repeated washes in high concentration EDTA

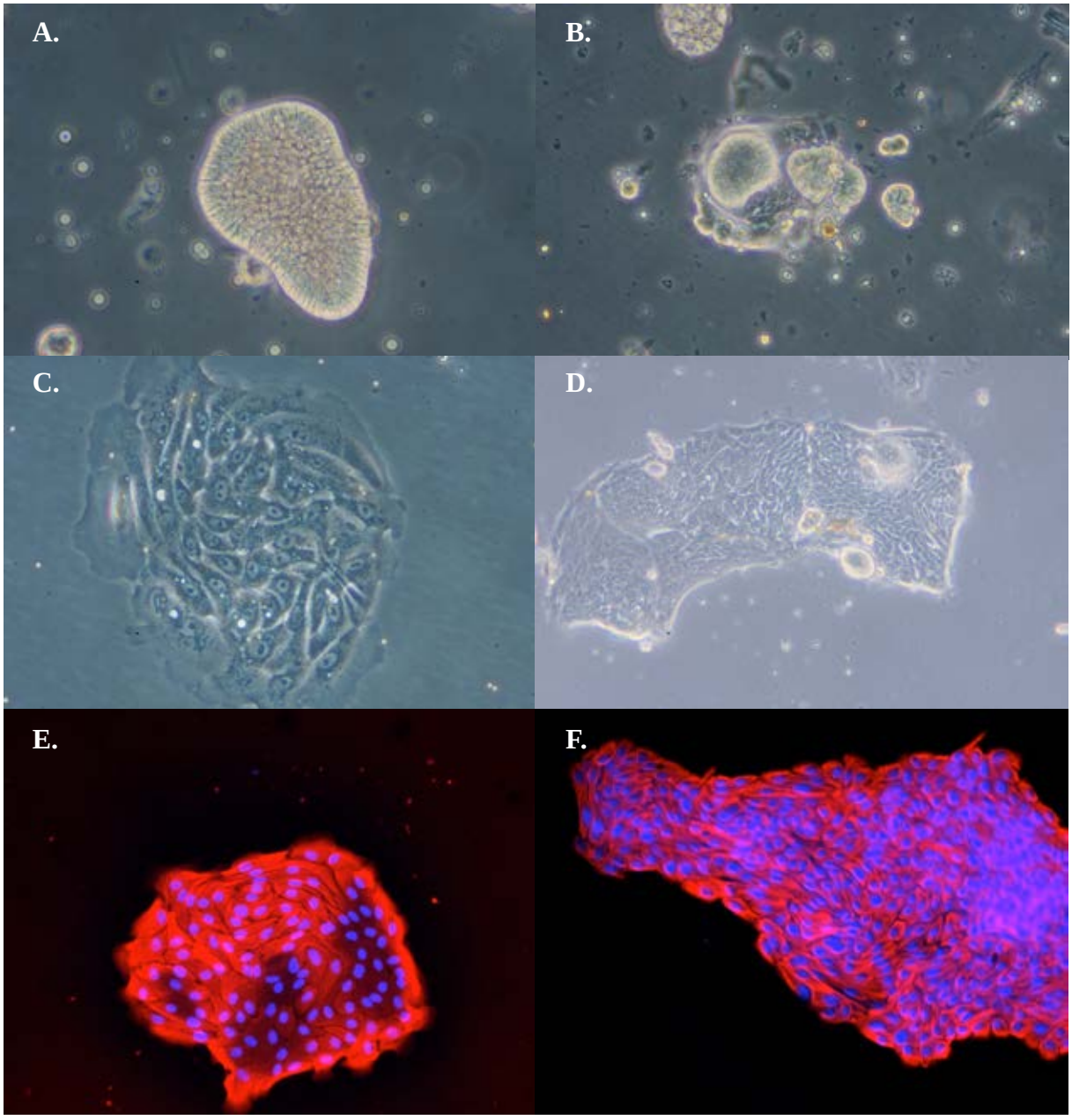

Figure 6.12. Freshly isolated PBGs adhere to plastic in Modified Kubota's Medium, form distinct, slow growing colonies colonies with biliary stem cell morphology and expression profile. Representative light microscopy images (200x magnification) of biliary tree stem cells isolated from explanted common bile duct and plated on plastic in modified Kubota's medium **A,** immediately after isolation and after **B,** 2 hours, **C,** 1 day and **D,** 3 days (100x magnification) culture. **E,** Cytokeratin 7 and **B,** cytokeratin 18 fluorescence immunohistochemistry of biliary tree stem cell colonies after 5 days culture in Kubota's modified media on plastic. Colonies were counterstained with DAPI

6.3. DISCUSSION

This study demonstrates the isolation of human hepatic stem cells from adult, explanted cirrhotic liver and non-pathological common bile duct from Whipple's procedures using techniques previously reported for the isolation of hepatic stem cells from foetal and uninjured liver[1]. The use of explanted liver tissue and common bile duct from Whipple's procedures as a source of hepatic stem cells is attractive as these sources negate the use of foetal and donor liver tissues. However, the use of these sources is challenging due to the heterogeneity of samples, due to range of aetiologies and severity of liver disease among individual livers. Hepatic stem cells isolated from diseased livers are likely to be altered compared to those from normal liver due to sustained exposure to the milieu of factors secreted in response to chronic liver injury. Due to the heterogeneous nature of explanted liver tissue used the behaviour of isolated hepatic stem cells colonies frequently demonstrated substantial variation. Hepatic stem cell colonies were observed after 2 to 3 days for most isolations then either proliferated consistently for weeks forming distinct colonies or underwent slowing of proliferation and colony collapse with all cells typically lost by around day 7. In rare instances, large numbers of hepatic stem cell colonies would be observed soon after isolation (within 24 hours of plating) and proliferate to confluence over a few days. Large variability in the numbers, viability and behaviour of isolated hepatic stem cells from individual explanted livers were observed, making comparisons between isolations difficult. Consequently, much of the work in this study is descriptive and observational.

Hepatic stem cells isolated from explanted liver have potential utility as a source of cells for basic research or for use as a cellular therapy. In both cases, understanding the differences

between cells isolated from normal and diseased tissues is important. This study revealed a number of differences between cells isolated from explanted tissue, and reports of hepatic stem cells isolated from normal, or foetal, tissues. Whilst the isolation of hepatic stem cells from normal and foetal tissues is relatively robust, with predictable numbers of colonies observed that are viable for weeks to months, there was a large degree of variability in isolations from explanted liver that were not accounted for by the amount of tissue used. Due to the nature of the isolation technique, the number of freshly isolated $EpCAM^{+}$ cells is hard to quantify. As the majority of cells isolated by EpCAM immuno-selection are mature BEC that are non-viable in the selective media used, it is difficult to quantify the number of hepatic stem cells obtained from individual isolations. Further, immuno-selection with beads commonly results in the isolation of clumps of cells rather than single cell suspensions making quantification by cytometric analysis challenging. From experience it appears greater viability and yields and result from isolations where greater clumping of isolated cells is observed, in keeping with the results from common bile duct where viable cultures only resulted from techniques isolating intact peri-biliary glands. Structural integrity of the glands is known to be important for keeping supportive stromal cells in close proximity to the biliary stem cells, increasing viability and maintaining physiological patterning of the niche. Previous attempts to isolate stem cells from a variety of organs have demonstrated greatly decreased viability when somatic stem cells are fully dissociated[11-13].

Primary BEC cultures in normal conditions can be passaged and cells gradually take on stromal, or fibroblastic, characteristics, and lose expression of biliary markers, with culture duration. In these conditions BEC proliferate as mono-layers and display a degree of contact

inhibition, The use of modified Kubota's media (MKM) is critical for the selection of hepatic stem cells. Culture of passage 3 BEC in MKM resulted in a decrease in cell number of 3 days, where in normal conditions cells proliferated rapidly to confluence. This experiment demonstrated mature BEC are not viable in MKM. Plating of freshly isolated immuno-selected $EpCAM^{+}$ cells however did result in the appearance of distinct colonies of tightly packed cells with typical hepatic stem cell morphology[3, 12, 191].

Culture of hepatic stem cell colonies in the presence of foetal calf serum (FCS) led to senescence and rapid loss of hepatic stem cell colonies over the course of 3 to 4 days. This observation either represents a stimulatory effect of FCS on hepatic stem cells leading to rapid initiation of hepatocytic differentiation and maturation, with mature hepatocytes lost due to lack of appropriate growth factors in MKM, or direct negative effects of FCS on hepatic stem cell colonies. The presence of $NCAM^{+}EpCAM^{-}$ cells on the peripheries of colonies potentially represent stromal supportive cells, or angioblasts, however there is great uncertainty regarding the presence, and characteristics, of these cells in liver[32, 192]. These cells may be important for maintaining the viability of isolated hepatic stem cells *in vitro* and further work fully characterising their identity and expression profile may increase our understanding of the role of these cells in maintaining hepatic stem cell colonies.

Experiments to assess the functional capacity of hepatic stem cells from explanted liver failed to definitively demonstrate differentiation into mature cell types. Subtle morphological changes with the use of media designed for the differentiation of adult human hepatic stem cells into mature biliary epithelial cells. After 4 days culture, hepatic stem cells demonstrated

a slightly elongated morphology more in keeping with mature biliary epithelial cells. However proliferation was greatly reduced by day 4 with some cells displaying changes suggestive of early apoptosis and cell death. The use of hepatocyte differentiation media invariably resulted in loss of hepatic stem cell colonies within 2 days. These findings again suggest that media with a greater number of growth factors and higher nutrient content may be required to support mature cell types derived from hepatic stem cell colonies.

The lack of media conclusively shown to support mature hepatocytes may also have impacted on the result of co-culture experiments with hepatic stem cell colonies and $CD14^{+}CD16^{+}$ PBMCs. For these reasons, the results of the co-culture experiment are hard to interpret as any hepatic stem cells differentiating into mature cell types may have died rapidly, masking any effects PBMCs may have had on the differentiation of hepatic stem cell colonies. Nevertheless, it was clearly demonstrated that PBMCs had a potent inhibitory effect on hepatic stem cells without altering the expression of EpCAM and NCAM by hepatic stem cells after 4 days co-culture.

Finally, the isolation of biliary tree/hepatic stem cells from common bile duct was demonstrated. Stem cell colonies obtained had very similar morphology and expression profiles to that of hepatic stem cells isolated from explanted liver and previous reports of hepatic stem cells from donor and foetal liver. The yields and growth characteristics of stem cells derived from common bile duct appeared to demonstrate less variability than cultures from explanted liver. Thus, common bile duct may provide a more robust source of biliary tree/hepatic stem cells as well as providing unaltered stem cell colonies allowing direct

comparison with those obtained from diseased explanted liver. Further work will attempt to optimise conditions for the long term maintenance and differentiation of biliary tree stem cells from Whipple's procedures and then apply modified techniques to cultures from explanted to try and reduce the variability of results and more informative comparisons between cultures from the two sources.

Ultimately, this study demonstrated the difficulty in using cirrhotic liver for the isolation of hepatic stem cells. Although hepatic stem cells could be isolated and their expression profile assessed, differentiation assays have to date failed to demonstrate production of functional parenchymal cell types, a key criteria needed to definitively prove cultured cells are adult hepatic stem cells. Further optimisation of culture conditions, possibly using 3D scaffolds or feeder/companion cells, are likely to be required if the isolation, long-term culture and maintenance of undifferentiated hepatic stem cells from explanted liver is to be demonstrated.

CHAPTER 7

CONCLUSIONS AND FUTURE WORK

7.1. OVERVIEW

There is increasing interest in hepatic stem cells as their role in tissue homeostasis, liver regeneration and carcinogenesis is further elucidated, potentially paving the way for targeted clinical interventions that may stimulate, or facilitate, more efficient activation and differentiation of the hepatic stem cell niche *in situ,* or development of hepatic stem cells as a efficacious cellular therapy. However there remain a number of unresolved questions, and apparent contradictions, concerning the function and behaviour of hepatic stem cells *in vivo*, particularly in the case of long-term chronic liver injury.

Native mature hepatocytes are known to have substantial regenerative capacity, thus, at least in conditions where hepatocytes retain significant proliferative capacity, hepatic stem cells appear to be a redundant secondary mechanism of liver regeneration. Thus, the contribution of hepatic stem cells to tissue homeostasis, the maintenance of parenchymal cell numbers and function, in normal conditions and regeneration in response to liver injury remains to be conclusively determined. This will likely require the use of animal models, particularly lineage tracing models that specifically identify hepatic stem cells and their progeny and disease models that accurately replicate the pathophysiology of chronic metabolic liver diseases.

Chapter 3 presents the characterisation of injury resulting from long-term administration of a previously reported dietary model of non-alcholic liver disease. This study demonstrated wild-type mice fed a diet containing high proportions of trans-fatty acids and fructose over 12

months developed the full spectrum of NAFLD, including significant fibrosis, and hepatocellular carcinoma. This result demonstrates for the first time that diet alone is sufficient to cause NASH and HCC. Activation of the hepatic stem cell niche was also demonstrated in the ALIOS model, establishing it as the most pathophysiological model for the study of hepatic stem cell activation as a result of chronic metabolic liver injury as it avoids the use of transgenic animals or toxic diets. Further, the demonstration of tumour cells expressing hepatic stem cell markers in ALIOS mice provided further evidence for a link between hepatic stem cell activation and the development of HCC.

The relationship between epithelial and mesenchymal populations in adult human liver is currently poorly understood despite the close spatial and temporal association between ductular reaction and fibrosis. In other organs, particularly skin[193] and intestine[90], it is increasingly recognised that stromal populations within epithelial stem cell niches are important mediators of epithelial stem cell activation and patterning. In the liver, the ductular reaction and fibrosis may represent a common process facilitating the proliferation, migration and differentiation of hepatic stem cells into mature hepatocytes through niche remodeling, secretion of mitogenic factors and recruitment of other cell types, particularly macrophages. The association between stromal and epithelial components of the hepatic stem cell niche is further complicated by recent reports of hepatic stellate cells expressing hepatocytic and epithelial stem cell markers[18, 194] and fate tracing experiments demonstrating hepatocytes derived from stromal populations in response to liver injury[181].

Chapter 4 demonstrates the prospective isolation of a resident population of hepatic stromal cells with high colony forming potential and ability to undergo rapid differentiation into myofibroblastic cells, potentially identifying them as significant contributors to liver fibrosis. The isolation of these cells (PαS) was based on the expression of PDGFRα and Sca1, a combination previously reported for mesenchymal stem cells of the bone marrow and other visceral organs. PαS cells were shown to reside in close proximity to the walls of hepatic veins, hepatic arteries and portal veins. The peri-portal location of PαS cells makes it conceivable that PαS cells contribute to fibrogenesis, ductular reaction and/or hepatic stem cell activation, processes that all originate from peri-portal locations. Further, culture of PαS cells in conditions designed for the selection and growth of hepatic stem cells, resulted in the appearance and rapid growth of epithelial stem cell colonies that could be passaged and cultured long-term. This observation potentially demonstrates PαS as a potent source of both stromal and epithelial populations in adult liver. However, more work is needed to demonstrate PαS directly transdifferentiate into epithelial cells and exclude the possibility of these colonies being derived from contaminating epithelial cells. Further, it needs to be demonstrated that epithelial cells selected from PαS cultures are capable of differentiation into mature epithelial cell types to definitively prove these cells are indeed hepatic stem/progenitor cells. The study of PαS cells may provide important information on the relationship between stromal and epithelial stem cell populations in adult liver and aid in elucidating whether epithelial to mesenchymal transition (EMT), and the reverse process (MET), occur and have relevance in response to liver injury.

Patients with end-stage liver disease, cirrhosis, are at greatly increased risk of hepatocellular carcinoma (HCC). Many HCC tumours are found to express biliary or epithelial stem cell markers, suggesting hepatic stem cells, or transitional cells within the maturational lineage, may be the cell of origin in some cases of HCC. This would be in-keeping with the concomitant and ongoing activation of the hepatic stem cell niche and increased numbers of hepatic stem cells and their progeny in cirrhotic livers. Experimental studies in animal models, and recent clinical studies, have provided further evidence linking hepatic stem cells and HCC.

Chapter 5 describes novel techniques for the objective quantification of hepatic stem cells and related histological phenomenon in liver biopsy tissue. These methods allow the ductular reaction, number of intermediate hepatobiliary cells, hepatic stem cells, and hepatocytes newly derived from hepatic stem cells to be fully quantified immunohistochemical analyses. This study identified a small cohort of NASH cirrhotic biopsies and demonstrated the ability to objectively quantify ductular reaction and identify intermediate hepatobiliary cells and hepatocytes newly derived from hepatic stem cells but, due to small numbers, the association between these cell types and patients' risk of HCC development could not be assessed. However, the presence of intermediate hepatobiliary cells in liver biopsies was found to confer a similar increased risk of HCC in this small cohort of NASH cirrhotic patients to that reported for HCV cirrhotic patients in a previous study[94], perhaps indicating the association is preserved across all chronic liver disease aetiologies. Therefore a much larger, 72 patient cohort of HCV cirrhotic patients' with liver biopsy material and follow-up at the Queen Elizabeth Hospital, Birmingham, was identified. Each of the quantification techniques have

been applied to this cohort allowing full quantification of each cell type and, along with clinical data, will allow the association to be fully assessed. Although much of this work is complete, due to blinding it has not been possible to make any preliminary observations or conclusions from this larger study.

There is currently a lack of suitable sources of human hepatic stem cells due to the scarcity of currently used tissues, foetal cadaveric livers and donor livers unused for transplant. This has inhibited *in vitro* research on human adult hepatic stem cells and is a major obstacle to their use as a clinical therapy.

In this study, the isolation of hepatic stem cells with typical morphology and expression profiles was demonstrated from explanted cirrhotic liver and common bile duct from Whipple's procedures. Although significant variability was observed between isolations, particularly from explanted liver, some cultures could be maintained long-term without loss of proliferation or alteration in expression profiles. However, this study failed to demonstrate differentiation of human hepatic stem cells from these sources in to functional parenchymal cell types. The production of hepatocytes from isolated hepatic stem cells is a critical step, not only in confirming isolated cells as hepatic stem cells, but in demonstrating their potential utility as a meaningful source of cells for research and cellular therapy applications.

7.2. FUTURE WORK

7.2.1. Hepatic stem cell activation and hepatocellular carcinoma in a mouse model of non-alcoholic steatohepatitis

- Further investigate the mechanisms mediating the effects of the ALIOS diet through the use of pharmacological interventions or transgenic models to rescue or attenuate liver injury and HCC development
- Use the ALIOS model with cell fate tracing models that specifically mark murine hepatic stem cells (Lgr5, Foxl1, Sox9) to assess the contribution of hepatic stem cells to regeneration and determine whether hepatic stem cells are the cell of origin for HCC as a result of ALIOS

7.2.2. Prospective isolation of stem/progenitor cells from adult murine liver

- Continue to optimise conditions for the selection of epithelial stem cells from PαS cells and their differentiation into mature parenchymal cell types to conclusively demonstrate them as hepatic stem cells
- Conduct gene expression fingerprinting analysis on freshly isolated PαS to further elucidate their identity and cell lineage
- Co-stain for PDGRα and Sca1 in sections from a range of liver injury models to assess the proliferation and fibrogenic potential of PαS in response to liver injury
- Use cell fate tracing models (PDGRα) to definitively determine the contribution of PαS to fibrogenic and epithelial cell types in response to liver injury

7.2.3. Activation of hepatic stem cells in chronic liver disease and association with risk of hepatocellular carcinoma

- Complete immunohistochemical analyses and quantification in HCV cirrhotic cohort and determine association with risk of HCC after adjusting for clinical risk factors
- Use confocal microscopy to stain for all markers simultaneously to further define the relationship between studied cellular populations and their place in the maturational lineage of hepatic stem cells
- Investigate the utility of more recently described markers of hepatic stem cells (Lgr5) in quantifying hepatic stem cells

7.2.4. Isolation of human adult hepatic stem cell from explanted liver and common bile duct

- Develop more robust isolation methods using hepatic stem cells from common bile duct to decrease variability observed in cultures from explanted cirrhotic liver
- Develop differentiation assays for the production of functional hepatocytes and biliary epithelial cells from isolated hepatic stem cell colonies to aid in assessing the potential and function of hepatic stem cells isolated from diseases liver
- Further optimise culture conditions allowing higher yields and viablity of hepatic stem cell colonies from explanted cirrhotic liver, most likely through the use of 3D culture systems, companion/feeder cells and hormonally defined media more representative of the hepatic stem cell niche

LIST OF REFERENCES

1. Schmelzer E, Zhang L, Bruce A, Wauthier E, Ludlow J, Yao HL, Moss N, Melhem A, McClelland R, Turner W, Kulik M, Sherwood S, Tallheden T, Cheng N, Furth ME, Reid LM. **Human hepatic stem cells from fetal and postnatal donors.** *J Exp Med.* 2007;204:1973-1987.
2. Schmelzer E, Wauthier E, Reid LM. **The phenotypes of pluripotent human hepatic progenitors.** *Stem Cells.* 2006;24:1852-1858.
3. Turner R, Lozoya O, Wang Y, Cardinale V, Gaudio E, Alpini G, Mendel G, Wauthier E, Barbier C, Alvaro D, Reid LM. **Human hepatic stem cell and maturational liver lineage biology.** *Hepatology.* 2011;53:1035-1045.
4. Sullivan GJ, Hay DC, Park IH, Fletcher J, Hannoun Z, Payne CM, Dalgetty D, Black JR, Ross JA, Samuel K, Wang G, Daley GQ, Lee JH, Church GM, Forbes SJ, Iredale JP, Wilmut I. **Generation of functional human hepatic endoderm from human induced pluripotent stem cells.** *Hepatology.* 2010;51:329-335.
5. Li F, Liu P, Liu C, Xiang D, Deng L, Li W, Wangensteen K, Song J, Ma Y, Hui L, Wei L, Li L, Ding X, Hu Y, He Z, Wang X. **Hepatoblast-like progenitor cells derived from embryonic stem cells can repopulate livers of mice.** *Gastroenterology.* 2010;139:2158-2169 e2158.
6. Touboul T, Hannan NR, Corbineau S, Martinez A, Martinet C, Branchereau S, Mainot S, Strick-Marchand H, Pedersen R, Di Santo J, Weber A, Vallier L. **Generation of functional hepatocytes from human embryonic stem cells under chemically defined conditions that recapitulate liver development.** *Hepatology.* 2010;51:1754-1765.
7. Spee B, Carpino G, Schotanus BA, Katoonizadeh A, Vander Borght S, Gaudio E, Roskams T. **Characterisation of the liver progenitor cell niche in liver diseases: potential involvement of Wnt and Notch signalling.** *Gut.* 2010;59:247-257.
8. Roskams TA, Libbrecht L, Desmet VJ. **Progenitor cells in diseased human liver.** *Semin Liver Dis.* 2003;23:385-396.
9. Furuyama K, Kawaguchi Y, Akiyama H, Horiguchi M, Kodama S, Kuhara T, Hosokawa S, Elbahrawy A, Soeda T, Koizumi M, Masui T, Kawaguchi M, Takaori K, Doi R, Nishi E, Kakinoki R, Deng JM, Behringer RR, Nakamura T, Uemoto S. **Continuous cell supply from a Sox9-expressing progenitor zone in adult liver, exocrine pancreas and intestine.** *Nat Genet.* 2011;43:34-41.
10. Roskams TA, Theise ND, Balabaud C, Bhagat G, Bhathal PS, Bioulac-Sage P, Brunt EM, Crawford JM, Crosby HA, Desmet V, Finegold MJ, Geller SA, Gouw AS, Hytiroglou P, Knisely AS, Kojiro M, Lefkowitch JH, Nakanuma Y, Olynyk JK, Park YN, Portmann B, Saxena R, Scheuer PJ, Strain AJ, Thung SN, Wanless IR, West AB. **Nomenclature of the finer branches of the biliary tree: canals, ductules, and ductular reactions in human livers.** *Hepatology.* 2004;39:1739-1745.
11. Cardinale V, Wang Y, Carpino G, Cui CB, Gatto M, Rossi M, Berloco PB, Cantafora A, Wauthier E, Furth ME, Inverardi L, Dominguez-Bendala J, Ricordi C, Gerber D, Gaudio E, Alvaro D, Reid L. **Multipotent stem/progenitor cells in human biliary**

tree give rise to hepatocytes, cholangiocytes, and pancreatic islets. *Hepatology.* 2011;54:2159-2172.
12. Carpino G, Cardinale V, Onori P, Franchitto A, Berloco PB, Rossi M, Wang Y, Semeraro R, Anceschi M, Brunelli R, Alvaro D, Reid LM, Gaudio E. **Biliary tree stem/progenitor cells in glands of extrahepatic and intraheptic bile ducts: an anatomical in situ study yielding evidence of maturational lineages.** *J Anat.* 2012;220:186-199.
13. Wang Y, Lanzoni G, Carpino G, Cui CB, Dominguez-Bendala J, Wauthier E, Cardinale V, Oikawa T, Pileggi A, Gerber D, Furth ME, Alvaro D, Gaudio E, Inverardi L, Reid LM. **Biliary Tree Stem Cells, Precursors to Pancreatic Committed Progenitors: Evidence for Possible Life-Long Pancreatic Organogenesis.** *Stem Cells.* 2013.
14. Fausto N, Campbell JS, Riehle KJ. **Liver regeneration.** *Hepatology.* 2006;43:S45-53.
15. Zajicek G. **Do livers "stream"?** *Am J Pathol.* 1995;146:772-776.
16. Dipaola F, Shivakumar P, Pfister J, Walters S, Sabla G, Bezerra JA. **Identification of intramural epithelial networks linked to peribiliary glands that express progenitor cell markers and proliferate after injury in mice.** *Hepatology.* 2013.
17. Wang Y, Yao HL, Cui CB, Wauthier E, Barbier C, Costello MJ, Moss N, Yamauchi M, Sricholpech M, Gerber D, Loboa EG, Reid LM. **Paracrine signals from mesenchymal cell populations govern the expansion and differentiation of human hepatic stem cells to adult liver fates.** *Hepatology.* 2010;52:1443-1454.
18. Michelotti GA, Xie G, Swiderska M, Choi SS, Karaca G, Kruger L, Premont R, Yang L, Syn WK, Metzger D, Diehl AM. **Smoothened is a master regulator of adult liver repair.** *J Clin Invest.* 2013;123:2380-2394.
19. Kallis YN, Robson AJ, Fallowfield JA, Thomas HC, Alison MR, Wright NA, Goldin RD, Iredale JP, Forbes SJ. **Remodelling of extracellular matrix is a requirement for the hepatic progenitor cell response.** *Gut.* 2011;60:525-533.
20. Asahina K, Zhou B, Pu WT, Tsukamoto H. **Septum transversum-derived mesothelium gives rise to hepatic stellate cells and perivascular mesenchymal cells in developing mouse liver.** *Hepatology.* 2011;53:983-995.
21. Yin C, Evason KJ, Asahina K, Stainier DY. **Hepatic stellate cells in liver development, regeneration, and cancer.** *J Clin Invest.* 2013;123:1902-1910.
22. Friedman SL. **Hepatic stellate cells: protean, multifunctional, and enigmatic cells of the liver.** *Physiol Rev.* 2008;88:125-172.
23. Troeger JS, Mederacke I, Gwak GY, Dapito DH, Mu X, Hsu CC, Pradere JP, Friedman RA, Schwabe RF. **Deactivation of hepatic stellate cells during liver fibrosis resolution in mice.** *Gastroenterology.* 2012;143:1073-1083 e1022.
24. Bilzer M, Roggel F, Gerbes AL. **Role of Kupffer cells in host defense and liver disease.** *Liver Int.* 2006;26:1175-1186.
25. Bird TG, Lu WY, Boulter L, Gordon-Keylock S, Ridgway RA, Williams MJ, Taube J, Thomas JA, Wojtacha D, Gambardella A, Sansom OJ, Iredale JP, Forbes SJ. **Bone marrow injection stimulates hepatic ductular reactions in the absence of injury via macrophage-mediated TWEAK signaling.** *Proc Natl Acad Sci U S A.* 2013;110:6542-6547.

26. Boulter L, Govaere O, Bird TG, Radulescu S, Ramachandran P, Pellicoro A, Ridgway RA, Seo SS, Spee B, Van Rooijen N, Sansom OJ, Iredale JP, Lowell S, Roskams T, Forbes SJ. **Macrophage-derived Wnt opposes Notch signaling to specify hepatic progenitor cell fate in chronic liver disease.** *Nat Med.* 2012;18:572-579.
27. Lorenzini S, Bird TG, Boulter L, Bellamy C, Samuel K, Aucott R, Clayton E, Andreone P, Bernardi M, Golding M, Alison MR, Iredale JP, Forbes SJ. **Characterisation of a stereotypical cellular and extracellular adult liver progenitor cell niche in rodents and diseased human liver.** *Gut.* 2010;59:645-654.
28. Cai J, Zhao Y, Liu Y, Ye F, Song Z, Qin H, Meng S, Chen Y, Zhou R, Song X, Guo Y, Ding M, Deng H. **Directed differentiation of human embryonic stem cells into functional hepatic cells.** *Hepatology.* 2007;45:1229-1239.
29. Schwartz RE, Linehan JL, Painschab MS, Hu WS, Verfaillie CM, Kaufman DS. **Defined conditions for development of functional hepatic cells from human embryonic stem cells.** *Stem Cells Dev.* 2005;14:643-655.
30. Naito H, Kidoya H, Sakimoto S, Wakabayashi T, Takakura N. **Identification and characterization of a resident vascular stem/progenitor cell population in preexisting blood vessels.** *EMBO J.* 2012;31:842-855.
31. Conigliaro A, Amicone L, Costa V, De Santis Puzzonia M, Mancone C, Sacchetti B, Cicchini C, Garibaldi F, Brenner DA, Kisseleva T, Bianco P, Tripodi M. **Evidence for a common progenitor of epithelial and mesenchymal components of the liver.** *Cell Death Differ.* 2013;20:1116-1123.
32. Li Y, Wang J, Asahina K. **Mesothelial cells give rise to hepatic stellate cells and myofibroblasts via mesothelial-mesenchymal transition in liver injury.** *Proc Natl Acad Sci U S A.* 2013;110:2324-2329.
33. Zhang L, Theise N, Chua M, Reid LM. **The stem cell niche of human livers: symmetry between development and regeneration.** *Hepatology.* 2008;48:1598-1607.
34. Kanwal F, Hoang T, Kramer JR, Asch SM, Goetz MB, Zeringue A, Richardson P, El-Serag HB. **Increasing prevalence of HCC and cirrhosis in patients with chronic hepatitis C virus infection.** *Gastroenterology.* 2011;140:1182-1188 e1181.
35. Ludwig J, Viggiano TR, McGill DB, Oh BJ. **Nonalcoholic steatohepatitis: Mayo Clinic experiences with a hitherto unnamed disease.** *Mayo Clin Proc.* 1980;55:434-438.
36. Clark JM, Brancati FL, Diehl AM. **The prevalence and etiology of elevated aminotransferase levels in the United States.** *Am J Gastroenterol.* 2003;98:960-967.
37. Browning JD, Szczepaniak LS, Dobbins R, Nuremberg P, Horton JD, Cohen JC, Grundy SM, Hobbs HH. **Prevalence of hepatic steatosis in an urban population in the United States: impact of ethnicity.** *Hepatology.* 2004;40:1387-1395.
38. Bedogni G, Miglioli L, Masutti F, Tiribelli C, Marchesini G, Bellentani S. **Prevalence of and risk factors for nonalcoholic fatty liver disease: the Dionysos nutrition and liver study.** *Hepatology.* 2005;42:44-52.
39. Machado M, Marques-Vidal P, Cortez-Pinto H. **Hepatic histology in obese patients undergoing bariatric surgery.** *J Hepatol.* 2006;45:600-606.
40. Angulo P. **Nonalcoholic fatty liver disease.** *N Engl J Med.* 2002;346:1221-1231.

41. Angulo P, Keach JC, Batts KP, Lindor KD. **Independent predictors of liver fibrosis in patients with nonalcoholic steatohepatitis.** *Hepatology.* 1999;30:1356-1362.
42. Feldstein AE, Wieckowska A, Lopez AR, Liu YC, Zein NN, McCullough AJ. **Cytokeratin-18 fragment levels as noninvasive biomarkers for nonalcoholic steatohepatitis: a multicenter validation study.** *Hepatology.* 2009;50:1072-1078.
43. Musso G, Gambino R, Cassader M, Pagano G. **Meta-analysis: natural history of non-alcoholic fatty liver disease (NAFLD) and diagnostic accuracy of non-invasive tests for liver disease severity.** *Ann Med.* 2011;43:617-649.
44. Kleiner DE, Brunt EM, Van Natta M, Behling C, Contos MJ, Cummings OW, Ferrell LD, Liu YC, Torbenson MS, Unalp-Arida A, Yeh M, McCullough AJ, Sanyal AJ. **Design and validation of a histological scoring system for nonalcoholic fatty liver disease.** *Hepatology.* 2005;41:1313-1321.
45. Wieckowska A, Feldstein AE. **Diagnosis of nonalcoholic fatty liver disease: invasive versus noninvasive.** *Semin Liver Dis.* 2008;28:386-395.
46. Ascha MS, Hanouneh IA, Lopez R, Tamimi TA, Feldstein AF, Zein NN. **The incidence and risk factors of hepatocellular carcinoma in patients with nonalcoholic steatohepatitis.** *Hepatology.* 2010;51:1972-1978.
47. Siddique A, Kowdley KV. **Insulin resistance and other metabolic risk factors in the pathogenesis of hepatocellular carcinoma.** *Clin Liver Dis.* 2011;15:281-296, vii-x.
48. Ertle J, Dechene A, Sowa JP, Penndorf V, Herzer K, Kaiser G, Schlaak JF, Gerken G, Syn WK, Canbay A. **Non-alcoholic fatty liver disease progresses to hepatocellular carcinoma in the absence of apparent cirrhosis.** *Int J Cancer.* 2011;128:2436-2443.
49. National Cholesterol Education Program Expert Panel on Detection E, Treatment of High Blood Cholesterol in A. **Third Report of the National Cholesterol Education Program (NCEP) Expert Panel on Detection, Evaluation, and Treatment of High Blood Cholesterol in Adults (Adult Treatment Panel III) final report.** *Circulation.* 2002;106:3143-3421.
50. Chitturi S, Abeygunasekera S, Farrell GC, Holmes-Walker J, Hui JM, Fung C, Karim R, Lin R, Samarasinghe D, Liddle C, Weltman M, George J. **NASH and insulin resistance: Insulin hypersecretion and specific association with the insulin resistance syndrome.** *Hepatology.* 2002;35:373-379.
51. Bugianesi E, Manzini P, D'Antico S, Vanni E, Longo F, Leone N, Massarenti P, Piga A, Marchesini G, Rizzetto M. **Relative contribution of iron burden, HFE mutations, and insulin resistance to fibrosis in nonalcoholic fatty liver.** *Hepatology.* 2004;39:179-187.
52. Patton HM, Yates K, Unalp-Arida A, Behling CA, Huang TT, Rosenthal P, Sanyal AJ, Schwimmer JB, Lavine JE. **Association between metabolic syndrome and liver histology among children with nonalcoholic Fatty liver disease.** *Am J Gastroenterol.* 2010;105:2093-2102.
53. De Bruyne RM, Fitzpatrick E, Dhawan A. **Fatty liver disease in children: eat now pay later.** *Hepatol Int.* 2010;4:375-385.
54. Ruhl CE, Everhart JE. **Determinants of the association of overweight with elevated serum alanine aminotransferase activity in the United States.** *Gastroenterology.* 2003;124:71-79.

55. Day CP. **Natural history of NAFLD: remarkably benign in the absence of cirrhosis.** *Gastroenterology.* 2005;129:375-378.
56. Ekstedt M, Franzen LE, Mathiesen UL, Thorelius L, Holmqvist M, Bodemar G, Kechagias S. **Long-term follow-up of patients with NAFLD and elevated liver enzymes.** *Hepatology.* 2006;44:865-873.
57. Soderberg C, Stal P, Askling J, Glaumann H, Lindberg G, Marmur J, Hultcrantz R. **Decreased survival of subjects with elevated liver function tests during a 28-year follow-up.** *Hepatology.* 2010;51:595-602.
58. Day CP, James OF. **Steatohepatitis: a tale of two "hits"?** *Gastroenterology.* 1998;114:842-845.
59. Monetti M, Levin MC, Watt MJ, Sajan MP, Marmor S, Hubbard BK, Stevens RD, Bain JR, Newgard CB, Farese RV, Sr., Hevener AL, Farese RV, Jr. **Dissociation of hepatic steatosis and insulin resistance in mice overexpressing DGAT in the liver.** *Cell Metab.* 2007;6:69-78.
60. Despres JP, Lemieux I. **Abdominal obesity and metabolic syndrome.** *Nature.* 2006;444:881-887.
61. Ruhl CE, Everhart JE. **Trunk fat is associated with increased serum levels of alanine aminotransferase in the United States.** *Gastroenterology.* 2010;138:1346-1356, 1356 e1341-1343.
62. Stranges S, Dorn JM, Muti P, Freudenheim JL, Farinaro E, Russell M, Nochajski TH, Trevisan M. **Body fat distribution, relative weight, and liver enzyme levels: a population-based study.** *Hepatology.* 2004;39:754-763.
63. van der Poorten D, Milner KL, Hui J, Hodge A, Trenell MI, Kench JG, London R, Peduto T, Chisholm DJ, George J. **Visceral fat: a key mediator of steatohepatitis in metabolic liver disease.** *Hepatology.* 2008;48:449-457.
64. Bataller R, Brenner DA. **Liver fibrosis.** *J Clin Invest.* 2005;115:209-218.
65. Popper H, Kent G, Stein R. **Ductular cell reaction in the liver in hepatic injury.** *J Mt Sinai Hosp N Y.* 1957;24:551-556.
66. Roskams T, Desmet V. **Ductular reaction and its diagnostic significance.** *Semin Diagn Pathol.* 1998;15:259-269.
67. Desmet VJ, van Eyken P, Roskams T. **Histopathology of vanishing bile duct diseases.** *Adv Clin Path.* 1998;2:87-99.
68. Libbrecht L, Desmet V, Van Damme B, Roskams T. **Deep intralobular extension of human hepatic 'progenitor cells' correlates with parenchymal inflammation in chronic viral hepatitis: can 'progenitor cells' migrate?** *J Pathol.* 2000;192:373-378.
69. Roskams T, Yang SQ, Koteish A, Durnez A, DeVos R, Huang X, Achten R, Verslype C, Diehl AM. **Oxidative stress and oval cell accumulation in mice and humans with alcoholic and nonalcoholic fatty liver disease.** *Am J Pathol.* 2003;163:1301-1311.
70. Demetris AJ, Seaberg EC, Wennerberg A, Ionellie J, Michalopoulos G. **Ductular reaction after submassive necrosis in humans. Special emphasis on analysis of ductular hepatocytes.** *Am J Pathol.* 1996;149:439-448.

71. Falkowski O, An HJ, Ianus IA, Chiriboga L, Yee H, West AB, Theise ND. **Regeneration of hepatocyte 'buds' in cirrhosis from intrabiliary stem cells.** *J Hepatol.* 2003;39:357-364.
72. Zhou H, Rogler LE, Teperman L, Morgan G, Rogler CE. **Identification of hepatocytic and bile ductular cell lineages and candidate stem cells in bipolar ductular reactions in cirrhotic human liver.** *Hepatology.* 2007;45:716-724.
73. Sasaki M, Ikeda H, Yamaguchi J, Miyakoshi M, Sato Y, Nakanuma Y. **Bile ductular cells undergoing cellular senescence increase in chronic liver diseases along with fibrous progression.** *Am J Clin Pathol.* 2010;133:212-223.
74. Yoon SM, Gerasimidou D, Kuwahara R, Hytiroglou P, Yoo JE, Park YN, Theise ND. **Epithelial cell adhesion molecule (EpCAM) marks hepatocytes newly derived from stem/progenitor cells in humans.** *Hepatology.* 2011;53:964-973.
75. Dorrell C, Erker L, Schug J, Kopp JL, Canaday PS, Fox AJ, Smirnova O, Duncan AW, Finegold MJ, Sander M, Kaestner KH, Grompe M. **Prospective isolation of a bipotential clonogenic liver progenitor cell in adult mice.** *Genes Dev.* 2011;25:1193-1203.
76. Shin S, Walton G, Aoki R, Brondell K, Schug J, Fox A, Smirnova O, Dorrell C, Erker L, Chu AS, Wells RG, Grompe M, Greenbaum LE, Kaestner KH. **Foxl1-Cre-marked adult hepatic progenitors have clonogenic and bilineage differentiation potential.** *Genes Dev.* 2011;25:1185-1192.
77. Ijzer J, Schotanus BA, Vander Borght S, Roskams TA, Kisjes R, Penning LC, Rothuizen J, van den Ingh TS. **Characterisation of the hepatic progenitor cell compartment in normal liver and in hepatitis: an immunohistochemical comparison between dog and man.** *Vet J.* 2010;184:308-314.
78. Van Den Heuvel MC, Slooff MJ, Visser L, Muller M, De Jong KP, Poppema S, Gouw AS. **Expression of anti-OV6 antibody and anti-N-CAM antibody along the biliary line of normal and diseased human livers.** *Hepatology.* 2001;33:1387-1393.
79. Theise ND, Saxena R, Portmann BC, Thung SN, Yee H, Chiriboga L, Kumar A, Crawford JM. **The canals of Hering and hepatic stem cells in humans.** *Hepatology.* 1999;30:1425-1433.
80. Saxena R, Theise ND, Crawford JM. **Microanatomy of the human liver-exploring the hidden interfaces.** *Hepatology.* 1999;30:1339-1346.
81. Roskams T, Katoonizadeh A, Komuta M. **Hepatic progenitor cells: an update.** *Clin Liver Dis.* 2010;14:705-718.
82. Roskams T. **Different types of liver progenitor cells and their niches.** *J Hepatol.* 2006;45:1-4.
83. Litvinov SV, Velders MP, Bakker HA, Fleuren GJ, Warnaar SO. **Ep-CAM: a human epithelial antigen is a homophilic cell-cell adhesion molecule.** *J Cell Biol.* 1994;125:437-446.
84. Litvinov SV, Bakker HA, Gourevitch MM, Velders MP, Warnaar SO. **Evidence for a role of the epithelial glycoprotein 40 (Ep-CAM) in epithelial cell-cell adhesion.** *Cell Adhes Commun.* 1994;2:417-428.

85. Anderson R, Schaible K, Heasman J, Wylie C. **Expression of the homophilic adhesion molecule, Ep-CAM, in the mammalian germ line.** *J Reprod Fertil.* 1999;116:379-384.
86. Stingl J, Eaves CJ, Zandieh I, Emerman JT. **Characterization of bipotent mammary epithelial progenitor cells in normal adult human breast tissue.** *Breast Cancer Res Treat.* 2001;67:93-109.
87. Schmelzer E, Reid LM. **EpCAM expression in normal, non-pathological tissues.** *Front Biosci.* 2008;13:3096-3100.
88. Yamashita T, Ji J, Budhu A, Forgues M, Yang W, Wang HY, Jia H, Ye Q, Qin LX, Wauthier E, Reid LM, Minato H, Honda M, Kaneko S, Tang ZY, Wang XW. **EpCAM-positive hepatocellular carcinoma cells are tumor-initiating cells with stem/ progenitor cell features.** *Gastroenterology.* 2009;136:1012-1024.
89. Yamashita T, Forgues M, Wang W, Kim JW, Ye Q, Jia H, Budhu A, Zanetti KA, Chen Y, Qin LX, Tang ZY, Wang XW. **EpCAM and alpha-fetoprotein expression defines novel prognostic subtypes of hepatocellular carcinoma.** *Cancer Res.* 2008;68:1451-1461.
90. Li L, Clevers H. **Coexistence of quiescent and active adult stem cells in mammals.** *Science.* 2010;327:542-545.
91. Hubscher SG. **Histological assessment of non-alcoholic fatty liver disease.** *Histopathology.* 2006;49:450-465.
92. Calvaruso V, Burroughs AK, Standish R, Manousou P, Grillo F, Leandro G, Maimone S, Pleguezuelo M, Xirouchakis I, Guerrini GP, Patch D, Yu D, O'Beirne J, Dhillon AP. **Computer-assisted image analysis of liver collagen: relationship to Ishak scoring and hepatic venous pressure gradient.** *Hepatology.* 2009;49:1236-1244.
93. Levene AP, Kudo H, Armstrong MJ, Thursz MR, Gedroyc WM, Anstee QM, Goldin RD. **Quantifying hepatic steatosis - more than meets the eye.** *Histopathology.* 2012;60:971-981.
94. Ziol M, Nault JC, Aout M, Barget N, Tepper M, Martin A, Trinchet JC, Ganne-Carrie N, Vicaut E, Beaugrand M, N'Kontchou G. **Intermediate hepatobiliary cells predict an increased risk of hepatocarcinogenesis in patients with hepatitis C virus-related cirrhosis.** *Gastroenterology.* 2010;139:335-343 e332.
95. Brunt EM, Blomenkamp K, Ahmed M, Ali F, Marcus N, Teckman J. **Hepatic progenitor cell proliferation and liver injury in alpha-1-antitrypsin deficiency.** *J Pediatr Gastroenterol Nutr.* 2010;51:626-630.
96. Clouston AD, Powell EE, Walsh MJ, Richardson MM, Demetris AJ, Jonsson JR. **Fibrosis correlates with a ductular reaction in hepatitis C: roles of impaired replication, progenitor cells and steatosis.** *Hepatology.* 2005;41:809-818.
97. Sackett SD, Li Z, Hurtt R, Gao Y, Wells RG, Brondell K, Kaestner KH, Greenbaum LE. **Foxl1 is a marker of bipotential hepatic progenitor cells in mice.** *Hepatology.* 2009;49:920-929.
98. Rountree CB, Ding W, Dang H, Vankirk C, Crooks GM. **Isolation of CD133+ liver stem cells for clonal expansion.** *J Vis Exp.* 2011.

99. Qiu Q, Hernandez JC, Dean AM, Rao PH, Darlington GJ. **CD24-positive cells from normal adult mouse liver are hepatocyte progenitor cells.** *Stem Cells Dev.* 2011;20:2177-2188.
100. Lowes KN, Brennan BA, Yeoh GC, Olynyk JK. **Oval cell numbers in human chronic liver diseases are directly related to disease severity.** *Am J Pathol.* 1999;154:537-541.
101. Tan J, Hytiroglou P, Wieczorek R, Park YN, Thung SN, Arias B, Theise ND. **Immunohistochemical evidence for hepatic progenitor cells in liver diseases.** *Liver.* 2002;22:365-373.
102. Maccallum WG. **Regenerative changes in the liver after acute yellow atrophy.** *Johns Hopkins Hosp Reports.* 1902;10:375-379.
103. Higgins GM, Anderson RM. **Experimental pathology of the liver 1. Restoration of the liver of the white rat following partial surgical removal.** *Arch Pathol* 1932;12:186-202.
104. Yoshida T. **Experimental Contribution to the Question of Metaplasic Episthelia.** *Virchows Archiv Fur Pathologische Anatomie Und Physiologie Und Fur Klinische Medizin.* 1932;283:29-40.
105. Kinosita R. **Studies on the cancerogenic chemical substances.** *Transactions of the Japanese Society for Pathology.* 1937;27:665-727.
106. Orr JW. **The histology of the rat's liver during the course of carcinogenesis by butter-yellow (p-dimethylaminoazobenzene).** *J. Pathol.* 1940;50:393-408.
107. Price JM, Harman JW, Miller EC, Miller JA. **Progressive microscopic alterations in the livers of rats fed the hepatic carcinogens 3'-methyl-4-dimethylaminoazobenzene and 4'-fluoro-4-dimethylaminoazobenzene.** *Cancer Res.* 1952;12:192-200.
108. Sasaki T, Yoshida T. **Experimentelle rzeugung des Leverkarzinoma durch Fuetterung mit o-amidoazotoluol.** *Virchows Archiv Fur Pathologische Anatomie Und Physiologie Und Fur Klinische Medizin.* 1935;295.
109. Farber E. **Similarities in the sequence of early histological changes induced in the liver of the rat by ethionine, 2-acetylamino-fluorene, and 3'-methyl-4-dimethylaminoazobenzene.** *Cancer Res.* 1956;16:142-148.
110. Wilson JW, Leduc EH. **Role of cholangioles in restoration of the liver of the mouse after dietary injury.** *J Pathol Bacteriol.* 1958;76:441-449.
111. Grisham JW, Porta EA. **Origin and Fate of Proliferated Hepatic Ductal Cells in the Rat: Electron Microscopic and Autoradiographic Studies.** *Exp Mol Pathol.* 1964;86:242-261.
112. Sell S, Nichols M, Becker FF, Leffert HL. **Hepatocyte proliferation and alpha 1-fetoprotein in pregnant, neonatal, and partially hepatectomized rats.** *Cancer Res.* 1974;34:865-871.
113. Evarts RP, Nagy P, Nakatsukasa H, Marsden E, Thorgeirsson SS. **In vivo differentiation of rat liver oval cells into hepatocytes.** *Cancer Res.* 1989;49:1541-1547.
114. Van de Velde H, Cauffman G, Tournaye H, Devroey P, Liebaers I. **The four blastomeres of a 4-cell stage human embryo are able to develop individually into**

blastocysts with inner cell mass and trophectoderm. *Hum Reprod.* 2008;23:1742-1747.
115. Huch M, Dorrell C, Boj SF, van Es JH, Li VS, van de Wetering M, Sato T, Hamer K, Sasaki N, Finegold MJ, Haft A, Vries RG, Grompe M, Clevers H. **In vitro expansion of single Lgr5+ liver stem cells induced by Wnt-driven regeneration.** *Nature.* 2013;494:247-250.
116. Jelnes P, Santoni-Rugiu E, Rasmussen M, Friis SL, Nielsen JH, Tygstrup N, Bisgaard HC. **Remarkable heterogeneity displayed by oval cells in rat and mouse models of stem cell-mediated liver regeneration.** *Hepatology.* 2007;45:1462-1470.
117. Arzumanyan A, Sambandam V, Clayton MM, Choi SS, Xie G, Diehl AM, Yu DY, Feitelson MA. **Hedgehog Signaling Blockade Delays Hepatocarcinogenesis Induced by Hepatitis B Virus X Protein.** *Cancer Res.* 2012.
118. Van Hul NK, Abarca-Quinones J, Sempoux C, Horsmans Y, Leclercq IA. **Relation between liver progenitor cell expansion and extracellular matrix deposition in a CDE-induced murine model of chronic liver injury.** *Hepatology.* 2009;49:1625-1635.
119. Towers M, Tickle C. **Growing models of vertebrate limb development.** *Development.* 2009;136:179-190.
120. Laurent TC, Fraser JR. **Hyaluronan.** *FASEB J.* 1992;6:2397-2404.
121. Hayes AJ, Tudor D, Nowell MA, Caterson B, Hughes CE. **Chondroitin sulfate sulfation motifs as putative biomarkers for isolation of articular cartilage progenitor cells.** *J Histochem Cytochem.* 2008;56:125-138.
122. Vongchan P, Warda M, Toyoda H, Toida T, Marks RM, Linhardt RJ. **Structural characterization of human liver heparan sulfate.** *Biochim Biophys Acta.* 2005;1721:1-8.
123. Roskams T, Rosenbaum J, De Vos R, David G, Desmet V. **Heparan sulfate proteoglycan expression in chronic cholestatic human liver diseases.** *Hepatology.* 1996;24:524-532.
124. Martinez-Hernandez A, Delgado FM, Amenta PS. **The extracellular matrix in hepatic regeneration. Localization of collagen types I, III, IV, laminin, and fibronectin.** *Lab Invest.* 1991;64:157-166.
125. Greenbaum LE, Wells RG. **The role of stem cells in liver repair and fibrosis.** *Int J Biochem Cell Biol.* 2011;43:222-229.
126. Lopez-Garcia C, Klein AM, Simons BD, Winton DJ. **Intestinal stem cell replacement follows a pattern of neutral drift.** *Science.* 2010;330:822-825.
127. Greco V, Guo S. **Compartmentalized organization: a common and required feature of stem cell niches?** *Development.* 2010;137:1586-1594.
128. Stocker E, Heine WD. **Regeneration of liver parenchyma under normal and pathological conditions.** *Beitr Pathol.* 1971;144:400-408.
129. Stocker E, Wullstein HK, Brau G. **[Capacity of regeneration in liver epithelia of juvenile, repeated partially hepatectomized rats. Autoradiographic studies after continous infusion of 3H-thymidine (author's transl)].** *Virchows Arch B Cell Pathol.* 1973;14:93-103.

130. Rhim JA, Sandgren EP, Degen JL, Palmiter RD, Brinster RL. **Replacement of diseased mouse liver by hepatic cell transplantation.** *Science.* 1994;263:1149-1152.
131. Overturf K, Al-Dhalimy M, Finegold M, Grompe M. **The repopulation potential of hepatocyte populations differing in size and prior mitotic expansion.** *Am J Pathol.* 1999;155:2135-2143.
132. Fattovich G, Stroffolini T, Zagni I, Donato F. **Hepatocellular carcinoma in cirrhosis: incidence and risk factors.** *Gastroenterology.* 2004;127:S35-50.
133. Sato Y, Nakata K, Kato Y, Shima M, Ishii N, Koji T, Taketa K, Endo Y, Nagataki S. **Early recognition of hepatocellular carcinoma based on altered profiles of alpha-fetoprotein.** *N Engl J Med.* 1993;328:1802-1806.
134. Mishra L, Banker T, Murray J, Byers S, Thenappan A, He AR, Shetty K, Johnson L, Reddy EP. **Liver stem cells and hepatocellular carcinoma.** *Hepatology.* 2009;49:318-329.
135. Armstrong MJ, Houlihan DD, Bentham L, Shaw JC, Cramb R, Olliff S, Gill PS, Neuberger JM, Lilford RJ, Newsome PN. **Presence and severity of non-alcoholic fatty liver disease in a large prospective primary care cohort.** *J Hepatol.* 2012;56:234-240.
136. Adams LA, Lymp JF, St Sauver J, Sanderson SO, Lindor KD, Feldstein A, Angulo P. **The natural history of nonalcoholic fatty liver disease: a population-based cohort study.** *Gastroenterology.* 2005;129:113-121.
137. Newsome PN, Hussain MA, Theise ND. **Hepatic oval cells: helping redefine a paradigm in stem cell biology.** *Curr Top Dev Biol.* 2004;61:1-28.
138. Richardson MM, Jonsson JR, Powell EE, Brunt EM, Neuschwander-Tetri BA, Bhathal PS, Dixon JB, Weltman MD, Tilg H, Moschen AR, Purdie DM, Demetris AJ, Clouston AD. **Progressive fibrosis in nonalcoholic steatohepatitis: association with altered regeneration and a ductular reaction.** *Gastroenterology.* 2007;133:80-90.
139. Dezso K, Papp V, Bugyik E, Hegyesi H, Safrany G, Bodor C, Nagy P, Paku S. **Structural analysis of oval-cell-mediated liver regeneration in rats.** *Hepatology.* 2012;56:1457-1467.
140. Yang S, Koteish A, Lin H, Huang J, Roskams T, Dawson V, Diehl AM. **Oval cells compensate for damage and replicative senescence of mature hepatocytes in mice with fatty liver disease.** *Hepatology.* 2004;39:403-411.
141. Bijl N, Sokolovic M, Vrins C, Langeveld M, Moerland PD, Ottenhoff R, van Roomen CP, Claessen N, Boot RG, Aten J, Groen AK, Aerts JM, van Eijk M. **Modulation of glycosphingolipid metabolism significantly improves hepatic insulin sensitivity and reverses hepatic steatosis in mice.** *Hepatology.* 2009;50:1431-1441.
142. Witek RP, Stone WC, Karaca FG, Syn WK, Pereira TA, Agboola KM, Omenetti A, Jung Y, Teaberry V, Choi SS, Guy CD, Pollard J, Charlton P, Diehl AM. **Pan-caspase inhibitor VX-166 reduces fibrosis in an animal model of nonalcoholic steatohepatitis.** *Hepatology.* 2009;50:1421-1430.
143. Horie Y, Suzuki A, Kataoka E, Sasaki T, Hamada K, Sasaki J, Mizuno K, Hasegawa G, Kishimoto H, Iizuka M, Naito M, Enomoto K, Watanabe S, Mak TW, Nakano T. **Hepatocyte-specific Pten deficiency results in steatohepatitis and hepatocellular carcinomas.** *J Clin Invest.* 2004;113:1774-1783.

144. Leclercq IA, Farrell GC, Field J, Bell DR, Gonzalez FJ, Robertson GR. **CYP2E1 and CYP4A as microsomal catalysts of lipid peroxides in murine nonalcoholic steatohepatitis.** *J Clin Invest.* 2000;105:1067-1075.
145. Lo L, McLennan SV, Williams PF, Bonner J, Chowdhury S, McCaughan GW, Gorrell MD, Yue DK, Twigg SM. **Diabetes is a progression factor for hepatic fibrosis in a high fat fed mouse obesity model of non-alcoholic steatohepatitis.** *J Hepatol.* 2011;55:435-444.
146. Yimin, Furumaki H, Matsuoka S, Sakurai T, Kohanawa M, Zhao S, Kuge Y, Tamaki N, Chiba H. **A novel murine model for non-alcoholic steatohepatitis developed by combination of a high-fat diet and oxidized low-density lipoprotein.** *Lab Invest.* 2012;92:265-281.
147. Kohli R, Kirby M, Xanthakos SA, Softic S, Feldstein AE, Saxena V, Tang PH, Miles L, Miles MV, Balistreri WF, Woods SC, Seeley RJ. **High-fructose, medium chain trans fat diet induces liver fibrosis and elevates plasma coenzyme Q9 in a novel murine model of obesity and nonalcoholic steatohepatitis.** *Hepatology.* 2010;52:934-944.
148. Tetri LH, Basaranoglu M, Brunt EM, Yerian LM, Neuschwander-Tetri BA. **Severe NAFLD with hepatic necroinflammatory changes in mice fed trans fats and a high-fructose corn syrup equivalent.** *Am J Physiol Gastrointest Liver Physiol.* 2008;295:G987-995.
149. Brunt EM. **Nonalcoholic steatohepatitis: definition and pathology.** *Semin Liver Dis.* 2001;21:3-16.
150. Germain L, Goyette R, Marceau N. **Differential cytokeratin and alpha-fetoprotein expression in morphologically distinct epithelial cells emerging at the early stage of rat hepatocarcinogenesis.** *Cancer Res.* 1985;45:673-681.
151. Weber A, Boger R, Vick B, Urbanik T, Haybaeck J, Zoller S, Teufel A, Krammer PH, Opferman JT, Galle PR, Schuchmann M, Heikenwalder M, Schulze-Bergkamen H. **Hepatocyte-specific deletion of the antiapoptotic protein myeloid cell leukemia-1 triggers proliferation and hepatocarcinogenesis in mice.** *Hepatology.* 2010;51:1226-1236.
152. Nejak-Bowen KN, Thompson MD, Singh S, Bowen WC, Jr., Dar MJ, Khillan J, Dai C, Monga SP. **Accelerated liver regeneration and hepatocarcinogenesis in mice overexpressing serine-45 mutant beta-catenin.** *Hepatology.* 2010;51:1603-1613.
153. Goodman ZD, Terraciano L, Wee A. **Tumours and tumour-like lesions of the liver.** *Macsween's Pathology of the Liver 6th Edition (Burt, A.D; Portmann, B.C.; Ferrell, L.D. editors).* 2012:761-851.
154. Park YN. **Update on precursor and early lesions of hepatocellular carcinomas.** *Arch Pathol Lab Med.* 2011;135:704-715.
155. Di Tommaso L, Franchi G, Park YN, Fiamengo B, Destro A, Morenghi E, Montorsi M, Torzilli G, Tommasini M, Terracciano L, Tornillo L, Vecchione R, Roncalli M. **Diagnostic value of HSP70, glypican 3, and glutamine synthetase in hepatocellular nodules in cirrhosis.** *Hepatology.* 2007;45:725-734.

156. Nhieu JT, Renard CA, Wei Y, Cherqui D, Zafrani ES, Buendia MA. **Nuclear accumulation of mutated beta-catenin in hepatocellular carcinoma is associated with increased cell proliferation.** *Am J Pathol.* 1999;155:703-710.
157. Tandra S, Yeh MM, Brunt EM, Vuppalanchi R, Cummings OW, Unalp-Arida A, Wilson LA, Chalasani N. **Presence and significance of microvesicular steatosis in nonalcoholic fatty liver disease.** *J Hepatol.* 2011;55:654-659.
158. Anstee QM, Goldin RD. **Mouse models in non-alcoholic fatty liver disease and steatohepatitis research.** *Int J Exp Pathol.* 2006;87:1-16.
159. Wang B, Hsu SH, Frankel W, Ghoshal K, Jacob ST. **Stat3-mediated activation of microRNA-23a suppresses gluconeogenesis in hepatocellular carcinoma by down-regulating Glucose-6-phosphatase and peroxisome proliferator-activated receptor gamma, coactivator 1 alpha.** *Hepatology.* 2012;56:186-197.
160. Nakanishi Y, Tsuneyama K, Nomoto K, Fujimoto M, Salunga TL, Nakajima T, Miwa S, Murai Y, Hayashi S, Kato I, Hiraga K, Hsu DK, Liu FT, Takano Y. **Nonalcoholic steatohepatitis and hepatocellular carcinoma in galectin-3 knockout mice.** *Hepatol Res.* 2008;38:1241-1251.
161. Jung Y, Brown KD, Witek RP, Omenetti A, Yang L, Vandongen M, Milton RJ, Hines IN, Rippe RA, Spahr L, Rubbia-Brandt L, Diehl AM. **Accumulation of hedgehog-responsive progenitors parallels alcoholic liver disease severity in mice and humans.** *Gastroenterology.* 2008;134:1532-1543.
162. Paradis V, Zalinski S, Chelbi E, Guedj N, Degos F, Vilgrain V, Bedossa P, Belghiti J. **Hepatocellular carcinomas in patients with metabolic syndrome often develop without significant liver fibrosis: a pathological analysis.** *Hepatology.* 2009;49:851-859.
163. Zhou CH, Ye LP, Ye SX, Li Y, Zhang XY, Xu XY, Gong LY. **Clinical significance of SOX9 in human non-small cell lung cancer progression and overall patient survival.** *J Exp Clin Cancer Res.* 2012;31:18.
164. Prevot PP, Simion A, Grimont A, Colletti M, Khalaileh A, Van den Steen G, Sempoux C, Xu X, Roelants V, Hald J, Bertrand L, Heimberg H, Konieczny SF, Dor Y, Lemaigre FP, Jacquemin P. **Role of the ductal transcription factors HNF6 and Sox9 in pancreatic acinar-to-ductal metaplasia.** *Gut.* 2012.
165. Sashikawa Kimura M, Mutoh H, Sugano K. **SOX9 is expressed in normal stomach, intestinal metaplasia, and gastric carcinoma in humans.** *J Gastroenterol.* 2011;46:1292-1299.
166. Borovski T, De Sousa EMF, Vermeulen L, Medema JP. **Cancer stem cell niche: the place to be.** *Cancer Res.* 2011;71:634-639.
167. Calabrese C, Poppleton H, Kocak M, Hogg TL, Fuller C, Hamner B, Oh EY, Gaber MW, Finklestein D, Allen M, Frank A, Bayazitov IT, Zakharenko SS, Gajjar A, Davidoff A, Gilbertson RJ. **A perivascular niche for brain tumor stem cells.** *Cancer Cell.* 2007;11:69-82.
168. Houlihan DD, Mabuchi Y, Morikawa S, Niibe K, Araki D, Suzuki S, Okano H, Matsuzaki Y. **Isolation of mouse mesenchymal stem cells on the basis of expression of Sca-1 and PDGFR-alpha.** *Nat Protoc.* 2012;7:2103-2111.

169. Mabuchi Y, Houlihan DD, Akazawa C, Okano H, Matsuzaki Y. **Prospective isolation of murine and human bone marrow mesenchymal stem cells based on surface markers.** *Stem Cells Int.* 2013;2013:507301.
170. Mabuchi Y, Morikawa S, Harada S, Niibe K, Suzuki S, Renault-Mihara F, Houlihan DD, Akazawa C, Okano H, Matsuzaki Y. **LNGFR(+)THY-1(+)VCAM-1(hi+) Cells Reveal Functionally Distinct Subpopulations in Mesenchymal Stem Cells.** *Stem Cell Reports.* 2013;1:152-165.
171. Morikawa S, Mabuchi Y, Kubota Y, Nagai Y, Niibe K, Hiratsu E, Suzuki S, Miyauchi-Hara C, Nagoshi N, Sunabori T, Shimmura S, Miyawaki A, Nakagawa T, Suda T, Okano H, Matsuzaki Y. **Prospective identification, isolation, and systemic transplantation of multipotent mesenchymal stem cells in murine bone marrow.** *J Exp Med.* 2009;206:2483-2496.
172. Bondue A, Tannler S, Chiapparo G, Chabab S, Ramialison M, Paulissen C, Beck B, Harvey R, Blanpain C. **Defining the earliest step of cardiovascular progenitor specification during embryonic stem cell differentiation.** *J Cell Biol.* 2011;192:751-765.
173. Chong JJ, Reinecke H, Iwata M, Torok-Storb B, Stempien-Otero A, Murry CE. **Progenitor cells identified by PDGFR-alpha expression in the developing and diseased human heart.** *Stem Cells Dev.* 2013;22:1932-1943.
174. Takamiya M, Haider KH, Ashraf M. **Identification and characterization of a novel multipotent sub-population of Sca-1(+) cardiac progenitor cells for myocardial regeneration.** *PLoS One.* 2011;6:e25265.
175. McQualter JL, Brouard N, Williams B, Baird BN, Sims-Lucas S, Yuen K, Nilsson SK, Simmons PJ, Bertoncello I. **Endogenous fibroblastic progenitor cells in the adult mouse lung are highly enriched in the sca-1 positive cell fraction.** *Stem Cells.* 2009;27:623-633.
176. Uezumi A, Ito T, Morikawa D, Shimizu N, Yoneda T, Segawa M, Yamaguchi M, Ogawa R, Matev MM, Miyagoe-Suzuki Y, Takeda S, Tsujikawa K, Tsuchida K, Yamamoto H, Fukada S. **Fibrosis and adipogenesis originate from a common mesenchymal progenitor in skeletal muscle.** *J Cell Sci.* 2011;124:3654-3664.
177. Futami I, Ishijima M, Kaneko H, Tsuji K, Ichikawa-Tomikawa N, Sadatsuki R, Muneta T, Arikawa-Hirasawa E, Sekiya I, Kaneko K. **Isolation and characterization of multipotential mesenchymal cells from the mouse synovium.** *PLoS One.* 2012;7:e45517.
178. Clayton E, Forbes SJ. **The isolation and in vitro expansion of hepatic Sca-1 progenitor cells.** *Biochem Biophys Res Commun.* 2009;381:549-553.
179. Tang Z, Wang A, Yuan F, Yan Z, Liu B, Chu JS, Helms JA, Li S. **Differentiation of multipotent vascular stem cells contributes to vascular diseases.** *Nat Commun.* 2012;3:875.
180. Knook DL, Seffelaar AM, de Leeuw AM. **Fat-storing cells of the rat liver. Their isolation and purification.** *Exp Cell Res.* 1982;139:468-471.
181. Swiderska-Syn M, Syn WK, Xie G, Kruger L, Machado MV, Karaca G, Michelotti GA, Choi SS, Premont RT, Diehl AM. **Myofibroblastic cells function as progenitors to regenerate murine livers after partial hepatectomy.** *Gut.* 2013.

182. Awuah PK, Nejak-Bowen KN, Monga SP. **Role and regulation of PDGFRalpha signaling in liver development and regeneration.** *Am J Pathol.* 2013;182:1648-1658.
183. Chen Y, Choi SS, Michelotti GA, Chan IS, Swiderska-Syn M, Karaca GF, Xie G, Moylan CA, Garibaldi F, Premont R, Suliman HB, Piantadosi CA, Diehl AM. **Hedgehog controls hepatic stellate cell fate by regulating metabolism.** *Gastroenterology.* 2012;143:1319-1329 e1311.
184. Ishak K, Baptista A, Bianchi L, Callea F, De Groote J, Gudat F, Denk H, Desmet V, Korb G, MacSween RN, et al. **Histological grading and staging of chronic hepatitis.** *J Hepatol.* 1995;22:696-699.
185. Chakravarty G, Rider B, Mondal D. **Cytoplasmic compartmentalization of SOX9 abrogates the growth arrest response of breast cancer cells that can be rescued by trichostatin A treatment.** *Cancer Biol Ther.* 2011;11:71-83.
186. Chakravarty G, Moroz K, Makridakis NM, Lloyd SA, Galvez SE, Canavello PR, Lacey MR, Agrawal K, Mondal D. **Prognostic significance of cytoplasmic SOX9 in invasive ductal carcinoma and metastatic breast cancer.** *Exp Biol Med (Maywood).* 2011;236:145-155.
187. Gouw AS, Clouston AD, Theise ND. **Ductular reactions in human liver: diversity at the interface.** *Hepatology.* 2011;54:1853-1863.
188. Rockey DC, Caldwell SH, Goodman ZD, Nelson RC, Smith AD, American Association for the Study of Liver D. **Liver biopsy.** *Hepatology.* 2009;49:1017-1044.
189. Selden C, Chalmers SA, Jones C, Standish R, Quaglia A, Rolando N, Burroughs AK, Rolles K, Dhillon A, Hodgson HJ. **Epithelial colonies cultured from human explanted liver in subacute hepatic failure exhibit hepatocyte, biliary epithelial, and stem cell phenotypic markers.** *Stem Cells.* 2003;21:624-631.
190. Nakatani K, Seki S, Kawada N, Kobayashi K, Kaneda K. **Expression of neural cell adhesion molecule (N-CAM) in perisinusoidal stellate cells of the human liver.** *Cell Tissue Res.* 1996;283:159-165.
191. Lee JH, Park HJ, Kim YA, Lee DH, Noh JK, Kwon CH, Jung SM, Lee SK. **The phenotypic characteristic of liver-derived stem cells from adult human deceased donor liver.** *Transplant Proc.* 2012;44:1110-1112.
192. Kabashima-Niibe A, Higuchi H, Takaishi H, Masugi Y, Matsuzaki Y, Mabuchi Y, Funakoshi S, Adachi M, Hamamoto Y, Kawachi S, Aiura K, Kitagawa Y, Sakamoto M, Hibi T. **Mesenchymal stem cells regulate epithelial-mesenchymal transition and tumor progression of pancreatic cancer cells.** *Cancer Sci.* 2013;104:157-164.
193. Mardaryev AN, Meier N, Poterlowicz K, Sharov AA, Sharova TY, Ahmed MI, Rapisarda V, Lewis C, Fessing MY, Ruenger TM, Bhawan J, Werner S, Paus R, Botchkarev VA. **Lhx2 differentially regulates Sox9, Tcf4 and Lgr5 in hair follicle stem cells to promote epidermal regeneration after injury.** *Development.* 2011;138:4843-4852.
194. Pritchett J, Harvey E, Athwal V, Berry A, Rowe C, Oakley F, Moles A, Mann DA, Bobola N, Sharrocks AD, Thomson BJ, Zaitoun AM, Irving WL, Guha IN, Hanley NA, Hanley KP. **Osteopontin is a novel downstream target of SOX9 with**

diagnostic implications for progression of liver fibrosis in humans. *Hepatology.* 2012;56:1108-1116.

195. Dolle L, Best J, Empsen C, Mei J, Van Rossen E, Roelandt P, Snykers S, Najimi M, Al Battah F, Theise ND, Streetz K, Sokal E, Leclercq IA, Verfaillie C, Rogiers V, Geerts A, van Grunsven LA. **Successful isolation of liver progenitor cells by aldehyde dehydrogenase activity in naive mice.** *Hepatology.* 2012;55:540-552.
196. Wang X, Foster M, Al-Dhalimy M, Lagasse E, Finegold M, Grompe M. **The origin and liver repopulating capacity of murine oval cells.** *Proc Natl Acad Sci U S A.* 2003;100 Suppl 1:11881-11888.
197. Overturf K, al-Dhalimy M, Ou CN, Finegold M, Grompe M. **Serial transplantation reveals the stem-cell-like regenerative potential of adult mouse hepatocytes.** *Am J Pathol.* 1997;151:1273-1280.